



8-2007

Construction of Bacteriophage-Based Bioluminescent Bioreporters for *Staphylococcus aureus* and *Salmonella* Monitoring

Aysu Ozen
University of Tennessee - Knoxville

Follow this and additional works at: https://trace.tennessee.edu/utk_graddiss

 Part of the [Microbiology Commons](#)

Recommended Citation

Ozen, Aysu, "Construction of Bacteriophage-Based Bioluminescent Bioreporters for *Staphylococcus aureus* and *Salmonella* Monitoring. " PhD diss., University of Tennessee, 2007.
https://trace.tennessee.edu/utk_graddiss/258

This Dissertation is brought to you for free and open access by the Graduate School at TRACE: Tennessee Research and Creative Exchange. It has been accepted for inclusion in Doctoral Dissertations by an authorized administrator of TRACE: Tennessee Research and Creative Exchange. For more information, please contact trace@utk.edu.

To the Graduate Council:

I am submitting herewith a dissertation written by Aysu Ozen entitled "Construction of Bacteriophage-Based Bioluminescent Bioreporters for *Staphylococcus aureus* and *Salmonella* Monitoring." I have examined the final electronic copy of this dissertation for form and content and recommend that it be accepted in partial fulfillment of the requirements for the degree of Doctor of Philosophy, with a major in Microbiology.

Gary S. Sayler, Major Professor

We have read this dissertation and recommend its acceptance:

Steven Ripp, Pamela Small, Stephen Oliver, Steven Wilhelm

Accepted for the Council:

Carolyn R. Hodges

Vice Provost and Dean of the Graduate School

(Original signatures are on file with official student records.)

To the Graduate Council:

I am submitting herewith a dissertation written by Aysu Ozen entitled “Construction of Bacteriophage-Based Bioluminescent Bioreporters for *Staphylococcus aureus* and *Salmonella* Monitoring.” I have examined the final electronic copy of this dissertation for form and content and recommend that it be accepted in partial fulfillment of the requirements for the degree of Doctor of Philosophy, with a major in Microbiology.

Gary S. Sayler, Major Professor

We have read this dissertation
and recommend its acceptance:

Steven Ripp

Pamela Small

Stephen Oliver

Steven Wilhelm

Accepted for the Council:

Carolyn R. Hodges, Vice Provost and
Dean of the Graduate School

(Original signatures are on file with official student records.)

**Construction of Bacteriophage-Based Bioluminescent
Bioreporters for *Staphylococcus aureus* and *Salmonella*
Monitoring**

A Dissertation Presented for
the Doctor of Philosophy
Degree
The University of Tennessee, Knoxville

Aysu Ozen
August 2007

ACKNOWLEDGEMENTS

I want to thank Dr. Gary Sayler for his guidance and for teaching me how to do good science. I also want to thank Dr. Steve Ripp for his support and for being a mentor and a friend. I want to acknowledge my committee members, Drs. Stephen Oliver, Pamela Small, and Steven Wilhelm for their helpful suggestions and input.

I am grateful to all previous and present members of CEB who I've had the pleasure to work with for being always nice, friendly and extremely helpful.

I want to thank my husband Can Ozen, my mother and father Emel and Ata Gunal, and my sisters, Asu Ozkan and Gursu Zimmermann for being there for me. Your love and support kept me going.

ABSTRACT

Construction of two recombinant *luxI* bacteriophage-based bioluminescent bioreporters was undertaken to develop detection and monitoring systems for *Staphylococcus aureus* and *Salmonella* spp. These systems take advantage of the high specificity of bacteriophage for their hosts and the *Vibrio fischeri lux* operon responsible for quorum sensing bioluminescence. The detection system is composed of two elements, a recombinant phage with *luxI* which is specific for the target pathogen, and an acylhomoserine lactone (AHL)-inducible bioreporter cell line carrying the reporter *lux* genes. The goal of this study was to construct *Salmonella*- and *S. aureus*-specific recombinant phages which contain *luxI*.

The *luxI* expression in *S. aureus* was controlled by cloning the gene into *S. aureus* under the control of a Gram-positive promoter and ribosomal binding site (RBS). The same construct was also placed into *Escherichia coli* and *Bacillus subtilis* for comparison purposes. Although light was produced by *E. coli* and *B. subtilis*, there was no light from *S. aureus*. The presence of *luxI* transcript was shown in all strains using real time qRT-PCR. Western blotting detected LuxI only in *E. coli* but not in *B. subtilis* and *S. aureus*. After the construct RBS was shown to be effective, the codon utilization of *luxI* was adapted to *S. aureus* phage P68 genome to eliminate a possible codon preference problem. Optimization had no effect on *S. aureus* while it resulted in a significant decrease of light from *E. coli* and a non-significant increase in *B. subtilis*. Additional studies are needed to determine reason(s) for *luxI* expression problem in *S. aureus*.

Salmonella choleraesuis, which carries *luxI* under the control of *Salmonella* phage P22 promoter and a Gram-negative RBS, produced high levels of light. The *luxI*,

under the control of the same promoter and RBS, was cloned into the phage P22 genome using homologous recombination. The recombinant phage P22luxI induced light from the bioreporter only when it was propagated using *S. choleraesuis* which harbored the homologous recombination plasmid. The bioluminescent bioreporter *E. coli* OHHLux was shown to produce light in the presence of P22luxI without the *S. choleraesuis* host. Bioluminescence tests showed P22luxI as the source of the problem. *Escherichia coli* OHHLux was shown not to be lysed by P22 or P22luxI and not to uptake the P22luxI genome during bioluminescence tests. P22luxI and *S. choleraesuis* in combination produced AHL by using an AHL bioreporter, *Agrobacterium tumefaciens* A136. Since *A. tumefaciens* A136 is not specific enough to use for quantification of AHL, another bioreporter was constructed by placing the *E. coli* OHHLux plasmid into *Klebsiella* strains. They produced light with P22luxI without the host like the previous bioreporter. Future studies should focus on constructing a bioreporter strain which does not produce light when mixed with P22luxI without its host. Optimization, and sensitivity and specificity determination studies of the system should be performed using this bioreporter strain.

TABLE OF CONTENTS

Chapter	Page
1. Introduction and General Information.....	1
2. Literature Review	
Quorum sensing.....	7
<i>V. fischeri</i> - <i>Euprymna scolopes</i> symbiosis.....	9
Bioluminescence reaction.....	9
Organization and regulation of the <i>lux</i> genes.....	10
Other regulators of <i>V. fischeri</i> bioluminescence.....	12
AHL synthesis and structure.....	14
Fatty acid biosynthesis (source of AHL acyl side chains).....	21
AHL substrate SAM.....	28
Quorum sensing in Gram-positive bacteria.....	31
Quorum sensing in <i>Salmonella</i> and <i>E. coli</i>	36
Bacteriophage.....	37
Bacterial pathogens <i>Salmonella</i> and <i>S. aureus</i>	42
Traditional, nucleic acid-based, and immunological bacterial pathogen detection methods.....	44
Bioluminescent bioreporters.....	48

Bacteriophage-based bioluminescent bioreporters for bacterial pathogen detection.....	51
The bacteriophage-based bioluminescent bioreporter system developed in this work.....	53
 3. Materials and Methods-Construction of <i>S. aureus</i> Bioreporter	
 Bacterial strains, plasmids, and bacteriophage.....	56
Growth and storage conditions.....	56
Molecular biology techniques.....	63
DNA sequencing.....	65
Preparation of chemically competent cells of <i>E. coli</i> DH5 α	65
Chemical transformation of <i>E. coli</i> DH5 α	65
Electroporation of <i>S. aureus</i>	66
Electroporation of <i>B. subtilis</i>	66
Plasmid purification using rapid boiling mini-prep method.....	67
Purification of <i>V. fischeri</i> genome.....	67
<i>luxI</i> cloning from <i>V. fischeri</i> genome.....	68
X8 promoter cloning from <i>S. aureus</i> phage Φ 85 genome.....	69
T ₁ T ₂ transcription termination site cloning.....	71
Construction of pMOD-2-kan ^r -prom-luxI-T1T2 #7 (or pMO-L) plasmid.....	71

Bioluminescent and fluorescent detection of OHHL from	
pMO-L #7 in <i>E. coli</i>	75
Construction of pMK4-prom-luxI #13.3 (or pMK-L #13.3).....	76
Transfer of pMK-L #13.3 into <i>B. subtilis</i> and <i>S. aureus</i>	80
Bioluminescent detection of OHHL from pMK-L #13.3 in <i>S.</i>	
<i>aureus</i> using Wallac 1450 Microbeta Plus Liquid Scintillation Counter.....	80
Fluorescent detection of OHHL from pMK-L #13.3 in <i>S.</i>	
<i>aureus</i> using Wallac Victor2 1420 Multilabel Counter.....	81
Construction of the pHPS9-luxI #7 (or pHP-L #7) plasmid.....	82
Transfer of pHP-L #7 into <i>S. aureus</i>	83
Fluorescent detection of OHHL from pHP-L #7 in <i>E. coli</i> and <i>S.</i>	
<i>aureus</i> using Wallac Victor2 1420 Multilabel Counter.....	85
Bioluminescent detection of OHHL from pHP-L #7 in <i>E. coli</i> and <i>S.</i>	
<i>aureus</i> using Wallac 1450 Microbeta Plus Liquid Scintillation Counter.....	86
Detection of OHHL from pHP-L #7 in <i>E. coli</i> and <i>S. aureus</i> using	
Liquid Chromatography Mass Spectrometry (LCMS).....	86
Construction of pHPS9-kanR #4 (or pHP-K #4).....	88
Transfer of pHP-K #4 into <i>S. aureus</i>	89
Detection and analysis of kanamycin resistance provided by	
pHP-K #4 in <i>E. coli</i> and <i>S. aureus</i>	89
Construction of pDG148-Stu-luxI #28 (or pDG-L #28).....	90
Transfer of pDG-L #28 into <i>S. aureus</i>	91
Construction of pHPS9-sht-Pspac-luxI-lacI #9 (or pHP-PL #9).....	92

Transfer of pHP-PL #9 into <i>B. subtilis</i> and <i>S. aureus</i>	95
Bioluminescent and fluorescent detection of OHHL from pDG-L #28 in <i>E. coli</i> and pHP-PL #9 in <i>E. coli</i> , <i>B. subtilis</i> , and <i>S. aureus</i> using Wallac Victor2 1420 Multilabel and 1450 Microbeta Plus Liquid Scintillation Counters.....	95
The <i>luxI</i> transcript detection from pHP-PL #9 and pDG-L #28 using real-time quantitative reverse transcriptase PCR.....	98
<i>luxI</i> translation product detection from pHP-PL #9 and pDG-L #28 using SDS-PAGE and Western Blotting.....	99
Construction of pHPS9-sht-Pspac-kanR-lacI #31 (or pHP-PK #31).....	101
Transfer of pHP-PK #31 and pUB110 into <i>S. aureus</i>	103
Detection and analysis of kanamycin resistance provided by pHP-PK #31 in <i>S. aureus</i>	105
<i>luxI</i> CDS codon optimization for adaptation to the codon bias of <i>S. aureus</i> phage P68.....	105
Construction of pHPS9-sht-Pspac-optluxI-lacI #5 (or pHP-POL #5).....	109
Transfer of pHP-POL #5 into <i>B. subtilis</i> and <i>S. aureus</i>	111
Bioluminescent and fluorescent detection of OHHL from pHP-POL #5 in <i>E. coli</i> , <i>B. subtilis</i> , and <i>S. aureus</i> using Wallac Victor2 1420 Multilabel and 1450 Microbeta Plus Liquid Scintillation Counters.....	111
Invitro packaging of <i>S. aureus</i> phage P68 genome.....	113
Statistical calculations.....	113

4.	Results-Construction of <i>S. aureus</i> Bioreporter	
	Bioluminescent and fluorescent detection of OHHL from pMO-L #7 in	
	<i>E. coli</i>	115
	Bioluminescent and fluorescent detection of OHHL from pMK-L #13.3 in	
	<i>S. aureus</i>	118
	Bioluminescent and fluorescent detection of OHHL from pHP-L #7	
	in <i>E. coli</i> and <i>S. aureus</i> using Wallac Victor2 1420 Multilabel and Wallac	
	1450 Microbeta Plus Liquid Scintillation Counters.....	121
	Detection of OHHL from pHP-L #7 in <i>E. coli</i> and <i>S. aureus</i> using	
	LCMS.....	126
	Detection and analysis of kanamycin resistance provided by pHP-K #4 in	
	<i>E. coli</i> and <i>S. aureus</i>	130
	Bioluminescent and fluorescent detection of OHHL from pDG-L #28 in	
	<i>E. coli</i> and pHP-PL #9 in <i>E. coli</i> , <i>B. subtilis</i> , and <i>S. aureus</i> using Wallac	
	Victor2 1420 Multilabel and 1450 Microbeta Plus Liquid Scintillation	
	Counters.....	131
	The <i>luxI</i> transcript detection from pHP-PL #9 and pDG-L #28 using	
	real-time quantitative reverse transcriptase PCR.....	147
	<i>luxI</i> translation product detection from pHP-PL #9 and pDG-L #28 using	
	SDS-PAGE and Western Blotting.....	152
	Detection and analysis of kanamycin resistance provided by pHP-PK #31	
	in <i>S. aureus</i>	154

	Bioluminescent and fluorescent detection of OHHL from pHP-POL #5 in <i>E. coli</i> , <i>B. subtilis</i> , and <i>S. aureus</i> using Wallac Victor2 1420 Multilabel and 1450 Microbeta Plus Liquid Scintillation Counters.....	157
	Invitro packaging of <i>S. aureus</i> phage P68 genome.....	165
	Summary of results obtained with plasmids used to determine the <i>luxI</i> expression efficiency in <i>S. aureus</i> ; and in <i>E. coli</i> and <i>B. subtilis</i> as controls.....	166
5.	Discussion and Conclusions-Construction of <i>S. aureus</i> Bioreporter.....	167
6.	Materials and Methods-Construction of <i>Salmonella</i> Bioreporter	
	Bacterial strains, plasmids, and bacteriophage.....	180
	Growth and storage conditions.....	180
	Molecular biology techniques.....	185
	DNA sequencing.....	185
	Electroporation of <i>S. choleraesuis</i>	186
	Electroporation of <i>Klebsiella</i> strains.....	187
	Plasmid purification using rapid boiling mini-prep method.....	187
	Construction of pCR2.1-P _L -luxI-T1T2 #3 (or pCR-L #3).....	188
	Transfer of pCR-L #3 into <i>Salmonella</i>	191

Bioluminescent and fluorescent detection of OHHL from pCR-L #3 in <i>S. choleraesuis</i> using Wallac Victor2 1420 Multilabel and 1450 Microbeta Plus Liquid Scintillation Counters.....	192
Construction of homologous recombination plasmid, pCR2.1-HA1-P _L -luxI-T1T2-HA2 #5 (or pCR-HAL #5).....	193
Transfer of pCR-HAL #5 into <i>S. choleraesuis</i>	196
Cloning of P _L , <i>luxI</i> , and T ₁ T ₂ into <i>Salmonella</i> phage P22 using homologous recombination.....	197
Propagation of phage from homologous recombination.....	197
Phage propagation for preparation of phage lysate stocks.....	198
Bioluminescent detection of OHHL from P22luxI phage propagated with <i>S. choleraesuis</i> or <i>S. choleraesuis</i> with pCR-HAL #5 using Wallac Victor2 1420 Multilabel and 1450 Microbeta Plus Liquid Scintillation Counters.....	199
Screening of P22luxI #3 and #7 phage by PCR.....	201
Testing the bioluminescent bioreporter <i>E. coli</i> OHHLux for infection by P22 and P22luxI #3 and #7 phage on an LB plate.....	201
Detection of bioluminescence from the bioluminescent bioreporter <i>E. coli</i> OHHLux and P22luxI mixture using Wallac Victor2 1420 Multilabel and 1450 Microbeta Plus Liquid Scintillation Counters.....	202
Control of phage stocks for contamination.....	204
Measurements from mixtures of bioluminescent bioreporter <i>E. coli</i> OHHLux and P22luxI #3 phage to determine the source of bioluminescence using Wallac 1450 Microbeta Plus Liquid Scintillation Counter.....	204

Test of pseudolysogeny.....	205
Qualitative detection of OHHL from P22luxI and <i>S. choleraesuis</i> mixture using AHL bioreporter <i>A. tumefaciens</i> A136.....	207
Construction of <i>Klebsiella</i> bioluminescent bioreporters.....	210
Bioluminescent detection of OHHL from <i>S. choleraesuis</i> and P22luxI phage using <i>Klebsiella</i> bioluminescent bioreporters and a Wallac 1450 Microbeta Plus Liquid Scintillation Counter.....	211
Bioluminescent detection of OHHL from P22luxI genome and bioluminescent bioreporters using a Wallac 1450 Microbeta Plus Liquid Scintillation Counter.....	213
Statistical calculations.....	215
 7. Results-Construction of <i>Salmonella</i> Bioreporter	
 Bioluminescent and fluorescent detection of OHHL from pCR-L #3 in <i>S.</i> <i>choleraesuis</i> using Wallac Victor2 1420 Multilabel and 1450 Microbeta Plus Liquid Scintillation Counters.....	216
Cloning of P _L , <i>luxI</i> , and T ₁ T ₂ into <i>Salmonella</i> phage P22 using homologous recombination.....	217
Bioluminescent detection of OHHL from P22luxI phage propagated with <i>S.</i> <i>choleraesuis</i> or <i>S. choleraesuis</i> with pCR-HAL #5 using Wallac Victor2 1420 Multilabel and 1450 Microbeta Plus Liquid Scintillation Counters.....	221
Screening of P22luxI #3 and #7 phages by PCR.....	222

Testing the bioluminescent bioreporter <i>E. coli</i> OHHLux for infection by P22 and P22luxI #3 and #7 phages on an LB plate.....	226
Detection of bioluminescence from the bioluminescent bioreporter <i>E. coli</i> OHHLux and P22luxI mixture using Wallac Victor2 1420 Multilabel and 1450 Microbeta Plus Liquid Scintillation Counters.....	226
Control of phage stocks for contamination.....	229
Measurements from the mixtures of bioluminescent bioreporter <i>E. coli</i> OHHLux and P22luxI #3 phage to determine the source of bioluminescence using Wallac 1450 Microbeta Plus Liquid Scintillation Counter.....	229
Test of pseudolysogeny.....	232
Qualitative detection of OHHL from P22luxI and <i>S. choleraesuis</i> mixture using AHL bioreporter <i>A. tumefaciens</i> A136.....	233
Bioluminescent detection of OHHL from <i>S. choleraesuis</i> and P22luxI phage using <i>Klebsiella</i> bioluminescent bioreporters and a Wallac 1450 Microbeta Plus Liquid Scintillation Counter.....	236
Bioluminescent detection of OHHL from P22luxI genome and bioluminescent bioreporters using a Wallac 1450 Microbeta Plus Liquid Scintillation Counter.....	242
8. Discussion and Conclusions-Construction of <i>Salmonella</i> Bioreporter.....	249
List of References.....	255
Appendix.....	298

Vita.....	300
-----------	-----

LIST OF TABLES

Table	Page
2-1. AHL types in various organisms.....	16
2-2. Gram-positive bacteria which carry SAM synthetase gene, <i>metK</i>	32
2-3. Bioluminescent bioreporters constructed for detection of chemicals.....	49
2-4. Bioluminescent bacteriophage-based bioreporters for bacterial pathogen detection.....	52
3-1. Bacterial strains used in this study.....	57
3-2. Plasmids used in this study.....	58
3-3. Bacteriophage used in this study.....	63
3-4. List of primers used in the study.....	64
3-5. The pairing of the phage Φ 85 X8 promoter sequence used and the sequence described by Carbonelli et al. (597).....	70
3-6. LCMS conditions used to detect OHHL from the standard and pHP-L #7 in <i>E. coli</i> and <i>S. aureus</i>	88
4-1. A summary of assays for bioluminescent and fluorescent OHHL detection from pHP-L #7 in <i>E. coli</i> and positive control.....	123
4-2. Kanamycin resistance patterns provided by pHP-K #4 in <i>E.coli</i> and <i>S. aureus</i> ..	130
4-3. Comparison of bioluminescence and fluorescence from pDG-L #28 in <i>E. coli</i> and pHP-PL #9 in <i>B. subtilis</i>	139

4-4.	Overnight Express Autoinduction System 1 (Novagen) effect on bioluminescence and fluorescence from constructs using IPTG-inducible <i>Pspac</i>	147
4-5.	Real-time qRT-PCR C _T values for <i>luxI</i> transcription from pDG-L #28 in <i>E. coli</i> and pHP-PL #9 in <i>E. coli</i> , <i>B. subtilis</i> , and <i>S. aureus</i>	151
4-6.	Kanamycin resistance patterns provided by pHP-PK #31 in <i>S. aureus</i>	155
4-7.	Comparison of bioluminescence and fluorescence from constructs that carry non-optimized or optimized <i>luxI</i> for adaptation to the codon bias of <i>S. aureus</i> phage P68.....	165
4-8.	A summary of results from all constructs used to determine <i>luxI</i> expression efficiency in <i>S. aureus</i> ; and in <i>E. coli</i> and <i>B. subtilis</i> as controls.....	166
5-1.	Comparison of copy numbers, RBSs, and promoters of constructs used for determination of <i>S. aureus</i> kanamycin resistance patterns.....	172
6-1.	Bacterial strains used in this study.....	181
6-2.	Plasmids used in this study.....	183
6-3.	Bacteriophage used in this study.....	184
6-4.	List of primers used in this study.....	186
6-5.	P22luxI amounts for bioluminescence detection from P22luxI propagated with <i>S. choleraesuis</i> or <i>S. choleraesuis</i> carrying pCR-HAL #5.	200
6-6.	Samples and amounts used for bioluminescence detection from <i>E. coli</i> OHHLux and P22luxI #7.....	203
6-7.	Samples and amounts used for bioluminescence detection from <i>E. coli</i> OHHLux and P22luxI #3.....	203

6-8.	Samples and amounts used to determine the source of bioluminescence from the <i>E. coli</i> OHHLux and P22luxI mixture.....	206
6-9.	Controls and amounts used to determine the source of bioluminescence from the <i>E. coli</i> OHHLux and P22luxI mixture.....	206
6-10.	Bioluminescence detection from <i>E. coli</i> OHHLux during its incubation with P22luxI and negative control, <i>E. coli</i> OHHLux using DeltaTox luminometer	206
6-11.	Samples, controls, and amounts used for OHHL detection from P22luxI and <i>S. choleraesuis</i> using AHL bioreporter <i>A. tumefaciens</i> A136.....	209
6-12.	Samples and amounts used for bioluminescence detection from P22luxI and its host <i>S. choleraesuis</i> using the <i>K. pneumoniae</i> bioreporter.....	211
6-13.	Samples and amounts used for bioluminescence detection from P22luxI and its host <i>S. choleraesuis</i> using the <i>K. oxytoca</i> bioreporter.....	212
6-14.	Negative controls and amounts used for bioluminescence detection P22luxI and its host <i>S. choleraesuis</i> using <i>Klebsiella</i> bioreporters.....	212
6-15.	Samples and amounts used for bioluminescence detection from P22luxI genome and <i>K. oxytoca</i> , <i>K. pneumoniae</i> , or <i>E. coli</i> OHHLux bioreporters.....	214
6-16.	Negative controls and amounts used for bioluminescence detection from P22luxI genome and <i>K. oxytoca</i> , <i>K. pneumoniae</i> , or <i>E. coli</i> OHHLux bioreporters.....	214
7-1.	Bioluminescence and fluorescence from pCR-L#3 in <i>S. choleraesuis</i>	221
7-2.	Bioluminescence from P22luxI #3, #7, 10^{-4} , and HR propagated using <i>S. choleraesuis</i> containing pCR-HAL #5.....	225

7-3.	Comparison of bioluminescence from P22luxI and <i>E. coli</i> OHHLux	
	dilutions determined to find the source of light from the P22luxI and	
	<i>E. coli</i> OHHLux mixture.....	230

LIST OF FIGURES

Figure	Page
2-1.	<i>Vibrio fischeri</i> Lux I/R quorum sensing system.....11
2-2.	Ain S/R and Lux S/PQ quorum sensing systems in <i>V. fischeri</i>13
2-3.	Some examples of different AHL structures.....15
2-4.	Synthesis of OHHL.....19
2-5.	FAB II pathway.....23
2-6.	SAM metabolism.....30
2-7.	Gram-positive quorum sensing oligopeptide autoinducers.....32
2-8.	<i>S. aureus</i> quorum sensing.....33
2-9.	<i>B. subtilis</i> quorum sensing.....35
2-10.	<i>S. typhimurium</i> AI-2, R-THMF.....37
2-11.	The bioluminescent bioreporter working mechanism.....49
2-12.	The bacteriophage-based bioluminescent bioreporter system for pathogen monitoring developed in this work.....54
3-1.	pMOD-2-kan ^r -prom-luxI-T1T2 #7 (or pMO-L #7) plasmid.....74
3-2.	Methodology for bioluminescent and fluorescent OHHL measurement from bacterial strains that carry <i>luxI</i>76
3-3.	Construction of pMK4-prom-luxI #13.3 (or pMK-L #13.3).....78
3-4.	pMK4-prom-luxI #13.3 (or pMK-L #13.3) plasmid.....79
3-5.	The construction of pHPS9-luxI #7 (or pHP-L #7).....84
3-6.	The construction of pHPS9-kanR #4 (or pHP-K #4).....90

3-7.	The construction of pDG148-Stu-luxI #28 (or pDG-L #28).....	92
3-8.	The construction of pHPS9-sht-Pspac-luxI-lacI #9 (or pHP-PL #9).....	94
3-9.	The construction of pHPS9-sht-Pspac-kanR-lacI #31 (or pHP-PK #31).	104
3-10.	Codon quality distribution plots provided by GENEART for non-optimized and optimized <i>luxI</i> for adaptation to the codon bias of <i>S. aureus</i> phage P68.....	106
3-11.	Codon quality plots provided by GENEART for non-optimized and optimized <i>luxI</i> for adaptation to the codon bias of <i>S. aureus</i> phage P68.....	107
3-12.	GC content plots provided by GENEART for non-optimized and optimized <i>luxI</i> for adaptation to the codon bias of <i>S. aureus</i> phage P68.....	107
3-13.	The pairing of non-optimized and optimized <i>luxI</i> for adaptation to the codon bias of <i>S. aureus</i> phage P68.....	108
3-14.	<i>luxI</i> , optimized for adaptation to the codon bias of <i>S. aureus</i> phage P68, in pPCR-Script.....	109
4-1 (A).	Bioluminescent OHHL detection from pMO-L #7 (or pMOD-2-kan ^r -prom-luxI-T1T2 #7) in <i>E. coli</i> at 28°C using bioreporter RoLux and Wallac Victor2 1420 Multilabel Counter.....	116
4-1 (B).	Fluorescent detection of OHHL from pMO-L #7 (or pMOD-2-kan ^r -prom-luxI-T1T2 #7) in <i>E. coli</i> at 28°C using bioreporter <i>E. coli</i> MT102 with pJBA132 and Wallac Victor2 1420 Multilabel Counter.....	117

4-2 (A).	Bioluminescent OHHL detection from pMK-L #13.3 (or pMK4-prom-luxI #13.3) in <i>S. aureus</i> at 28°C using bioreporter RoLux and Wallac 1450 Microbeta Plus Liquid Scintillation Counter.....	119
4-2 (B).	Fluorescent OHHL detection from pMK-L #13.3 (or pMK4-prom-luxI #13.3) in <i>S. aureus</i> at 28°C using bioreporter <i>E. coli</i> MT102 with pJBA132 and Wallac Victor2 1420 Multilabel Counter.....	120
4-3 (A).	Bioluminescent OHHL detection from pHP-L #7 (or pHPS9-luxI #7) in <i>E. coli</i> and <i>S. aureus</i> at 28°C using the bioreporter RoLux and Wallac 1450 Microbeta Plus Liquid Scintillation Counter.....	124
4-3 (B).	Fluorescent OHHL detection from pHP-L #7 (or pHPS9-luxI #7) in <i>E. coli</i> and <i>S. aureus</i> at 28°C using the bioreporter <i>E. coli</i> MT102 with pJBA132 and Wallac Victor2 1420 Multilabel Counter.....	125
4-4.	The LC chromatogram and mass/charge spectrum of the peak shown in LC chromatogram to detect OHHL molecule in standard (OHHL in dH ₂ O).....	127
4-5.	The LC chromatogram and mass/charge spectrum of the peak in LC chromatogram to detect OHHL molecule in 24 h-culture of <i>E. coli</i> carrying pHP-L #7.....	128
4-6.	The LC chromatogram and mass/charge spectrum of the peak in LC chromatogram to detect OHHL molecule in 24 h-culture of <i>S. aureus</i> carrying pHP-L #7.....	129

4-7 (A).	Bioluminescent OHHL detection from pDG-L #28 (or pDG148-Stu-luxI #28) in <i>E. coli</i> at 28°C with and without IPTG using the bioreporter <i>E. coli</i> OHHLux and Wallace 1450 Microbeta Plus Liquid Scintillation Counter.....	133
4-7 (B).	Fluorescent OHHL detection from pDG-L #28 (or pDG148-Stu-luxI #28) in <i>E. coli</i> at 28°C with and without IPTG using the bioreporter <i>E. coli</i> MT102 with pJBA132 and Wallace Victor2 1420 Multilabel Counter.....	134
4-8 (A).	Bioluminescent OHHL detection from pHP-PL #9 (or pHPS9-sht-Pspac-luxI-lacI #9) in <i>B. subtilis</i> at 28°C with and without IPTG using the bioreporter <i>E. coli</i> OHHLux and Wallace 1450 Microbeta Plus Liquid Scintillation Counter.....	135
4-8 (B).	Fluorescent OHHL detection from pHP-PL #9 (or pHPS9-sht-Pspac-luxI-lacI #9) in <i>B. subtilis</i> at 28°C with and without IPTG using the bioreporter <i>E. coli</i> MT102 with pJBA132 and Wallace Victor2 1420 Multilabel Counter.....	136
4-9 (A).	Bioluminescent OHHL detection from pHP-PL #9 (or pHPS9-sht-Pspac-luxI-lacI #9) in <i>S. aureus</i> at 28°C with and without IPTG using the bioreporter <i>E. coli</i> OHHLux and Wallace 1450 Microbeta Plus Liquid Scintillation Counter.....	137

4-9 (B).	Fluorescent OHHL detection from pHP-PL #9 (or pHPS9-sht-Pspac-luxI-lacI #9) in <i>S. aureus</i> at 28°C with and without IPTG using the bioreporter <i>E. coli</i> MT102 with pJBA132 and Wallac Victor2 1420 Multilabel Counter.....	138
4-10 (A).	Bioluminescent OHHL detection from pHP-PL #9 (or pHPS9-sht-Pspac-luxI-lacI #9) in <i>E. coli</i> in Overnight Express Autoinduction System 1 at 28°C using the bioreporter <i>E. coli</i> OHHLux and Wallac 1450 Microbeta Plus Liquid Scintillation Counter.....	141
4-10 (B).	Fluorescent OHHL detection from pHP-PL #9 (or pHPS9-sht-Pspac-luxI-lacI #9) in <i>E. coli</i> in Overnight Express Autoinduction System 1 at 28°C using the bioreporter <i>E. coli</i> MT102 with pJBA132 and Wallac Victor2 1420 Multilabel Counter.....	142
4-11 (A).	Bioluminescent OHHL detection from pHP-PL #9 (or pHPS9-sht-Pspac-luxI-lacI #9) in <i>B. subtilis</i> in Overnight Express Autoinduction System 1 at 28°C using the bioreporter <i>E. coli</i> OHHLux and Wallac 1450 Microbeta Plus Liquid Scintillation Counter.....	143

4-11 (B).	Fluorescent OHHL detection from pHP-PL #9 (or pHPS9-sht-Pspac-luxI-lacI #9) in <i>B. subtilis</i> in Overnight Express Autoinduction System 1 at 28°C using the bioreporter <i>E. coli</i> MT102 with pJBA132 and Wallac Victor2 1420 Multilabel Counter.....	144
4-12 (A).	Bioluminescent OHHL detection from pHP-PL #9 (or pHPS9-sht-Pspac-luxI-lacI #9) in <i>S. aureus</i> in Overnight Express Autoinduction System 1 at 28°C using the bioreporter <i>E. coli</i> OHHLux and Wallac 1450 Microbeta Plus Liquid Scintillation Counter.....	145
4-12 (B).	Fluorescent OHHL detection from pHP-PL #9 (or pHPS9-sht-Pspac-luxI-lacI #9) in <i>S. aureus</i> in Overnight Express Autoinduction System 1 at 28°C using the bioreporter <i>E. coli</i> MT102 with pJBA132 and Wallac Victor2 1420 Multilabel Counter.....	146
4-13 (A).	Real-time qRT-PCR plots for <i>luxI</i> transcription from wild-type <i>S. aureus</i> (negative control).....	149
4-13 (B).	Real-time qRT-PCR plots for <i>luxI</i> transcription from pDG-L #28 (or pDG148-Stu-luxI #28) in <i>E. coli</i>	149
4-13 (C).	Real-time qRT-PCR plots for <i>luxI</i> transcription from pHP-PL #9 (or pHPS9-sht-Pspac-luxI-lacI #9) in <i>E. coli</i>	150
4-13 (D).	Real-time qRT-PCR plots for <i>luxI</i> transcription from pHP-PL #9 (or pHPS9-sht-Pspac-luxI-lacI #9) in <i>B. subtilis</i>	150
4-13 (E).	Real-time qRT-PCR plots for <i>luxI</i> transcription from pHP-PL #9 (or pHPS9-sht-Pspac-luxI-lacI #9) in <i>S. aureus</i>	151

4-14.	SDS-PAGE of total protein extracts from <i>E. coli</i> , <i>B. subtilis</i> and <i>S. aureus</i> with pHP-PL #9; and <i>E. coli</i> containing pDG-L #28.....	153
4-15.	Western blotting for LuxI detection from <i>E. coli</i> , <i>B. subtilis</i> and <i>S. aureus</i> with pHP-PL #9; and <i>E. coli</i> containing pDG-L #28.....	154
4-16.	Kanamycin resistance patterns provided by pHP-PK #31 in <i>S. aureus</i> compared to those from pUB110 in <i>S. aureus</i>	156
4-17 (A).	Bioluminescent OHHL detection of from pHP-POL #5 (or pHPS9-sht-Pspac-optluxI-lacI #5) in <i>E. coli</i> at 28°C using the bioreporter <i>E. coli</i> OHHLux and Wallace 1450 Microbeta Plus Liquid Scintillation Counter.....	159
4-17 (B).	Fluorescent OHHL detection from pHP-POL #5 (or pHPS9-sht-Pspac-optluxI-lacI #5) in <i>E. coli</i> at 28°C using the bioreporter <i>E. coli</i> MT102 with pJBA132 and Wallace Victor2 1420 Multilabel Counter.....	160
4-18 (A).	Bioluminescent OHHL detection from pHP-POL #5 (or pHPS9-sht-Pspac-optluxI-lacI #5) in <i>B. subtilis</i> at 28°C using the bioreporter <i>E. coli</i> OHHLux and Wallace 1450 Microbeta Plus Liquid Scintillation Counter.....	161
4-18 (B).	Fluorescent OHHL detection from pHP-POL #5 (or pHPS9-sht-Pspac-optluxI-lacI #5) in <i>B. subtilis</i> at 28°C using the bioreporter <i>E. coli</i> MT102 with pJBA132 and Wallace Victor2 1420 Multilabel Counter.....	162

4-19 (A).	Bioluminescent OHHL detection from pHP-POL #5 (or pHPS9-sht-Pspac-optluxI-lacI #5) in <i>S. aureus</i> at 28°C using the bioreporter <i>E. coli</i> OHHLux and Wallace 1450 Microbeta Plus Liquid Scintillation Counter.....	163
4-19 (B).	Fluorescent OHHL detection from pHP-POL #5 (or pHPS9-sht-Pspac-optluxI-lacI #5) in <i>S. aureus</i> at 28°C using the bioreporter <i>E. coli</i> MT102 with pJBA132 and Wallace Victor2 1420 Multilabel Counter.....	164
5-1 (A).	The aligning of phage Φ85 genome sequence and the X8 promoter sequence used in construction of pMO-L #7 using BLAST.....	169
5-1 (B).	The aligning of phage Φ85 genome sequence and the X8 promoter sequence described by Carbonelli et al. (605) using BLAST.....	170
6-1.	pCR2.1-P _L -luxI-T1T2 #3 (or pCR-L #3) plasmid.....	191
6-2.	pCR2.1-HA1-P _L -luxI-T1T2-HA2 #5 (or pCR-HAL #5) plasmid used for homologous recombination.....	196
6-3.	Methodology for bioluminescent OHHL detection of from recombinant P22luxI phage.....	200
6-4.	Assay diagram for qualitative detection of OHHL using AHL bioreporter <i>A. tumefaciens</i> A136.....	209
7-1 (A).	Bioluminescent OHHL detection from pCR-L #3 (or pCR2.1-P _L -luxI-T1T2 #3) in <i>S. choleraesuis</i> at 28°C using the bioreporter <i>E. coli</i> OHHLux and Wallace 1450 Microbeta Plus Liquid Scintillation Counter.....	218

7-1 (B).	Bioluminescent OHHL detection from pCR-L #3 (or pCR2.1-P _L -luxI-T1T2 #3) in <i>S. choleraesuis</i> at 28°C using the bioreporter <i>E. coli</i> OHHLux and Wallace Victor2 1420 Multilabel Counter.....	219
7-1 (C).	Fluorescent OHHL detection from pCR-L #3 (or pCR2.1-P _L -luxI-T1T2 #3) in <i>S. choleraesuis</i> at 28°C using the bioreporter <i>E. coli</i> MT102 with pJBA132 and Wallace Victor2 1420 Multilabel Counter.....	220
7-2 (A).	Bioluminescent OHHL detection from P22luxI #3, #7, 10 ⁻⁴ , and HR using the bioreporter <i>E. coli</i> OHHLux, the host <i>S. choleraesuis</i> , and Wallace 1450 Microbeta Plus Liquid Scintillation Counter.....	223
7-2 (B).	Bioluminescent OHHL detection from P22luxI #3, #7, 10 ⁻⁴ , and HR using the bioreporter <i>E. coli</i> OHHLux, the host <i>S. choleraesuis</i> , and Wallace Victor2 1420 Multilabel Counter.....	224
7-3.	Products from PCR to check the presence of <i>luxI</i> in P22luxI #3 and #7 propagated using <i>S. choleraesuis</i> or <i>S. choleraesuis</i> carrying pCR-HAL #5.....	225
7-4 (A).	Bioluminescent OHHL detection from P22luxI and the bioreporter <i>E. coli</i> OHHLux using Wallace 1450 Microbeta Plus Liquid Scintillation Counter.....	227
7-4 (B).	Bioluminescent OHHL detection from P22luxI and the bioreporter <i>E. coli</i> OHHLux using Wallace Victor2 1420 Multilabel Counter.....	228

7-5.	Bioluminescence detection to find the source of light from the P22luxI and <i>E. coli</i> OHHLux mixture.....	231
7-6.	Products from PCR to check the presence of <i>luxI</i> in genome and plasmid purifications of <i>E. coli</i> OHHLux after incubation with P22luxI.....	233
7-7.	Qualitative OHHL detection using AHL bioreporter <i>A. tumefaciens</i> A136. Sample names are shown on top of pictures.....	235
7-8 (A).	Bioluminescent OHHL detection from P22luxI #3 using the host <i>S. choleraesuis</i> and the <i>K. oxytoca</i> bioreporter.....	238
7-8 (B).	Bioluminescent OHHL detection from P22luxI #7 using the host <i>S. choleraesuis</i> and the <i>K. oxytoca</i> bioreporter.....	239
7-9 (A).	Bioluminescent OHHL detection from P22luxI #3 using the host <i>S. choleraesuis</i> and the <i>K. pneumoniae</i> bioreporter.....	240
7-9 (B).	Bioluminescent OHHL detection from P22luxI #7 using the host <i>S. choleraesuis</i> and the <i>K. pneumoniae</i> bioreporter.....	241
7-10 (A).	Bioluminescent OHHL detection from P22luxI #3 genome using the <i>K. pneumoniae</i> bioreporter and Wallac 1450 Microbeta Plus Liquid Scintillation Counter.....	244
7-10 (B).	Bioluminescent OHHL detection from P22luxI #7 genome using the <i>K. pneumoniae</i> bioreporter and Wallac 1450 Microbeta Plus Liquid Scintillation Counter.....	245

7-11 (A).	Bioluminescent OHHL detection from P22luxI #3 genome using the <i>K. oxytoca</i> bioreporter and Wallac 1450 Microbeta Plus Liquid Scintillation Counter.....	246
7-11 (B).	Bioluminescent OHHL detection from P22luxI #7 genome using the <i>K. oxytoca</i> bioreporter and Wallac 1450 Microbeta Plus Liquid Scintillation Counter.....	247
7-12.	Bioluminescent OHHL detection from P22luxI genome using the <i>E.</i> <i>coli</i> OHHLux bioreporter and Wallac 1450 Microbeta Plus Liquid Scintillation Counter.....	248

CHAPTER I

INTRODUCTION AND GENERAL INFORMATION

Various methods have been used to monitor the environment, agricultural products, food, fermentors, and wastewater treatment plants to detect pollutants and pathogens and also to observe biological processes for clinical and pharmaceutical purposes (1-15). Although these methods can be sensitive, specific, and powerful, they are usually costly, laborious, time-consuming, and need to be performed in special laboratories by trained personnel. Furthermore, chemical detection methods such as gas or high pressure liquid chromatography and mass and atomic absorption spectrometry do not take into account bioavailability; the interactions with other chemicals in mixtures and the effects on organisms (13-15). Frequently, pathogen detection methods cannot differentiate between dead and alive and/or living and viable but not culturable (VBNC) organisms and may have specificity and cross-contamination problems (1-12). These problems with the existing methods create a need for alternative systems.

Bioluminescent bioreporters offer a good alternative. They are genetically engineered microbial organisms that react to the presence of specific analyte(s) by generating light (see reviews 13-22). Light-producing reporter genes are placed under the control of a promoter which is inducible only by the particular analyte. Bioreporters are integrated into biosensors, forming devices which are a combination of biological and electrical components so that the light produced can be measured to detect and quantify the target analyte. They provide a rapid, non-invasive, sensitive, and specific alternative

to existing methods. Bioluminescent bioreporters can be used to determine effects of chemicals on organisms and their bioavailability and to differentiate living pathogens from those which are dead or VBNC.

Bioluminescent bioreporters have been constructed previously in our lab for detection of naphthalene (23-27), salicylate (24, 25, 28, 29), polychlorinated biphenyls (30), benzene, toluene, ethylbenzene, and xylene (BTEX) (31), trichloroethylene (32), polycyclic aromatic hydrocarbons (33, 34), 2, 4-dichlorophenoxyacetic acid and 2,4-dichlorophenol (35), phenol (36), and for toxicity monitoring in biological wastewater treatment systems (37). These systems used *Vibrio fischeri lux* genes as reporter genes. Integrated circuit luminometers have been developed to measure and record the light generated by bioreporters. They are called bioluminescent bioreporter integrated circuits (BBICs) (38). The BBIC is composed of a photodetector and a signal processor which are contained in a 1cm³ area. While the photodetector captures light, the signal processor digitizes and transmits it to a data receiver. This is a mobile unit in a hand-held format. The bioluminescent bioreporter interfaced with the BBIC is an ideal system for monitoring of different environments for chemicals and pathogens. It is a small and portable self-sustained device which allows for remote sensing. Testing is performed by exposing the device to the sample with no requirement for trained personnel. It is a cheap and low power drain system. All these capabilities of the system make it suitable for continuous and remote monitoring of different environments in real-time for any analyte of interest.

Infectious diseases caused by the contamination of food and environment by bacterial pathogens have been on the rise recently (1, 39-43). An important route of

contamination is transfer of pathogens including *Salmonella* from animal and human feces to soil as a result of poorly treated sewage sludge applications on the land (39, 40, 44-48). Pathogens are eventually transported to water from soil (39). Contaminated water may infect humans and animals or contaminate agricultural products (39, 40, 45, 49-52). Pathogens which become airborne after waste application and agricultural irrigation may also cause infections (50-53). Among them is *Staphylococcus aureus* which can be a lower human colon organism (53). *Staphylococcus aureus* and other opportunistic pathogens are also found on surfaces and as airborne in health care centers, causing nosocomial infections (43, 54-57). Therefore, there is a need for detection methods to monitor environments such as soil, water, and surfaces and agricultural products. Another environment that needs to be monitored for pathogens is within the spacecraft. Spacecrafts are especially susceptible to contamination due to use of reconditioned air and recycled water and the closed environment (58, 59). Opportunistic pathogens, including *S. aureus*, have been detected frequently in space flights from various surfaces of the craft and astronauts (58-60). This may pose serious health risks to the astronauts whose immune systems are weakened in space (58, 61). Contamination in spacecrafts may also lead to allergic reactions, food spoilage, release of toxins, infection of plants, and deterioration of structural materials (58, 62).

The aim of this study was to construct a bioluminescent bioreporter system for detection of bacterial pathogens in various environments by applying the same principles used for developing previous pollutant monitoring bioreporters. The system takes advantage of the high specificity of the bacteriophage for their hosts and *V. fischeri* quorum sensing *lux* system. Unlike previous bacteriophage-based bioluminescent

bioreporters, this system utilizes all components of the *V. fischeri lux* operon (see below). *luxI* is carried by the recombinant phage whose host is the target pathogen while the rest of the *lux* operon genes are inside a recombinant bioreporter cell line. The bioreporter cannot generate light without *luxI*-synthesized acylhomoserine lactones (AHLs). The recombinant phage and bioreporter are ultimately designed to be integrated in a BBIC (38). When the system is exposed to a sample contaminated with the target pathogen, AHL, the product of LuxI, is produced upon infection of pathogen by the recombinant phage. AHL diffuses into the bioreporter cell where it induces *lux* genes, which results in light production. Eventually, a BBIC will measure and transmit the signal obtained. The bioreporter cell was constructed previously and tested for *Escherichia coli* monitoring with successful results (63). This study aims to construct *luxI* recombinant phages that will be used for detecting *S. aureus* and *Salmonella*, separately. In the end, these will be self-sufficient and fully-automated systems without the need for addition of any exogenous substrates, use of laborious methods, and trained personnel. The mobile format does not require power or optic cables with transmission of data to a receiver, making them suitable for field use. They will be highly specific and sensitive devices, capable of monitoring various environmental samples and food for *Salmonella* and *S. aureus* continuously with remote sensing.

Chapter 2 provides information about the physiological, biochemical, and genetic aspects of quorum sensing and bioluminescence in *V. fischeri*, *S. aureus*, *Bacillus subtilis*, *Salmonella*, and *E. coli*. It includes a literature review for previous bioluminescent bioreporters for chemical and pathogen detection and describes details of the system developed for this work and difference from previous systems. General

information about the bacteriophage and contamination problems with *Salmonella* and *S. aureus* are also mentioned in this chapter. Chapters 3 and 6 discuss the details of the methods and experiments performed to develop appropriate vector and expression systems for bacteriophage-based bioluminescent bioreporters for monitoring *S. aureus* and *Salmonella*, respectively. Results obtained from these experiments are given in chapters 4 (*S. aureus*) and 7 (*Salmonella*). Chapters 5 and 8 discuss the *S. aureus* and *Salmonella* results, respectively, and present suggestions for their explanation.

Results obtained from this study point to some conclusions listed below:

- Expression of *V. fischeri luxI* in *S. aureus* is problematic because of reasons other than the promoter and ribosomal binding site (RBS) compatibility. These reasons are unknown at the present time since there is no other study of *V. fischeri luxI* expression in *S. aureus* in the literature. They may include *luxI* mRNA or protein instability; or the presence of acylhomoserine lactonases or AHL antagonists in *S. aureus*. Further studies are needed to determine the cause of this problem.
- Homologous recombination appears to be an efficient and significant mechanism used by *Salmonella* phage P22 frequently during the infection.
- Recombinant *Salmonella* phage P22 may be infecting *E. coli*, *Klebsiella pneumoniae*, and *Klebsiella oxytoca* although the only host stated for wild-type P22 phage in the literature is *Salmonella*. However, the nature of this possible infection is not clear. It may be following a pseudolysogenic pathway. Further studies are required to determine the certainty and nature of possible infections of *E. coli*, *K. pneumoniae*, and *K. oxytoca* by P22.

- If further tests confirm infection of *E. coli*, *K. pneumoniae*, and *K. oxytoca* by P22, the recombinant phage P22luxI developed for *Salmonella* monitoring in this study may be used to test different bacterial strains (especially those belonging to enterobacteria) for P22 infection which does not lead to lysis. Also, principles used here to construct P22luxI can be applied to other phage strains for development of similar recombinant constructs which can be used for tests of phage infection that does not result in lysis.

CHAPTER II

LITERATURE REVIEW

Quorum sensing

Quorum sensing, first described by Nealson and colleagues and Eberhard (64-67), is the production, release and subsequent detection of signal molecules called autoinducers by bacteria, indicative of population density. As the population of bacteria grows, cells secrete autoinducers into the environment. Therefore, the extracellular concentration of autoinducer is correlated with the population density. When the autoinducer reaches a critical threshold level, bacteria respond by altering gene expression. This allows bacteria to perform certain cell functions only when they reach a sufficiently large population, a quorum. Some of the functions controlled by quorum sensing are virulence, competence, biofilm formation, conjugation, antibiotic production, motility, sporulation and bioluminescence (68).

There are three main classes of quorum sensing that use different types of autoinducer molecules: the LuxI/R systems of Gram-negative bacteria that utilize AHLs, the oligopeptide two-component systems of Gram-positive bacteria, and the autoinducer-2 (AI-2) system widespread among Gram-negative and Gram-positive bacteria which use a furanosyl borate diester as the autoinducer.

LuxI/R quorum sensing is common among α , β , and γ subclasses of Proteobacteria (69, 70). This system has two major components: a *V. fischeri* LuxI homologue that synthesizes the AHL autoinducer and a *V. fischeri* LuxR homologue that

binds AHL (69-76). The autoinducer diffuses into and out of the cell or is transported across the cell membrane. When its concentration reaches a threshold level, the LuxR type receptor protein binds AHL. The resulting complex controls expression of quorum-sensing-regulated genes. LuxI/R systems have been identified in over 70 species of Gram-negative bacteria although there are no Gram-positive bacteria known that produce AHL (69, 73-75).

Gram-positive bacteria use modified oligopeptides as autoinducers. Small linear or cyclic peptides are produced in the cytoplasm as precursors (72, 75). Later, they are modified and transported into the environment where they interact with the membrane-bound two-component sensor kinase proteins. This interaction causes phosphorylation of the associated response regulator that changes expression of target genes.

LuxI/R and oligopeptide two-component quorum sensing systems are used for intraspecies communication (73, 75). The autoinducer can be recognized only by the bacterial species that produces it. The structure of the autoinducer produced by each bacterial species is different from that of other species and receptors can only recognize their own cognate autoinducers.

The AI-2-based quorum sensing is shared by both Gram-negative and -positive bacteria. It is a furanosyl borate diester produced by the *luxS* gene (72, 73). Homologues of *luxS* have been found in many species so this system has been implicated in interspecies communication (72, 77). However, the signaling mechanism has not been defined in most of the bacteria that carry *luxS* homologues and there are questions as to whether AI-2 is a true quorum sensing signal molecule or a metabolic side product (69, 72).

***V. fischeri*- *Euprymna scolopes* symbiosis**

Quorum sensing was first discovered and described in the bioluminescent marine bacteria *V. fischeri* and *Vibrio harveyi* (65-67). Most of the early quorum sensing research focused on *V. fischeri* which lives in a symbiotic relationship with the Hawaiian bobtail squid *Eu. scolopes* (78-80). Bacterial cells colonize the specialized light organ of the squid. *Vibrio fischeri* grow to very high cell densities (10^{10} - 10^{11} cells/ ml) in the nutrient-rich light organ (65, 81-85). When the autoinducer produced by the growing culture reaches a critical concentration inside the light organ, bioluminescence genes are induced for expression (86-88). Autoinducer concentrations inside the light organ can exceed 100 nM which is higher than the level required to induce bioluminescence with laboratory cultures (89). However, *V. fischeri* is found at low cell densities (a few cells/ml) in nutrient-limiting ocean conditions where autoinducer diffuses away and can not accumulate (82, 90). Therefore, the light organ is a primary niche in the ocean for *V. fischeri* to exist at high densities. *Euprymna scolopes* is a nocturnal animal that lives in the shallow sand flats (78, 79). It benefits from the symbiosis by using the light provided by *V. fischeri* to escape from its predators (78-80, 84, 85). In this strategy called counterillumination, the squid projects light downward to mask its shadow at night (79, 82, 84, 85, 88). It can control the amount of light emitted by *V. fischeri* by opening and closing a shutter beneath the light organ.

Bioluminescence reaction

Luminescence created during *V. fischeri* cell growth is generated by the reaction of reduced flavomononucleotide (FMNH₂), long-chain aliphatic aldehyde (RCHO), and

oxygen (91-96). This reaction produces oxidized flavomononucleotide (FMN), aliphatic acid (RCOOH) and water with the simultaneous release of excess free energy as blue-green light at 490 nm that results in bioluminescence (91, 92, 97-99).



luxA and *luxB* genes encode α and β subunits of the heterodimeric luciferase enzyme which catalyzes the reaction (86, 91, 92). The aldehyde substrate used by luciferase is converted from fatty acids by a multienzyme complex. The reductase, thioesterase and synthetase components of this fatty acid reductase complex are encoded by *luxC*, *luxD* and *luxE* genes, respectively (91, 92, 100, 101). *luxG* is thought to encode a flavin mononucleotide reductase which produces FMNH₂ substrate for luciferase (92, 102).

Organization and regulation of *lux* genes

Bioluminescence genes of *V. fischeri* are organized into two operons which are transcribed in opposite directions with a 150 bp-intergenic regulatory region between them (Figure 2-1). Structural genes, *luxA*, *luxB*, *luxC*, *luxD*, *luxE*, and *luxG*, and the regulator gene *luxI*, are located on the rightward *luxICDABEG* operon. The other operon consists of *luxR* whose product is the transcriptional activator of the *luxICDABEG* operon (86, 87, 95, 103-105). The LuxI protein is the autoinducer synthase and it produces an AHL, *N*-(3-oxohexanoyl)-L-homoserine lactone (OHHL) (86, 106, 107). The LuxR regulatory protein activates *luxICDABEG* operon transcription after binding the autoinducer (86, 103).

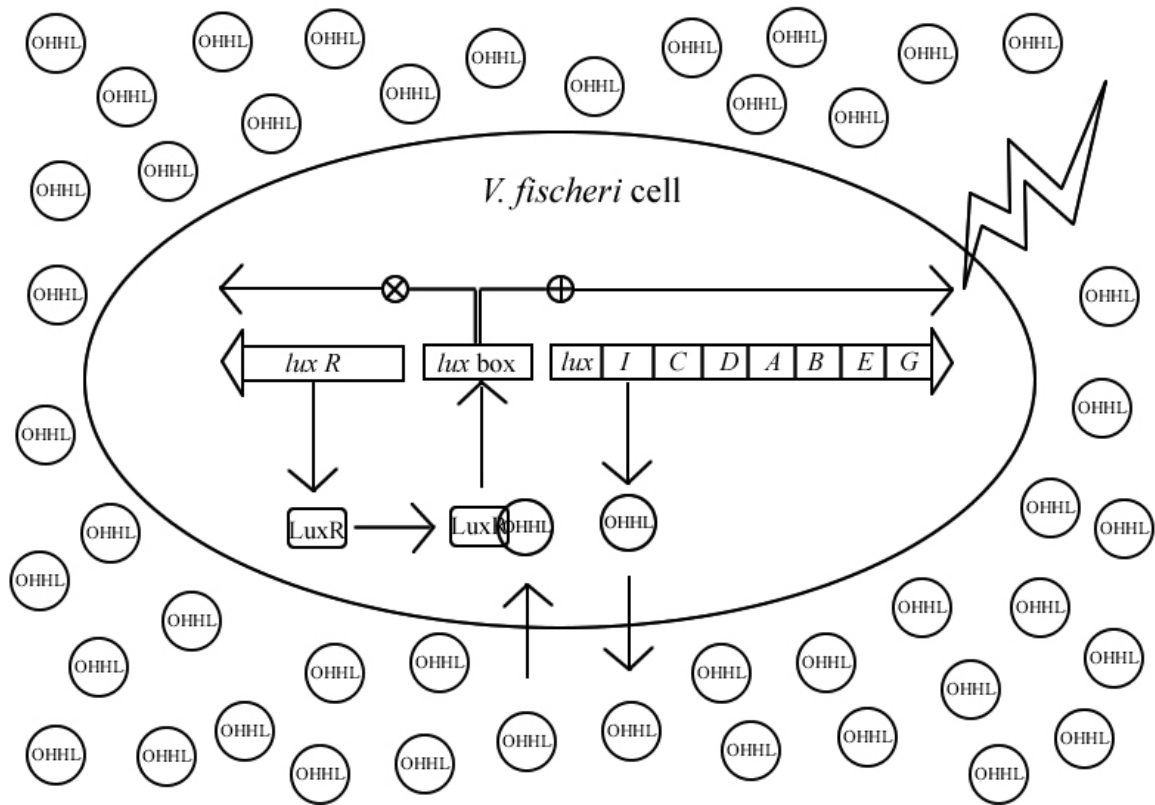


Figure 2-1. *Vibrio fischeri* Lux I/R quorum sensing system (64, 66, 67, 86, 87, 95, 103-128) (⊗ = Repression ⊕ = Induction)

When *V. fischeri* cell density is low, the *luxICDABEG* operon is transcribed weakly (Figure 2-1). Therefore, the autoinducer level is low and almost no light is produced (66, 67, 108). Since OHHL can freely diffuse in and out of the cell, intracellular and extracellular concentrations become the same (109). As the cell density increases, it accumulates in the environment. When OHHL reaches a critical, threshold concentration (10 nM) it binds to the amino-terminal OHHL-binding domain of LuxR (66, 86, 87, 110-112). The interaction induces a conformational change in the LuxR protein. This allows it to dimerise, which leads to unmasking of the DNA binding domain, carboxy-terminal (64, 112-118). The complex binds to the *lux* box which is a 20-bp inverted repeat sequence around 40 bp upstream of the *luxICDABEG* operon transcriptional start site (119-123). Binding stimulates expression of the *lux* cassette resulting in an exponential increase in both OHHL production and light generation (66, 108, 115, 124). While this creates a positive feedback loop on *luxICDABEG* transcription, it represses *luxR* expression (87, 125-128). Therefore, these loops keep light production under control at high population densities.

Other regulators of *V. fischeri* bioluminescence

Vibrio fischeri possesses two more signals that have a role in regulation of bioluminescence: *N*-octanoyl-L-homoserine lactone (C8-HSL) synthesized by AinS (129-133) and AI-2, a furanosyl borate diester, produced by LuxS (134, 135) (Figure 2-2). C8-HSL is sensed by AinR (129, 130) while AI-2 is sensed by LuxP and LuxQ (134, 135). These two signals stimulate bioluminescence by relieving the repression of LitR which is the transcriptional activator of the *luxR* operon (134, 136-138).

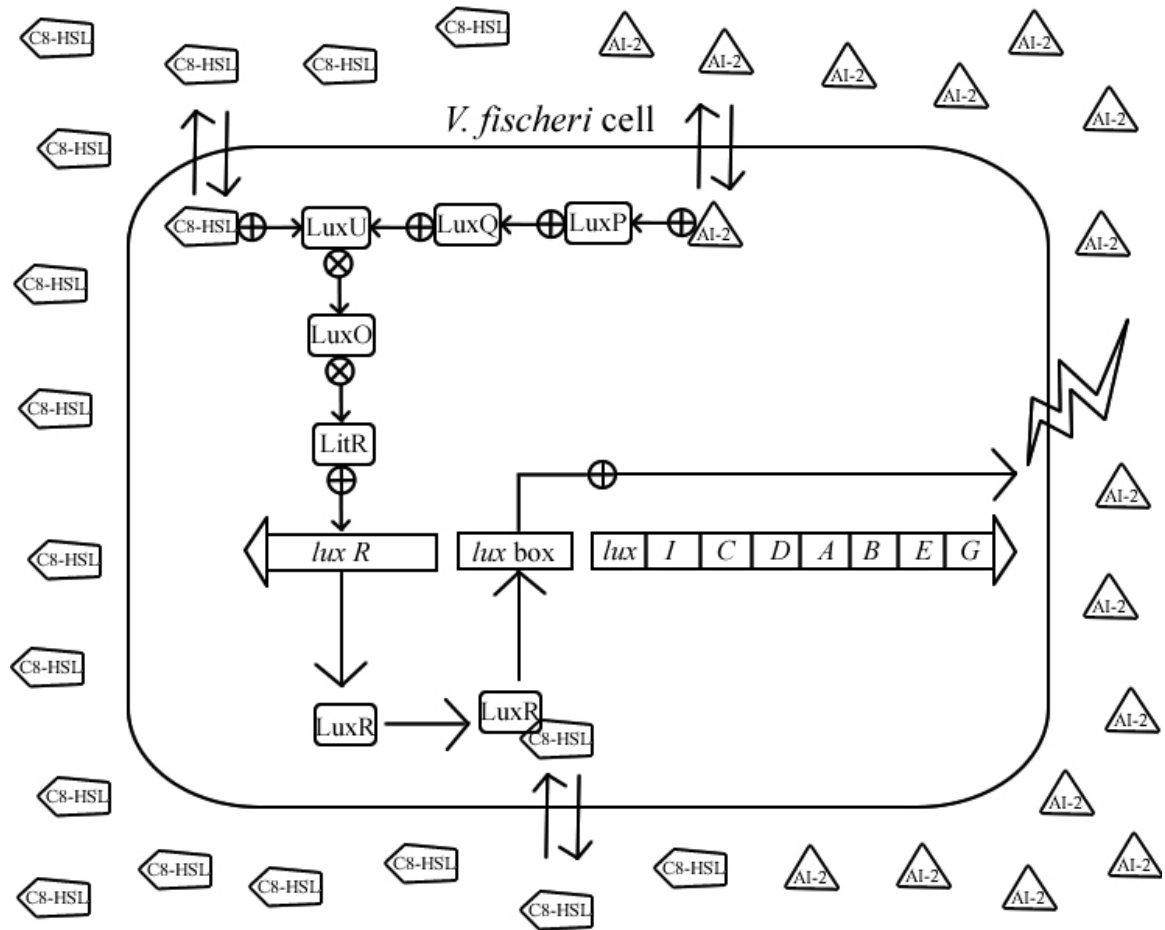


Figure 2-2. Ain S/R and Lux S/PQ quorum sensing systems in *V. fischeri* (129-140) (⊗ = Repression ⊕ = Induction)

At low cell densities ($<10^8$ cells/ml) found in the ocean, luminescence is repressed through inhibition of LitR by LuxO (134, 136-138) (Figure 2-2). When C8-HSL accumulates to a threshold level that correlates with intermediate cell densities (10^8 - 10^9 cells/ml) obtained in lab cultures and early stages of squid colonization, it induces bioluminescence partially by (i) activating a phosphorelay cascade that results in LuxO inactivation, and by (ii) binding LuxR (134, 138, 139). OHHL is at a low level to induce luminescence at this stage. C8-HSL binds its cognate receptor AinR to induce the cascade that inactivates LuxO through LuxU (134, 138, 139). This relieves repression of LitR and thus LitR stimulates expression of LuxR (136, 140). Binding of C8-HSL to LuxR causes a weak induction of *luxICDABEG* operon transcription. OHHL reaches significant amounts at high cell densities ($>10^{10}$ cells/ml) achieved only inside the light organ of the squid and binds LuxR. This causes full induction of bioluminescence (138, 139).

Although both C8-HSL and OHHL can induce bioluminescence by binding to LuxR, OHHL binding results in much higher light emission than C8-HSL binding does (Figure 2-2). Therefore, it acts as an antagonist of light induction by OHHL (131, 141). One role of C8-HSL may be to competitively inhibit premature activation of bioluminescence at low cell densities (131, 132).

AHL synthesis and structure

Quorum sensing autoinducer signals of Gram-negative bacteria are AHLs. AHLs are composed of an acyl side chain linked to a homoserine lactone ring with an amide bond. While all AHLs carry the same homoserine lactone, their acyl side chains differ in length and substitution (Figure 2-3, Table 2-1) (142-150). Acyl chains range from 4 to 14

carbons with either an oxo- or hydroxy- or no substituent at their third carbon atom. However, two AHLs with acyl chains up to 16 and 18 carbons have been found in *Rhodobacter capsulatus* and *Sinorhizobium meliloti* (151, 152). Acyl chains may also be saturated or unsaturated. 7,8-*cis*-*N*-(3-hydroxytetradecenoyl) homoserine lactone and 7,8-*cis*-*N*-(tetradecenoyl) homoserine lactone produced by *Rhizobium leguminosarum* (153, 154) and *Rhodobacter sphaeroides* (155), respectively, are two examples of AHL which carry acyl chains with double bonds. Most bacterial AHLs discovered carry an even number of carbons in their acyl chain. Pathogenic Gram-negative bacteria which do not produce AHL are *Actinobacillus pleuropneumoniae*, *E. coli*, *Haemophilus influenza*, *K. pneumoniae*, *Neisseria meningitidis*, *Salmonella* spp., *Vibrio cholerae*, *Campylobacter jejuni*, and *Helicobacter pylori* (156).

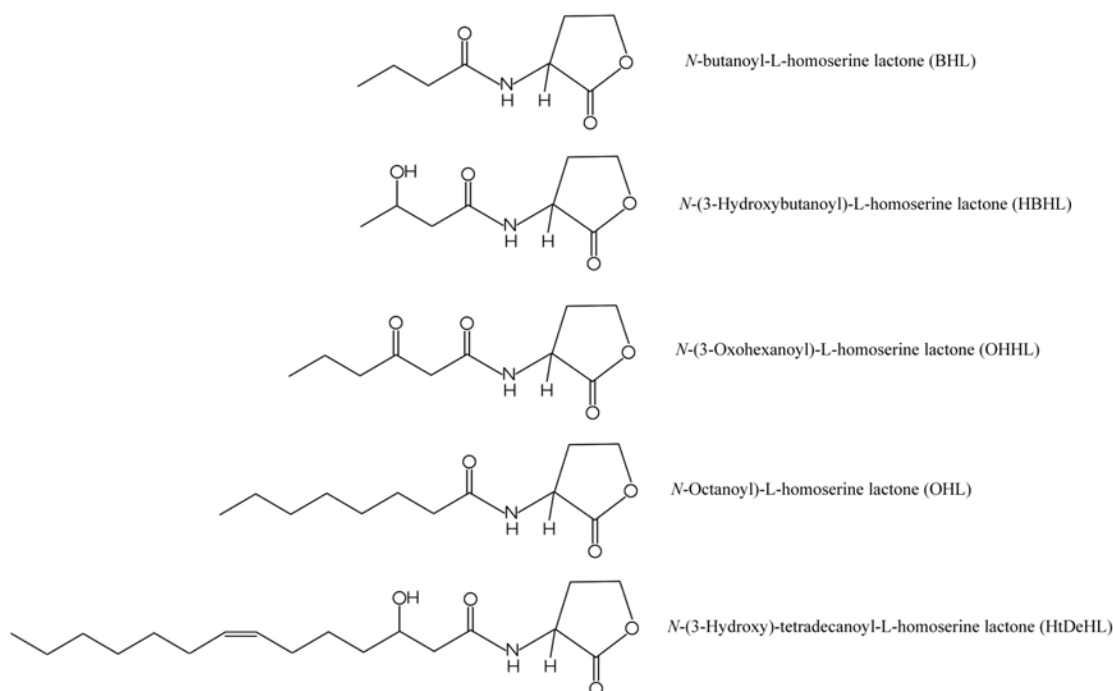


Figure 2-3. Some examples of different AHL structures (see Table 2-1 for references)

Table 2-1. AHL types in various organisms

Organism	LuxI/LuxR Homologue(s)	AHL Type	References
<i>V. fischeri</i>	LuxI/LuxR-	<i>N</i> -(3-oxohexanoyl)-L-homoserine lactone	(86, 87, 106)
<i>V. fischeri</i>	AinR/AinS	<i>N</i> -(octanoyl)-L-homoserine lactone	(129, 130)
<i>Aeromonas hydrophila</i>	AhyI/AhyR	<i>N</i> -butanoyl-L-homoserine lactone	(157)
<i>Aeromonas salmonicida</i>	AsaI/AsaR	<i>N</i> -butanoyl-L-homoserine lactone	(157, 158)
<i>A. tumefaciens</i>	TraI/TraR-TraM	<i>N</i> -(3-oxooctanoyl)-L-homoserine lactone	(159-165)
<i>Brucella melitensis</i>	Unknown	<i>N</i> -(3-oxododecanoyl)-L-homoserine lactone	(69)
<i>Burkholderia cepacia</i>	CepI/CepR	<i>N</i> -octanoyl-L-homoserine lactone	(166)
<i>Chromobacterium violaceum</i>	CviI/CviR	<i>N</i> -hexanoyl-L-homoserine lactone	(142, 167)
<i>Enterobacter agglomerans</i>	EagI/EagR	<i>N</i> -(3-oxohexanoyl)-L-homoserine lactone	(145, 168)
<i>Erwinia carotovora</i>	ExpI/ExpR, CarI/CarR, HsII/?	<i>N</i> -(3-oxohexanoyl)-L-homoserine lactone	(168-174)
<i>Erwinia chrysanthemi</i>	ExpI/ExpR	<i>N</i> -(3-oxohexanoyl)-L-homoserine lactone	(175, 176)
<i>E. chrysanthemi</i>	Unknown	<i>N</i> -decanoyl)-L-homoserine lactone	(175)
<i>Erwinia stewartii</i>	EsaI/EsaR	<i>N</i> -(3-oxohexanoyl)-L-homoserine lactone	(177)
<i>E. coli</i>	Unknown/SdiA	Unknown	(178-181)
<i>Pantoea stewartii</i>	EsaR/EsaI	<i>N</i> -(3-oxohexanoyl)-L-homoserine lactone	(177, 182)
<i>Pseudomonas aereofaciens</i>	PhzI/PhzR	<i>N</i> -hexanoyl-L-homoserine lactone	(183-185)
<i>Pseudomonas aeruginosa</i>	LasI/LasR	<i>N</i> -(3-oxododecanoyl)-L-homoserine lactone	(186-191)
<i>P. aeruginosa</i>	RhlI/RhlR	<i>N</i> -butyryl-L-homoserine lactone	(150, 192-197)
<i>Ralstonia solanacearum</i>	SolI/SolR	<i>N</i> -hexanoyl-L-homoserine lactone, <i>N</i> -octanoyl-L-homoserine lactone	(198)

Table 2-1. Continued

Organism	LuxI/LuxR Homologue(s)	AHL Type	References
<i>R. leguminosarum</i>	RhlI/RhlR	<i>N</i> -hexanoyl-L-homoserine lactone	(153, 199, 200)
<i>R. leguminosarum</i>	CinI/CinR	<i>N</i> -(3-hydroxy-7- <i>cis</i> -tetradecenoyl)-L-homoserine lactone	(153, 154, 199, 201, 202)
<i>R. sphaeroides</i>	CerI/CerR	7,8- <i>cis-N</i> -(tetradecanoyl)-L-homoserine lactone	(155)
<i>Salmonella typhimurium</i>	Unknown/SdiA	Unknown	(203)
<i>Serratia liquefaciens</i>	SwrI/Unknown	<i>N</i> -butanoyl-L-homoserine lactone	(204, 205)
<i>Vibrio anguillarum</i>	VanI/VanR	<i>N</i> -(3-oxodecanoyl)-L-homoserine lactone	(206)
<i>V. harveyi</i>	LuxM/LuxN-LuxO-LuxR	<i>N</i> - β -(hydroxybutyryl)-L-homoserine lactone	(207-211)
<i>V. harveyi</i>	Lux?/LuxPQ-LuxO-LuxR	<i>N</i> - β -(hydroxybutyryl)-L-homoserine lactone	(212)
<i>Yersinia enterocolitica</i>	YenI/YenR	<i>N</i> -hexanoyl-HSL, <i>N</i> -(3-oxohexanoyl)-L-homoserine lactone	(213)
<i>Yersinia pestis</i>	YpeR/YpeI	Unknown	(69)
<i>Yersinia pseudotuberculosis</i>	YpsI/YpsR	<i>N</i> -(3-oxohexanoyl)-L-homoserine lactone	(214)
<i>Y. pseudotuberculosis</i>	YtbI/YtbR	<i>N</i> -octanoyl-L-homoserine lactone	(214)

The LuxI protein and its homologues are responsible for synthesis of AHLs. LuxI-type proteins have the ability to produce AHLs in heterologous hosts as determined by studies on various bacteria transformed with *luxI* and its homologues (87, 159, 186, 192, 213). This points to the fact that AHL substrates are from cellular pools of metabolites. The *V. fischeri* AHL was the first AHL discovered. It was identified as *N*-(3-oxohexanoyl) homoserine lactone or OHHL (Figure 2-3, Table 2-1) (106). *Vibrio fischeri* crude extracts were shown to synthesize OHHL in the presence of *S*-adenosylmethionine (SAM) and 3-oxo-hexanoyl-CoA (124). Later studies found that SAM (107, 124, 159, 215-219) and acyl-acyl carrier proteins (acyl-ACPs) (107, 159, 217-220) were substrates for LuxI-directed AHL synthesis. The homoserine lactone ring of AHL is derived from a common cellular amino acid substrate, SAM (221), while the acyl side chain is obtained from fatty acid biosynthesis metabolite, acyl-ACP. 3-oxohexanoyl-ACP is the specific acyl-ACP used for synthesis of OHHL.

Synthesis of AHL starts with binding of SAM to the active site of the LuxI enzyme (Figure 2-4) (107, 218, 222). The acyl side chain of the appropriate acyl-ACP (3-oxohexanoyl-ACP in the case of OHHL) forms an amide bond with SAM after a nucleophilic attack on the C1 position of the acyl-ACP by the amino nitrogen of SAM. Another nucleophilic attack, this time on the γ carbon of SAM by the SAM carboxylate oxygen, causes lactonization of the intermediate. This results in production of AHL and release of 5'-methylthioadenosine (MTA), a toxic byproduct. MTA is cleaved by Pfs, a nucleoside enzyme, into adenine and methylthioribose (MTR) which are not toxic (107, 218, 222).

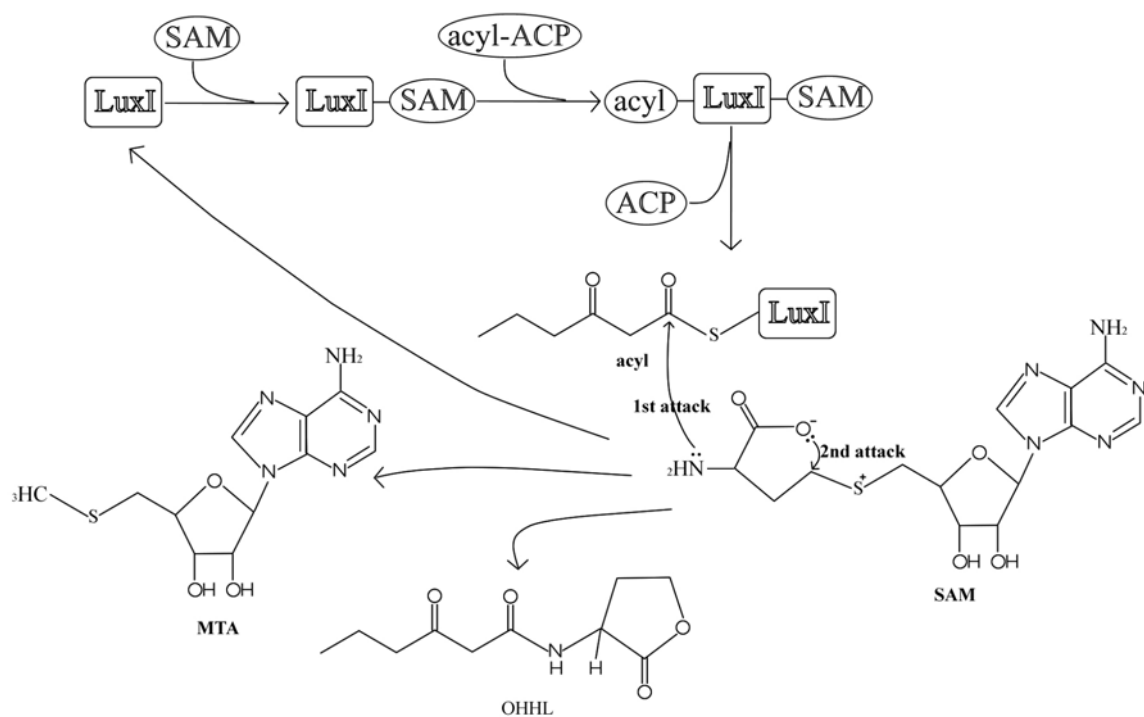


Figure 2-4. Synthesis of OHHL (107, 218, 222)

LuxI and its homologues change from 194 to 226 amino acids in size (149). When their protein sequences are compared, <5% similarity is detected (223, 224). Although LuxI-type proteins produce AHL molecules with specific acyl side chains, the difference between protein sequences can not be used to determine the type of AHL synthesized by a particular sequence (223, 224). Comparison of protein sequences detected ten conserved amino acids with seven of them charged, mostly in the amino-terminal region (149, 225). Furthermore, mutational studies on LuxI-type proteins identified conserved charged residues in the amino-terminal half (LuxI residues 25-70) (225, 226). Most mutations resulted in production of nonfunctional LuxI proteins and five of the amino acids mutated are conserved in all LuxI-type proteins (LuxI Arg25, Glu44, Asp46, Asp49 and Arg70) (226). These results suggest that highly conserved amino-terminal regions may be the parts responsible for functions consistent in all LuxI-type proteins while the carboxy-terminal regions may have roles in recognition of specific acyl side chains of acyl-ACPs (226).

LuxI-type proteins synthesize specific AHLs which are used for intraspecies communication of bacterial species that produce them. Some species produces more than one type of AHL although only one acts as the main quorum sensing signal (107, 149, 150, 152, 218). Secondary AHLs produced by LuxI-type proteins act as competitors of the main AHL signal (131, 141, 227, 228). These AHLs bind the LuxR-type protein in place of the main AHL without activating the protein. The specificity of the AHL molecule originates from its acyl side chain, so it has been suggested that recognition of the appropriate acyl-ACP by the LuxI-type protein creates this specificity in the production of AHL (149). Structural studies on EsaI in *P. stewartii* and LasI in *P.*

aeruginosa showed that the size of the cavity which interacts with the acyl side chain may be responsible for the selectivity of LuxI-type proteins for certain acyl-ACPs (222, 229). The cavity of LasI which produces a longer AHL is larger than the cavity of EsaI which synthesizes a shorter AHL. However, the specificity in quorum-sensing systems is also provided by binding of LuxR-type proteins only to their cognate AHLs (230-232).

Short-chain AHLs like OHHL of *V. fischeri* can freely diffuse across the cell membrane while long-chain AHLs (e.g., 12-carbon AHL of *P. aeruginosa*) need to be transported actively with efflux or influx pumps (109, 233, 234). Larger AHLs have higher hydrophobicity because of their longer hydrophobic acyl side chains, decreasing their permeability through cell membranes. Short-chain AHLs which usually contain a 3-oxo- or 3-hydroxy group have low octanol/water partition coefficients (235). The presence of the hydrophilic homoserine lactone in the structure of AHLs in addition to the hydrophobic acyl side chain makes them capable of existing in both cell membrane and aqueous intracellular and extracellular media (236).

Fatty acid biosynthesis (source of AHL acyl side chains)

Fatty acids are produced by fatty acid biosynthesis (FAB) pathways which are divided into FAB I and FAB II. Type I pathway is found in mammals. It is a single protein with separate domains that catalyze different reactions of the pathway (237). Type II, or dissociated pathway, used by bacteria, plants, and parasites is composed of discrete proteins. Each protein catalyzes a single reaction in the pathway (238-241). Although different structurally, FAB I and FAB II are responsible for the same chemical reactions (242). FAB II pathway does not only produce fatty acids but also a variety of

cellular metabolism precursors. Fatty acids are components of membrane phospholipids (243-246). Intermediates of the FAB pathway are used in synthesis of lipoic acid, vitamins (247, 248), polysaccharides (249), adenylate cyclase, hemolysin (250), and quorum sensing AHL autoinducers (107, 159, 219).

Gram-negative bacteria produce straight-chain saturated and unsaturated fatty acids at different lengths via FAB II pathway. The *E. coli* pathway is the most-studied type II system and serves as the model system for FAB II research in other organisms. The following is a summary of the *E. coli* straight-chain FAB reaction (241, 246, 251, 252):



The acyl carrier protein (ACP) is an important cofactor of this pathway that transfers the acyl side chain from enzyme to enzyme during FAB (241, 246, 253). Precursors for the pathway are provided by cellular acetyl-CoA supply (241). Individual steps of the pathway are explained below (see also Figure 2-5):

- 1- The first reaction catalyzed by a multiunit enzyme complex, acetyl-CoA carboxylase (ACC), produces malonyl-CoA from acetyl-CoA and CO₂ (254, 255).
- 2- Malonyl-CoA:ACP transacylase (FabD) transfers the malonate group from malonyl-CoA to ACP to form malonyl-ACP (241, 256).
- 3- FAB starts with condensation of malonyl-ACP with acetyl-CoA. This reaction catalyzed by β -ketoacyl-ACP synthase III (FabH) releases β -ketobutyryl-ACP and CO₂ (238, 251, 257-263).

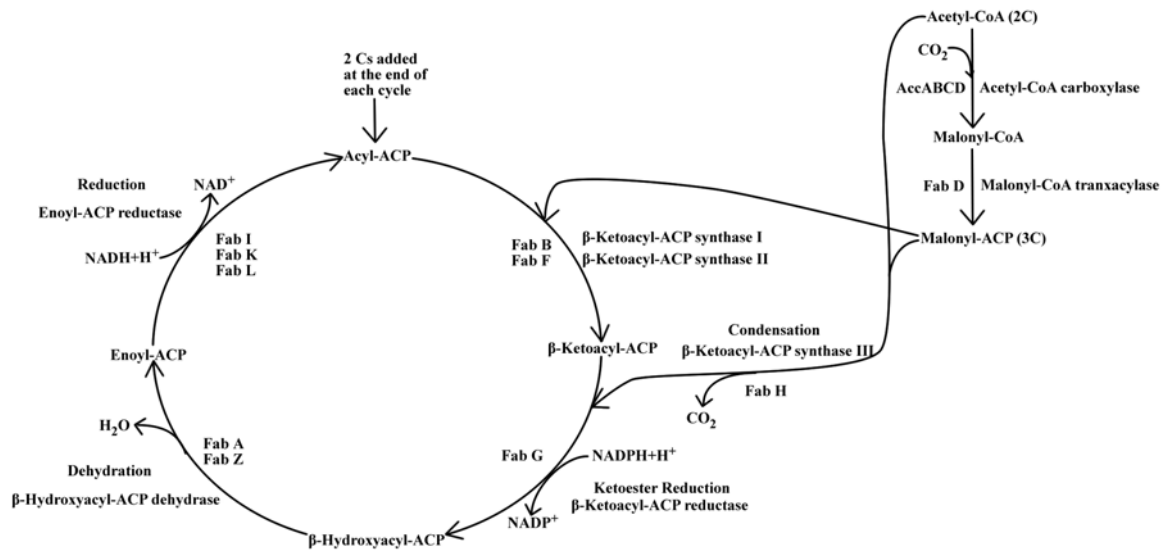


Figure 2-5. FAB II pathway (238, 241, 245, 251, 254-287)

4- β -ketobutyryl-ACP enters the elongation cycle which is catalyzed by four enzymes.

The acyl side chain is elongated by two carbons with each cycle.

a- The keto group is reduced to a hydroxyl group by β -ketoacyl-ACP reductase (FabG) in the NADPH-dependent first reaction of the cycle (264, 265).

b- The resulting β -hydroxyacyl-ACP is dehydrated by β -hydroxyacyl-ACP dehydratase (FabA or FabZ) to form an enoyl-ACP (266-270).

c- The cycle is completed by production of an acyl-ACP after reduction of the double bond in enoyl-ACP by NADH-dependent enoyl-ACP reductase (FabI, FabK, or FabL) (271-274).

5- The product formed is condensed with malonyl-ACP by β -ketoacyl-ACP synthase (KAS) I or II (FabB or FabF, respectively) to extend the acyl-ACP by two carbons. Elongation cycles are repeated until the target acyl chain length is reached (245, 275-287).

FAB II pathway can also synthesize unsaturated fatty acids (UFAs). FabA isomerizes *trans*-2-decenoyl-ACP to *cis*-3-decenoyl-ACP at the 10-carbon intermediate, preserving the double bond in the acyl chain (266, 267, 269, 270, 288-293). The *cis*-3-decenoyl-ACP is elongated by FabB-catalyzed condensation with malonyl-ACP to form UFAs as final products (266, 279, 288, 290, 294-298).

Genes encoding FAB II pathway enzymes are highly conserved among bacteria. Homologues of *E. coli* pathway genes can be identified in genomes of other species by a simple BLAST search (242, 299). However, there are some differences between the type II pathways of Gram-positive and -negative bacteria. Gram-positive bacteria make their UFAs by desaturation of saturated fatty acids (300-302). Furthermore, many Gram-positive bacteria possess branched-chain fatty acids as the largest component of their fatty acid pool while most Gram-negative bacteria have mainly straight-chain fatty acids (252, 303-305). Bacterial genera which have branched-chain fatty acids as the major fatty acid include *Staphylococcus* and *Bacillus* (252, 305). The percentage of fatty acids which are branched is 81% in *S. aureus* and 95% in *B. subtilis* (252). This percentage is lower than 20% in *E. coli* and *Salmonella* which have straight-chain fatty acids in high amounts (252). Type II pathway is used for synthesis of all bacterial fatty acids. The determining factor for production of straight- or branched-chain fatty acids during type II pathway is substrate specificity of the elongation-condensing FabH enzyme (70, 238, 251, 252, 262, 303, 306, 307). Although the amino acid sequence of the FabH active site is conserved among bacteria and all FabH enzymes have similar catalytic mechanisms, there are significant differences in substrate specificities of FabH from Gram-negative and -positive bacteria. FabH from branched-chain fatty acid-synthesizing bacteria show broad

substrate specificity whereas FabH from bacteria with mostly straight-chain fatty acids are highly selective for acetyl-CoA (70, 238, 251, 252, 257, 259, 262, 263, 303, 305-317). FabH with broad substrate specificity can use 2-to-6-carbon straight chain and branched-chain acyl-CoAs (70, 252, 303, 306, 307, 309-312, 314-318). Branched-chain fatty acids contain either iso- or anteiso-methyl branches (252, 303, 309-312, 318-320). α -ketoisocaproate, α -keto- β -methylvalerate, and α -ketoisovalerate act as precursors for synthesis of iso-odd, anteiso-odd, and iso-even fatty acids, respectively (252).

Escherichia coli FabH which can not utilize substrates with chains longer than 4 carbons and branched-chain CoAs especially prefers acetyl-CoA. Thus, *E. coli* can only synthesize straight-chain fatty acids (238, 251, 257-259, 261-263, 303, 304, 308, 317).

There are two homologues of FabH in *B. subtilis*: FabH1 and FabH2. *B. subtilis* FabH1 is 45% identical and 56% similar to *E. coli* FabH, and *B. subtilis* FabH2 is 38% identical and 48% similar to *E. coli* FabH. However, unlike *E. coli* FabH, *B. subtilis* FabH homologues exhibit high activity with 4-to-8-carbon straight-chain acyl-CoA and all branched-chain acyl-CoA substrates while they are less active with acetyl-CoA. *B. subtilis* FabH1 and FabH2 expression in *E. coli* lead to the production of 17-carbon branched-chain fatty acids (252, 303, 307, 309-312, 314, 315, 318-320).

The *S. aureus* membrane is made of 80% branched-chain fatty acids (70, 252, 316, 317). *Staphylococcus aureus* FabH can use 4-to-6-carbon straight- and branched-chain acyl-CoA substrates to make both straight-chain and branched-chain fatty acids. The *S. aureus* FabH activity order for various acyl-CoA substrates was determined as follows: isobutyryl-CoA>hexanoyl-CoA>butyryl-CoA>isovaleryl-CoA>>acetyl-CoA. In contrast, *E. coli* FabH showed the lowest activity with the same substrates except for

acetyl-CoA. The *S. aureus* FabH amino acid sequence has 57, 40, and 34% identity with FabH proteins of *B. subtilis*, *E. coli*, and *Mycobacterium tuberculosis*, respectively. The crystal structure of *S. aureus* FabH is similar to the *E. coli* FabH structure; and amino acid sequences of *S. aureus* and *E. coli* FabH acyl chain binding pockets are the same. In spite of the similarity between structures and amino acid sequences of two FabH, their binding pocket sizes are different. Acetyl- or propionyl-CoA can fit into the small *E. coli* FabH pocket. The *S. aureus* FabH pocket, which is larger, can accept 4-to-6-carbon straight- and branched-chain acyl-CoA substrates while exhibiting low activity with shorter substrates (70, 252, 316, 317). Other enzymes of the FAB II pathway are not selective for straight- or branched-chain fatty acids. All can use both straight- and branched-chain acyl-ACPs (252, 303).

There are two more isoforms of elongation condensing enzymes other than FabH in *E. coli* FAB II pathway: FabB and FabF. FabH catalyzes only the first condensation reaction between acetyl-CoA and malonyl-ACP, whereas FabB and FabF are responsible for elongation of the fatty acid by condensing acyl-ACP substrates with malonyl-ACP. FabB can catalyze condensations up to 10-carbon acyl-ACP while FabF can catalyze conversion of 16-carbon palmitoleic acid to 18-carbon *cis*-vaccenic acid. Amino acid sequences of FabB and FabF are 40% identical and do not have high sequence homology with FabH. FabB, FabF, and FabH have similar structures but there are significant differences between active sites of FabH and Fab/F. Gram-positive bacteria contain FabH and either FabB or FabF as isoforms of elongation condensing enzymes. FabB/F are highly conserved among bacteria, being essential enzymes for the FAB II pathway (238, 245, 251, 257-261, 263, 275-287, 296-299, 303, 321-324).

There are two isoforms of elongation dehydratases in *E. coli*: FabA and FabZ. FabA not only acts as the dehydratase during the elongation cycle but also isomerizes *trans*-2- to *cis*-3- to add a double bond into the 10-carbon acyl-ACP to produce UFAs. FabA is essential for UFA synthesis in Gram-negative bacteria and found only in the γ subdivision of Proteobacteria. Unlike FabA, FabZ has a role in dehydration but not in isomerization. Gram-positive bacteria contain only the FabZ isoform of the dehydratase (266-270, 288-295, 299).

FabI, FabK, and FabL are the three isoforms of bacterial enoyl-ACP reductases which regulate the rate of FAB. Each bacterial species has different isoform(s). FabI is found in *E. coli* and *M. tuberculosis* (271, 274, 325-331). Gram-positive *Streptococcus pneumoniae*, *Enterococcus faecalis*, *Enterococcus faecium*, and Gram-negative *Pseudomonads* have the FabK isoform (273, 299). *Staphylococcus aureus* contains only FabI, whereas *B. subtilis* possesses both FabI and FabL (272, 299, 332). *Bacillus subtilis* and *S. aureus* FabI are structurally very similar to *E. coli* FabI (272, 303, 332). *Staphylococcus aureus* FabI protein sequence is 48% identical to *E. coli* FabI sequence (332). Both have the same active sites and their substrate activities are highly similar (332). *Staphylococcus aureus* FabI which substituted *E. coli* FabI was shown to be functional (332).

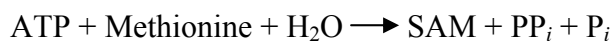
The rest of the FAB II enzymes are highly conserved among bacteria and have single isoforms. Domains of ACPs which transport the growing fatty acid chain from enzyme to enzyme during FAB can be exchanged between different organisms. Binding sites for FAB intermediates and enzymes are conserved among over a hundred ACP protein sequences. ACP proteins from different bacterial species are also structurally very

similar (242, 246, 253, 333-356). ACC catalyzes the first reaction of the fatty acid synthesis which is the rate-limiting step in the FAB II pathway (254, 255). The *S. aureus* and *E. coli* ACC structures show 52% sequence identity and both have a small, zinc-binding region which has an acetyl-CoA binding site (255). The *fabG* and *fabD* genes are found in the genomes of all bacteria sequenced and their amino acid sequences are all highly similar (256, 264, 265, 299, 325-331, 357-360).

Some FAB II pathway genes are clustered together in the *E. coli* genome in the order, *fabH-fabD-fabG-acpP-fabF*. The rest of the genes are dispersed throughout the chromosome. *Salmonella typhimurium* was determined to have the same cluster of genes in the identical order in a study (264). The sequence of the *S. typhimurium* cluster of *fab* genes was 85% identical to the *E. coli* cluster. Presumed protein sequences from the *S. typhimurium* cluster were found to contain the same number of residues and to have 90% identity to the *E. coli* cluster of Fab sequences. A 55-bp deletion in *S. typhimurium acpP* promoter region was the only difference between clusters of the two organisms. This deletion has been suggested to cause a difference in transcription of *S. typhimurium acpP* compared to *E. coli acpP*. *Salmonella typhimurium* and *E. coli* FAB II pathway proteins are interchangeable since they are identical (261, 264, 361).

AHL substrate SAM

SAM is synthesized from methionine and ATP by *S*-adenosylmethionine synthetase (ATP:L-methionine *S*-adenosyltransferase, EC 2.5.1.6) (362-387) which is encoded by the *metK* gene in *E. coli* (388-394) as shown below:



SAM levels in the cell are retained by a cycle of reactions which are a part of methionine biosynthesis metabolism (Figure 2-6) (395, 396). The cycle starts with a reaction where *S*-adenosylhomocysteine, which is created by SAM-dependent methylation reactions, is hydrolyzed to form adenosine and homocysteine. Homocysteine is converted to methionine using the methyl group from methyltetrahydrofolate by methionine synthase. Methionine synthase needs to be activated by SAM to mediate this reaction. Methionine and ATP are used to generate SAM in the final reaction of the cycle.

SAM is the major methyl donor for a wide variety of biological reactions in both prokaryotic and eukaryotic cells (Figure 2-6) (363) and the second most used enzyme substrate after ATP (397). Molecules which are methylated by SAM include RNA (398) and DNA (389, 399, 400) for modulation of transcription and translation, norepinephrine for production of epinephrine (401), membrane phospholipids (401), and proteins (402). SAM is also the donor of the aminopropyl group for synthesis of polyamine (399, 403, 404) and spermidine (405), and the amino donor for the synthesis of biotin (406). It is used in the activation of free radical enzymes (407) and endonucleases of *E. coli* type I restriction and modification systems (408-411). SAM has a role in generation of cyclopropane fatty acids from UFAs in *E. coli* (412) and acts as the corepressor of methionine biosynthesis in *E. coli*, *S. typhimurium*, and Gram-positive bacteria (221, 413-417). Finally, the homoserine lactone ring for the quorum sensing AHL autoinducer synthesis is provided by SAM (see above).

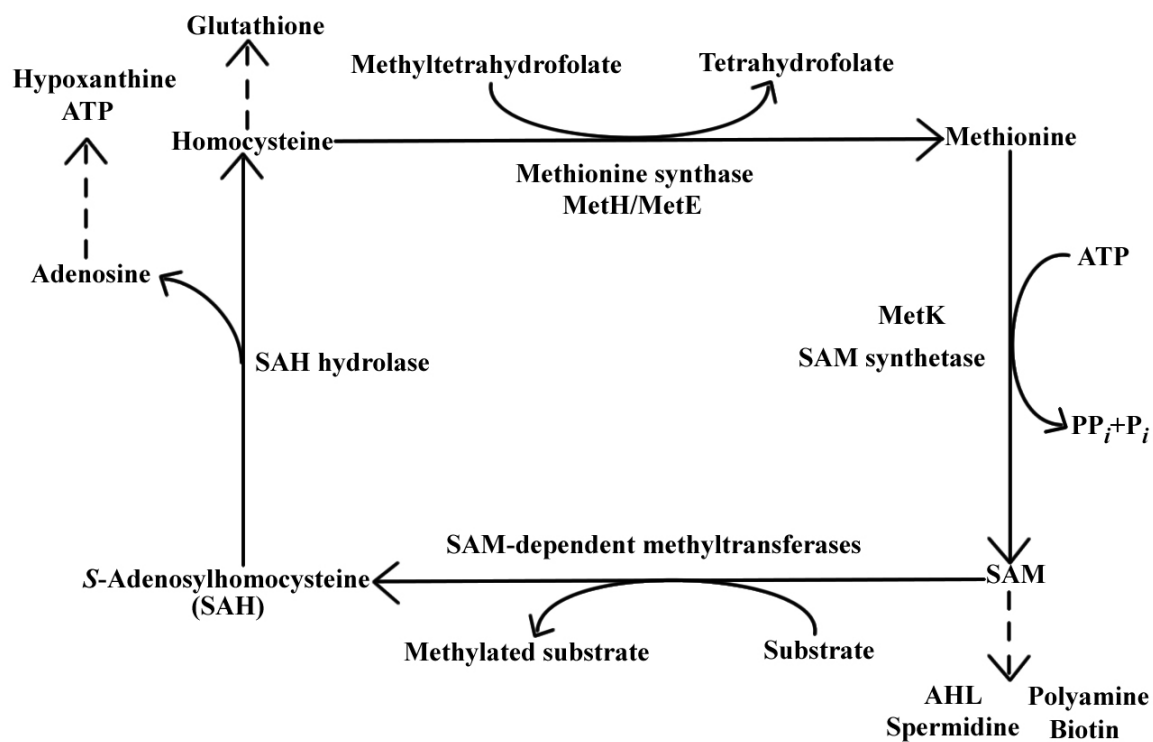


Figure 2-6. SAM metabolism (362-396, 399, 403-406)

SAM synthetase protein sequence is highly conserved among organisms (Table 2-2). The *E. coli* and *B. subtilis* enzyme sequences are 57% identical while *B. subtilis* protein sequence is 77% and 63% identical to the enzyme sequences of *S. aureus* and *S. typhimurium*, respectively (417, 418). Amino acid sequences of *E. coli* and human enzymes show 54% identity (362). Also, the active site residues of SAM synthetase are conserved in over 30 enzyme sequences reported, including the rat liver enzyme (363, 368). However, various isoforms of the enzyme have k_{cat} values different from one another up to 100-fold and the domain of the synthetase which covers the active site is the least conserved region in enzymes from different organisms (362).

Quorum sensing in Gram-positive bacteria

Gram-positive bacteria use modified oligopeptides instead of AHLs as quorum sensing signals (Figure 2-7). These peptides function by activating two component sensor/signal transduction systems. Examples of processes which are regulated by peptide-mediated quorum sensing in Gram-positive bacteria include virulence in *S. aureus* and competence and sporulation in *B. subtilis* (419-422).

In *S. aureus*, quorum sensing is regulated by *agr* (accessory gene regulator). This system controls expression of virulence factors in a density-dependent manner (420, 423-431). The *agr* system consists of two transcriptional units, RNAII and RNAIII which are controlled by promoters P2 and P3, respectively (Figure 2-8) (423, 424). RNAII unit encodes the sensor (*agrC*) and the response regulator (*agrA*) of a two-component signal transduction system and proteins (by the *agrD* and *agrB* genes) responsible for generation of the autoinducing peptide (AIP) of quorum sensing (423, 424, 432-435).

Table 2-2. Gram-positive bacteria which carry SAM synthetase gene, *metK* (413, 416)

<i>B. subtilis</i>	<i>Leuconostoc mesenteroides</i>	<i>Clostridium botulinum</i>
<i>Bacillus cereus</i>	<i>Pediococcus pentosaceus</i>	<i>Clostridium tetani</i>
<i>Bacillus halodurans</i>	<i>Lactococcus lactis</i>	<i>Clostridium difficile</i>
<i>Bacillus stearothermophilus</i>	<i>Streptococcus agalactiae</i>	<i>Thermoanaerobacter tengcong.</i>
<i>Oceanobacillus iheyensis</i>	<i>Streptococcus mutans</i>	<i>Streptomyces coelicolor</i>
<i>S. aureus</i>	<i>Streptococcus pneumoniae</i>	<i>Thermobifida fusca</i>
<i>L. monocytogenes</i>	<i>Streptococcus pyogenes</i>	<i>Chlorobium tepidum</i>
<i>E. faecalis</i>	<i>Streptococcus suis</i>	<i>Chloroflexus aurantiacus</i>
<i>Lactobacillus plantarum</i>	<i>Streptococcus thermophilus</i>	<i>Cytophaga hutchinsonii</i>
<i>Lactobacillus casei</i>	<i>Streptococcus uberis</i>	<i>Thermotogales</i>
<i>Lactobacillus delbrueckii</i>	<i>Clostridium acetobutylicum</i>	<i>Fusobacterium nucleatum</i>
<i>Oenococcus oeni</i>	<i>Clostridium perfringens</i>	<i>Deinococcus radiodurans</i>

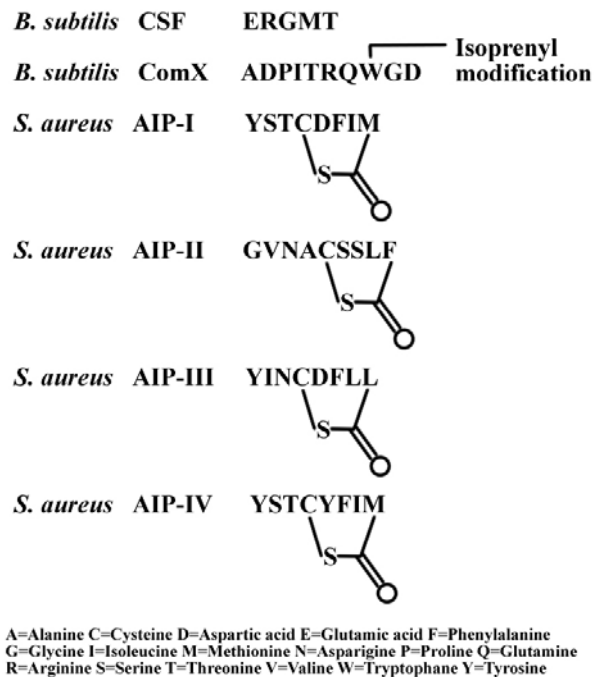


Figure 2-7. Gram-positive quorum sensing oligopeptide autoinducers (432, 436-445)

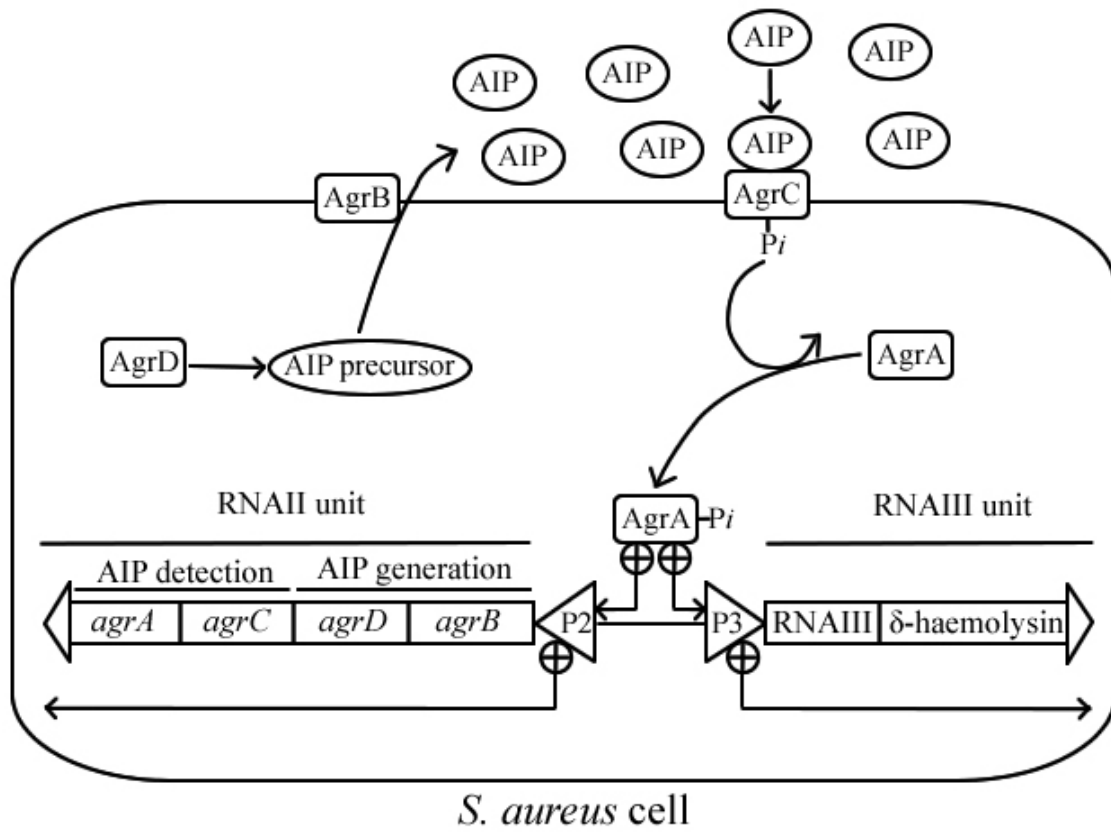


Figure 2-8. *S. aureus* quorum sensing (420, 423-435, 446-453) (⊕ = Induction)

RNAIII unit encodes δ -haemolysin and RNAIII transcript (423, 424, 427, 428, 446, 447). RNAII operon is expressed continuously at a low level. The *agrD* gene encodes a precursor protein (424, 448), which is exported into the extracellular environment by the action of the *agrB* product (449-451). AgrB cleaves the precursor during this transport forming the quorum sensing signal AIP which is a thiolactone-carrying octapeptide (424). AIP accumulates in the environment as cell numbers increase until reaching a threshold level during the transition stage from exponential to stationary growth (420). Then, AIP binds to the membrane-associated sensor protein, AgrC, which activates AgrC by autophosphorylation (423, 424, 452). Phosphate is transferred from AgrC to the cytoplasmic response regulator, AgrA (435). Phosphorylated AgrA activates RNAII and RNAIII operons (423, 424, 453). RNAII operon induction results in an autoinduction feedback loop, producing more AIP (423, 424). RNAIII transcript produced from RNAIII operon acts as the effector molecule for regulating the production of various *S. aureus* virulence factors (420, 427, 428, 430, 433, 447, 454-460).

Staphylococcus aureus AIPs are 8-9 amino acids-long and all contain a thiolactone ring which is essential for signal activity (Figure 2-7) (432, 436-439). The ring is formed by a linkage between a central conserved cysteine residue and the C-terminal carboxylic acid and is common to all AIPs. AIPs produced by different *S. aureus* strains vary in their amino acid sequence. *S. aureus* strains are categorized into four groups based on the AIP signal they produce. The AIP signal of each *S. aureus* group inhibits activation of *agr* systems in other *S. aureus* groups (424, 432, 436, 437, 461-463). This interference is believed to help the *S. aureus* strain which activates its quorum sensing system in the host organism first to outcompete other strains.

Two quorum sensing signal peptides control competence and sporulation in *B. subtilis* (Figure 2-9). These peptides are released into the environment as the number of cells increases. The peptide ComX, which is obtained by ComQ processing, is the activator of two-component system ComP/ComA (440-443). Phosphorylated ComA induces expression of *comS*. ComS inhibits degradation of ComK which is responsible for activation of competence development genes (464-467). The other peptide signal is CSF (competence and sporulation factor) which is internalized by an ABC (ATP-binding cassette) transporter (441, 444, 445). At low concentrations, CSF stimulates competence by inhibiting ComA phosphatase RapC (444, 468-470). This increases the level of phosphorylated ComA, eventually leading to competence development. However, CSF at high concentrations promotes sporulation and inhibits ComS, which results in competence repression (444, 468, 471-473).

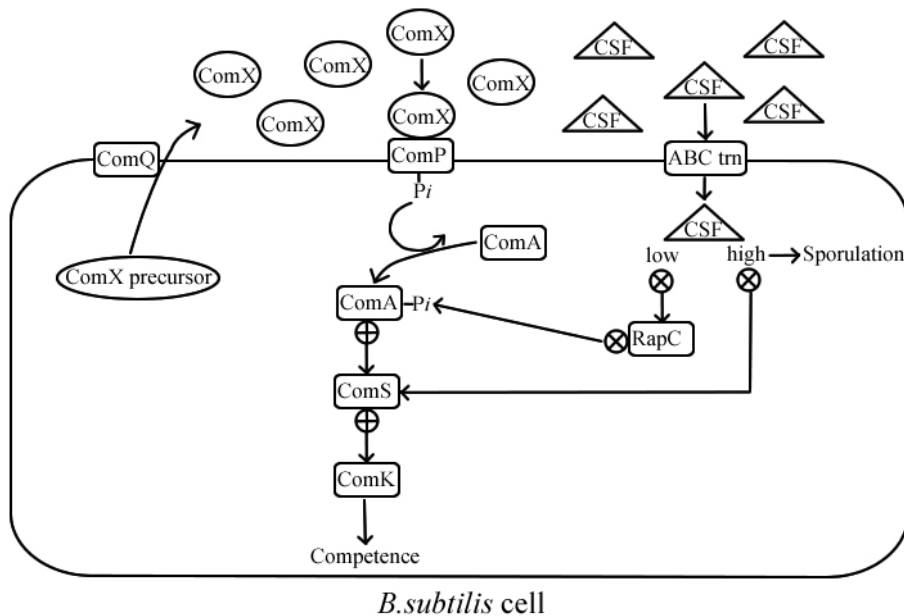


Figure 2-9. *B. subtilis* quorum sensing (440-445, 464-473) (⊗=Repression ⊕=Induction)

Bacillus species contain *aiiA* genes which encode AHL lactonases (474-476). AHL lactonases inactivate AHLs by hydrolyzing their lactone ring. *Bacillus* species, which use peptides as quorum sensing signals, are not affected by these enzymes. It has been suggested that *Bacillus* use AHL lactonases to interfere with AHL-mediated quorum sensing to compete with other bacteria.

Quorum sensing in *Salmonella* and *E. coli*

Salmonella typhimurium and *E. coli* produce an AI-2 molecule which is encoded by *luxS* when grown in the presence of glucose or another carbohydrate (Figure 2-10) (477, 478). AI-2 was identified as (2*R*, 4*S*)-2-methyl-2,3,3,4-tetrahydroxytetrahydrofuran (*R*-THMF) in *S. typhimurium* (479). The *S. typhimurium* and *E. coli luxS* gene sequences show significant identity with *V. harveyi luxS* sequence (477). The only genes which are known to be regulated by LuxS in *S. typhimurium* form the *lsr* operon (LuxS-regulated) (480, 481). This operon encodes a sugar ABC transporter which is used to import AI-2 into the cell in *S. typhimurium* and *E. coli* (480-482). AI-2 is produced and released into the environment where it accumulates during mid-exponential growth phase (478, 483). It is taken up by cells through the Lsr transporter during stationary growth (478, 480-483). AI-2 is modified inside the cell, leading to loss of its activity (481, 482). The function of this system is not known. It has been hypothesized that *S. typhimurium* uses this process to interfere with quorum sensing of other AI-2-producing bacteria (74). Acidic pH and high osmolarity, which are similar to conditions found in a host, induce AI-2 production as well (484). Therefore, some researchers have suggested that AI-2 activates virulence genes in *S. typhimurium* (483).

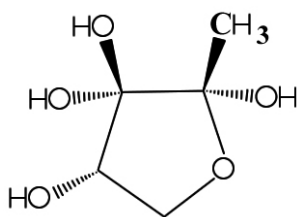


Figure 2-10. *S. typhimurium* AI-2, *R*-THMF (479)

Escherichia coli and *S. typhimurium* have a LuxR homologue, SdiA, (181, 485) but no LuxI homologue and do not produce AHLs (158, 486). SdiA promotes virulence genes, the *rck* operon, and other genes which provide resistance to host defense mechanisms in *S. typhimurium* (203, 487-489). This LuxR homologue also activates cell division genes (178, 179, 181), regulates virulence factors (490, 491), and increases resistance to xenobiotics (485, 492) in *E. coli*. SdiA does not sense AI-2s produced by *E. coli* and *S. typhimurium* but it responds to AHLs produced by other bacterial species (486, 493, 494). Some suggested that *E. coli* and *S. typhimurium* utilize SdiA to detect the presence of other bacteria (203, 486, 494), while others proposed that sensing other bacteria provide them with the information that they are inside a host (203). It is not clear whether SdiA and LuxS interact in *S. typhimurium* and *E. coli* (483, 484).

Bacteriophage

Bacteriophage or phage are viruses that infect bacteria and are highly specific for their hosts (495). Each phage can infect a certain species or strain(s) of a species. Phage particles or virions are composed of DNA or RNA genetic material and a protein or lipoprotein coat called the head or capsid (495). The number of bases found in phage

genomes varies from a few thousand to a few hundred thousand. Phage are obligate parasites that take over host cell machinery after infection to produce their own genetic material and proteins (495). They are found in very high numbers in the environments where their hosts occupy. When phage are outside a host, they can survive for long periods of time; but are susceptible to various chemical and physical agents such as UV light, sunlight, acidic pH, ascorbic acid, urea, detergents, alcohols, and heat (495).

More than 95% of all known phage belong to the order *Caudovirales* or tailed phage. The phage of this group have one molecule of linear dsDNA and icosahedral heads of protein with no envelope (495-500). Heads have binary symmetry which is a combination of both cubic and helical symmetry. Isometric or elongated heads range from 45-170 nm in diameter. Elongated heads can reach up to 230 nm. The G+C content of their genome is similar to that of their host DNA. Genes of proteins with similar functions are found in clusters in the genome. This group of phage has tails which are composed of helical rows or stacked discs, and base plates, fibers, or spikes for adsorption to the host cell surface. There are three families in this group based on tail morphology: *Siphoviridae*, *Myoviridae*, and *Podoviridae* (495-500). *Siphoviridae* phage which make up to 61% of tailed phage have long and noncontractile tails of 65-570 x 7-10 nm (495-500). Coliphage λ is the best-known phage in this family. *Myoviridae* form 25% of tailed phage (495-500). Their tails are made up of a sheath and a central tube which form a double layer. They measure 80-455 x 16-20 nm and are contractile. T4 is the type species in this family. Finally, 15% are in *Podoviridae* family which carries short, noncontractile tails capable of extension during infection (495-500). Tails are around 20 x 8 nm. Coliphage T7 is a member of this family.

Phage are termed virulent or temperate depending on their life cycle. Virulent phage take over host cell machinery to reproduce after infection and then lyse the cell to release newly-formed phage particles (495, 496, 501-503). Virulent phage have various mechanisms to take control of host metabolism. These include degradation of the host genome, inhibition of host DNA replication, transcription, and translation, blocking the restriction system, and changing the host membrane (495, 496, 501-503). Only a limited number of phage genes are expressed during the lysogenic cycle. Temperate phage which form more than 50% of all tailed phage enter either the lytic or lysogenic cycle after infection depending on the physiological condition of the host cell (495, 496, 501-503). The presence of a poor medium, host cell starvation, low temperatures, and infection with more than one phage are some of the factors that induce the lysogenic cycle. The phage genome is inserted into the host chromosome or exists as a plasmid in the bacterial cytoplasm during the lysogenic cycle. Usually a specific integrase enzyme places the genome into a certain site at the chromosome. The phage genome is replicated together with the host cell chromosome. A phage in this state is called a prophage (495, 496, 501-503). Prophage may remain in hosts for many generations. The prophage produce a repressor protein to suppress the expression of lytic cycle genes. However, some chemical and physical agents such as mitomycin C and UV light which damage host DNA or inhibit its replication can induce prophage to start the lytic cycle. Prophage usually prevent infection of their hosts by other phage in the same immunity group and also may provide them with virulence factors, restriction systems, and antimicrobial resistance (495, 496, 501-503). This process, in which prophage gene expression changes the host cell phenotype, is called lysogenic conversion.

There are five stages of the phage life cycle: adsorption, penetration, replication, assembly, and lysis. Phage first bind to receptors on the surface of bacteria (495, 501-505). These can be lipopolysaccharide components or outer membrane proteins of Gram-negative bacteria while phage of Gram-positive bacteria bind to teichoic acids, specific to each species, which are found inside the peptidoglycan layer. Some phage can recognize multiple types of receptors and others bind only to a single type. Phage use their tail fibers (adhesin regions) to interact with receptors (495, 501-505). Adhesin regions are specific to each phage species. This attachment between the adhesin and host receptor is responsible for host specificity of a phage. Penetration stage starts with degradation of the peptidoglycan layer of the host cell by a lysozyme released from the tail tip (495, 501-505). Then the tail degrades or makes contact with the bacterial inner membrane, inducing release of phage DNA. The genome of the phage enters the bacterial cell after passing through the tail. The capsid is left outside the cell. Phage have various mechanisms to protect their genomes from degradation by bacterial nucleases and restriction enzymes (495, 501-505). Their genomes may carry an unusual nucleotide or lack restriction enzyme recognition sequences. Some phage inhibit host cell nucleases. The phage genome may circularize itself while other phage have proteins to protect the linear ends upon entering the host. The genome of most phage is circularized by recombination of redundant ends after DNA transfer. In case of the lysogenic cycle, the circularized genome is integrated into the host chromosome while the circular genome of the lytic cycle-phage replicates via theta mode. The phage genome becomes latent in the host until it is induced to enter the lytic cycle (495, 501-505). Large lytic phage have a totally different mechanism for DNA replication in which the linear genome is replicated

by the phage's own DNA polymerase. Lytic cycle transcription starts with recognition of the strong phage promoters which induce early phage genes by bacterial RNA polymerase (495, 501-505). Products of these genes have roles in protection of the phage genome from host defense mechanisms, in decision between the lytic and lysogenic cycle, or in capturing host cell machinery. Then, middle genes are expressed with production of molecules which function in phage DNA replication. Lastly, late phage genes are transcribed, producing components of the capsid and tail, sigma proteins, RNA polymerase-related proteins, assembly factors, and lysis proteins. Phage may alter and use bacterial RNA polymerase and/or synthesize its own polymerase(s) for transcription (495, 501-505). Most phage form a linear concatemer of multiple genomes by a rolling-circle replication mechanism. Virion assembly starts with packaging of DNA from the concatemer into the preformed capsid until the capsid is full or specific termination sequences are reached (495, 501-505). Assembly pathways for capsids, tails, and tail fibers are separate. The capsid filled with DNA attaches to the preformed tail, resulting in formation of a complete, infective virion. In the final lysis phase, holins produced by the phage aggregate to construct hole formations in the inner membrane which provide access to the peptidoglycan layer for endolysins (495, 501-505). Endolysins disrupt the peptidoglycan layer through which the virions are released. Lysis is a scheduled event which is under the control by the phage (495, 501-505). If the number of target bacteria in the environment is high, lysis happens earlier while it is delayed if bacterial cell numbers are low.

Bacterial pathogens *Salmonella* and *S. aureus*

Animal and human feces contain various bacterial pathogens such as *Campylobacter*, *Salmonella*, *Shigella*, *Yersinia*, *Aeromonas*, *Pasteurella*, *Franciella*, *Leptospira*, *Vibrio*, *Escherichia*, *Legionella*, *Neisseria*, *Bacillus*, *Francisella*, *Burkholderia*, *Clostridium*, and *Brucella* (39, 44, 45). *Salmonella* has been detected in high amounts in feces (46) and was isolated from 55% of treated sewage sludge samples in Sweden (47). Application of poorly treated human and animal wastes on land causes contamination of soil with these bacterial pathogens (39, 45, 48). Half of the seven million dry tonne sewage sludge produced annually is used for land application each year in USA (39, 45). Treatment methods used in wastewater-treatment plants to produce sludge with reduced pathogen concentrations include composting, aerobic and anaerobic digestion, alkaline stabilization, conditioning, dewatering, and heat drying (39). Contamination of soil may also occur after utilization of human and animal wastes for land fertilization (39, 40). Pathogens which survive in soil for long periods of time may reach ground and surface water (39). *Salmonella* was shown to remain in soil alive for 20 days and it is also resistant to freezing and drying (39). If contaminated water is used for irrigation and/or drinking, this results in a potential source of infection of animals and humans. Furthermore, contaminated soil could lead to transfer of these pathogens to food products (39, 40, 45, 49-52). Contaminated produce was the cause of 41% of outbreak cases from 1990 to 1998 in the USA (39, 40). There are more than 200 types of foodborne diseases. Seventy-six million cases and 5,000 deaths are caused by diseases transmitted by food each year in the USA (41). *Salmonella* is one of the main causative agents for foodborne diseases worldwide. *Salmonella enterica* and *Campylobacter* were

responsible for 70% of all cases between 1995 and 2001 in Finland (1, 42). Additionally, salmonellosis leads to reactive arthritis and increases the fatality 3.1 times compared to controls (506, 507). *Salmonella* is also a Centers for Disease Control and Prevention (CDC) Category B bioterrorism threat agent.

Pathogens can be dispersed into the air after use of wastes and wastewater for land application and agricultural irrigation (50-53) and may cause airborne diseases by being transferred to humans via winds. People who reside within 1 km of sewage sludge application regions were found to be highly infected by pathogens from application sites (53). One forth of all residents were infected with *S. aureus* which can be a lower human colon organism resistant to desiccation. This pathogen is an opportunistic pathogen which can infect irritated tissues (53). *Staphylococcus aureus* is also detected commonly in the air and surface samples from hospitals (54). It is thought to be an important causative agent for airborne nosocomial infections in hospitals (54). Besides, it has been suggested to cause late onset biomaterial infections as a result of exposure of these materials to contaminated air before an operation (54). The number of patients nosocomially infected by opportunistic pathogens in hospitals is more than 2 million with more than \$4.5 billion cost each year in the USA (43). The major source of contamination in hospitals is various surfaces such as computer keyboards, faucet handles, and fabrics. *Staphylococcus aureus*, *Enterococci*, *E. coli*, *Pseudomonas*, and *Enterobacter* are the most common etiologic agents (43, 55). *Staphylococcus aureus* has been shown to survive on dry surfaces for long periods of time (56, 57). This pathogen is also known to commonly infect humans by contaminating recreational waters (508, 509).

Traditional, nucleic acid-based, and immunological bacterial pathogen detection methods

Microscopy and culturing on selective media have been traditional methods to detect bacterial pathogens in various types of samples (see reviews 2-6). These methods are easy to perform and cheap. However, there are some problems with traditional detection methods. While the disadvantage of microscopy is that it can not be used to identify bacteria, there are several problems with culture methods as well (see reviews 2-6). Some bacteria found in the environment are VBNC on general culture media. These include some pathogenic bacterial species such as *H. pylori*, *Campylobacter*, *E. coli*, *V. cholerae*, *Vibrio* spp., and *Legionella pneumophila*. Therefore, traditional culture methods may select for organisms which can grow fast and easily adapt to growth conditions. Also, bacteria isolated from the environment can be injured or stressed physically because of various environmental stressors such as nutrient deficiency, disinfectants, and UV light (see reviews 2-6). *Enterobacteriaceae* including *Salmonella* species, which are deficient or slow in lactose fermentation, have been shown to be underrepresented during traditional culturing methods. Therefore, VBNC and injured bacteria need to be enriched before detection using nonselective media under conditions without stress, which can take up to 8-24 h. Detection itself can take up to several days. These problems make culturing methods time-consuming and laborious, and also decrease the sensitivity.

Various PCR-based methods are used for detection and identification of bacterial pathogens in environmental, clinical, and food samples (see reviews 1, 2-5, 7-9). Nested PCR, multiplex PCR, real time quantitative PCR, amplified ribosomal DNA restriction

analysis (ARDRA), ribosomal RNA intergenic spacer analysis (RISA), denaturing gradient gel electrophoresis (DGGE), amplified fragment length polymorphism (AFLP), enterobacterial repetitive intergenic consensus polymerase chain reaction (ERIC-PCR), the repetitive sequence-based polymerase chain reaction (rep-PCR), terminal restriction fragment length polymorphism (TRFLP), length heterogeneity PCR (LH-PCR), and ligase chain reaction (LCR) are examples of PCR-based molecular detection methods. Some of these methods such as ARDRA, RISA, DGE, and TRFLP analyze sequences amplified from rRNA gene regions (see reviews 1, 2-5, 7-9). Unlike DNA-based PCR methods, rRNA-based PCR methods can determine viable cells because of the relationship between copy numbers and the metabolic activity of the cell.

PCR-based techniques have various advantages over traditional methods such as rapidness and sensitivity with low detection limits (theoretically as low as one cell) (see reviews 1, 2-5, 7-9). Identification range of these techniques includes VBNC, injured, and slow-growing bacteria as well as healthy cells. PCR-based methods do not require culturing of samples. However, these tests are not without limitations. Samples usually contain substrates which inhibit PCR, leading to false-negative results (see reviews 1, 2-5, 7-9). This problem increases especially with concentrated samples since inhibitors are also concentrated during the process. DNA-specific PCR-based methods can not differentiate between viable and nonviable organisms. This may require an additional culturing step before PCR, increasing the testing time and eliminating detection of VBNC cells. Efficiency of these methods is limited to the specificity of the primers for the target organism and PCR conditions used. Also, primer target sequences need to be represented in the gene database (see reviews 1, 2-5, 7-9). If primers are not specific enough for the

target organism, cross-reactivity with other bacteria present in the sample may result. Contamination by exogenous DNA from test materials and reagents or carryover from a positive sample is another common problem. Since the sensitivity of PCR is very high, even very low amounts of contaminating DNA will be increased to detectable levels during PCR. Interpretation of results is not easy; false-positive results due to contamination or false-negative results which are caused by poorly-designed primers and assay conditions or PCR inhibition are always possible (see reviews 1, 2-5, 7-9). Some PCR-based assays are technically quite complex and need to be performed by well-trained personnel, take long periods of time, and require expensive equipment.

There are also hybridization assays which are used for bacterial pathogen detection. Fluorescent in situ hybridization (FISH) uses DNA probes which can hybridize with genus- or species-specific 16S rRNA sequences (see reviews 2-4, 7, 9). FISH has a high sensitivity and does not require culturing of the sample. This hybridization method can detect VBNC cells as well and can be used to quantify specific organisms. However, it may not detect injured cells, and bacterial debris and materials other than organisms found in the sample may nonspecifically bind probes and affect test results. Nucleic acid microarray is another type of hybridization assay based on DNA or RNA sequences (see reviews 2-4, 7, 9). It is quite specific and sensitive, being able to perform very high numbers of reactions at one time. Inhibition by substrates found in samples is a significant problem. Nucleic acid microarray detects VBNC, living, and dead cells without being able to distinguish between them. This technique is highly complex in terms of processing and data analysis, and costly, which makes it unsuitable to use as a routine detection method. Both types of hybridization assays can detect organisms whose

target sequence is already in the database, limiting the detection range of the test (see reviews 2-4, 7, 9).

Immunological methods which are used commonly for pathogen detection take advantage of the specificity of an antibody for an antigen (see reviews 2, 6, 10-12). The antigen can be various types of molecules on the surface of the bacterial pathogen. Both monoclonal and polyclonal antibodies can be used (see reviews 2, 6, 10-12). The specificity of the assay can be adjusted to detect organisms at the family, genus, species, or serotype level. Some examples of immunological detection methods are ELISA (enzyme-linked immunosorbent assay), fluorescently labeled immunoassay, and enzyme immunoassay (see reviews 2, 6, 10-12). While immunological methods are easy to perform, rapid, sensitive, and suitable for automation, they do have some disadvantages. The detection limit is not as high as that of nucleic acid-based molecular methods because of the low affinity of the antibody for its antigen (see reviews 2, 6, 10-12). The detection limit of ELISA is between 10^3 and 10^5 colony forming units (cfu)/ml. The efficiency of immunological tests depends on the condition of the antigen in the environment. If the antigen is changed in the environment, the antibody can not bind it as effectively as it does under laboratory conditions (see reviews 2, 6, 10-12). There may also be cross-reaction problems with other organisms which may share some antigens with the target organism. The debris found in the environment may nonspecifically bind to antigens or antibodies, and thus may interfere with results (see reviews 2, 6, 10-12). In addition, immunological techniques can not differentiate between viable and dead cells.

Various disadvantages of current techniques described previously create the need for alternative bacterial pathogen detection methods. Public health concerns demand rapid, sensitive, easy-to-perform, and cheap detection methods which can be automated for continuous and real-time monitoring of pathogens.

Bioluminescent bioreporters

Bioluminescent bioreporters are usually recombinant bacteria which are genetically engineered to emit light in the presence of a specific analyte (Figure 2-11) (see reviews 13-22). These bioreporters carry a construct, formed by placing reporter gene expression under the control of the promoter which is induced only by the target analyte. The construct can be in the form of a plasmid or can be integrated into the bacterial chromosome. The most common bioluminescence reporter genes are the *lux* genes of *Photobacterium luminescens*, *V. harveyi*, or *V. fischeri*. The reporter gene product, bioluminescence, is easily detected and measured by luminescence-measuring devices. The intensity of the response is correlated with the quantity of the analyte. The analyte to be detected can be an environmental pollutant, toxic chemicals in wastewaters, bacterial nutrients, and pathogens (Table 2-3).

Bioluminescent bioreporters provide a very rapid, specific, and sensitive method of detection which is not invasive in organisms. Properties of a highly detectable bioluminescence signal make it ideal for construction of high-throughput, continuous and real-time monitoring systems.

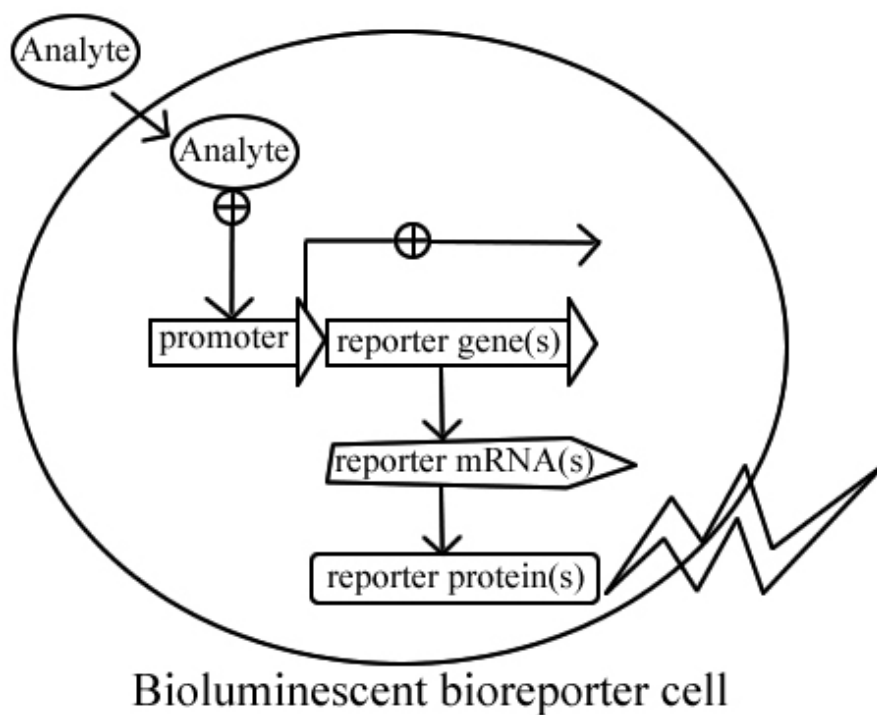


Figure 2-11. The bioluminescent bioreporter working mechanism (see reviews 13-22)

(\oplus = Induction)

Table 2-3. Bioluminescent bioreporters constructed for detection of chemicals

Chemical	References
Cadmium	510-513
Nickel	514, 515
Antimonite	516
Lead	511
Zn, Cu, and Cd, alone and in combination	517
Metals in soils amended with sewage sludge	518
Aluminum	519
Arsenate	520, 521
Arsenite	516, 520
Arsenic	512
Chromate	514, 521
Copper	521, 522
Iron	523
Inorganic mercury	522, 524-530
Nitrate	531

Table 2-3. Continued

Chemical	References
Zinc	532
Heavy metals	533-535
Metal salts	536
Pentachlorophenol	510
Dioxins	537
Endocrine disruptors	538
Polycyclic aromatic hydrocarbons (PAHs) naphthalene and salicylate	23-30, 33, 539, 540
Alkanes	541
m-xylene	542
4-chlorobenzoate	543
Hydrocarbon	544
Phenol	36, 545-547
Phenolic compounds	548
Organotin pollutants and their initial breakdown products (tributyltin, dibutyltin, triphenyltin and diphenyltin)	549
Biocides	550
Bioavailable linear alkylbenzene sulfonate	551
BTEX	31, 552
Tetracyclines	553
Polychlorinated biphenyls	30
Pesticides 2,4-dichlorophenoxyacetic acid and 2,4-dichlorophenol	35
Trichloroethane	32
Organic solvents	536
Hydrophobic pollutants	544
Gas toxicants	554
Ethanol	555, 556
Benzene derivatives	557
Wastewater toxicity	37, 558
Various pollutants	536, 559-571
Oxidative stress chemicals	564, 572
Cell membrane-damaging chemicals	571, 573
DNA-damaging chemicals	565, 573
Protein-damaging chemicals	560, 573
PAH bioavailability	34
Nitrogen bioavailability	574-576
Phosphorus bioavailability	576, 577
Iron bioavailability	578, 579
Carbon bioavailability	576
Arsenic bioavailability	580

Bacteriophage-based bioluminescent bioreporters for bacterial pathogen detection

High specificity of phage for their hosts makes them ideal candidates for specific bacterial pathogen detection (Table 2-4). Phage can be used to develop systems which identify bacteria with high sensitivity, selectivity, and rapidity. High amounts of phage can be produced in short times inexpensively while antibiotics are much more costly and slower to make. Furthermore, a phage-based system can detect living and VBNC cells unlike PCR- and antibiotic-based methods. However, a phage-based system can be practical, economical, and simple only if the phage can be screened quickly and easily. Also, the phage formed should be measured quantitatively to be able to determine the amount of the target organism. The combination of the phage-based detection with bioluminescence offers this system (see reviews 581-585). In such a system, the recombinant phage carries the bacterial *lux* or eukaryotic *luc* genes from a naturally-luminescent organism. Since phage do not have transcriptional and translational machinery in the absence of a host, they can not produce light. When they infect the host which is the target organism to detect, *lux* genes are transferred into the host cell and expressed. In the presence of exogenous substrate, this results in generation of bioluminescence which can be readily measured, determining the presence and amount of the target organism.

Table 2-4. Bioluminescent bacteriophage-based bioreporters for bacterial pathogen detection (Det=Detection, Min=Minimum, Ref=References, NK=Not known)

Target Species	Phage used	Bioluminescence genes	Sample	Det Time	Min Det Limit	Ref
<i>Listeria monocytogenes</i>	A511	<i>V. harveyi luxAB</i>	Culture Spiked salad	2 h 22-24 h	100-10 ³ cells/ml 1 cell/g	586
<i>L. monocytogenes</i>	A511	<i>V. harveyi luxAB</i>	Spiked pudding and cabbage Spiked meat and cheese	20 h 20 h	1 cell/g 10-100 cells/g	587
<i>M. tuberculosis</i>	TM4	<i>Fflux</i> (firefly luciferase)	Clinical isolates and sputum	2-3 days	Not known	588, 589
<i>M. tuberculosis</i>	TM4	<i>Fflux</i>	Sputum	24-48 h	Not known	590-593
<i>Mycobacterium smegmatis</i> and <i>M. tuberculosis</i>	TM4	<i>Fflux</i>	Culture	24 h	10 ⁴ -10 ⁵ cells	594
<i>M. smegmatis</i>	L5	<i>Fflux</i>	Culture	20 h 40 h	10 ³ cells 100 cells	595
<i>S. typhimurium</i>	P22	<i>luxAB</i>	Soil, water, and sewage sludge	24 h	1 cell/ml	596
<i>Salmonella</i>	P22 and 2 unknown	<i>V. fischeri luxAB</i>	Culture Whole eggs	6 h 24 h	10 cells/ml 10 cells/egg	597
Enteric indicator bacteria	ΦV10	<i>V. fischeri luxAB</i>	Meat	50 min 4h	10 ⁴ cells/g 10 cells/g	598
<i>E. coli</i> O157:H7	ΦV10	<i>V. harveyi luxAB</i>	Culture	1h	NK	599
<i>Salmonella</i>	Felix 01	<i>Vibrio luxAB</i>	Culture	NK	NK	600
<i>E. coli</i>	λCharon 30	<i>V. fischeri luxAB</i>	Milk and urine	1 h	10-100 cells/ml	601

The bacteriophage-based bioluminescent bioreporter system developed in this work

Previous bacteriophage-based bioluminescent bioreporters of bacterial pathogens (Table 2-4) have all used only the luciferase-coding genes (prokaryotic *luxAB* or eukaryotic *Fflux*), and thus could not function without addition of an inducer (aldehydes for prokaryotic and luciferin for eukaryotic systems) which is necessary for light generation. Therefore, these were not self-sufficient techniques which are required for construction of automated, high-throughput methods to monitor pathogens continuously. Also, such methods prevent optimization of bioreporter response since inducer concentration and addition time will be changed for each assay. Research of the present study aims to construct *S. aureus*- and *Salmonella*- monitoring systems which have the advantages but not the disadvantages of previous methods. The system will be composed of two elements: *S. aureus*- or *Salmonella*-specific recombinant phage which has the *luxI* gene from *V. fischeri* and a bioreporter cell line which is an *E. coli* strain with the *V. fischeri luxR* gene, promoter site (P_{lux}), and *luxCDABE* cassette (Figure 2-12). The system is not capable of producing light in the absence of the phage host organism. Since the phage itself is metabolically inactive, *luxI* can not be expressed. Light will not be emitted without the AHL autoinducer, synthesized by the *luxI* gene product. When there is the target organism which is the host of the *luxI*⁺ phage in the environment, it will be infected by the phage. This will result in transfer of the phage genome carrying *luxI* into the host cell and its subsequent expression. The LuxI protein formed in the target pathogen will synthesize AHL which can freely diffuse across the cell membrane. AHL will then be taken up by the bioreporter cell, leading to induction of *lux* genes and light generation.

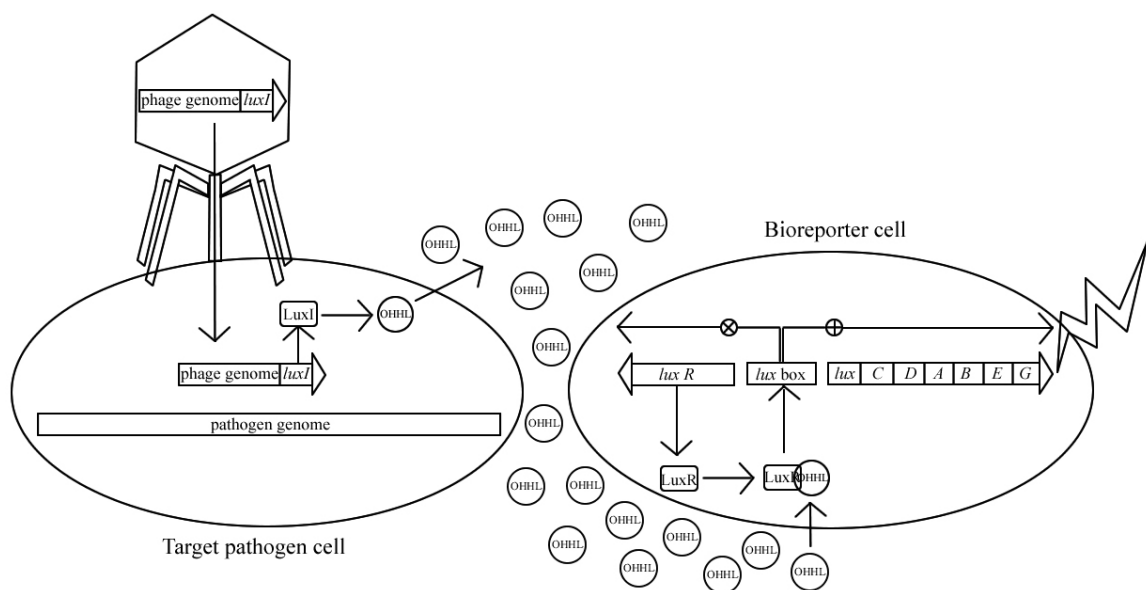


Figure 2-12. The bacteriophage-based bioluminescent bioreporter system for pathogen monitoring developed in this work

The bioreporter cell line was already constructed and tested for *E. coli* detection using a λ phage engineered to carry *V. fischeri luxI* gene in our lab (63). The system could detect 10^8 cfu/ml and as low as 1 cfu/ml in 1.5 h and 10.3 hours, respectively, in culture. When the system was tested with spiked lettuce leaves, 10^8 cfu/ml and 130 cfu/ml were detected in 2.6 and 22.4 hours, respectively. The aim of this research is to construct *luxI*-carrying recombinant phage, one specific for *S. aureus* and one specific for *Salmonella*. Each of phage will be used in combination with the bioreporter cell line which has the other genes of the *lux* operon. Ultimately, these two autonomous systems are aimed to be used for applications that will monitor *S. aureus* and *Salmonella* separately in a continuous and totally automated format in real time. The recombinant phage and the bioreporter cell will be fixed on a BBIC which contains a photodetector

and a signal processor (38). The BBIC will measure light generated after exposure to the target pathogen in the environment. The value determined will be digitized and transmitted to a data receiver. The system will be portable with no requirement for power and optic cables, which is suitable for field detection. It will be able to be used easily by non-trained personnel for quick pathogen detection with high sensitivity and specificity.

CHAPTER III

MATERIALS AND METHODS

CONSTRUCTION OF *S. AUREUS* BIOREPORTER

Bacterial strains, plasmids, and bacteriophage

Bacterial strains, plasmids, and bacteriophage used in this study are shown in Tables 3-1, 3-2, and 3-3, respectively.

Growth and storage conditions

Escherichia coli, *B. subtilis*, and *S. aureus* strains were grown in LB (Luria-Bertani broth; 10 g tryptone, 5 g yeast extract, 10 g NaCl, pH 7.5) at 37°C at 220 rpm overnight unless stated otherwise. Media were sterilized by autoclaving at 121°C and 15 psi for 20 min. Agar plates were prepared by adding 15 g/L of agar into the medium before autoclaving. Overnight cultures of bacterial strains were stored at -80°C in 25% glycerol.

Table 3-1. Bacterial strains used in this study.

Species	Strain	Description and/or Genotype	Reference and/or Source
<i>V. fischeri</i>	NCMB 1281	Type strain	ATCC 7744, 602
<i>E. coli</i>	DH5 α	General cloning, blue/white screening without IPTG; F ⁻ ϕ 80 <i>lacZ</i> Δ M15 Δ (<i>lacZYA-argF</i>)U169 <i>recA1 endA1 hsdR17</i> (r _k ⁻ , m _k ⁺) <i>phoA supE44 thi-1 gyrA96 relA1</i>	Invitrogen, Carlsbad, CA
<i>E. coli</i>	TOP10	Chemically competent cloning strain, blue/white screening without IPTG; F ⁻ <i>mcrA</i> Δ (<i>mrr-hsdRMS-mcrBC</i>) Φ 80 <i>lacZ</i> Δ M15 Δ <i>lacX74 recA1 araD139</i> Δ (<i>ara-leu</i>)7697 <i>galU galK rpsL</i> (Str ^R) <i>endA1 nupG</i>	Invitrogen, Carlsbad, CA
<i>E. coli</i>	RoLux	OHHL bioluminescent bioreporter, phage λ sensitive; STBL4 (EZ::TN <i>luxRoCDABE</i>)	603
<i>E. coli</i>	OHHLux	OHHL bioluminescent bioreporter, phage λ resistant; EZ::TN pMOD (Epicentre Biotechnologies, Madison, WI)- <i>V. fischeri luxR-P_{luxI}-P. luminescens luxCDABE-rrnB</i> T ₁ T ₂ , Kan ^r	63
<i>E. coli</i> carrying pJBA132	MT102	OHHL fluorescent bioreporter; pME6031- <i>luxR-P_{luxI}-RBSII-gfp</i> (ASV)-T ₀ -T ₁ , Tc ^r	604
<i>E. coli</i>	K12 XL10-GOLD	Cloning of 0602285pPCR-Script, <i>dam</i> ⁺ <i>dcm</i> ⁺	GENEART (Regensburg, Germany)
<i>B. subtilis</i>	BD170	pUB110, Kan ^r , Neo ^r	ATCC 37015
<i>S. aureus</i>	SA113	Restriction deficient mutant from strain NCTC 8325	ATCC 35556
<i>S. aureus</i>	RN4220	Restriction deficient strain which accepts DNA from <i>E. coli</i>	Dr. Richard Novick, New York Un.
<i>S. aureus</i>	CDC 85	Host of phage Φ 85	ATCC27708, 605, 606
<i>S. aureus</i>	Twort	Host of phage Twort	Felix d'Herelle Center, Canada, 606, 607
<i>S. aureus</i>	RN451	Host of phage P68	Dr. John Iandolo, Un. of Oklahoma , 608

Table 3-2. Plasmids used in this study.

Plasmid	Description	Function	Reference and/or Source
pCR2.1	3929 bp, <i>LacZ</i> α , MCS, pUC origin, Kan ^r , Amp ^r	Overnight TA cloning of PCR products	Invitrogen, Carlsbad, CA
pCR2.1-TOPO	3931 bp, <i>LacZ</i> α , MCS, pUC origin, Kan ^r , Amp ^r	5 min-cloning of <i>Taq</i> polymerase-amplified PCR products	Invitrogen, Carlsbad, CA
pCR2.1-luxI #13	4537 bp, <i>luxI</i> CDS with <i>S. aureus</i> RBS carrying 5' <i>Bam</i> HI and 3' <i>Kpn</i> I sites	Cloning of <i>luxI</i> CDS under the control of <i>S. aureus</i> RBS	This work
pCR2.1-phage85prom #8	4354 bp, phage Φ 85 X8 promoter with 5' NotI and 3' <i>Sal</i> I sites	Cloning of <i>S. aureus</i> phage Φ 85 X8 promoter	This work
pMOD-1-T1T2	2901 bp, T ₁ T ₂ in EZ::TN pMOD-1 (Epicentre Biotechnologies, Madison, WI)	Source of <i>rrnB</i> ribosomal terminator T ₁ T ₂ of pKK223-3	Lab stock
pCR2.1-T1T2 #9	4367 bp, T ₁ T ₂ with 5' <i>Sac</i> I and 3' <i>Cla</i> I sites	Cloning of <i>rrnB</i> ribosomal terminator T ₁ T ₂ of pKK223-3	This work
pYES2.1/V5-His-TOPO-kan ^r	8227 bp, Gram-negative kan ^r with 5' <i>Hind</i> III-NotI and 3' <i>Hind</i> III sites (x2) in pYES2.1/V5-His-TOPO yeast expression cloning plasmid (Invitrogen, Carlsbad, CA), pMB1 ori, Amp ^r , Kan ^r	Source of Gram-negative kan ^r of Invitrogen, Carlsbad, CA TA cloning vector pCR2.1	Lab stock
EZ::TN pMOD-2<MCS>	2545 bp, MCS, 2X mosaic ends (MEs) for transposition, pUC ori, Amp ^r	Transposon construction vector	Epicentre Biotechnologies, Madison, WI
pMOD-2-kan ^r #2	3763 bp, Gram-negative pCR2.1 kan ^r with 5' <i>Hind</i> III-NotI and 3' <i>Hind</i> III sites	Cloning of Gram-negative pCR2.1 kan ^r of into EZ::TN pMOD-2<MCS> between MEs	This work

Table 3-2. Continued

Plasmid	Description	Function	Reference and/or Source
pMOD-2-kan ^r -luxI #6	4356 bp, <i>kan^r-luxI</i> CDS under the control of <i>S. aureus</i> RBS with 5' <i>Bam</i> HI and 3' <i>Kpn</i> I sites	Cloning of <i>luxI</i> CDS under the control of <i>S. aureus</i> RBS into pMOD-2-kan ^r #2 between MEs	This work
pMOD-2-kan ^r -luxI-T1T2 #2	4747 bp, <i>kan^r-S. aureus</i> RBS- <i>luxI</i> CDS-T ₁ T ₂ with 5' <i>Sac</i> I and 3' <i>Cla</i> I sites	Cloning of <i>rrnB</i> ribosomal terminator T ₁ T ₂ of pKK223-3 into pMOD-2-kan ^r -luxI #6 after <i>luxI</i> CDS and between MEs	This work
pMOD-2-kan ^r -prom-luxI-T1T2 #7 (also referred to as pMO-L #7 in text and tables)*	5231 bp, <i>kan^r-S. aureus</i> phage Φ85 X8 promoter with 5' <i>Not</i> I and 3' <i>Sal</i> I sites- <i>S. aureus</i> RBS- <i>luxI</i> CDS-T ₁ T ₂ between MEs in EZ::TN pMOD-2<MCS>	Cloning of <i>kan^r-S. aureus</i> phage Φ85 X8 promoter- <i>S. aureus</i> RBS- <i>luxI</i> CDS-T ₁ T ₂ into <i>S. aureus</i> phage Twort genome using transposition	This work
pCR2.1-TOPO P _L - <i>luxI</i>	pCR2.1-TOPO-phage λ left arm promoter P _L - <i>V. fischeri luxI</i> , pUC origin, Kan ^r , Amp ^r	OHHL-producing positive control plasmid	63
pMK4	5575 bp, MCS, <i>lacZ</i> , pUC9 ori, pC194 ori, Amp ^r , Cam ^r	Gram-positive/Gram-negative shuttle vector	ATCC 37315, 609
pMK4-prom-luxI #13.3 (also referred to as pMK-L #13.3 in text and tables)*	6674 bp, pMK4- <i>S. aureus</i> phage Φ85 X8 promoter- <i>S. aureus</i> RBS- <i>luxI</i> CDS, pUC9 ori, pC194 ori, Amp ^r , Cam ^r	Testing OHHL production from <i>luxI</i> CDS under the control of <i>S. aureus</i> RBS and phage Φ85 X8 promoter	This work
pCR2.1-luxI #30	4539 bp, <i>S. aureus</i> RBS- <i>luxI</i> CDS with 5' <i>Sal</i> I and 3' <i>Bam</i> HI sites	Addition of 5' <i>Sal</i> I and 3' <i>Bam</i> HI sites to <i>S. aureus</i> RBS- <i>luxI</i> CDS for insertion into pHPS9	This work

Table 3-2. Continued

Plasmid	Description	Function	Reference and/or Source
pHPS9	5700 bp, MCS, <i>cat</i> -86:: <i>lacZ</i> α , <i>L. lactis</i> promoter P59, Gram positive ori rep60 from pTA1060, Gram-negative ori from pUC, Em ^r , Cam ^r	Gram-positive/Gram-negative shuttle expression vector	ATCC 37816, 610
pHPS9-luxI #7 (also referred to as pHP-L #7 in text and tables)*	5684 bp, <i>S. aureus</i> RBS- <i>luxI</i> CDS under the control of <i>L. lactis</i> promoter P59, Gram positive ori rep60 from pTA1060, Gram-negative ori from pUC, Em ^r , Cam ^r	Testing OHHL production from <i>luxI</i> CDS under the control of <i>S. aureus</i> RBS and <i>L. lactis</i> promoter P59	This work
pCR2.1-kanR #10	4719 bp, <i>S. aureus</i> RBS- <i>kan</i> ^r CDS from pDG148-Stu with 5' <i>Sa</i> I and 3' <i>Ba</i> mHI sites	Cloning of <i>kan</i> ^r CDS from pDG148-Stu under the control of <i>S. aureus</i> RBS used for <i>luxI</i> expression in pHPS9	This work
pHPS9-kanR #4 (also referred to as pHP-K #4 in text and tables)*	5862 bp, <i>S. aureus</i> RBS-pDG148-Stu <i>kan</i> ^r CDS under the control of <i>L. lactis</i> promoter P59, Gram positive ori rep60 from pTA1060, Gram-negative ori from pUC, Em ^r , Cam ^r	Determination of pHPS9 promoter P59 efficiency by placing <i>S. aureus</i> RBS- <i>kan</i> ^r CDS from pDG148-Stu under its control into pHPS9	This work
pCR2.1-luxI #3	4525 bp, <i>luxI</i> CDS with 5' and 3' <i>Stu</i> I sites	Addition of 5' and 3' <i>Stu</i> I sites to <i>luxI</i> CDS for insertion into pDG148-Stu	This work
pDG148-Stu	8272 bp, <i>Pspac</i> (hybrid promoter of <i>B. subtilis</i> phage SPO-1/ <i>lac</i> operator regulated by the IPTG-inducible LacI repressor), a Gram-positive RBS, <i>lacI</i> , <i>E. coli</i> Amp ^r , <i>E. coli</i> or <i>B. subtilis</i> Kan ^r , <i>E. coli</i> or <i>B. subtilis</i> Ble ^r	Gram-positive/Gram-negative shuttle inducible expression vector	BGSC ECE145, 611

Table 3-2. Continued

Plasmid	Description	Function	Reference and/or Source
pDG148-Stu-luxI #28 (also referred to as pDG-L #28 in text and tables)*	8854 bp, <i>Pspac</i> -the Gram-positive RBS- <i>luxI-lacI</i> , Amp ^r , Kan ^r , Ble ^r	Testing OHHL production from <i>luxI</i> under the control of Gram-positive inducible promoter <i>Pspac</i> and RBS of pDG148-Stu	This work
pHPS9-sht #7	5000 bp, MCS, <i>lacZα</i> , <i>L. lactis</i> promoter P59, Gram positive ori rep60 from pTA1060, Gram-negative ori from pUC, Em ^r , Cam ^r	Shortening pHPS9 by removing <i>cat</i> -86	This work
pHPS9-sht-Pspac-luxI-lacI #9 (also referred to as pHP-PL #9 in text and tables)*	7256 bp, pHPS9-sht #7 carrying <i>Pspac</i> -Gram positive RBS- <i>luxI-lacI</i> fragment from pDG148-Stu-luxI #28 (or pDG-L #28)	Shortening the construct which carries <i>luxI</i> under the control of <i>Pspac</i> and RBS of pDG148-Stu for transfer into <i>S. aureus</i> instead of longer pDG148-Stu-luxI #28 (pDG-L #28)	This work
pCR2.1-kanRStuI #12	4704 bp, <i>kan^r</i> CDS from pDG148-Stu with 5' and 3' <i>StuI</i> sites	Addition of 5' and 3' <i>StuI</i> sites to <i>S. aureus kan^r</i> CDS from pDG148-Stu	This work
pDG148-Stu-kanR #8	9017 bp, <i>Pspac</i> -the Gram-positive RBS- <i>S. aureus kan^r</i> CDS from pDG148-Stu- <i>lacI</i> , Amp ^r , Kan ^r , Ble ^r	Cloning of <i>S. aureus kan^r</i> CDS from pDG148-Stu into pDG148-Stu under the control of the Gram-positive RBS and <i>Pspac</i>	This work

Table 3-2. Continued

Plasmid	Description	Function	Reference and/or Source
pHPS9-sht-Pspac-kanR-lacI #31 (also referred to as pHP-PK #31 in text and tables)*	7419 bp, pHPS9-sht #7 carrying <i>Pspac</i> -Gram positive RBS- <i>S. aureus kan^r</i> CDS from pDG148-Stu - <i>lacI</i> fragment from pDG148-Stu-kanR #8	Determination of pHPS9-sht-Pspac-luxI-lacI #9 (or pHP-PL #9) RBS efficiency by replacing <i>luxI</i> with <i>S. aureus kan^r</i> CDS	This work
pUB110	4548 bp, Kan ^r , Neo ^r	<i>S. aureus</i> natural plasmid used as a cloning vector for <i>Bacillus</i>	ATCC 37015
0602285pPCR-Script	3462 bp, optimized <i>luxI</i> CDS with 5' and 3' <i>StuI</i> sites, fl (+) ori, Col E1 ori, Amp ^r	Cloning of <i>luxI</i> CDS whose codon usage was adapted to the codon bias of <i>S. aureus</i> phage P68 by GENEART (Regensburg, Germany)	GENEART (Regensburg, Germany)
pDG148-Stu-optluxI #16	8857 bp, <i>Pspac</i> -the Gram-positive RBS-optimized <i>luxI-lacI</i> , Amp ^r , Kan ^r , Ble ^r	Cloning of optimized <i>luxI</i> CDS under the control of the Gram-positive RBS and <i>Pspac</i>	This work
pHPS9-sht-Pspac-optluxI-lacI #5 (also referred to as pHP-POL #5 in text and tables)*	7259 bp, pHPS9-sht #7 carrying <i>Pspac</i> -Gram positive RBS-optimized <i>luxI-lacI</i> fragment from pDG148-Stu-optluxI #16	Testing OHHL production from <i>luxI</i> whose codon usage was optimized for <i>S. aureus</i> phage P68	This work

(*See Table A in the appendix for a complete list of alternative names used for plasmids.)

Table 3-3. Bacteriophage used in this study.

Phage	Host	Description	Reference and/or Source
Φ85	<i>S. aureus</i> CDC 85 (ATCC 27708)	Temperate, serogroup B, long/non-contractile tail, 44,283 bp	ATCC 27708-B1, 605, 606
Twort	<i>S. aureus</i> Twort	<i>Myoviridae</i> , 90 nm diameter, 203 nm tail, virulent, single linear ds DNA genome (130,706 bp)	Felix d'Herelle Center, Canada, 606, 607
P68	<i>S. aureus</i> RN451	<i>Podoviridae</i> , 75 nm diameter, short/non-contractile tail (40 nm), virulent, single linear ds DNA genome (18,227 bp)	Felix d'Herelle Center, Canada, 608, GenBank AF513033

Molecular biology techniques

All molecular biology techniques were performed using protocols from Molecular Cloning: A Laboratory Manual (612) unless stated otherwise. All procedures which were carried out with kits followed manufacturer's instructions. All restriction enzymes were provided by Promega (Madison, WI). Electrophoresis was done using TBE buffer which contained 0.045 M Tris-Borate and 0.001 M EDTA, pH 8.0. All PCR reactions were performed using PCR Ready-To-Go beads (Amersham Biosciences, Buckinghamshire, England) following manufacturer's instructions on a PTC-225 DNA Engine Tetrad Peltier Thermal Cycler (MJ Research, Inc., Waltham, MA). All primers were obtained from Sigma Genosys (The Woodlands, TX) or Operon Biotechnologies, Inc. (Huntsville, AL). A list of primers is given in Table 3-4. Primers, arrived lyophilized, were suspended in sterile dH₂O to make a stock solution with 1 nmol/μl concentration. The stock solution was diluted to a working solution of 5 pmol/μl concentration using sterile dH₂O. All PCR and sequencing reactions were carried out using working solutions. DNA quantifications were done using a DyNA 200 Fluorometer (GE Healthcare, Buckinghamshire, UK).

Table 3-4. List of primers used in this study.

Name	Sequence (5'-3')	References
luxIBamHI forward	GGATCCGAGGAGGAGTTGGTATGAC TATAATG	This work
luxIKpnI reverse	GGTACCCATTAATTTAAGACTGCTT	This work
prom85NotI forward	GCGGCCGCGAGAATATGTCATAACC TG	This work
prom85Sall reverse	GTCGACCTGAATTCGGTAACGATG	This work
T1T2SacI forward	GAGCTCAAGAGTTTGTAGAAACGC	This work
T1T2ClaI reverse	ATCGATTCTGTTTTGGCGGATG	This work
luxISall forward	GTCGACGAGGAGGAGTTGGTATGAC TATAATG	This work
luxIBamHI reverse	GGATCCCATTAATTTAAGACTGCTT	This work
kanRSall forward	GTCGACGAGGAGGAGTTGGTGTGAA TGGACCAATAATAATGA	This work
kanRBamHI reverse	GGATCCTCAAAATGGTATGCGTTTTG	This work
luxIStuI forward	AGGCCTATGACTATAATGATAAAAA	This work
luxIStuI reverse	AGGCCTTTAATTTAAGACTGCTT	This work
LuxI-qRT forward	GCAATTCCATCGGAGGAGTA	Dr. Michael Allen, University of Tennessee, Knoxville
LuxI-qRT reverse	AAACGCCAGCATCCACTTAC	Dr. Michael Allen, University of Tennessee, Knoxville
kanRStuI forward	AGGCCTGTGAATGGACCAATAATAA TGACT	This work
kanRStuI reverse	AGGCCTTCAAAATGGTATGCGTTTTG ACA	This work

DNA sequencing

Sequencing reactions were done by the Molecular Biology Resource Facility at The University of Tennessee, Knoxville with an ABI Prism 3100 Genetic Analyzer and a 3730 DNA Analyzer (Applied Biosystems, Foster City, CA). M13 reverse and forward primers (Invitrogen, Carlsbad, CA) were used for sequencing reactions of genes which were cloned into pCR2.1-TOPO or pCR2.1 (Invitrogen, Carlsbad, CA). Sequencing for genes cloned into other plasmids was done using primers which were used for cloning.

Preparation of chemically competent cells of *E. coli* DH5 α

One ml of overnight culture of *E. coli* DH5 α was inoculated into 100 ml of fresh LB and was grown at 37°C at 220 rpm until reaching an OD₆₀₀ of ~0.4. It was put into ice for at least 15 min. The ice-cold culture was centrifuged at 10,000 x g for 5 min at 4°C. The pellet was resuspended gently in 50 ml ice-cold wash buffer (5 mM Tris-HCL pH 7.6, 10 mM MgCl₂, 50 mM NaCl), centrifuged, and resuspended as before. After another centrifugation, the pellet was dissolved in 25 ml ice-cold calcium buffer (10 mM Tris-HCL pH 7.6, 10 mM MgCl₂, 100 mM CaCl₂) and stored on ice for 30 min. Cells were centrifuged as before and then resuspended in 4 ml ice-cold storage buffer (43 ml calcium buffer, 7 ml glycerol). Finally, cells were stored at -80°C in 100 μ l aliquots up to 3 months.

Chemical transformation of *E. coli* DH5 α

The chemically competent cell aliquot (100 μ l) was thawed on ice. One μ l of plasmid or 5 μ l ligation reaction was added into the cell suspension, mixed by tapping on

the bottom of the tube, and then stored on ice for 30 min. After incubation, the suspension was heat shocked for 30 sec at 37°C followed by storage on ice for 5 min. LB (150 µl) was added into the tube. Then it was shaken at 37°C for 1 h. Dilutions of the cell suspension were plated onto selective LB plates which were incubated at 37°C overnight.

Electroporation of *S. aureus*

The method of Schenk and Laddaga (613) was used for preparation of electrically competent cells and electroporation of *S. aureus*. Briefly, the cultures at mid-log phase were washed with dH₂O once and with 10% glycerol twice at room temperature. After incubation at room temperature for 15 min, they were resuspended in 10% glycerol. Then, cells were centrifuged, resuspended in 10% glycerol, and stored at -80°C in 60 µl aliquots. Electroporation was performed by mixing 60 µl electrocompetent cells with 1 µl DNA in a 1-mm gap electroporation cuvette. Cells and DNA were electroporated at 20°C, 100 ohms resistance, 25 µF capacitance (optimum time constant of 2.5 ms), and 2.3 kV.

Electroporation of *B. subtilis*

The *B. subtilis* electroporation protocol 0010a (BTX ID #1361) which was prepared using the method of Stephenson and Jarrett (614) as suggested by the Electro Cell Manipulator ECM 600 Manual (BTX Applications, Holliston, MA) was followed for preparation of electrically competent cells and electroporation of *B. subtilis* strains. Briefly, the mid-log phase cultures were washed with sterile ice-cold dH₂O three times and resuspended in 30% glycerol, and stored at -80°C in 100 µl aliquots. Electroporation was performed by mixing 100 µl electrocompetent cells with 1 µl DNA in a 2-mm gap

electroporation cuvette. Cells and DNA were electroporated at 4°C, 150 ohms resistance, 25 µF capacitance (optimum time constant of 6.5-8 ms), and 2.5 kV.

Plasmid purification using rapid boiling mini-prep method

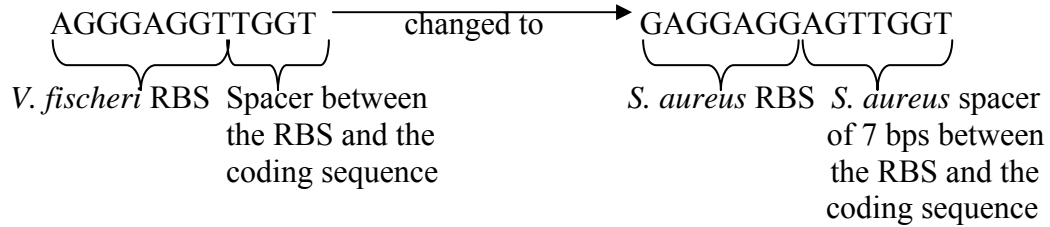
One ml of an overnight culture was centrifuged at 10,000 x g for 5 min at room temperature in a microcentrifuge. The pellet was resuspended in 40 µl of STET buffer (50 mM EDTA, 50 mM Tris pH 8.0, 5% Triton, 8% sucrose). Four µl of freshly prepared lysozyme solution (10 mg/ml in 20% sucrose, 50 mM Tris pH 8.0) were added to the suspension. The tube was placed in a boiling water bath for 1 min, and centrifuged at 14,000 x g for 10 min at room temperature. The pellet was removed with a sterile toothpick and then 150 µl of 0.3 M KAc, pH 8.0 and 500 µl ice-cold ethanol were added to the supernatant. After mixing by inversion, the solution was stored on ice for 10 min, centrifuged at 14,000 x g for 15 min at 4°C, and the supernatant was discarded. The DNA pellet was washed with 500 µl of 70% ethanol. The pellet was dried at room temperature, resuspended in enzyme digestion buffer, and used for digestion.

Purification of *V. fischeri* genome

A colony of *V. fischeri* strain ATCC 7774 was placed into 100 µl of sterile dH₂O in a sterile 1.5 ml Eppendorf tube, boiled for 10 min, and then centrifuged at 14,000 x g for 5 min in a tabletop centrifuge at 4°C. The supernatant containing genomic DNA was stored at -20°C.

***luxI* cloning from *V. fischeri* genome**

luxI gene was amplified from purified *V. fischeri* genome using luxIBamHI forward and luxIKpnI reverse primers. The RBS of *V. fischeri luxI* gene was changed into a typical *S. aureus* RBS (615) during amplification by including the *S. aureus* RBS in the luxIBamHI forward primer. The RBS change is shown below:



The PCR conditions were 94°C for 5 min followed by 39 cycles of 94°C for 30 sec, 56°C for 30 sec, and 72°C for 1 min, and then 72°C for 10 min extension time. Fifteen µl of the PCR reaction were run on a 1% agarose gel with ethidium bromide (EtBr) in 0.5xTBE (Tris-Borate EDTA) to verify PCR product size. After confirmation, the PCR product was cloned into a TA cloning vector pCR2.1 (Invitrogen, Carlsbad, CA) according to manufacturer's instructions. Plasmids were purified from overnight cultures of selected transformant colonies using the rapid boiling mini-prep method (see above). They were screened for the presence of PCR product by *EcoRI* (Promega, Madison, WI) restriction analysis. Plasmids of selected transformants, which are positive for the insert, were purified with Wizard Plus Midi-Preps DNA Purification Systems (Promega, Madison, WI) according to manufacturer's instructions and sequenced. After sequence confirmation, the construct selected was named pCR2.1-luxI #13.

X8 promoter cloning from *S. aureus* phage Φ85 genome

The genome of *S. aureus* phage Φ85 was isolated using Wizard Lambda Phage DNA Purification System (Promega, Madison, WI) following manufacturer's instructions and used as a template for amplifying the X8 promoter sequence (605). The PCR was performed with prom85NotI forward and prom85SalI reverse primers under the following conditions: 94°C for 5 min, then 35 cycles of 94°C for 30 sec, 52°C for 30 sec, and 72°C for 30 sec, followed by 72°C for 15 min. To verify the PCR product size, 15 µl of the reaction were electrophoresed on a 1% agarose gel with EtBr in 0.5xTBE. Then, the product was integrated into the TA cloning vector pCR2.1 (Invitrogen, Carlsbad, CA). Transformant colonies were screened with *Eco*RI restriction analysis as described previously. Transformants pCR2.1-phage85prom #2 and #8 were sequenced. Sequencing results of both constructs were the same. There were some differences between promoter sequences obtained and the sequence described by Carbonelli et al. (605) (Table 3-5). Since differences were outside the putative promoter area determined by Carbonelli et al. (605), studies were continued with plasmid pCR2.1-phage85prom #8. Table 3-5 shows these differences and the putative promoter region with the motifs determined by Carbonelli et al. (605).

Table 3-5. The pairing of the phage Φ85 X8 promoter sequence used (top) and the X8 sequence described by Carbonelli et al. (605) (bottom). Differences between sequences are shown in bold. The putative promoter region is underlined and motifs are in boxes.

(X=missing nucleotides)

X GAGAATATGTCATAACCTGCATCCGTCTTATGATTTCG
T GAGAATATGTCATAACCTGCATCCGTCTTATGATTTCG
TTCGGG C ATTCTAGCATT TTTTTGXXXXXXXXXXATAAT
TTCGGG C ATTCTAGCATT TTTTTGATAATATGTCATAAT
AGTTTTACTTGTAATGTGTTAGTCATT TTCTATTCT
AGTTTTACTTGTAATGTGTTAGTCATTXXXXXXXXXX
CCTCATATTTATAGACA CTTGACCTGCCATAATCC
XXXXXXXXXXXXXXXXXXXXXXXXXXXXXXXXXXXX
CTACTGCTTCATCAAGTTCAATACCTTCTTTAACTGAA
XXXXXXXXXXXXAAGTTCAATACCTTCTTTAACTGAA
TGTTGAATAGCATTGTGCAT TCCCTCAAGTATTTCAT
TGTTGAATAGCATTGTGCAT CCAAGATTTCACAACAG
CAAACGCTTGCGCTTTCTTATACACGTCCTCAATCTCT
CTTGACGAXXX CTTTCTTATACACGTCCTCAATCTCT
TTTAGCAACCCCTCTGTGTCATTACCGTTATACGCACTA
TTTAGCAACCCCTCTGTGTCATTACCGTTATACGCACTA
GCACTAATAACGGACTGTTTCGATTTTTTCGCGATTATTC
GCACTAATAACGGACTGTTTCGA TTTTTTC GCGA TTATTC
-54 -44
ATTGTGTCATCCTCCATAAAAATTTTATTGTTTAAT
ATT GTGTCA TCCTCC ATAAAAATTTTATT TGTTTAAT
-35 homopyrimidines extended -10
TCCATTCCGAATTTAACTCTTTCATCATCGTTACCGAA
<u>TCCATTCCGAATTTAACTCTTTCATCATCGTTACCGAA</u>
TTCAGXXXXXXXXX
TTCAGCTCGGTAA

T₁T₂ transcription termination site cloning

The *rrnB* ribosomal terminator T₁T₂ of pKK223-3 plasmid (Pharmacia, Uppsala, Sweden) which was cloned into a pMOD-1 vector (Epicentre Biotechnologies, Madison, WI) previously in our lab was amplified using T1T2SacI forward and T1T2ClaI reverse primers. The PCR protocol was as follows: 94°C for 5 min followed by 35 cycles of 94°C for 30 sec, 43°C for 30 sec, and 72°C for 1 min, and then a final step of 72°C for 15 min. Size confirmation and cloning of PCR product and restriction analysis of constructs (except for *ClaI/SacI* digestion instead of *EcoRI* digestion) were performed as described previously. The transformant pCR2.1-T1T2 #9 was chosen after sequence confirmation.

Construction of pMOD-2-kan^r-prom-luxI-T1T2 #7 (or pMO-L #7) plasmid

pMOD-2-kan^r-prom-luxI-T1T2 #7 (or pMO-L #7) plasmid was constructed to clone *kan^r*-*S. aureus* phage Φ85 X8 promoter-*S. aureus* RBS-*luxI* CDS-T₁T₂ fragment into *S. aureus* phage Twort genome using transposition since phage genome was not sequenced at that point. The fragment to be transposed was placed in between two ME sites which are recognized by the EZ::TN transposase (Invitrogen, Carlsbad, CA).

kan^r gene was cloned into EZ::TN pMOD-2<MCS> plasmid (Epicentre Biotechnologies, Madison, WI). The source of the gene was pYES2.1/V5-His-TOPO plasmid (Invitrogen, Carlsbad, CA) carrying two copies of *kan^r* from TA cloning vector pCR2.1 (Invitrogen, Carlsbad, CA). This plasmid was constructed in our lab previously (lab stock). The pYES2.1/V5-His-TOPO-*kan^r* and pMOD-2 plasmids were digested with *HindIII* (Promega, Madison, WI) at 37°C for 105 min according to manufacturer instructions. The pMOD-2 digest was purified using QIAquick Gel Extraction Kit

(Qiagen Inc., Valencia, CA) following the manufacturer protocol. Then, it was dephosphorylated with calf intestine alkaline phosphatase (CIAP; Promega, Madison, WI) at 37°C according to manufacturer's procedure. Digested and dephosphorylated pMOD-2 and digested pYES2.1/V5-His-TOPO-*kan*^r plasmids were run on a 1% agarose gel with EtBr in 0.5XTBE for 90 min. DNA bands of pMOD-2 and *kan*^r were screened under UV light, excised from the gel, and purified with QIAquick Gel Extraction Kit (Qiagen Inc., Valencia, CA). Concentrations of pMOD-2 plasmid and *kan*^r insert purified from the gel were measured as 33 ng/μl and 2 ng/μl, respectively. The ligation reaction set after this contained 5.1 ng pMOD-2 vector, 24 ng *kan*^r insert, 1x ligase buffer, and 1 unit T4 DNA ligase (Promega, Madison, WI). The reaction was incubated at 16°C overnight. Five μl of the ligation reaction were chemically transformed into *E. coli* DH5α. Plasmids from overnight cultures of selected transformant colonies were purified using rapid boiling mini-prep method (see above) and screened with *Hind*III digestion (Promega, Madison, WI) for the presence of the *kan*^r insert. Plasmids from selected transformants with the insert were purified using Wizard Plus Midi-Preps DNA Purification Systems (Promega, Madison, WI) according to manufacturer's instructions and sequenced. The transformant carrying the correct *kan*^r sequence in the correct orientation was selected and named pMOD-2-*kan*^r #2.

To integrate *luxI* into pMOD-2-*kan*^r #2 vector, pCR2.1-*luxI* #13 and pMOD-2-*kan*^r #2 were digested with *Kpn*I and *Bam*HI in the presence of 1X multicore buffer (Promega, Madison, WI) following manufacturer instructions. After digestion, pMOD-2-*kan*^r #2 was purified from the solution by QIAquick Gel Extraction Kit (Qiagen Inc., Valencia, CA) and dephosphorylated with CIAP. Then pMOD-2-*kan*^r #2 and *Kpn*I and

*Bam*HI-digested pCR2.1-luxI #13 were run on a gel and screened as described previously. The pMOD-2-kan^r #2 and *luxI* bands were purified using QIAquick Gel Extraction Kit (Qiagen Inc., Valencia, CA). For ligation of *luxI* into the pMOD-2-kan^r #2 vector, 100 ng vector and 167.34 ng insert were mixed in the presence of 1X buffer and one unit T4 DNA ligase (Promega, Madison, WI). After overnight incubation at 16°C, *E. coli* DH5α cells were transformed with the reaction. Transformants obtained were screened as described previously using *Kpn*I and *Bam*HI. Transformant pMOD-2-kan^r-luxI #6 was chosen for further experiments after sequencing.

The rRNB ribosomal terminator T₁T₂ cut out of pCR2.1-T₁T₂ #9 was integrated into pMOD-2-kan^r-luxI #6 in the same way as described previously. *Cla*I and *Sac*I were used in the presence of buffer E (Promega, Madison, WI) for digestion of plasmids and for restriction analysis. Final DNA concentrations for ligation reaction were 293 ng pMOD-2-kan^r-luxI #6 and 28 ng T₁T₂. The selected construct was named pMOD-2-kan^r-luxI-T₁T₂ #2.

The X8 promoter sequence (605) of phage Φ85 was cloned from pCR2.1-phage85prom #8 into pMOD-2-kan^r-luxI-T₁T₂ #2 using the same methods described previously. *Sal*I and *Not*I (Promega, Madison, WI) were used for digestion of plasmids which were ligated while restriction analysis was performed with *Sal*I and *Pst*I (Promega, Madison, WI). Concentrations of pMOD-2-kan^r-luxI-T₁T₂ #2 vector and X8 promoter insert were 196 ng and 176.37 ng, respectively, in the ligation reaction. The construct pMOD-2-kan^r-prom-luxI-T₁T₂ #7 (or pMO-L #7; see Table A in the appendix for a complete list of alternative names used for plasmids) was selected for further experiments (Figure 3-1).

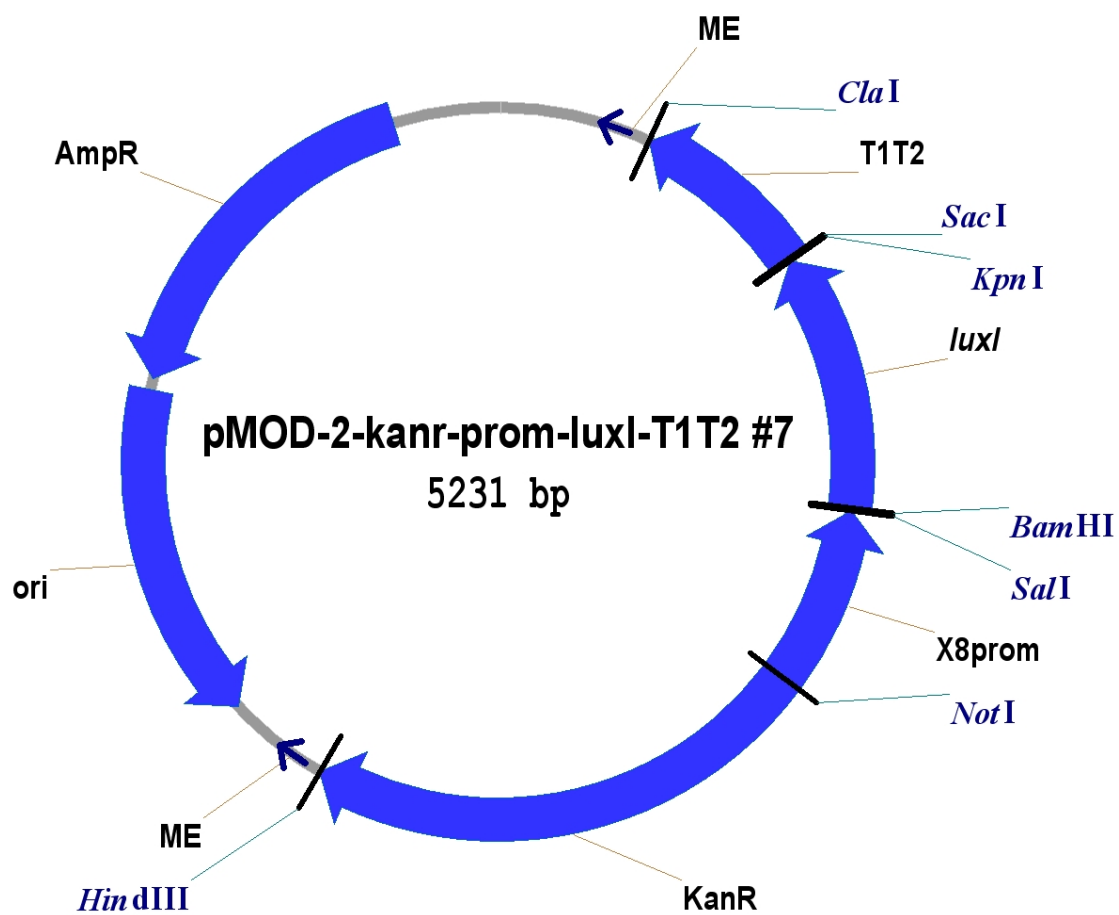


Figure 3-1. pMOD-2-kan^r-prom-luxI-T1T2 #7 (or pMO-L #7) plasmid

Bioluminescent and fluorescent detection of OHHL from pMO-L #7 in *E. coli*

Bacterial cultures were prepared by growing strains overnight in LB with antibiotics at 37°C and 220 rpm. Strains were OHHL bioreporters, RoLux and *E. coli* MT102 with pJBA132; positive and negative controls, *E. coli* strains carrying pCR2.1-TOPO P_L-*luxI* and pMOD-2-kan^r #2, respectively; and *E. coli* harboring pMO-L #7. Overnight cultures of controls and pMO-L #7-carrying *E. coli* were diluted 100 times in fresh LB without antibiotics and grown at 37°C and 220 rpm until they reached mid-exponential growth (OD₆₀₀=0.5-0.7). Supernatants were collected and used for the experiment after cultures were centrifuged at 10,000 x g for 20 min. Pellets of bioreporter overnight cultures were resuspended in the same volume of fresh LB after centrifugation at 10,000 x g for 20 min. Resuspended cells were diluted to OD₆₀₀=0.1 with fresh LB containing antibiotics to use for the experimental setup. One hundred µl of the supernatant from the strain to be tested for OHHL production was combined with 100 µl of the bioreporter in a well of a Costar 96-well black microtiter plate with a clear bottom (Corning Inc. Life Sciences, Lowell, MA) in triplicate. Bioluminescence, fluorescence, and absorbance were measured at 28°C overnight with a Wallac Victor2 1420 Multilabel Counter (PerkinElmer Life and Analytical Sciences, Waltham, MA). A diagram of the methodology is shown in Figure 3-2. The protocol consisted of a cycle of shaking for 10 sec, absorbance measurement at 450 nm, shaking for 10 sec, bioluminescence measurement (CPS), shaking for 10 sec, fluorescence measurement (GFP), and incubation for 20 min. Bioluminescence and fluorescence values were normalized by dividing CPS and GFP values by OD₄₅₀ values of bioreporters. Then, the average of triplicate measurements at each time point was calculated and used to construct charts.

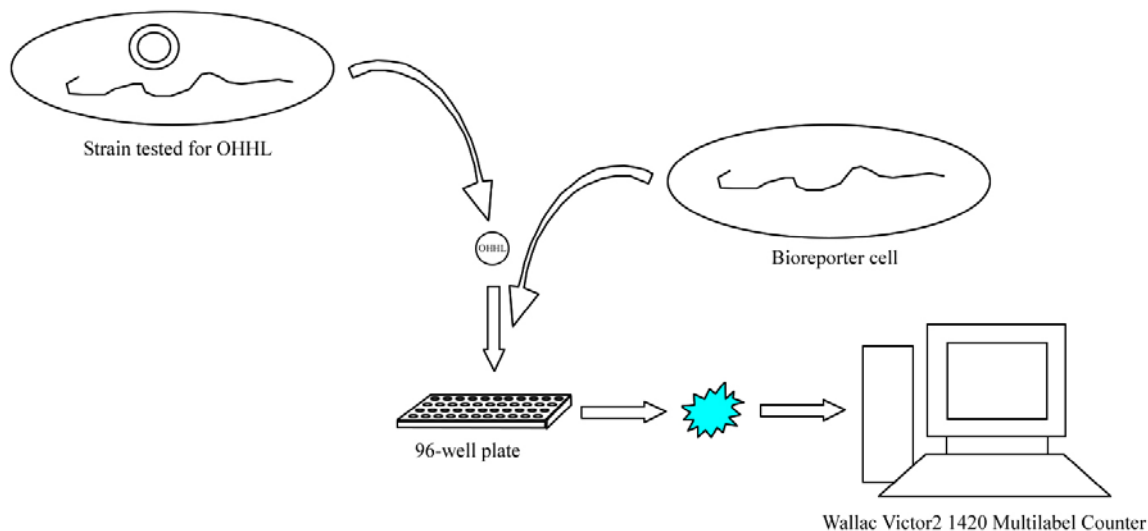


Figure 3-2. Methodology for bioluminescent and fluorescent OHHL measurement from bacterial strains that carry *luxI*.

Construction of pMK4-prom-*luxI* #13.3 (or pMK-L #13.3)

pMK4 is a Gram-positive and -negative shuttle vector. *luxI* CDS was cloned into pMK4 under the control of *S. aureus* RBS and phage Φ85 X8 promoter to test OHHL production from *luxI* inside *S. aureus*.

To clone the phage Φ85 X8 promoter sequence (605) and the *luxI* gene from pMO-L #7 into pMK4, both plasmids were digested with *Hae*II (Promega, Madison, WI) at 37°C according to manufacturer's instructions. pMK4 digest (5.6 µg) was purified with QIAquick Gel Extraction Kit (Qiagen Inc., Valencia, CA) and then dephosphorylated with CIAP (Promega, Madison, WI). This was followed by another purification step with QIAquick Gel Extraction Kit this time from the dephosphorylation solution. The remaining portion of pMK4 digest (620 ng) and 3 µg pMO-L #7 digest were run on a

0.4% agarose gel with EtBr in 0.5xTBE. The gel was screened using UV illumination to detect whether pMK4 digestion was successful and to determine the pMO-L #7 digestion products based on size. The DNA band which contained the promoter and *luxI* genes from pMO-L #7 were excised from the gel and purified using the QIAquick Gel Extraction Kit (Qiagen Inc., Valencia, CA). The promoter and *luxI* genes were integrated into dephosphorylated and purified pMK4 plasmid in a ligation reaction with 742 ng insert and 277 ng vector in the presence of one unit T4 DNA Ligase (Promega, Madison, WI). The reaction was incubated at 16°C overnight and then transformed into chemically competent *E. coli* DH5 α . Plasmids obtained from transformants were screened with *HaeII/XbaI*, *SmaI*, *PstI*, *HaeII*, *HindIII*, *SacI/XbaI*, *NotI/SacI*, *PvuII/SacI*, and *XbaI/NotI* (Promega, Madison, WI) digestions and sequenced in the same manner described previously. Two copies of the promoter and *luxI* genes were integrated into pMK4. To eliminate one of the copies, the selected construct was digested with *SacI* (Promega, Madison, WI) and the digest was run on the gel as described previously. The DNA band which included pMK4 with one copy of the promoter and *luxI* was purified from the gel and ligated onto itself in the presence of T4 DNA Ligase (Promega, Madison, WI). After transformation, screening with *KpnI* (Promega, Madison, WI) digestion, and sequencing (following protocols described previously), the construct which carried one copy of the promoter and *luxI* in pMK4 was selected and named pMK4-prom-luxI #13.3 (or pMK-L #13.3; see Table A in the appendix for a complete list of alternative names used for plasmids). A construction scheme and a diagram of the plasmid are shown in Figures 3-3 and 3-4, respectively.

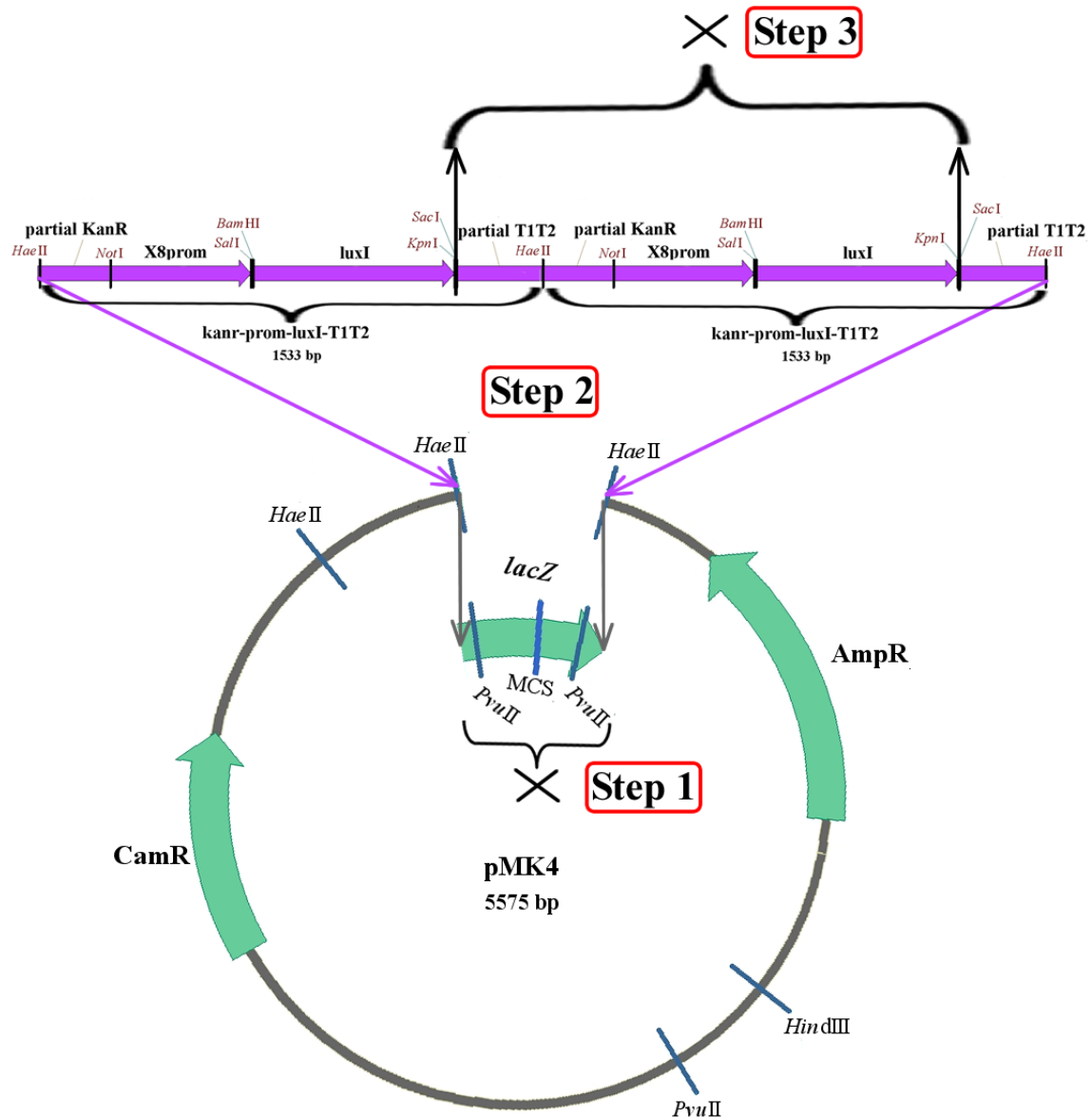


Figure 3-3. Construction of pMK4-prom-luxI #13.3 (or pMK-L #13.3). *lacZ* of pMK4 was exchanged with two copies of the fragment that contained partial *kan^r*, X8 promoter, *luxI*, and partial T₁T₂ from pMO-L #7 (steps 1 and 2). One of the copies was removed in step 3. (MCS=*HindIII*/*PstI*/*SalI*/*BamHI*/*SmaI*/*EcoRI*)

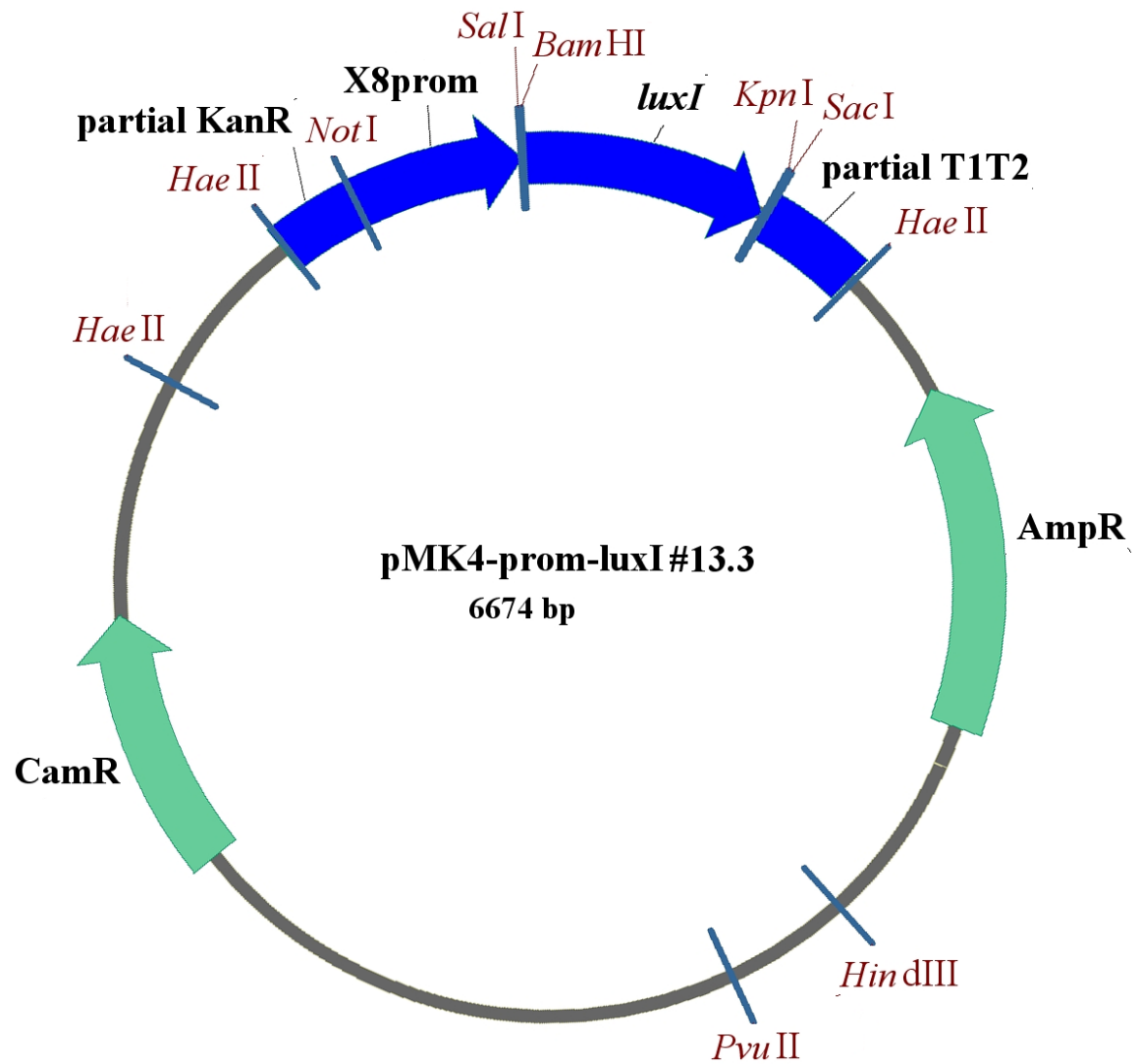


Figure 3-4. pMK4-prom-luxI #13.3 (or pMK-L #13.3) plasmid

Transfer of pMK-L #13.3 into *B. subtilis* and *S. aureus*

pMK-L #13.3 was electroporated into electrically competent *B. subtilis* cells. Plasmids were purified from overnight cultures of resulting transformants in LB with the antibiotic using Wizard Plus Midi-Preps DNA Purification Systems (Promega, Madison, WI). Plasmids were screened for the presence of pMK-L #13.3 by *Xba*I (Promega, Madison, WI) restriction analysis at 37°C. Digests were run on a 0.3% agarose gel with EtBr in 0.5xTBE. The *B. subtilis* transformants which carry pMK-L #13.3 were detected based on digest size after screening the gel with UV illumination.

The plasmid of the selected *B. subtilis* transformant was used to electroporate electrically competent cells of *S. aureus* SA113 strain. Plasmids were purified from transformants using MasterPure Gram Positive DNA Purification Kit (Epicentre Biotechnologies, Madison, WI) and digested with *Xba*I (Promega, Madison, WI) at 37°C. They were run on a 0.4% agarose gel with EtBr in 0.5xTBE. The *S. aureus* SA113 cell containing pMK-L #13.3 was determined by screening the gel with UV light and tested for OHHL production.

Bioluminescent detection of OHHL from pMK-L #13.3 in *S. aureus* using Wallac 1450 Microbeta Plus Liquid Scintillation Counter

Bioluminescent bioreporter RoLux, negative control (*E. coli* carrying pMO-L #7), positive control (*E. coli* with pCR2.1-TOPO PL-*luxI*), and *S. aureus* harboring pMK-L #13.3 were grown overnight in LB with antibiotics at 37°C and 220 rpm. Overnight cultures except for the bioreporter culture were inoculated into fresh LB without antibiotics (100 µl culture into 10 ml LB), and grown at 37°C with 220 rpm until their

OD₆₀₀ reached 0.5-0.7. Then, cells were centrifuged at 10,000 x g for 20 min and supernatants were collected. The bioreporter overnight culture cells, after being washed with LB twice, were resuspended in LB with the antibiotic, diluted to OD₆₀₀=0.1 with antibiotic-containing LB, and used for the assay. A Costar 24-well black microtiter plate with a black bottom (Corning Inc. Life Sciences, Lowell, MA) was used to combine 100 µl supernatant of the strain to be tested for OHHL production, 100 µl of the bioreporter resuspension, and 100 µl LB with the antibiotic in each well. Each sample was prepared in triplicate. Bioluminescence values were measured with a Wallac 1450 Microbeta Plus Liquid Scintillation Counter (PerkinElmer Life and Analytical Sciences, Waltham, MA). The methodology is shown in Figure 3-2. The protocol was repetition of bioluminescence measurement (CPS) followed by incubation for 20 min which carried on overnight at 28°C. Average CPS measurement in triplicate was calculated for each sample. Bioluminescence versus time charts were constructed using these average values.

Fluorescent detection of OHHL from pMK-L #13.3 in *S. aureus* using Wallac Victor2 1420 Multilabel Counter

Experimental conditions and strains used were the same as described previously with several exceptions. The fluorescent bioreporter *E. coli* MT102 with pJBA132 which was diluted to OD₆₀₀ = 0.1 with LB was used instead of RoLux. The supernatant (100 µl) of the strain to be tested for OHHL production and 100 µl of the bioreporter resuspension were mixed in each well of the 96-well black microtiter plate with a clear bottom. The negative control was the fluorescent bioreporter, 100 µl of which was combined with 100 µl dH₂O in the microtiter well. Wallac Victor2 1420 Multilabel Counter recorded the

fluorescence and absorbance measurements where a cycle of shaking for 10 sec, absorbance measurement at 450 nm, shaking for 20 sec, fluorescence measurement (GFP), and incubation for 20 min was repeated overnight at 28°C. Fluorescence measurements were normalized by dividing GFP by OD₄₅₀ values. The average of normalized fluorescence values in triplicate were calculated and used for construction of charts.

Construction of the pHPS9-luxI #7 (or pHP-L #7) plasmid

luxI CDS was placed into pHPS9 under the control of *S. aureus* RBS and *L. lactis* promoter P59 to control *luxI* OHHL production in *S. aureus*. To integrate *luxI* into Gram-positive and -negative shuttle expression vector pHPS9, *Sall* and *Bam*HI sites were added to the 5' and 3' ends of *luxI*, respectively. For this, *luxI* was amplified from the *V. fischeri* genome using luxISall forward and luxIBamHI reverse primers. This process also added the *luxI* RBS region used for construction of pMO-L #7 to the sequence. Conditions for PCR included a step of 94°C for 5 min followed by 35 cycles of 94°C for 30 sec, 48°C for 30 sec, and 72°C for 40 sec, and a final step of 72°C for 15 min. Cloning of the PCR product into the TOPO TA cloning vector pCR2.1 (Invitrogen, Carlsbad, CA) and screening of transformants (with *Eco*RI digestion) were performed as described previously. The construct pCR2.1-luxI #30 was selected.

pCR2.1-luxI #30 and pHPS9 were digested with *Sall*/*Bam*HI (Promega, Madison, WI) in a reaction with 1x buffer D at 37°C. Digests were run on a 0.5% agarose gel with EtBr in 0.5xTBE. After screening gel with UV light, DNA bands to be purified were determined based on size. To clone *luxI* under the control of the P59 promoter in place of

cat-86 in pHPS9, the larger size pHPS9 fragment was purified leaving the smaller band in the gel after digestion with *Sall/BamHI*, which removed the *cat-86* gene. Also, the *luxI* fragment cut out of pCR2.1-*luxI* #30 was purified from the gel using QIAquick Gel Extraction Kit (Qiagen Inc., Valencia, CA). DNA Ligation Kit Ver.2.1 (Takara Bio Inc., Shiga, Japan) was used to ligate 528 ng of purified *luxI* fragment to 502 ng of the purified pHPS9 fragment following manufacturer instructions. The reaction was incubated overnight at 16°C. Then 9 µl of the reaction were mixed with one µl Solution III of DNA Ligation Kit Ver.2.1 (Takara Bio Inc., Shiga, Japan) to increase transformation efficiency. The mixture was chemically transformed into *E. coli* DH5α. Transformants were screened as described previously with *Sall/BamHI* digestion followed by sequencing. The construct chosen was named pHPS9-*luxI* #7 (or pHP-L #7; see Table A in the appendix for a complete list of alternative names used for plasmids) (Figure 3-5).

Transfer of pHP-L #7 into *S. aureus*

pHP-L #7 was electroporated into electrically competent *S. aureus* RN4220 cells. Plasmids from overnight transformant cultures were purified using the Plasmid Midi Kit (Qiagen Inc., Valencia, CA) following the protocol suggested by the manufacturer for *Staphylococcus* spp. plasmid purification. They were screened for the presence of *luxI* insert by *Sall/BamHI* digestion at 37°C followed by electrophoresis with a 0.5% agarose gel with EtBr in 0.5xTBE. The *S. aureus* RN4220 transformant which carried pHP-L #7 was selected after screening the gel for the insert with UV illumination. The selected plasmid was sequenced to confirm results. *Staphylococcus aureus* RNN4220 strain containing pHP-L #7 was tested for OHHL production.

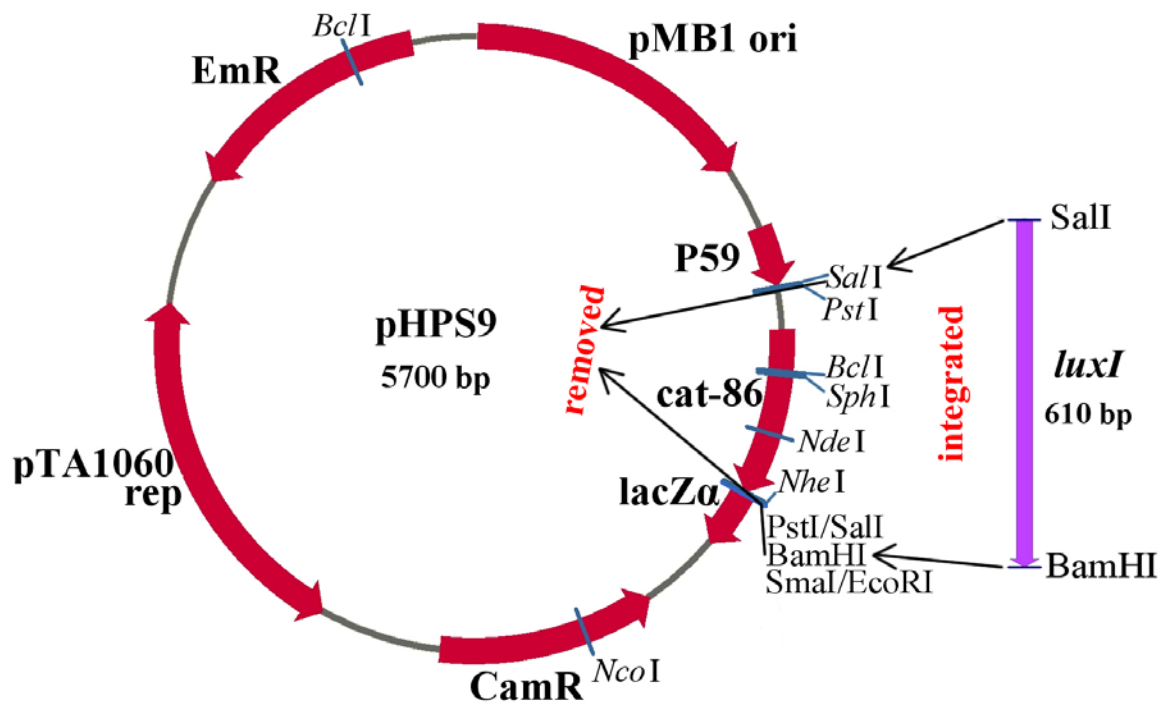


Figure 3-5. Construction of pHPS9-luxI #7 (or pHP-L #7). *cat-86* of pHPS9 was exchanged with *luxI*, which placed *luxI* under the control of Gram-positive P59 promoter.

Fluorescent detection of OHHL from pHP-L #7 in *E. coli* and *S. aureus* using Wallac Victor2 1420 Multilabel Counter

Two different negative controls were used for these assays, a bioreporter alone mixed with dH₂O which replaced the sample supernatant for *E. coli* with pCR2.1-TOPO P_L-*luxI* (positive control), and *E. coli* carrying pHP-L #7. The bioluminescent detection bioreporter was RoLux and the fluorescent detection bioreporter was *E. coli* MT102 with pJBA132. For *S. aureus* with pHP-L #7, the wild type *S. aureus* RN4220 strain was used as the negative control. Strains were grown overnight in LB with antibiotics at 37°C. Overnight cultures, except for bioreporter strain cultures, were reinoculated into fresh LB without antibiotics (100 µl culture into 10 ml LB), and grown at 37°C until they reached mid-log phase (OD₆₀₀= 0.5-0.6 for *E. coli* and 0.6-1.5 for *S. aureus*). Supernatants collected after centrifugation at 10,000 x g for 15 min were passed through 0.22 µm filters and used for assays. Overnight cultures of bioreporters, washed with LB, were diluted to OD₆₀₀ = 0.1 with LB containing antibiotics. Each assay was carried out in a Costar 96-well black microtiter plate with a clear bottom (Corning Inc. Life Sciences, Lowell, MA). For samples which were tested for OHHL production, the positive control, and the *S. aureus* negative control, 100 µl of supernatant of each strain were mixed with 100 µl bioreporter dilution in a well while 100 µl dH₂O combined with 100 µl bioreporter solution was used as the negative control for *E. coli* strains (Figure 3-2). Each was prepared in triplicate. Fluorescence and absorbance from samples were monitored by a Wallac Victor2 1420 Multilabel Counter. The protocol consisted of shaking for 10 sec, absorbance measurement at 450 nm, shaking for 20 sec, fluorescence measurement (GFP), and incubation for 20 min. This cycle was repeated overnight at 28°C.

Measurements were normalized by dividing GFP by OD₄₅₀ values, averages were calculated, and used for bioluminescence or fluorescence versus time charts.

Bioluminescent detection of OHHL from pHP-L #7 in *E. coli* and *S. aureus* using Wallac 1450 Microbeta Plus Liquid Scintillation Counter

Experiments were completed in the same way as described previously with the following exceptions. A Costar 96-well black microtiter plate with a black bottom (Corning Inc. Life Sciences, Lowell, MA) was used in measurements made by a Wallac 1450 Microbeta Plus Liquid Scintillation Counter (PerkinElmer Life and Analytical Sciences, Waltham, MA). The bioluminescence measurement (CPS) following incubation for 20 min repeated overnight was the experimental protocol. Assays 1, 2, and 5 were done at 28°C while assays 3 and 4 were performed at 30°C. The average of CPS measurements was calculated for each sample to construct charts.

Detection of OHHL from pHP-L #7 in *E. coli* and *S. aureus* using Liquid Chromatography Mass Spectrometry (LCMS)

Overnight cultures of *E. coli* and *S. aureus* harboring pHP-L #7 were diluted 100 times in fresh LB with antibiotics. These 100 ml cultures were grown at 37°C with 220 rpm in 500 ml flasks for 24 h. Twenty ml of each 24 hour-culture were completed to 200 ml by adding fresh LB with antibiotics. These 200ml-cultures were incubated at 37°C with 220 rpm in one liter flasks. Fifty ml samples from each culture were collected after incubations of 2 (the time₀ sample) and 24 h (the time₂₄ sample). These samples were used for OHHL extraction.

To extract OHHL from cultures, each 50 ml sample was mixed with 50 ml ethyl acetate in a 125 ml separation funnel and shaken manually for 30 min with frequent ventilations. The mixture was allowed to stand for 10 min for separation. The top layer, which is OHHL-containing ethyl acetate, was collected in a 250 ml flask. The bottom layer of medium and cells were left in the funnel. Fresh ethyl acetate (50 ml) was added to this and shaken manually for another 30 min with frequent ventilations. After separation, the top layer was transferred to the flask which contained the first top layer collected and the bottom layer was discarded. Ethyl acetate was evaporated. The OHHL that remained in the flask was dissolved in 6 ml methanol and transferred to a 10 ml vial. Methanol was evaporated by exposing the solution to nitrogen gas. The OHHL that remained in the tube was stored at -20°C until it was used for LCMS analysis. Each OHHL sample was brought to room temperature and dissolved in 500 µl methanol just before analysis. The standard was a synthetic OHHL solution (Sigma-Aldrich Co., St. Louis, MO) dissolved in dH₂O (1 mg/ml). The instrument and equipment used for OHHL detection were LCQ Deca XP^{plus} LCMS and Ace 3 C18 column (Advanced Chromatography Technologies, Aberdeen, Scotland) #ACE-111-1046 with dimensions of 10 cmx4.6 mm Id. Four scans were done within a mass range of 100-350 for MS. APCI was used for MS with the following specifications: source heater temperature of 300°C, sheath gas flow rate of 35 arb, aux/sweep gas flow rate of 10 arb, discharge current of 5 µA, capillary temperature of 250° C, capillary voltage of 17 V, and tube lens offset of 20 V. The LCMS conditions used are shown in Table 3-6.

Table 3-6. LCMS conditions used to detect OHHL from the standard (OHHL in dH₂O) and pHP-L #7 in *E. coli* and *S. aureus*.

Minute	Water%	Methanol%	Flow rate (µl/minute)
0	80	20	200
1	80	20	200
21	30	70	200
24	30	70	200

Construction of pHPS9-kanR #4 (or pHP-K #4)

kan^r coding sequence (CDS) from pDG148-Stu was cloned into the pHPS9 plasmid under the control of the pHPS9 promoter P59 and the RBS which was used for *luxI* expression in the pHP-L #7 construct. This was done to determine the pHPS9 promoter P59 efficiency by placing a gene other than *luxI* under its control. *kan^r* CDS was amplified using kanRSalI forward and kanRBamHI reverse primers from pDG148-Stu. The PCR protocol consisted of a step of 94°C for 5 min, 35 cycles of 94°C for 30 sec, 55°C for 30 sec, and 72°C for 50 sec, and finally a step of 72°C for 15 min. The PCR product screening and cloning into the TOPO TA cloning vector pCR2.1 (Invitrogen, Carlsbad, CA) were carried out as described previously. Transformants were screened with *EcoRI* restriction analysis and sequenced. The clone selected was named pCR2.1-kanR #10.

pHPS9 and pCR2.1-kanR #10 were cut with *SalI* and *BamHI* (Promega, Madison, WI) at 37°C in the presence of 1X buffer D. Digests were run on a 0.5% agarose gel with EtBr in 0.5XTBE. The gel was screened under UV illumination to detect DNA fragments to be used based on size. Digestion of the pHPS9 plasmid resulted in two fragments, the region between *SalI* and *BamHI* sites which is mostly the *cat-86* gene and the remaining

part of the plasmid. The goal was to replace the region between *SalI* and *BamHI* sites with *kan^r*. Therefore, the pHPS9 portion without the *cat-86* gene was cut out of the gel and purified using the QIAquick Gel Extraction Kit (Qiagen Inc., Valencia, CA). *kan^r* from the digested pCR2.1-kanR #10 was purified from the gel in the same way. *kan^r* (54 ng) was integrated into 81 ng pHPS9 which was purified from the gel using one unit T4 DNA Ligase (Promega, Madison, WI). After overnight incubation at 16°C, 4 µl of the solution were transformed into chemically competent *E. coli* TOP10 cells (Invitrogen, Carlsbad, CA). Transformants obtained were screened with *SalI/BamHI* restriction analysis and sequenced as explained above. The selected transformant was called pHPS9-kanR #4 (or pHP-K #4; see Table A in the appendix for a complete list of alternative names used for plasmids) (Figure 3-6).

Transfer of pHP-K #4 into *S. aureus*

pHP-K #4 was electroporated into electrically competent *S. aureus* RN4220 cells. *Staphylococcus aureus* transformants were screened using *SalI/BamHI* digestion. The *S. aureus* transformant which carried the construct was tested for kanamycin resistance.

Detection and analysis of kanamycin resistance provided by pHP-K #4 in *E. coli* and *S. aureus*

Cultures of *E. coli* and *S. aureus* with pHP-K #4 were plated onto LB plates containing kanamycin concentrations in the range of 2.5-70 µg/ml. Results were compared to kanamycin resistance patterns provided by the other plasmids and constructs which carry *kan^r* under the control of various promoters and RBSs.

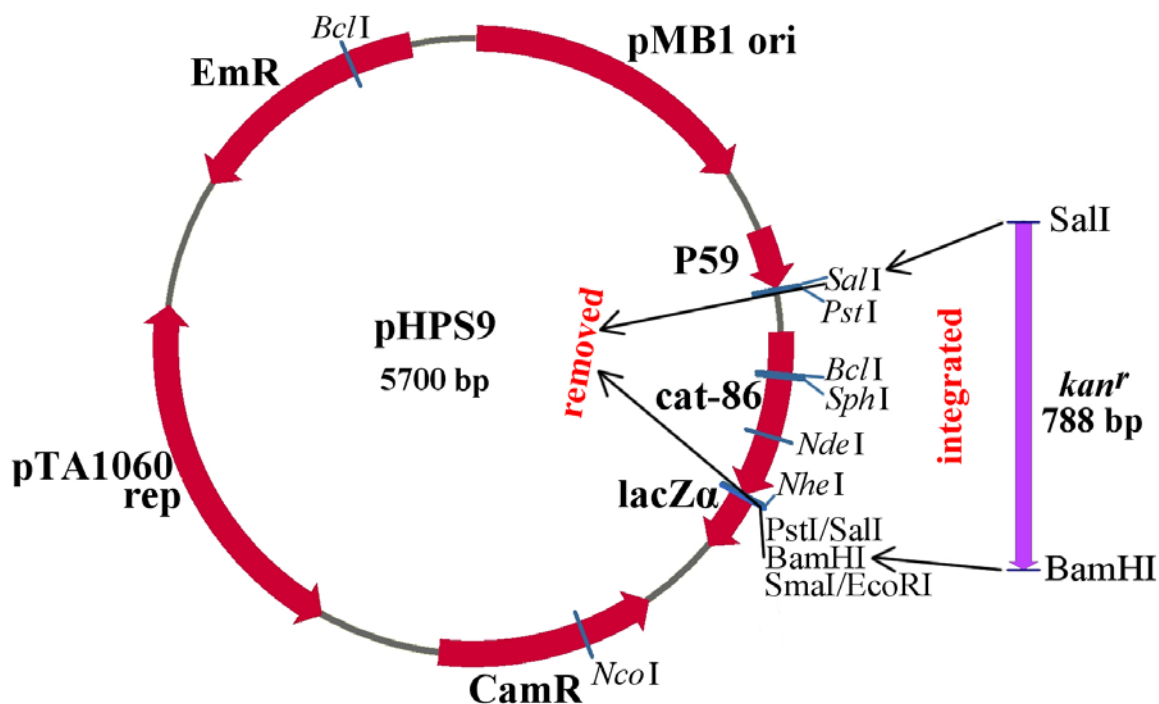


Figure 3-6. Construction of pHPS9-kanR #4 (or pHP-K #4). *cat-86* was exchanged with *kan^r* from pDG148-Stu, which placed *kan^r* under the control of Gram-positive P59.

Construction of pDG148-Stu-luxI #28 (or pDG-L #28)

The *luxI* CDS was cloned into a Gram-positive and -negative shuttle expression vector, pDG148-Stu, under the control of the plasmid's Gram-positive promoter and RBS. pDG148-Stu promoter is a hybrid promoter of the *B. subtilis* phage SPO-1 and the *lac* operator, *Pspac*, which is regulated by the IPTG-inducible LacI repressor.

First, *luxI* CDS was amplified from pMO-L #7 using luxIStuI forward and luxIStuI reverse primers to add *StuI* enzyme sites to the 5' and 3' ends of the gene. The PCR protocol consisted of a first step of 94°C for 5 min followed by 35 cycles of 94°C for 30 sec, 42°C for 30 sec, and 72°C for 42 sec, and a final step of 72°C for 15 min. PCR product screening and cloning into the TOPO TA cloning vector pCR2.1 (Invitrogen,

Carlsbad, CA); and transformant screening with *EcoRI* digestion and sequencing were performed as described previously. The construct pCR2.1-luxI #3 was selected for further cloning.

pCR2.1-luxI #3 and pDG148-Stu were digested with *StuI* enzyme (Promega, Madison, WI) at 37°C. pCR2.1-luxI #3 digest (8080 ng) and an aliquot of pDG148-Stu digest (601 ng) were run on a 0.5% agarose gel with EtBr in 0.5xTBE. UV illumination of the gel showed the resulting DNA fragments, confirming the digestion of pDG148-Stu and spotting the *luxI* bands from pCR2.1-luxI #3. *luxI* bands were cut out of the gel and purified with QIAquick Gel Extraction Kit (Qiagen Inc., Valencia, CA) to use for ligation. The portion of the pDG148-Stu digest which was not run on the gel was purified the same way for ligation. *luxI* (221 ng) integration into pDG148-Stu (50 ng) was done using the DNA Ligation Kit<Mighty Mix> (Takara Bio Inc., Shiga, Japan). The ligation reaction was transformed into chemically competent *E. coli* TOP10 cells (Invitrogen, Carlsbad, CA). Transformants were screened with *EcoRI/BamHI* restriction analysis and sequenced. The transformant which was chosen was called pDG148-Stu-luxI #28 (or pDG-L #28; see Table A in the appendix for a complete list of alternative names used for plasmids) (Figure 3-7).

Transfer of pDG-L #28 into *S. aureus*

Attempts to electroporate pDG-L #28 into electrically competent *S. aureus* RN4220 cells was unsuccessful. pDG148-Stu could not be electroporated into *S. aureus* RN4220 either.

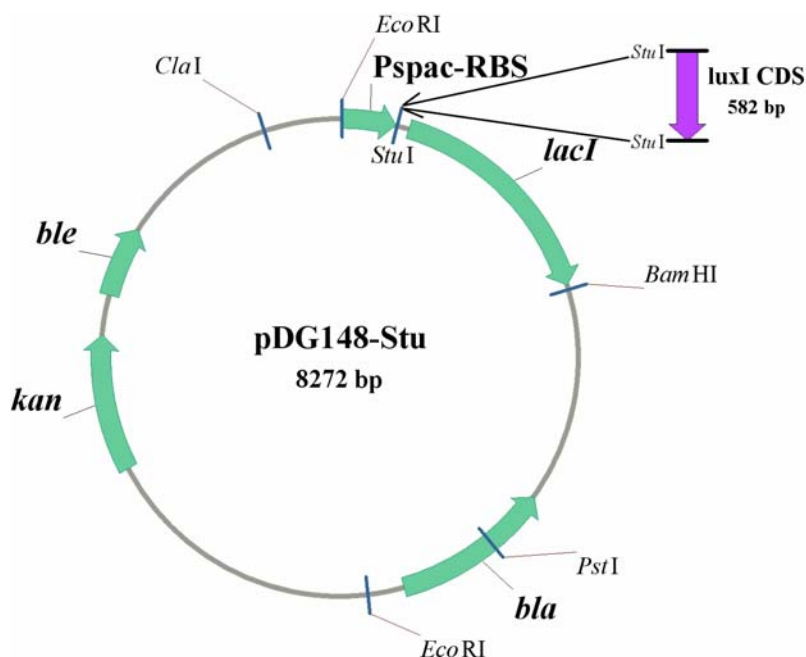


Figure 3-7. Construction of pDG148-Stu-*luxI* #28 (or pDG-L #28). *luxI* was placed under the control of Gram-positive *Pspac* and RBS.

Construction of pHPS9-sht-*Pspac*-*luxI*-*lacI* #9 (or pHP-PL #9)

pDG148-Stu which is 8.3 kb and pDG-L #28 which is 8.85 kb could not be electroporated into *S. aureus* RN4220. A smaller construct was formed to electroporate *luxI* under the control of *Pspac* and RBS of pDG148-Stu into *S. aureus* more easily.

First, a smaller version of the pHPS9 plasmid was created. For this, pHPS9 was first digested with *PstI* (Promega, Madison, WI) and run on a 0.5% agarose gel with EtBr in 0.5xTBE. The digestion produced two fragments: the 0.7 kb-region between two *PstI* sites which contained *cat-86* and the remaining part of the plasmid which is 5 kb. The 5-kb fragment of the plasmid was purified from the gel using QIAquick Gel Extraction Kit (Qiagen Inc., Valencia, CA) after UV light screening. This fragment (360 ng) was

religated onto itself using DNA Ligation Kit Ver.2.1 (Takara Bio Inc., Shiga, Japan). The ligation reaction was transformed into chemically competent *E. coli* TOP10 cells (Invitrogen, Carlsbad, CA). Transformants were screened with *Pst*I (Promega, Madison, WI) digestion as described previously. The transformant selected was named pHPS9-sht #7. This process shortened the plasmid from 5.7 kb to 5 kb.

To clone pDG-L #28 region between *Eco*RI and *Bam*HI sites which contained *Pspac*, RBS, *luxI*, and *lacI* into pHPS9-sht #7, both plasmids were digested with *Eco*RI and *Bam*HI in the presence of 1x buffer E (Promega, Madison, WI) at 37°C. Digests were run on a 0.5% agarose gel with EtBr in 0.5xTBE. DNA bands on the gel which contained digested-pHPS9 and the pDG-L #28 fragment of *Pspac*, RBS, *luxI*, and *lacI* were spotted based on size using UV illumination. They were cut out of the gel and purified with QIAquick Gel Extraction Kit (Qiagen Inc., Valencia, CA). Two ligation reactions were set up using DNA Ligation Kit Ver.2.1 (Takara Bio Inc., Shiga, Japan): the reaction with the vector:insert ratio of 1:5 (82 ng pHPS9-sht #7:190 ng *Pspac*, RBS, *luxI*, and *lacI*) and the reaction with the vector:insert ratio of 1:10 (41 ng pHPS9-sht #7:190 ng *Pspac*, RBS, *luxI*, and *lacI*). Reactions were transformed into chemically competent *E. coli* TOP10 cells (Invitrogen, Carlsbad, CA). Transformants obtained were screened with *Pst*I digestion and sequenced as described previously. Based on these results, the construct pHPS9-sht-Pspac-luxI-lacI #9 (or pHP-PL #9; see Table A in the appendix for a complete list of alternative names used for plasmids) was selected. A construction scheme for the plasmid is shown in Figure 3-8. The size of the plasmid which carries *luxI* under the control of pDG148-Stu promoter *Pspac* and RBS was decreased from 8854 bp to 7256 bp with the construction of pHPS9-sht-Pspac-luxI-lacI #9 (or pHP-PL #9)

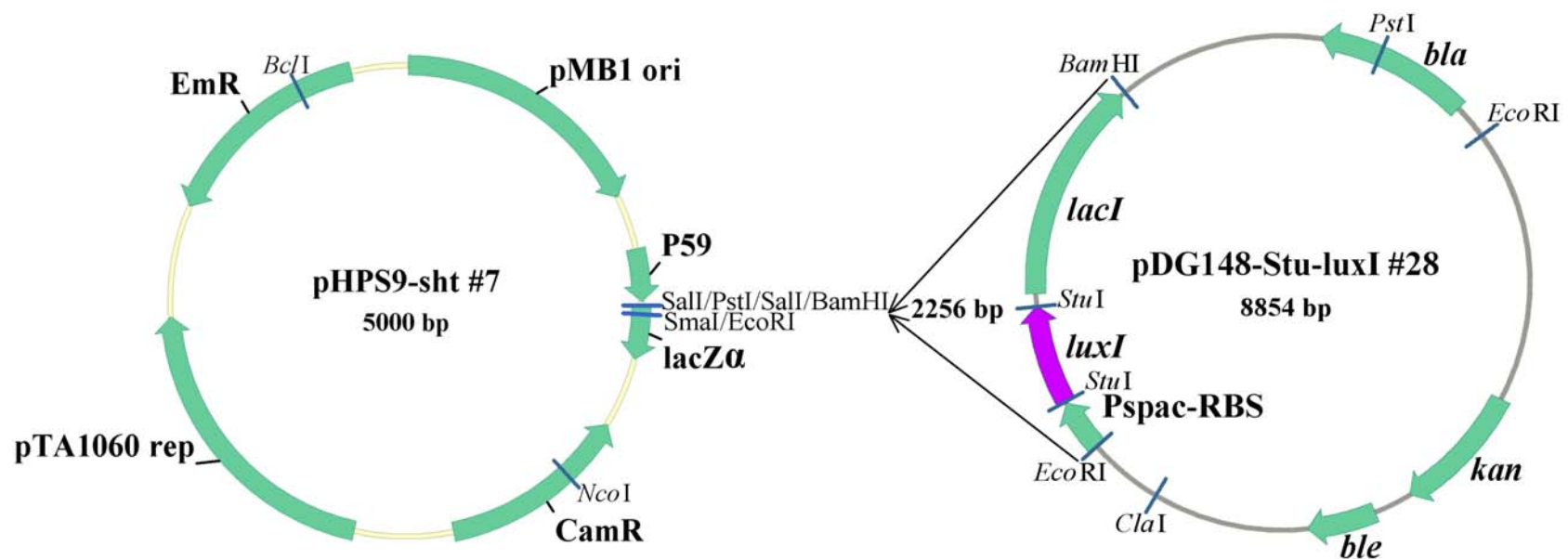


Figure 3-8. Construction of pHPS9-sht-Pspac-luxI-lacI #9 (or pHP-PL #9). *Pspac*, RBS, *luxI*, and *lacI* from pDG-L #28 (or pDG148-Stu-luxI #28) were inserted into pHPS9-sht #7, which resulted in construction of a smaller plasmid with *luxI* under the control of *Pspac* and RBS of pDG148-Stu.

Transfer of pHP-PL #9 into *B. subtilis* and *S. aureus*

pHP-PL #9 was electroporated into electrically competent *B. subtilis* and *S. aureus* RN4220 cells. Plasmids of *B. subtilis* transformant overnight cultures were purified using Wizard Plus Midi-Preps DNA Purification Systems (Promega, Madison, WI) according to manufacturer instructions. Instructions suggested by the manufacturer for Wizard Plus Midi-Preps DNA Purification Systems (Promega, Madison, WI) were modified to purify plasmids from transformant *S. aureus* overnight cultures. Cells of each *S. aureus* transformant culture were suspended in 1/10 volume with the suspension buffer of the kit. Fifty µl (for every 10 ml of the overnight culture) lysostaphin enzyme solution (0.5 mg/ml) which is capable of specifically degrading *S. aureus* cell walls were added into the resuspended culture. The solution was incubated at 37°C for 17 min. The remainder of the protocol was carried out as suggested by the manufacturer. Plasmids were screened with *Pst*I/*Bam*HI restriction analysis for both *B. subtilis* and *S. aureus* and also sequenced for *S. aureus* as described previously. The selected *B. subtilis* and *S. aureus* transformants which carried pHP-PL #9 were tested for OHHL production.

Bioluminescent and fluorescent detection of OHHL from pDG-L #28 in *E. coli* and pHP-PL #9 in *E. coli*, *B. subtilis*, and *S. aureus* using Wallac Victor2 1420 Multilabel and 1450 Microbeta Plus Liquid Scintillation Counters

For OHHL detection from pDG-L #28 in *E. coli*, the strain itself, bioluminescent bioreporter *E. coli* OHHLux, and fluorescent bioreporter *E. coli* MT102 with pJBA132 were grown overnight in LB with antibiotics at 37°C. The overnight culture of *E. coli* harboring pDG-L #28 (100 µl) was inoculated into fresh LB without antibiotic (10 ml)

and grown at 37°C until mid-log phase ($OD_{600} = 0.86$). To induce the *Pspac* promoter of pDG-L #28, the culture was divided into 3 tubes with 3.2 ml in each, following procedures described by Joseph et al. (611). The control tube contained no IPTG while 0.5 mM IPTG was added into one tube and 2 mM IPTG was added into the other. Cultures continued to grow at 37°C for 2 h. After this, supernatants were collected, passed through 0.22 μ m filters, and used for the experimental set-up. Overnight cultures of bioreporters were washed with LB, diluted to $OD_{600} = 0.1$ in fresh LB containing antibiotics, and used for the experiment. A Costar 96-well black microtiter plate with a clear bottom (Corning Inc. Life Sciences, Lowell, MA) was used for Wallac Victor2 1420 Multilabel Counter (PerkinElmer Life and Analytical Sciences, Waltham, MA) measurements and a Costar 96-well black microtiter plate with a black bottom (Corning Inc. Life Sciences, Lowell, MA) was used for Wallac 1450 Microbeta Plus Liquid Scintillation Counter (PerkinElmer Life and Analytical Sciences, Waltham, MA) measurements. Each sample was prepared by combining 100 μ l supernatant with 100 μ l bioreporter dilution in triplicate (Figure 3-2). Negative controls contained 100 μ l bioreporter dilution (*E. coli* OHHLux or *E. coli* MT102 with pJBA132) combined with 100 μ l dH₂O instead of the supernatant, each in triplicate. Wallac Victor2 1420 Multilabel Counter measurements of fluorescence and absorbance followed a protocol of shaking for 10 sec, absorbance measurement at 450 nm, shaking for 20 sec, fluorescence measurement (GFP), and incubation for 20 min. The protocol was repeated overnight at 28°C. Fluorescence data obtained were normalized by dividing GFP values by OD_{450} values. The mean of normalized values for triplicate measurements of each sample was used for construction of the graphs. Wallac 1450 Microbeta Plus Liquid Scintillation

Counter protocol consisted of bioluminescence measurement (CPS) every 20 min of incubation repeated overnight at 28°C. Charts were prepared using the mean of each sample's triplicate measurement versus time.

OHHL detection from pHP-PL #9 in *B. subtilis* and *S. aureus* was performed assertively in the same way with a few differences. The negative control for *S. aureus* with pHP-PL #9 was the wild type *S. aureus* strain RN4220 whose supernatant was combined with the bioreporter dilution for measurements. Cultures from which supernatants were collected were grown to mid-log phase with OD₆₀₀= 0.62 for the positive control, 1.1 for the negative control *S. aureus* RN4220, 1 for *S. aureus* carrying pHP-PL #9, and 0.57 for *B. subtilis* harboring pHP-PL #9. The IPTG concentrations used for promoter *Pspac* induction were 2 and 3 mM. Incubation continued for 1 h after IPTG addition.

OHHL production from pHP-PL #9 in *E. coli*, *B. subtilis* and *S. aureus* was determined with bioluminescent and fluorescent measurements using the Overnight Express Autoinduction System 1 (Novagen, Darmstadt, Germany) instead of IPTG to induce the promoter *Pspac*. The Overnight Express Autoinduction System provided optimized media components to combine with a glucose-free complex medium, such as LB. The resulting medium allowed bacteria to reach high cell densities and then induced protein expression by its lactose component. It was developed to induce protein expression, without IPTG and needs to be used with IPTG-inducible hosts. *Escherichia coli*, *B. subtilis* and *S. aureus* containing pHP-PL #9 and *S. aureus* RN4220 as the negative control for plasmid-carrying *S. aureus* were grown in Overnight Express Autoinduction System 1 medium without antibiotics at 37°C overnight as suggested by

the manufacturer with the exception of 260 rpm shaking instead of 300 rpm. Supernatants of overnight cultures were collected, filtered through 0.22 μ m filters and used for the experiment. Overnight cultures of bioluminescent and fluorescent bioreporters in LB with antibiotics were diluted to OD₆₀₀= 0.1 in fresh LB with antibiotics and used. Negative controls for *B. subtilis* and *E. coli* strains were bioreporters combined with dH₂O instead of supernatants. The remainder of the experiment was carried out as described previously.

The *luxI* transcript detection from pHP-PL #9 and pDG-L #28 using real-time quantitative reverse transcriptase PCR

Real-time quantitative reverse transcriptase PCR (qRT-PCR) was used to test the efficiency of *Pspac* promoter in *E. coli*, *B. subtilis* and *S. aureus* by detecting the *luxI* transcript. Overnight cultures of *E. coli*, *B. subtilis* and *S. aureus* containing pHP-PL #9, *E. coli* with pDG-L #28, and the wild type *S. aureus* RN4220 (negative control) were diluted (1:100) into fresh LB with antibiotics and grown at 37°C until mid-log phase. The RNAp Protect Bacteria Reagent (Qiagen Inc., Valencia, CA) was added to cultures. RNA from cultures was extracted using the RNeasy kit (Qiagen Inc., Valencia, CA) and the RNase-Free DNase Set (Qiagen Inc., Valencia, CA) which provided on-column DNase digestion. Protocols were carried out as suggested by the manufacturer with several modifications. Disruption of *E. coli* and *B. subtilis* cell walls was done by incubating cells with lysozyme for 30 min; while *S. aureus* was incubated with lysostaphin (7.5 ng/ml culture) for 45 min and then with lysozyme for 15 min. The extracted RNA was quantified using the Quant-iT RiboGreen RNA Assay Kit (Molecular Probes-Invitrogen, Carlsbad, CA) and The Versafluo Fluorometer (Bio-Rad, Hercules, CA). Quantified

DNA was subjected to real-time qRT-PCR using QuantiTect Probe RT-PCR reagents (Qiagen Inc., Valencia, CA) in an Opticon DNA Engine (MJ Research, Inc., Waltham, MA) thermocycler with fluorescence detector. LuxI-qRT forward and reverse primers and LuxI-q5'P probe with a 5' fluorophore, FAM, and a 3' quencher, BHQ (black hole quencher) were used for reactions. The LuxI-q5'P probe sequence from 5' to 3' is CAGTATCATCACAAGCATAAATATA TTCTGCATT. Each sample was prepared in triplicate with an additional reaction which lacked the reverse transcriptase to control DNA contamination. The same amount of RNA (125 ng) was used for each reaction. Reactions were placed into a 96-well microtiter plate and measured. The protocol for real-time qRT-PCR followed these steps: 50°C RT reaction for 30 min, 95°C RT inactivation for 15 min, and then 45 cycles of 95°C denaturation for 15 sec, 58°C annealing/extension for 30 sec, and a fluorescence measurement. Baseline start and end cycles were 3 and 7, respectively. Data were analyzed using Opticon Monitor Analysis Software Version 1.08.

***luxI* translation product detection from pHP-PL #9 and pDG-L #28 using SDS-PAGE and Western Blotting**

The presence of LuxI protein in *E. coli*, *B. subtilis* and *S. aureus* harboring pHP-PL #9, and *E. coli* carrying pDG-L #28 was tested by Sodium Dodecyl Sulfate-Polyacrylamide Gel Electrophoresis (SDS-PAGE) and Western Blotting. Pellets from mid-log phase cultures (20 ml each) of experimental strains and wild type *S. aureus* RN4220 (negative control) were subjected to protein extraction. Soluble and insoluble proteins of samples were extracted using the B-PER Bacterial Protein Extraction Reagent

(Pierce, Rockford, IL) with the midi-scale protocol supplied by the manufacturer. Incubation time for *B. subtilis* soluble protein extraction was changed from 10 min to 26 min. Also, *S. aureus* soluble protein extraction was performed with 50 mg lysostaphin and the B-PER reagent at 37°C for 25 min. The whole protocol was carried out in the presence of Halt Protease Inhibitor Cocktail, EDTA Free (Pierce, Rockford, IL) as suggested by the manufacturer.

Since *B. subtilis* soluble protein yield was low with B-PER Bacterial Protein Extraction Reagent (Pierce, Rockford, IL), the extraction was repeated using a French Press. The pellet of a 500 ml mid-log phase culture of *B. subtilis* harboring pHP-PL #9 was dissolved in 50 ml lysis buffer (50 mM Tris pH 8.0, 5 mM EDTA, 200 mM NaCl, 1 mM PMSF). After homogenization with a glass homogenizer, the solution was lysed by a French Press using three cycles at 16,000 psi. The supernatant of the cell lysate was used as the soluble protein fraction.

SDS-PAGE was used to check protein yields from extractions. Extracts were loaded into wells of a Criterion Precast Gel, 12.5% Tris-HCL, 1 mm, 12+2 comb, 45 µl (Bio-Rad, Hercules, CA). The gel was run at 200 V for about 1 h in a Criterion vertical electrophoresis cell (Bio-Rad, Hercules, CA). Proteins on the gel were stained using GelCode Blue Stain Reagent (Pierce, Rockford, IL) following instructions of the manufacturer.

To detect the LuxI protein, Western Blotting was performed using the LuxI antibody from rabbit antisera (Genemed Synthesis Inc., San Francisco, CA; Lot No: 31465 Antiserum; ID: Antibody Rabbit #1423) which targets the LuxI sequence, AVGKNSSKINNSASEITM. Another SDS-PAGE was done for Western Blotting. After

the SDS-PAGE, proteins were transferred from the unstained gel onto a Sequi-Blot PVDF Membrane (0.2 μ m; Bio-Rad, Hercules, CA) using the EBU-4000 Semi-Dry Blotter System (C.B.S. Scientific Co., Del Mar, CA) which was run at 200 mA for 1 h. The membrane was blocked in 10% milk blocking solution (in 1X TTBS; 20mM Tris-HCL pH 7.6, 150 mM NaCl, 0.1% Tween 20) for 2 h at room temperature with gentle shaking. After blocking, it was incubated with the LuxI antibody (100-250X diluted) in 2.5% milk (in 1X TTBS) overnight at 4°C without shaking. The membrane was washed in 1X TTBS for 30 min at room temperature with gentle shaking by changing the buffer every 10 min. This was followed by incubation of the membrane with the secondary antibody (2800-3000X diluted) in 1X TTBS for 2 h at RT with gentle shaking. ImmunoPure Goat Anti-Rabbit IgG, (H+L), Alkaline Phosphatase Conjugated (Pierce, Rockford, IL) was used as the secondary antibody. The membrane was washed as before. Color development was carried out using the Alkaline Phosphatase Conjugate Substrate Kit (Bio-Rad, Hercules, CA) as suggested by the manufacturer. The membrane was incubated with color development solution for 7 min at room temperature with gentle shaking. The reaction was stopped by washing the membrane in dH₂O for 10-25 min at room temperature with gentle shaking.

Construction of pHPS9-sht-Pspac-kanR-lacI #31 (or pHP-PK #31)

The RBS efficiency of the construct pHP-PL #9 in *S. aureus* which produces the *luxI* transcript but not the LuxI protein and light was tested by replacing the *luxI* CDS with the CDS of a *S. aureus*-native gene, *kan^r*.

kan^r CDS with the 5' and 3' *Stu*I enzyme sites was placed into TOPO TA cloning vector pCR2.1 (Invitrogen, Carlsbad, CA) after PCR using the *kanRStu*I forward and reverse primers and pDG148-Stu as the template. PCR conditions were a first step of 94°C for 5 min, then 35 cycles of 94°C for 30 sec, 58°C for 30 sec, and 72°C for 47 sec, and a final step of 72°C for 15 min. Transformant screening with *Eco*RI restriction analysis and sequencing were done as described previously. The construct was named pCR2.1-*kanRStu*I #12.

kan^r CDS did not directly replace *luxI* CDS in pHP-PL #9 construct since *Stu*I enzyme was found not only at the 5' and 3' ends of *luxI*. *kan^r* CDS was first integrated into pDG148-Stu. pCR2.1-*kanRStu*I #12 and pDG148-Stu were digested with *Stu*I (Promega, Madison, WI) at 37°C. All of the pCR2.1-*kanRStu*I #12 digest (9.45 µg) and 975 ng of the pDG148-Stu digest were run on a 0.5% agarose gel with EtBr in 0.5xTBE. Digestion products were screened on the gel with UV light to detect *kan^r* fragments and to verify digestion of pDG148-Stu. *kan^r* fragments were cut out of the gel and purified using QIAquick Gel Extraction Kit (Qiagen Inc., Valencia, CA). The part of the pDG148-Stu digest which was not run on the gel (1.17 µg) was purified using the same kit after digestion. Purified *kan^r* (331.5 ng) and pDG148-Stu (122 ng) were ligated using the DNA Ligation Kit<Mighty Mix> (Takara Bio Inc., Shiga, Japan) at 16°C overnight. The reaction was transformed into chemically competent *E. coli* TOP10 cells (Invitrogen, Carlsbad, CA). Transformants were screened with *Eco*RI/*Bam*HI restriction analysis and sequenced. The construct determined that contained the correct insert in the correct orientation was selected and called pDG148-Stu-*kanR* #8.

The region of pDG148-Stu-kanR #8 which contained *Pspac*, RBS, *kan^r*, and *lacI* was inserted into pHPS9-sht #7. For this, both plasmids were digested with *EcoRI* and *BamHI* in the presence of 1x buffer E (Promega, Madison, WI) at 37°C and run on a 0.5% agarose gel with EtBr in 0.5xTBE. UV illumination screening showed digestion products based on size. The digested pHPS9-sht #7 and the fragment containing *Pspac*, RBS, *kan^r*, and *lacI* were cut out of the gel and purified with QIAquick Gel Extraction Kit (Qiagen Inc., Valencia, CA). The ligation reaction was carried out with 40 ng pHPS9-sht #7 and 296 ng insert of *Pspac*, RBS, *kan^r*, and *lacI* using the DNA Ligation Kit<Mighty Mix> (Takara Bio Inc., Shiga, Japan). After overnight incubation at 16°C, the reaction was transformed into chemically competent *E. coli* TOP10 cells (Invitrogen, Carlsbad, CA). The construct pHPS9-sht-Pspac-kanR-lacI #31 (or pHP-PK #31; see Table A in the appendix for a complete list of alternative names used for plasmids) was selected after screening of transformants with *PstI* digestion and sequencing (Figure 3-9).

Transfer of pHP-PK #31 and pUB110 into *S. aureus*

pHP-PK #31 and pUB110 (for comparison) were electroporated into electrically competent *S. aureus* RN4220 cells. Plasmids of the transformants were purified as described previously with the exception that the incubation time with lysostaphin was decreased from 17 min to 10 min. pUB110 plasmid purifications were run on a 0.5% agarose gel with EtBr in 0.5xTBE. The gel was screened with UV light to detect plasmids based on size. pHP-PK #31 purifications were sequenced to determine *S. aureus* transformants which harbored the plasmid. Selected *S. aureus* transformants which carried pUB110 or pHP-PK #31 were tested for kanamycin resistance patterns.

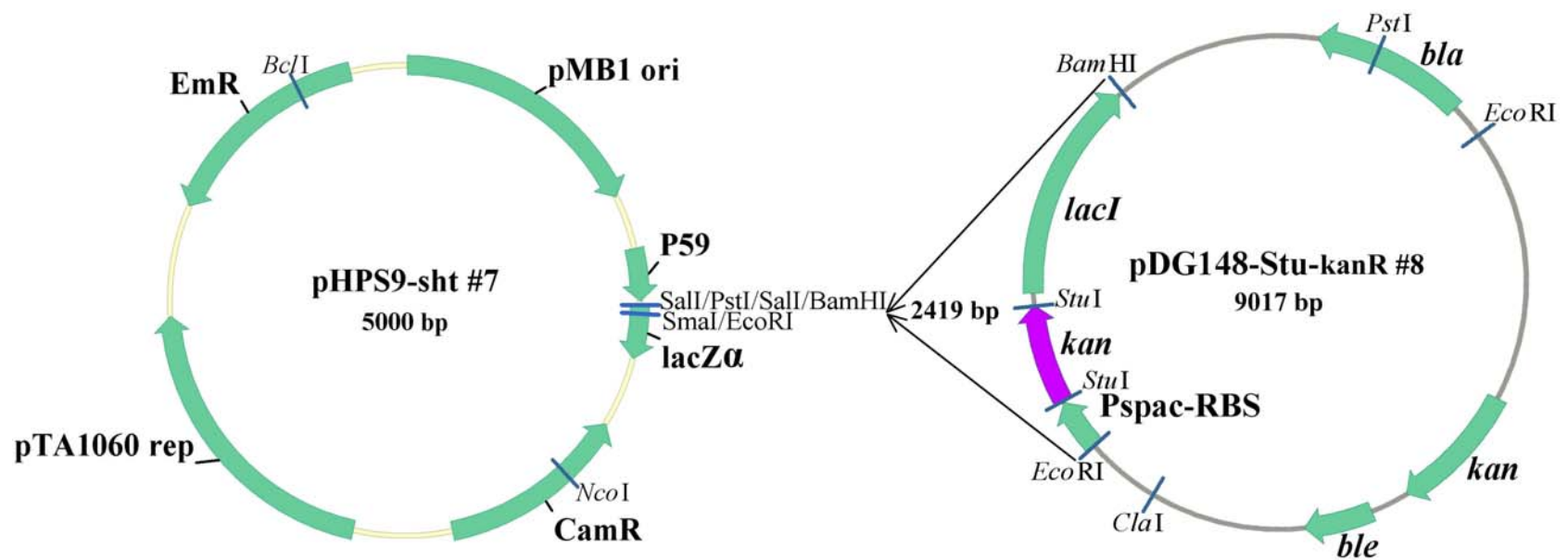


Figure 3-9. Construction of pHPS9-sht-Pspac-kanR-lacI #31 (or pHP-PK #31). *Pspac*, RBS, *kan*^r, and *lacI* were inserted into pHPS9-sht #7, which resulted in construction of a smaller plasmid with *S. aureus kan*^r under the control of *Pspac* and RBS of pDG148-Stu.

Detection and analysis of kanamycin resistance provided by pHP-PK #31 in *S. aureus*

Cultures of *S. aureus* with pHP-PK #31 and pUB110 were streaked onto LB plates containing different concentrations of kanamycin. Kanamycin resistance patterns were compared to those of the other plasmids and constructs which have the *kan^r* gene under the control of various promoters and RBSs in *S. aureus* and one another.

***luxI* CDS codon optimization for adaptation to the codon bias of *S. aureus* phage P68**

The presence of *luxI* transcript was shown in *S. aureus* with pHP-PL #9 while the LuxI protein was not detected using LuxI antibody. Also, the RBS of the construct was demonstrated to work after replacing the *luxI* CDS with *S. aureus*-native *kan^r* CDS. Therefore, to determine if the codon preference is a problem for *luxI* translation in *S. aureus*, the *luxI* CDS codon usage was adapted to the codon bias of *S. aureus* phage P68. The reason for not adapting *luxI* codons to the codon bias of *S. aureus* strain RN4220 which was used for pHP-PL #9 expression was that its genome is not sequenced yet. P68 is the phage which was planned to clone the *luxI* gene into for the construction of the recombinant phage for monitoring *S. aureus*. Phage P68 was also shown to carry genes most of which have high translation efficiency (616).

Codon optimization using the GeneOptimizer software and synthesis of the optimized gene were carried out by GENEART (Regensburg, Germany). During the process, the company avoided regions of very high (> 80%) or very low (< 30%) GC

content and cis-acting sequence motifs such as internal TATA-boxes, chi-sites and ribosomal entry sites, AT-rich or GC-rich sequence stretches, and repeat sequences and RNA secondary structures. Two negatively cis-acting motifs, one consensus TATA box and one -35 box, were found and corrected. Optimization increased the codon adaptation index (CAI) value from 0.62 to 0.98 (1 being the best score) which shows a high and stable degree of expression for the gene. Average GC content of *luxI* decreased from 33% to 27% after the optimization. Figures 3-10, 3-11, and 3-12 show details of the optimization process as reported by GENEART (Regensburg, Germany). Figure 3-13 shows sequences of non-optimized versus optimized *luxI* CDS.

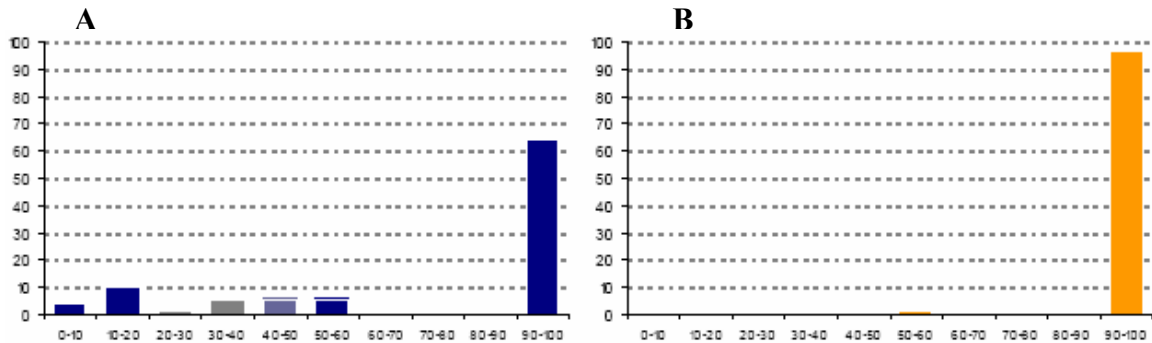


Figure 3-10. Codon quality distribution plots provided by GENEART (Regensburg, Germany) for (A) non-optimized and (B) optimized *luxI* for adaptation to the codon bias of *S. aureus* phage P68. The X-axis shows the quality class and the Y-axis shows the percentage of codons. A quality value of 100 represents the most-used codon for P68 gene expression.

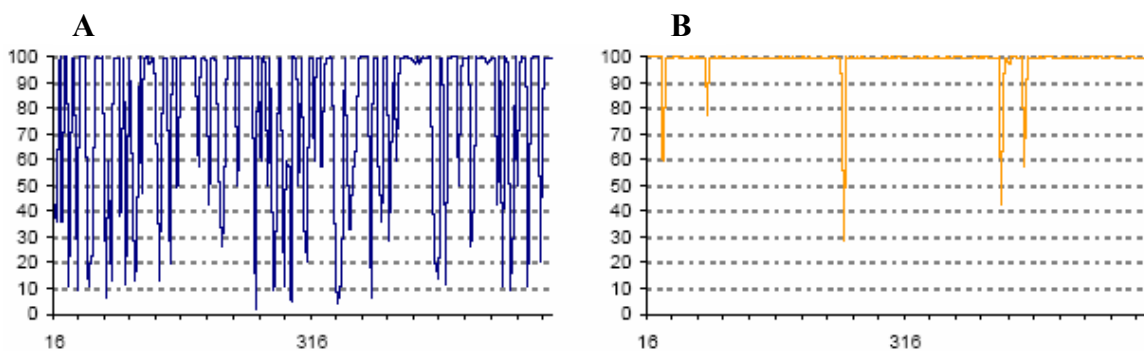


Figure 3-11. Codon quality plots provided by GENEART (Regensburg, Germany) for (A) non-optimized and (B) optimized *luxI* for adaptation to the codon bias of *S. aureus* phage P68. The X-axis shows the codon position and the Y-axis shows the quality. A quality value of 100 represents the most-used codon for P68 gene expression.

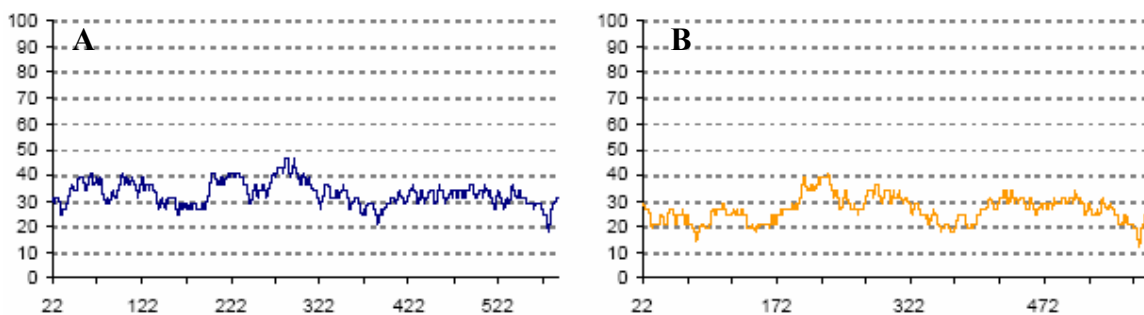


Figure 3-12. GC content plots provided by GENEART (Regensburg, Germany) for (A) non-optimized and (B) optimized *luxI* for adaptation to the codon bias of *S. aureus* phage P68. The X-axis shows the nucleotide position and the Y-axis shows the GC content.

1	ATGACTATAATGATAAAAAAATCGGATTTTTTGGCAATTCATCGGAGGA	50
	
1	ATGACAATTATGATTAAAAAAGTGATTTTTTAGCAATTCATCAGAAGA	50
51	GTATAAAGGTATTCTAAGTC--TTCGTTATCAAGTGTTAAGCAAAGACT	98
	
51	ATATAAAGGTATTTTA--TCATTAAGATATCAAGTTTTTAAACAACGTTT	98
99	TGAGTGGGACTTAGTTGTAGAAAATAACCTTGAATCAGATGAGTATGATA	148
	
99	AGAATGGGATTTAGTTGTTGAAAATAATTTAGAATCAGATGAATATGATA	148
149	ACTCAAATGCAGAATATATTTATGCTTGTGATGATACTGAAAATGTAAGT	198
	
149	ATTCAAATGCAGAATATATTTATGCATGTGATGATACAGAAAATGTTTCA	198
199	GGATGCTGGCGTTTATTACCTACAACAGGTGATTATATGCTGAAAAGTGT	248
	
199	GGTTGTTGGCGTTTATTACCAACAACAGGTGATTACATGTTAAAAATCAGT	248
249	TTTTCTGAATTGCTTGGTCAACAGAGTGTCCCAAAGATCCTAATATAG	298
	
249	TTTTCCAGAATTATTAGGTCAACAATCAGCACCAAAGATCCAAATATTG	298
299	TCGAATTAAGTCGTTTTGCTGTAGGTAAAAATAGCTCCAAGATAAATAAC	348
	
299	TGAATTATCACGTTTTGCAGTTGGTAAAAATTCATCAAAAATTAATAAT	348
349	TCTGCTAGTGAAATTACAATGAAACTATTTGAAGCTATATATAAACACGC	398
	
349	TCAGCATCAGAAATTACAATGAAATTATTTGAAGCAATTTATAAACATGC	398
399	TGTTAGTCAAGGTATTACAGAATATGTAACAGTAACATCAACAGCAATAG	448
	
399	AGTTTCACAAGGTATTACTGAATATGTAACAGTTACATCAACAGCTATTG	448
449	AGCGATTTTTTAAAGCGTATTAAAGTTTCTTGTGTCATCGTATTGGAGACAAA	498
	
449	AACGTTTTTTTAAACGTATTAAAGTTCCATGTCATCGTATTGGTGATAAA	498
499	GAAATTCATGTATTAGGTGATACTAAATCGGTTGTATTGTCTATGCCTAT	548
	
499	GAAATTCATGTTTTAGGTGATACAAAATCAGTTGTTTTATCAATGCCAAT	548
549	TAATGAACAGTTTTAAAAAAGCAGTCTTAAATTAA	582
	
549	TAATGAACAATTTAAAAAAGCAGTTTTTAAATTAATAA	585

Figure 3-13. The pairing of non-optimized (top sequence) and optimized (bottom sequence) *luxI* for adaptation to the codon bias of *S. aureus* phage P68. (Vertical lines show identical bases and dots show non-identical bases.)

Construction of pHPS9-sht-Pspac-optluxI-lacI #5 (or pHP-POL #5)

Optimized *luxI* was synthesized by assembling synthetic oligonucleotides by GENEART (Regensburg, Germany) as follows: The gene was cloned into pPCR-Script (amp^R) at the *KpnI* and *SacI* restriction sites into *E. coli* K12 XL10-GOLD. The plasmid was purified with Pure Yield Plasmid Midiprep (Promega, Madison, WI) and confirmed the sequence of *luxI* by sequencing. A map of the plasmid which was provided by GENEART (Regensburg, Germany) is shown in Figure 3-14.

The *luxI* gene integrated into plasmid pPCR-Script (0602285pPCR-Script) was transformed into chemically competent *E. coli* TOP10 cells (Invitrogen, Carlsbad, CA). Resulting transformants were screened with *KpnI*/*SacI* restriction analysis and sequenced. The transformant carrying the plasmid was selected for further experiments.

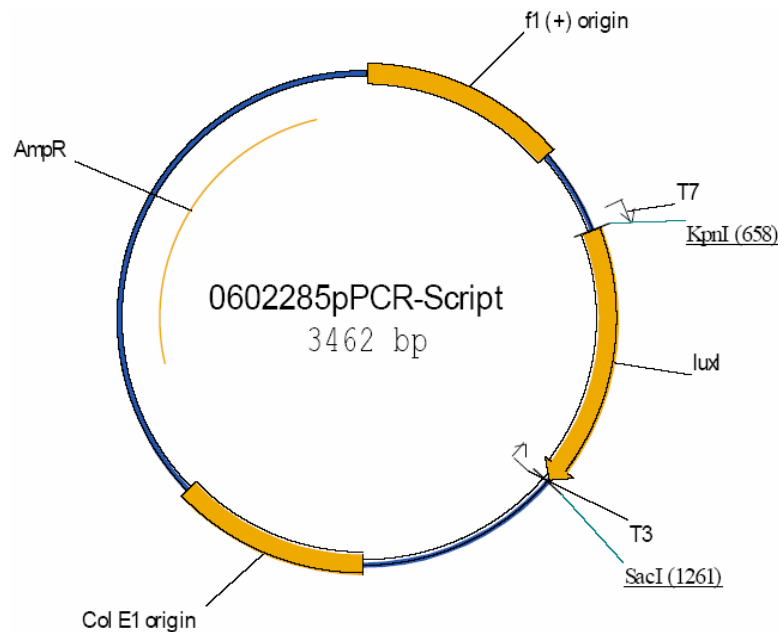


Figure 3-14. *luxI*, optimized for adaptation to the codon bias of *S. aureus* phage P68, in pPCR-Script (provided by GENEART, Regensburg, Germany)

Optimized *luxI* was first cloned into pDG148-Stu instead of directly replacing *luxI* in pHP-PL #9 which has more than two sites for *StuI*, used for *luxI* cloning. 0602285pPCR-Script and pDG148-Stu were digested with *StuI* (Promega, Madison, WI) at 37°C. While pDG148-Stu was directly purified from the reaction after digestion, the 0602285pPCR-Script digest was run on a 0.5% agarose gel with EtBr in 0.5XTBE. The gel was screened using a UV light to spot *luxI* bands based on size. *luxI* was cut out of the gel and purified. QIAquick Gel Extraction Kit (Qiagen Inc., Valencia, CA) was used for all purifications. The ligation reaction containing 69 ng digested pDG148-Stu and 290 ng *luxI* was carried out using DNA Ligation Kit<Mighty Mix> (Takara Bio Inc., Shiga, Japan). After the overnight incubation at 16°C, reactions were transformed into chemically competent *E. coli* TOP10 cells (Invitrogen, Carlsbad, CA). Transformants were screened using *EcoRI/BamHI* digestion and sequenced. The construct carrying the correct insert at the correct orientation was named pDG148-Stu-optluxI #16.

The fragment of *Pspac*, RBS, optimized *luxI*, and *lacI* was cloned from pDG148-Stu-optluxI #16 into pHPS9-sht #7. For this, pHPS9-sht #7 and pDG148-Stu-optluxI #16 were cut with *EcoRI* and *BamHI* in the presence of 1X buffer E (Promega, Madison, WI) at 37°C and then run on a 0.5% agarose gel with EtBr in 0.5xTBE. The fragment of *Pspac*, RBS, optimized *luxI*, and *lacI* and digested pHPS9-sht #7 which were spotted with UV illumination were cut out of the gel and purified using QIAquick Gel Extraction Kit (Qiagen Inc., Valencia, CA). The ligation was performed with the DNA Ligation Kit<Mighty Mix> (Takara Bio Inc., Shiga, Japan) at 16°C overnight. Two reactions were prepared, one with 86 ng pHPS9-sht #7 and 400 ng fragment of *Pspac*, RBS, *kan^r*, and *lacI* using 1:10 ratio of vector to insert and the other with 150 ng pHPS9-sht #7 and 346

ng fragment using 1:5 ratio. Transformants obtained after transfer of reactions into chemically competent *E. coli* TOP10 cells (Invitrogen, Carlsbad, CA) were screened with *Pst*I digestion and sequencing. The construct selected was called pHPS9-sht-Pspac-optluxI-lacI #5 (or pHP-POL #5; see Table A in the appendix for a complete list of alternative names used for plasmids). The construction of the plasmid was done in the same way as shown in Figure 3-8.

Transfer of pHP-POL #5 into *B. subtilis* and *S. aureus*

pHP-POL #5 was electroporated into electrically competent *B. subtilis* and *S. aureus* RN4220 cells. Plasmids were purified from transformants as before. Plasmids from *B. subtilis* were screened with *Pst*I/*Bam*HI restriction analysis while *S. aureus* plasmids were screened with both *Pst*I/*Bam*HI digestion and sequencing. Transformants which carried plasmids were tested for OHHL production.

Bioluminescent and fluorescent detection of OHHL from pHP-POL #5 in *E. coli*, *B. subtilis*, and *S. aureus* using Wallac Victor2 1420 Multilabel and 1450 Microbeta Plus Liquid Scintillation Counters

Escherichia coli, *B. subtilis*, and *S. aureus* strains carrying pHP-POL #5, wild type *S. aureus* RN4220 (negative control for *S. aureus*), *E. coli* harboring pCR2.1-TOPO PL-*luxI* (positive control), bioluminescent bioreporter *E. coli* OHHLux, and fluorescent bioreporter *E. coli* MT102 with pJBA132 were grown overnight in LB with antibiotics at 37°C. Bioreporter cultures were washed with LB, diluted to OD₆₀₀= 0.1 in LB with antibiotics and used for the assay. Cultures of other strains were diluted 100X in fresh LB

without antibiotics and grown at 37°C until mid-log phase (OD_{600} = 0.55 for positive control, 0.95 for *S. aureus* negative control, 0.88 for *E. coli* sample, 1.6 for *B. subtilis* sample, and 0.75 for *S. aureus* sample). Supernatants were collected, passed through 0.22 μ m filters and used for the assay. Each sample was prepared in triplicate by mixing 100 μ l of supernatant with 100 μ l of bioreporter dilution in Costar 96-well black microtiter plates (Corning Inc. Life Sciences, Lowell, MA). Plates with clear and black bottoms were used for Wallac Victor2 1420 Multilabel and Wallac 1450 Microbeta Plus Liquid Scintillation Counters (PerkinElmer Life and Analytical Sciences, Waltham, MA), respectively (Figure 3-2). Supernatant of *S. aureus* RN4220 was combined with bioreporter solution and used as the negative control for *S. aureus* sample. The bioreporter dilution (*E. coli* OHHLux or *E. coli* MT102 with pJBA132) mixed with dH₂O instead of supernatant was used as the negative control for *E. coli* and *B. subtilis* samples. All controls were in triplicate. The protocol followed by Wallac Victor2 1420 Multilabel Counter contained shaking for 10 sec, absorbance measurement at 450 nm, shaking for 20 sec, fluorescence measurement (GFP), and incubation for 20 min which was repeated overnight at 28°C. Fluorescence measurements were normalized by dividing GFP values by OD_{450} values. The mean of triplicate measurements for each sample was calculated to construct charts. Wallac 1450 Microbeta Plus Liquid Scintillation Counter protocol was bioluminescence measurement (CPS) followed by 20 min incubation continued repeatedly overnight at 28°C. Charts for these measurements were prepared using mean values for triplicate measurements of each sample.

Invitro packaging of *S. aureus* phage P68 genome

Staphylococcus aureus phage P68 was selected for the construction of recombinant phage carrying *luxI*. Before cloning of *luxI* into the phage genome, the phage genome alone was used for packaging to develop a method. P68 genome (0.8-1 µg) which was purified using Wizard Lambda Preps DNA Purification System (Promega, Madison, WI) was packaged invitro with MaxPlax Lambda Packaging Extracts (Epicentre Biotechnologies, Madison, WI). The packaging reaction (50-140 µl) was placed onto an LB plate with top agar (LB, 0.5% agar) containing *S. aureus* RN451 overnight culture (20 µl). The plate was incubated overnight at 37°C. The area of lysis obtained the next day was scraped off and mixed with one ml LB in a sterile tube. The solution was kept at room temperature for 1.5 h and then vortexed. The supernatant collected after the centrifugation at 8,000 x g for 10 min was passed through a 0.22 µm-filter, and tested for infectivity by pouring 600 µl of the solution mixed with top agar (LB, 0.5% agar) and *S. aureus* RN451 overnight culture (15 µl) onto an LB plate. Lysis was obtained on the plate after overnight incubation at 37°C. The remainder of the phage solution was stored at 4°C.

Statistical calculations

Bioluminescence and fluorescence values were normalized by dividing the CPS and GFP values obtained, respectively, by absorbance values at OD₄₅₀ of the bioreporter culture measured at the same time point where available. The average of triplicate measurements was calculated for each time point. Normalized values were used if the absorbance of the bioreporter culture was measured. Error bars were generated by

calculating the standard deviation (SD) of triplicate bioluminescence or fluorescence values at each time point as follows: The average of triplicate measurements (normalized where available) for a time point was subtracted from each measurement (normalized where available) at that time point. The squares of the differences were calculated. The average of all three squared differences was determined. The square root of the value found was used as the standard deviation for the average value at each time point. Significance levels were determined by comparing average bioluminescence or fluorescence values of a sample to those of the negative control using Student's *t*-test ($P < 0.05$). Maximum induction value of a sample for an assay was calculated by dividing the highest amount of light obtained from the sample during the assay by the amount of light from the negative control at the same time point.

CHAPTER IV

RESULTS

CONSTRUCTION OF *S. AUREUS* BIOREPORTER

Bioluminescent and fluorescent detection of OHHL from pMO-L #7 in *E. coli*

The *kan^r*-*S. aureus* phage Φ 85 X8 promoter-*S. aureus* RBS-*luxI* CDS-T₁T₂ fragment was placed into EZ::TN pMOD-2<MCS> plasmid (Epicentre Biotechnologies, Madison, WI) in between two MEs. MEs are sites which are recognized by the EZ::TN transposase (Epicentre Biotechnologies, Madison, WI) for transposition to occur. The aim was to clone *luxI* under the control of the *S. aureus* phage Φ 85 X8 promoter and *S. aureus* RBS into the *S. aureus* phage Twort genome randomly using transposition since the Twort genome sequence was not known at the time.

OHHL production by pMO-L #7 in *E. coli* was determined by bioluminescence and fluorescence measurements at 28°C overnight on a Wallac Victor2 1420 Multilabel Counter (PerkinElmer Life and Analytical Sciences, Waltham, MA). Bioluminescent and fluorescent OHHL bioreporters were RoLux and *E. coli* MT102 with pJBA132, respectively. The *E. coli* strains carrying pCR2.1-TOPO PL-*luxI* and pMOD-2-*kan^r* #2 were used as positive and negative controls, respectively. Each measurement represents the average of triplicate samples. Results (Figure 4-1) showed no OHHL production by pMO-L #7 in *E. coli*. Bioluminescence and fluorescence values were not significantly different from those of the negative control. The positive control produced bioluminescence and fluorescence values of 13,000 and 11,000 units, respectively.

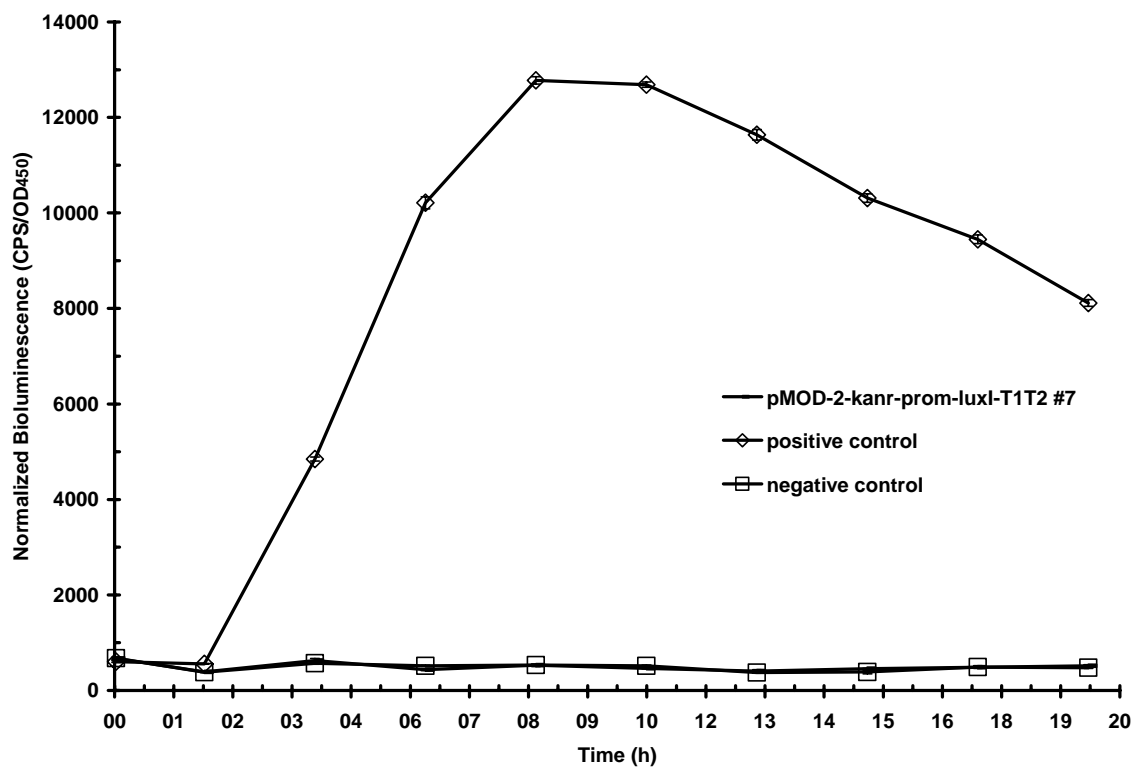


Figure 4-1 (A). Bioluminescent OHHL detection from pMO-L #7 (or pMOD-2-kan^r-prom-luxI-T1T2 #7) in *E. coli* at 28°C using bioreporter RoLux and Wallac Victor2 1420 Multilabel Counter. Results represent the mean bioluminescence values (n=3) \pm SD (bars).

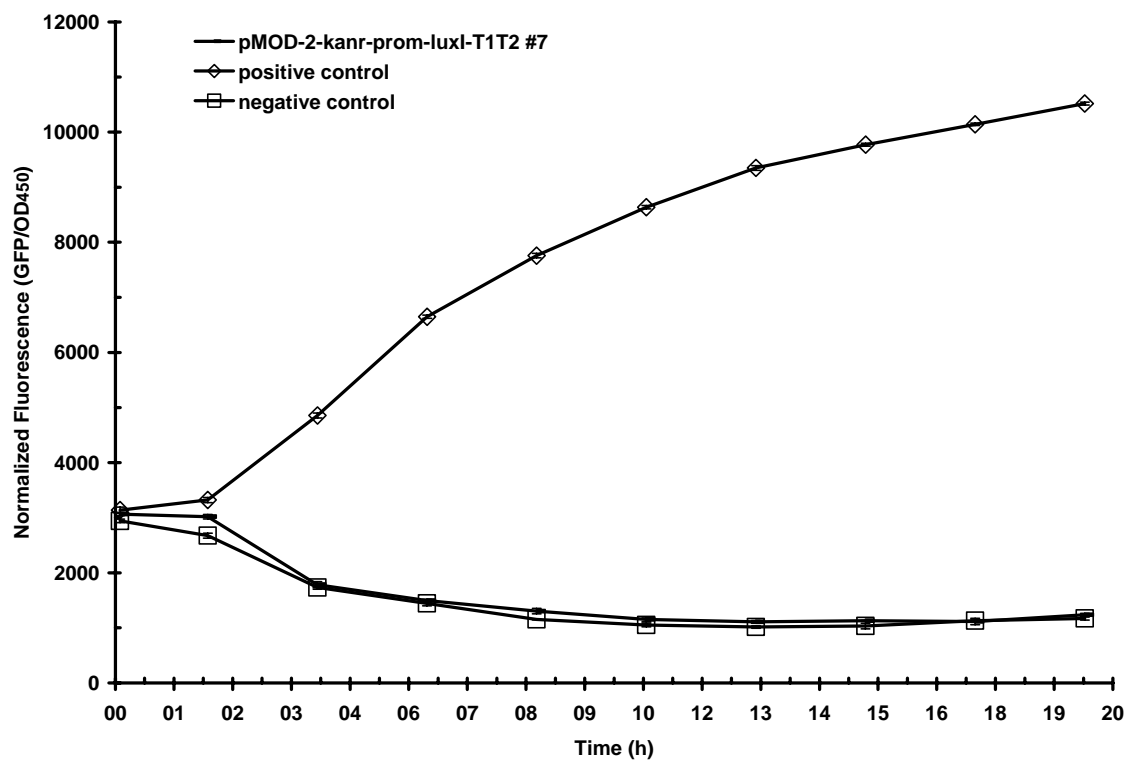


Figure 4-1 (B). Fluorescent OHHL detection from pMO-L #7 (or pMOD-2-kan^r-prom-luxI-T1T2 #7) in *E. coli* at 28°C using bioreporter *E. coli* MT102 with pJBA132 and Wallac Victor2 1420 Multilabel Counter. Results represent the mean fluorescence values (n=3) \pm SD (bars).

Bioluminescent and fluorescent detection of OHHL from pMK-L #13.3 in *S. aureus*

pMK-L #13.3 was constructed to test OHHL production from *luxI* CDS under the control of *S. aureus* RBS and phage Φ 85 X8 promoter inside *S. aureus*. pMK4 is a Gram-positive and -negative shuttle vector so construction using it can be transferred into a *S. aureus* strain.

Bioluminescent detection of OHHL from pMK-L #13.3 in *S. aureus* was done using RoLux as the bioreporter, *E. coli* with pMO-L #7 as the negative control, and *E. coli* with pCR2.1-TOPO PL-*luxI* as the positive control. The fluorescent detection bioreporter was *E. coli* MT102 with pJBA132 and the positive control was *E. coli* with pCR2.1-TOPO PL-*luxI*. The bioreporter itself was used as the negative control in the presence of dH₂O replacing the sample supernatant in fluorescence measurements. Samples were set up in a 24-well black microtiter plate with a black bottom for fluorescent detection and in a 96-well black microtiter plate with a clear bottom for bioluminescent detection in triplicate. Bioluminescence measurements taken at 28°C were collected with a Wallac 1450 Microbeta Plus Liquid Scintillation Counter (PerkinElmer Life and Analytical Sciences, Waltham, MA). Fluorescence and absorbance data were measured with a Wallac Victor2 1420 Multilabel Counter (PerkinElmer Life and Analytical Sciences, Waltham, MA) at 28°C. Bioluminescence charts represent CPS values versus time, while fluorescence charts show GFP per absorbance values versus time. Results are shown in Figure 4-2. While positive control bioluminescence and fluorescence measurements reached ~19,000 and ~34,000 units, respectively, the pMK-L #13.3 plasmid-carrying *S. aureus* produced values which were not significantly different from negative control values. Thus, the plasmid did not produce OHHL in *S. aureus* cells.

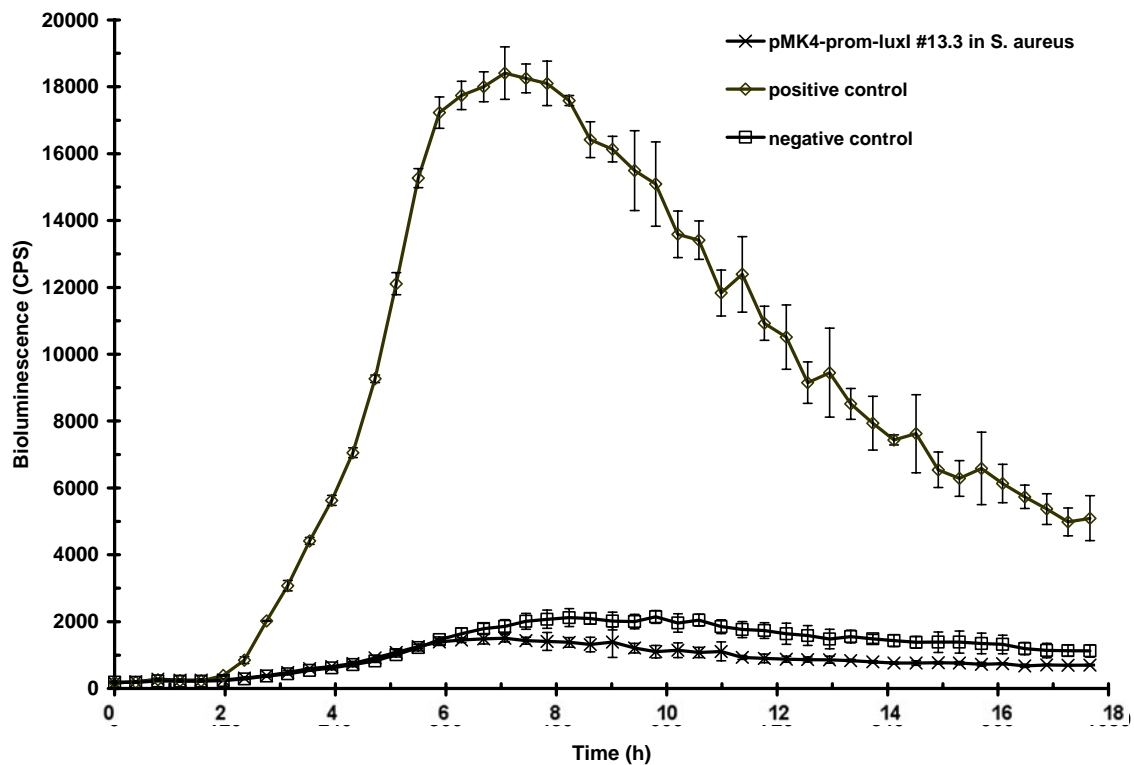


Figure 4-2 (A). Bioluminescent OHHL detection from pMK-L #13.3 (or pMK4-prom-luxI #13.3) in *S. aureus* at 28°C using bioreporter RoLux and Wallac 1450 Microbeta Plus Liquid Scintillation Counter. Results represent the mean bioluminescence values ($n=3$) \pm SD (bars).

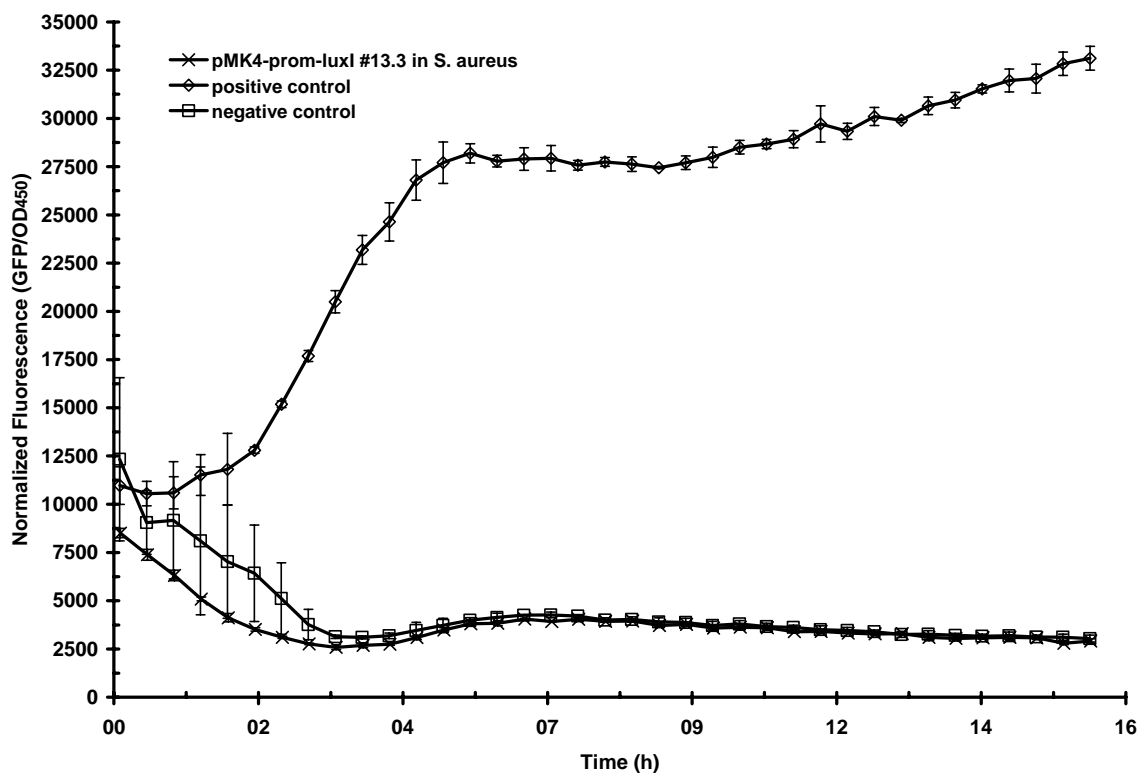


Figure 4-2 (B). Fluorescent OHHL detection from pMK-L #13.3 (or pMK4-prom-luxI #13.3) in *S. aureus* at 28°C using bioreporter *E. coli* MT102 with pJBA132 and Wallac Victor2 1420 Multilabel Counter. Results represent the mean fluorescence values ($n=3$) \pm SD (bars).

Bioluminescent and fluorescent detection of OHHL from pHP-L #7 in *E. coli* and *S. aureus* using Wallac Victor2 1420 Multilabel and Wallac 1450 Microbeta Plus Liquid Scintillation Counters

The efficiency of *L. lactis* promoter P59 from pHPS9 was tested for expression of *luxI* CDS under the control of *S. aureus* RBS by detecting OHHL produced from pHP-L #7 in *E. coli* and *S. aureus*.

The positive control used for all experiments was *E. coli* harboring pCR2.1-TOPO PL-*luxI*. The negative control for *E. coli* strains was the bioreporter used for the assay, RoLux for bioluminescence and *E. coli* MT102 carrying pJBA132 for fluorescence, while it was the wild type *S. aureus* RN4220 strain for *S. aureus* with pHP-L #7. Each sample was prepared in triplicate and measured with Wallac Victor2 1420 Multilabel and Wallac 1450 Microbeta Plus Liquid Scintillation Counters. Values from the Wallac Victor2 1420 Multilabel Counter were divided by the absorbance values to construct the graphs. Data from the Wallac 1450 Microbeta Plus Liquid Scintillation Counter were used directly since this device has no capability to measure absorbance. Each CPS or GFP value represents the average of triplicate measurements.

Five assays were performed to detect OHHL from pHP-L #7 in *E. coli* and *S. aureus* where the bioluminescence and fluorescence were measured with the Wallac Victor2 1420 Multilabel Counter and only bioluminescence was measured with the Wallac 1450 Microbeta Plus Liquid Scintillation Counter. Therefore, three sets of data were obtained from five different assays. There was no bioluminescence or fluorescence

obtained from the pHP-L #7 plasmid in *S. aureus* in any of the assays. The levels of light obtained were not significantly different from those produced by the *S. aureus* negative control. The pHP-L #7 plasmid in *E. coli* produced bioluminescence and fluorescence in varying amounts in all assays performed.

A summary of these results and the positive control results as a comparison are presented in Table 4-1. The highest induction of the bioluminescent or fluorescent bioreporter obtained with *E. coli* with pHP-L #7 in each assay changed from 1.5 to 17.4 times, compared to values obtained with the negative control. Induction values for the positive control were between 4.9 and 296.5. These values were acquired in a time period of 4.5-17.5 hours for both strains.

A bioluminescence graph formed by measurements from assay 2 by the Wallac 1450 Microbeta Plus Liquid Scintillation Counter and a fluorescence graph constructed from assay 2 measurements by the Wallac Victor2 1420 Multilabel Counter are shown as representative examples of these assays in Figure 4-3.

Table 4-1. A summary of assays for bioluminescent and fluorescent OHHL detection from pHP-L #7 in *E. coli* and positive control. The table shows maximum induction (MI; the highest amount of light from a sample divided by the negative control value at the same time point) value for each assay. RoLux and *E. coli* MT102 carrying pJBA132 were used as bioluminescent and fluorescent bioreporters, respectively. (T = Time period in h to obtain MI, Wallac 1450 = Wallac 1450 Microbeta Plus Liquid Scintillation Counter, Wallac Victor2 = Wallac Victor2 1420 Multilabel Counter)

	pHP-L #7 in <i>E. coli</i>		Positive control	
	MI	T	MI	T
Wallac 1450 Bioluminescence				
Assay 1	6.5X	8.5	7X	8.5
Assay 2	13X	6	26X	14
Assay 3	1.8X	8	5X	7.5
Assay 4	1.9X	10	5X	7.5
Assay 5	2.3X	7	297X	7
Wallac Victor2 Bioluminescence				
Assay 1	4.3X	10	4.9X	8
Assay 2	17.4X	13.5	9X	13
Assay 3	4.6X	8	23.6X	9.5
Assay 4	3.5X	10.5	22.3X	9.5
Assay 5	2X	7.5	185X	7.5
Wallac Victor2 Fluorescence				
Assay 1	4X	16.5	4.9X	12.5
Assay 2	10X	17.5	22.4X	17.5
Assay 3	2.8X	15.5	17.5X	15.5
Assay 4	3X	4.5	9X	4.5
Assay 5	1.5X	16	14X	16

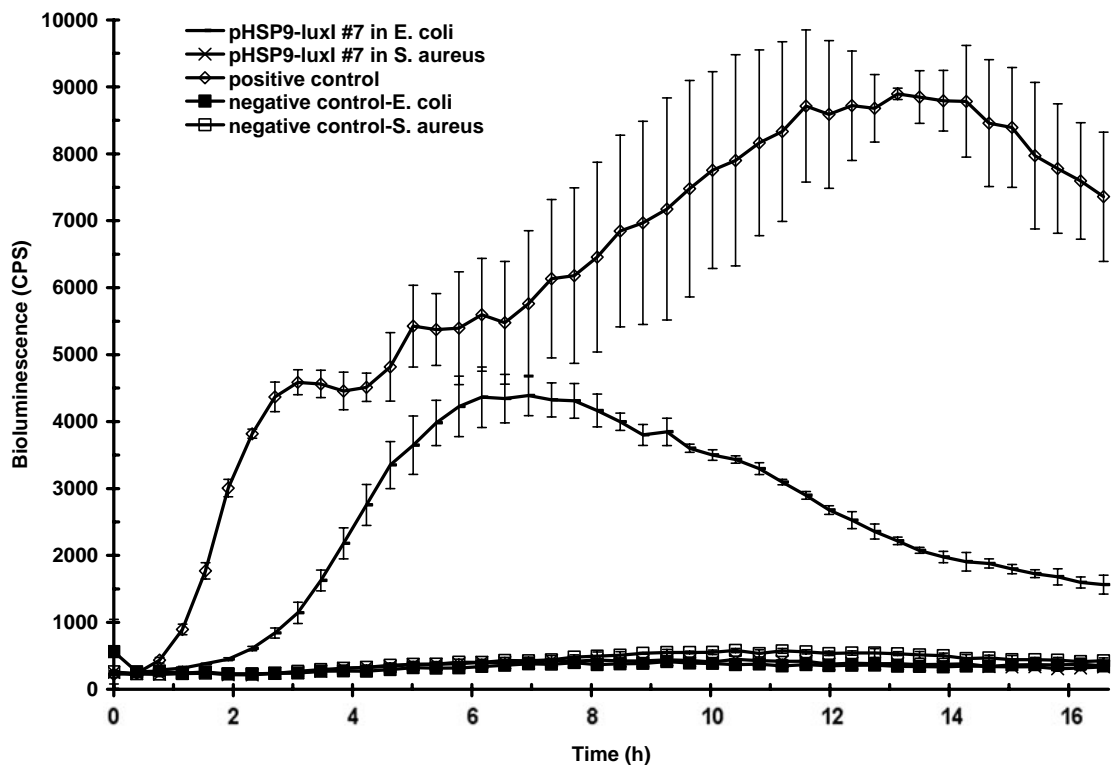


Figure 4-3 (A). Bioluminescent OHHL detection from pHP-L #7 (or pHSP9-luxI #7) in *E. coli* and *S. aureus* at 28°C using the bioreporter RoLux and Wallac 1450 Microbeta Plus Liquid Scintillation Counter. Results represent the mean bioluminescence values ($n=3$) \pm SD (bars) from assay 2.

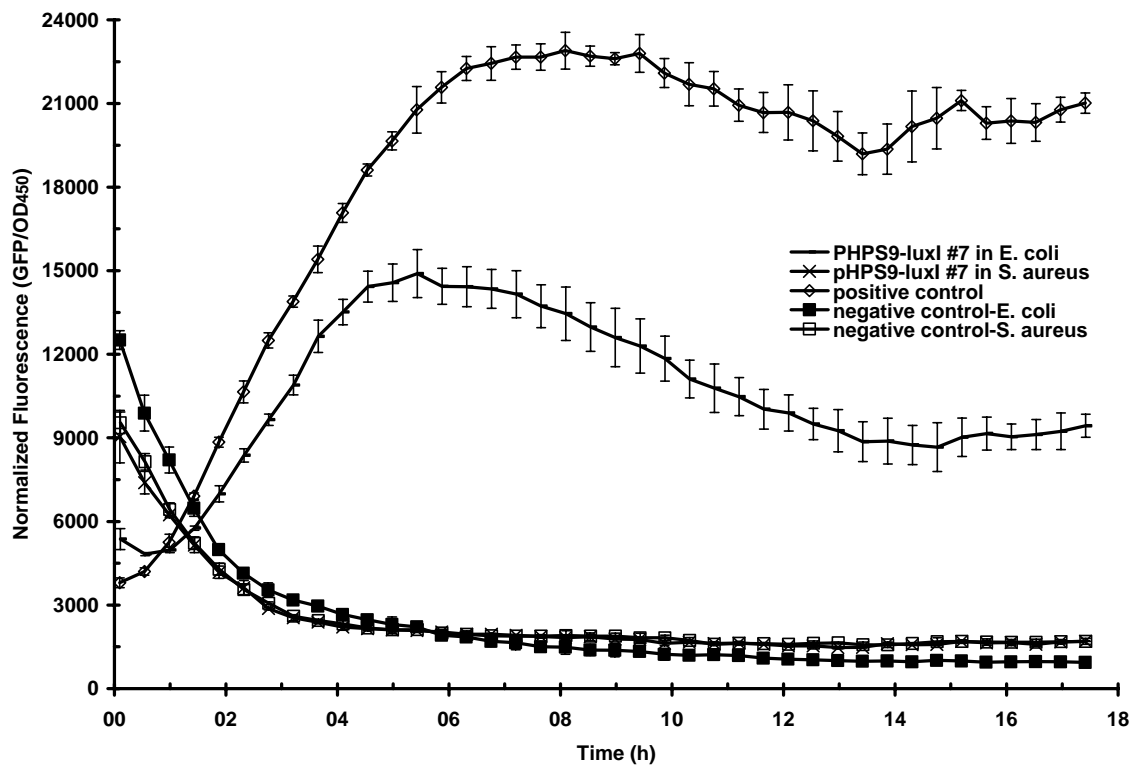


Figure 4-3 (B). Fluorescent OHHL detection from pHP-L #7 (or pHPS9-luxI #7) in *E. coli* and *S. aureus* at 28°C using the bioreporter *E. coli* MT102 with pJBA132 and Wallac Victor2 1420 Multilabel Counter. Results represent the mean fluorescence values ($n=3$) \pm SD (bars) from assay 2.

Detection of OHHL from pHP-L #7 in *E. coli* and *S. aureus* using LCMS

There was generation of light from pHP-L #7 in *E. coli* while there was not any from pHP-L #7 in *S. aureus*. To determine if the problem is at OHHL or LuxI synthase production level, OHHL production from *E. coli* and *S. aureus* harboring pHP-L #7 was detected with LCMS. Synthetic OHHL (Sigma-Aldrich Co., St. Louis, MO) dissolved in sterile dH₂O (1 mg/ml) was used as the standard. Cultures were grown at 37°C with 220 rpm. Samples collected after 2 h (time₀) and 24 h (time₂₄) were used to detect OHHL. The method was LCQ Deca XP^{plus} LCMS utilizing Ace 3 C18 column (Advanced Chromatography Technologies, Aberdeen, Scotland) #ACE-111-1046. There was no OHHL produced by *S. aureus* carrying pHP-L #7 (Figure 4-6). While it is probable that *E. coli* with pHP-L #7 produced OHHL, this was not certain because the retention time (RT) of *E. coli* sample OHHL (13.45) (Figure 4-5) is not the same as the standard OHHL RT (13.60) (Figure 4-4). Peaks at 213.9 and 214.0 m/Z in the standard and *E. coli* spectra, respectively, represent OHHL in samples (Figures 4-4 and 4-5). The *E. coli* and *S. aureus* spectra were prepared with time₂₄ samples and the standard spectrum was constructed using 1 ppm OHHL (Figures 4-4 through 4-6).

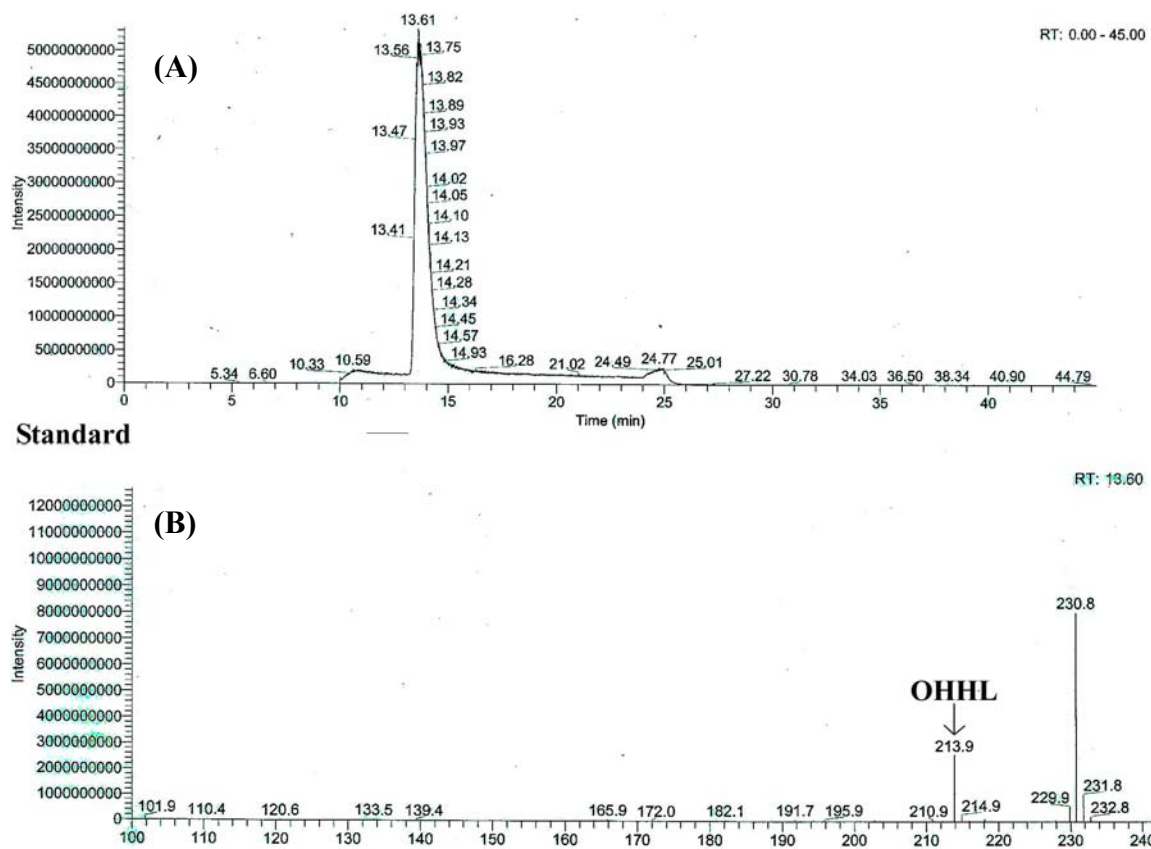
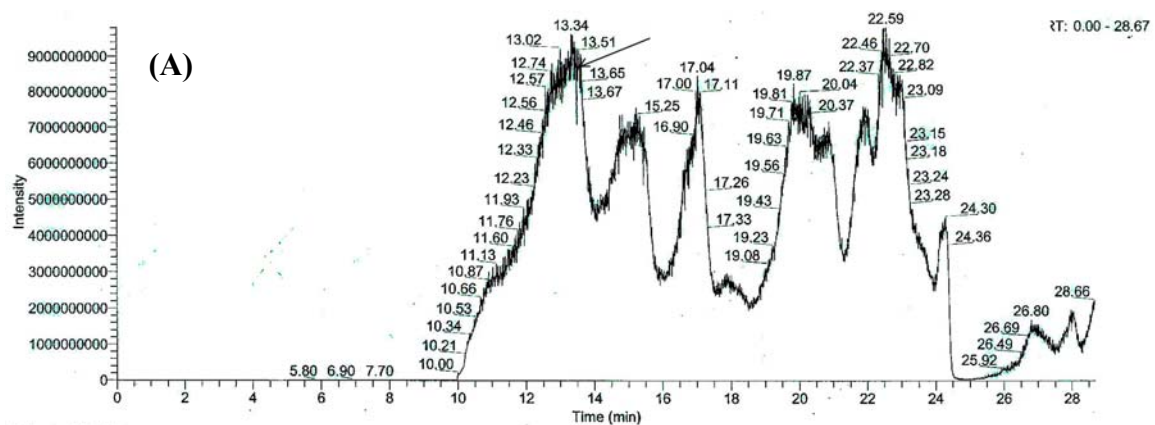


Figure 4-4. (A) The LC chromatogram and (B) mass/charge spectrum of the peak shown in LC chromatogram to detect OHHL molecule in standard (OHHL in dH₂O).



E. coli time₂₄

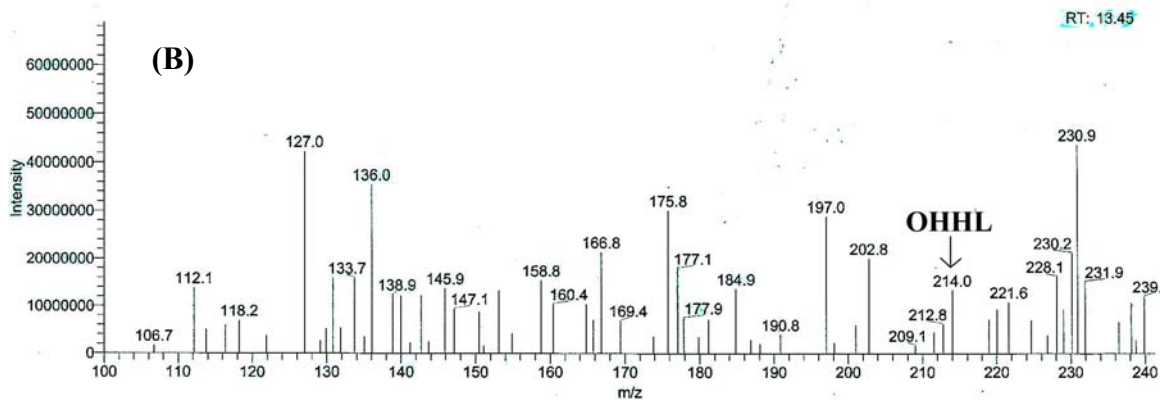


Figure 4-5. (A) The LC chromatogram and (B) mass/charge spectrum of the peak (marked with an arrow) in LC chromatogram to detect OHHL molecule in 24 h-culture of *E. coli* carrying pHP-L #7.

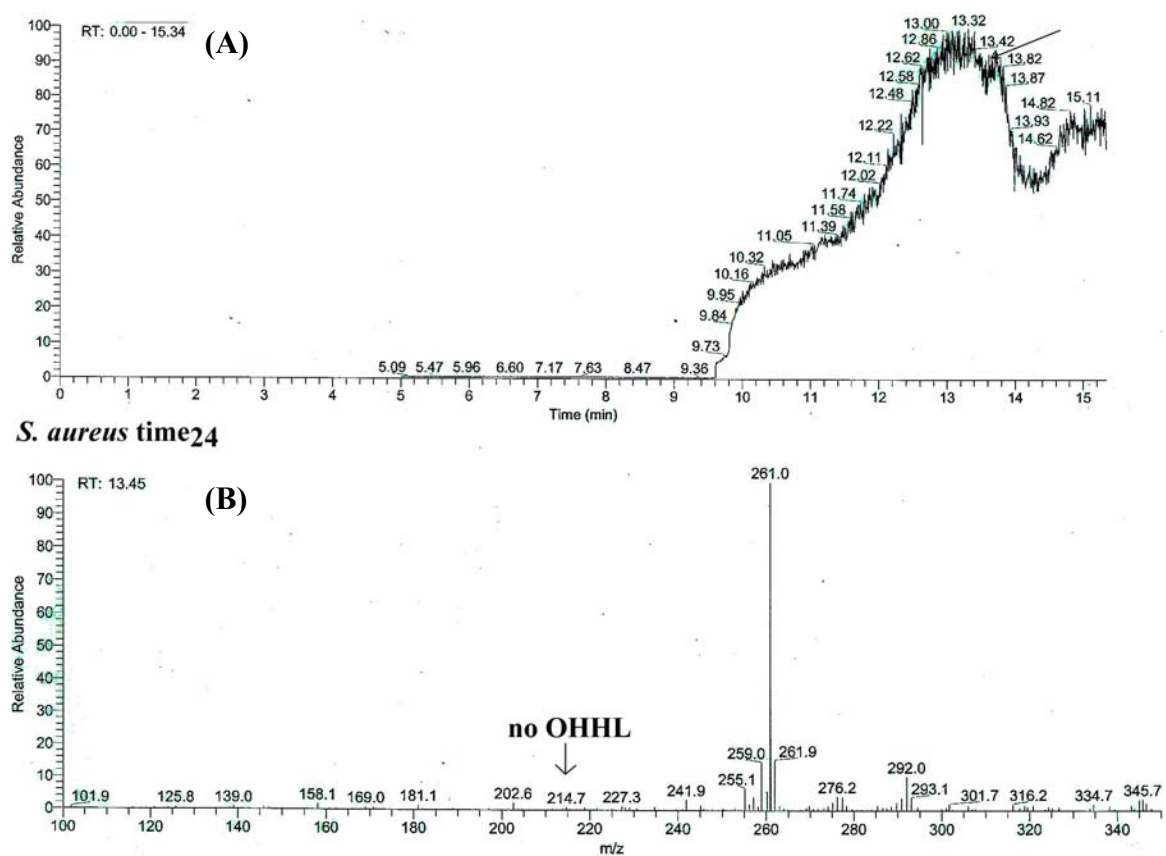


Figure 4-6. (A) The LC chromatogram and (B) mass/charge spectrum of the peak (marked with an arrow) in LC chromatogram to detect OHHL molecule in 24 h-culture of *S. aureus* carrying pHP-L #7.

Detection and analysis of kanamycin resistance provided by pHP-K #4 in *E. coli* and *S. aureus*

Since pHP-L #7 produced OHHL in *E. coli* but not in *S. aureus* as shown by bioluminescence, fluorescence and LCMS tests, the efficiency of the construct promoter P59 which controls the *luxI* expression was tested. *kan^r* was put in place of *luxI* into the construct to function as a bioreporter. The *E. coli* and *S. aureus* cultures with pHP-K #4 were streaked onto LB plates containing different concentrations of kanamycin. Results were compared to kanamycin resistance patterns provided by other plasmids and constructs which contained the *kan^r* gene under the control of different promoters and RBSs (Table 4-2). Compared to other plasmids, pHP-K #4 provided less resistance to kanamycin in *S. aureus*. On the other hand, the kanamycin resistance level from *E. coli* with pHP-K #4 was higher than those from other plasmids in *E. coli*.

Table 4-2. Kanamycin resistance patterns provided by pHP-K #4 in *E. coli* and *S. aureus*. Patterns were compared to those of other constructs which contained *kan^r* under the control of different promoters and RBSs. (R=Resistant, S=Sensitive, ND=Not determined, *=please see below for the construction of plasmid.)

	Kanamycin concentration (µg/ml)								
	2.5	5	10	15	20	35	45	50	70
pHP-K #4 in <i>S. aureus</i>	R	R	R	R	S	S	S	S	S
Wild type <i>S. aureus</i> RN4220	R	R	S	S	S	S	S	S	S
pUB110 in <i>S. aureus</i>	R	R	R	R	R	R	S	S	S
pHP-PK #31 in <i>S. aureus</i> *	R	R	R	R	R	R	R	R	R
pHP-K #4 in <i>E. coli</i>	R	R	R	R	R	ND	ND	ND	ND
pHP-PK #31 in <i>E. coli</i> *	R	R	R	ND	S	S	S	S	S
pDG-L #28 in <i>E. coli</i> *	R	R	R	ND	S	S	S	S	S

These results are consistent with bioluminescent, fluorescent, and LCMS OHHL detection results from pHP-L #7 in *E. coli* and *S. aureus*. While the *E. coli* strain produced OHHL whose production is catalyzed by the product of *luxI* under the P59 control, *S. aureus* strain did not. However, these results can not show with certainty that the P59 promoter of pHPS9 does not work efficiently because promoters and RBSs which control *kan^r* expression and copy numbers of plasmids are different. The problem may be with the promoter, the RBS, or the copy number of pHPS9. Nevertheless, the results exhibit that the expression of a gene under the same conditions used for expression of *luxI* in pHP-L #7 construct is not efficient compared to conditions provided by other plasmids.

Bioluminescent and fluorescent detection of OHHL from pDG-L #28 in *E. coli* and pHP-PL #9 in *E. coli*, *B. subtilis*, and *S. aureus* using Wallac Victor2 1420 Multilabel and 1450 Microbeta Plus Liquid Scintillation Counters

pDG-L #28 was formed by placing *luxI* CDS under the control of the Gram-positive promoter and RBS of pDG148-Stu which is a Gram-positive and -negative expression shuttle vector. The promoter of the vector, *Pspac*, is a hybrid of the *B. subtilis* phage SPO-1 promoter and the *lac* operator which is regulated by the IPTG-inducible LacI repressor. Although the plasmid was transformed into *E. coli*, it could not be electroporated into *S. aureus*. To be able to clone *luxI*, which is under the control pDG148-Stu *Pspac* and RBS with *lacI* into *S. aureus*, these fragments were transferred into pHPS9-sht #7 (a 5 kb, shortened version of pHPS9). The resulting plasmid pHP-PL

#9 which is 7,256 bp was smaller than pDG-L #28 which is 8,854 bp. pHP-PL #9 could be electroporated into *S. aureus* and *B. subtilis*.

The OHHL from pDG-L #28 in *E. coli* and pHP-PL #9 in *B. subtilis* and *S. aureus* was measured using bioluminescent bioreporter *E. coli* OHHLux, and fluorescent bioreporter *E. coli* MT102 with pJBA132. The negative control for *E. coli* and *B. subtilis* strains was the bioreporter alone combined with dH₂O instead of the sample supernatant. The negative control for *S. aureus* sample was the wild type *S. aureus* strain RN4220 supernatant combined with the bioreporter. The IPTG induction of light from plasmids was tested using 0.5 and 2 mM IPTG with *E. coli* containing pDG-L #28 and 2 and 3 mM IPTG with *B. subtilis* and *S. aureus* carrying pHP-PL #9.

Bioluminescent and fluorescent values obtained with IPTG-induced strains were not significantly different from values obtained without IPTG (Figures 4-7 through 4-9). IPTG does not seem to have an inducing effect on light production. However, pDG-L #28 in *E. coli* and pHP-PL #9 in *B. subtilis* were able to produce OHHL in the absence of IPTG as shown by the bioluminescence (Figures 4-7 (A) and 4-8 (A)) and fluorescence levels (Figures 4-7 (B) and 4-8 (B)) obtained. There was no bioluminescent or fluorescent OHHL detection from pHP-PL #9 in *S. aureus* (Figure 4-9). Bioluminescence and fluorescence detected from pDG-L #28 in *E. coli* were very high compared to those produced by pHP-PL #9 in *B. subtilis*. A comparison of the two systems is shown in Table 4-3. The maximum amount of light from pDG-L #28 in *E. coli* was 604 (bioluminescent) and 20 (fluorescent) times higher than those from the negative control, while the highest light levels from pHP-PL #9 in *B. subtilis* were only ~3 (bioluminescent) and ~2 (fluorescent) times higher than those from the negative control.

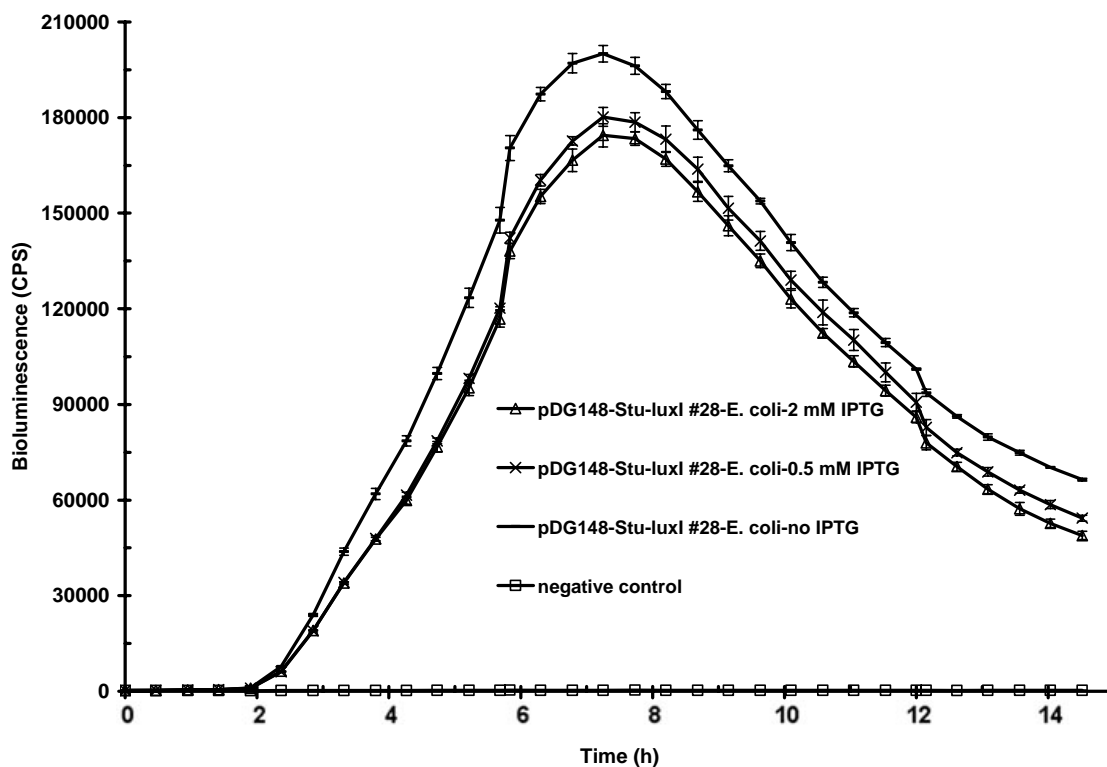


Figure 4-7 (A). Bioluminescent OHHL detection from pDG-L #28 (or pDG148-Stu-luxI #28) in *E. coli* at 28°C with and without IPTG using the bioreporter *E. coli* OHHLux and Wallac 1450 Microbeta Plus Liquid Scintillation Counter. Results represent the mean bioluminescence values ($n=3$) \pm SD (bars).

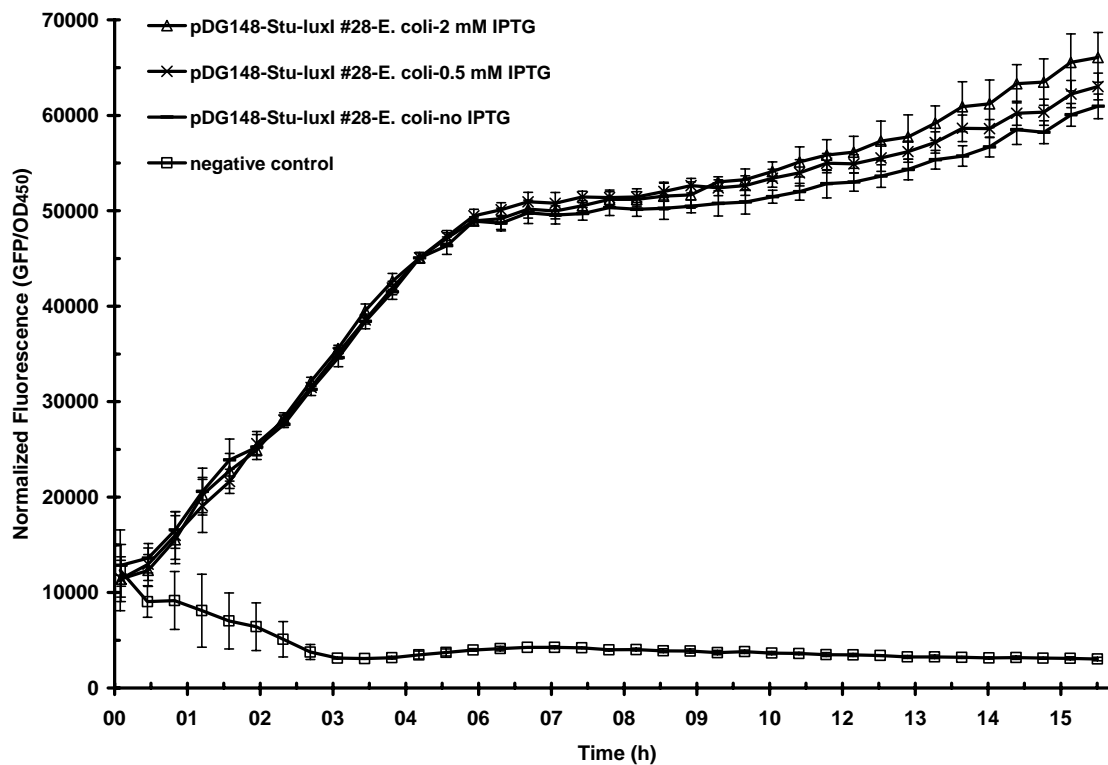


Figure 4-7 (B). Fluorescent OHHL detection from pDG-L #28 (or pDG148-Stu-luxI #28) in *E. coli* at 28°C with and without IPTG using the bioreporter *E. coli* MT102 with pJBA132 and Wallac Victor2 1420 Multilabel Counter. Results represent the mean fluorescence values ($n=3$) \pm SD (bars).

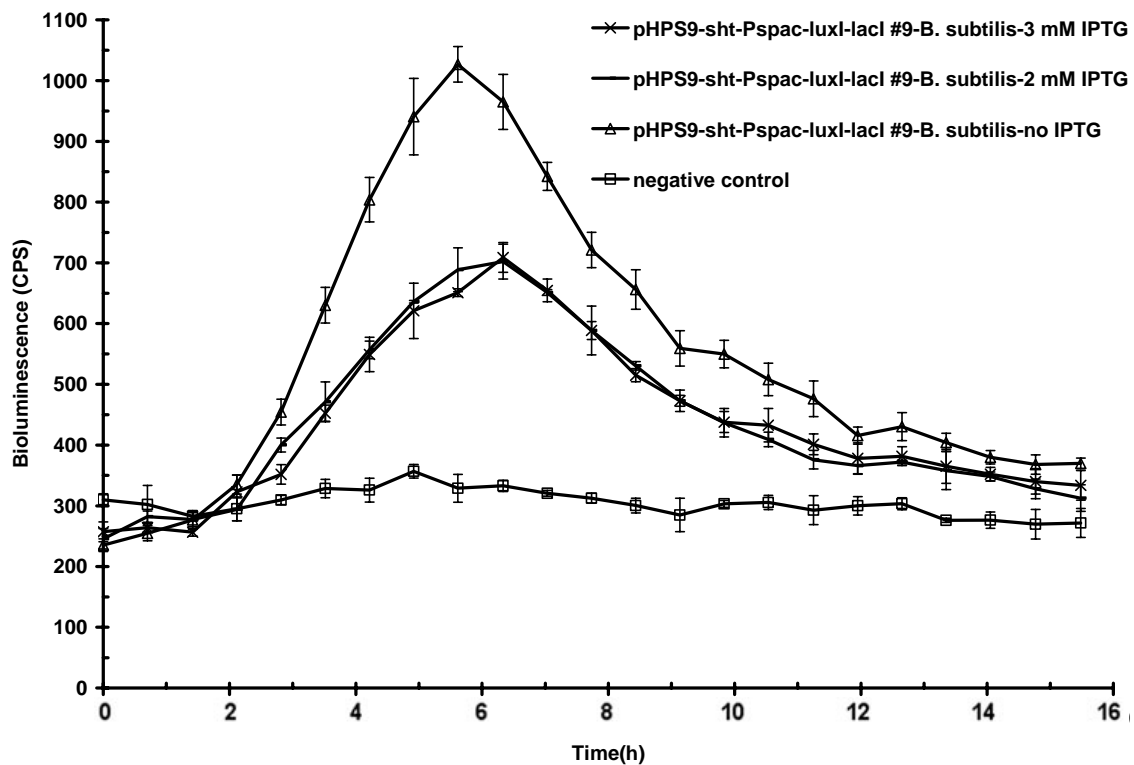


Figure 4-8 (A). Bioluminescent OHHL detection from pHP-PL #9 (or pHPS9-sht-Pspac-luxI-lacI #9) in *B. subtilis* at 28°C with and without IPTG using the bioreporter *E. coli* OHHLux and Wallac 1450 Microbeta Plus Liquid Scintillation Counter. Results represent the mean bioluminescence values ($n=3$) \pm SD (bars).

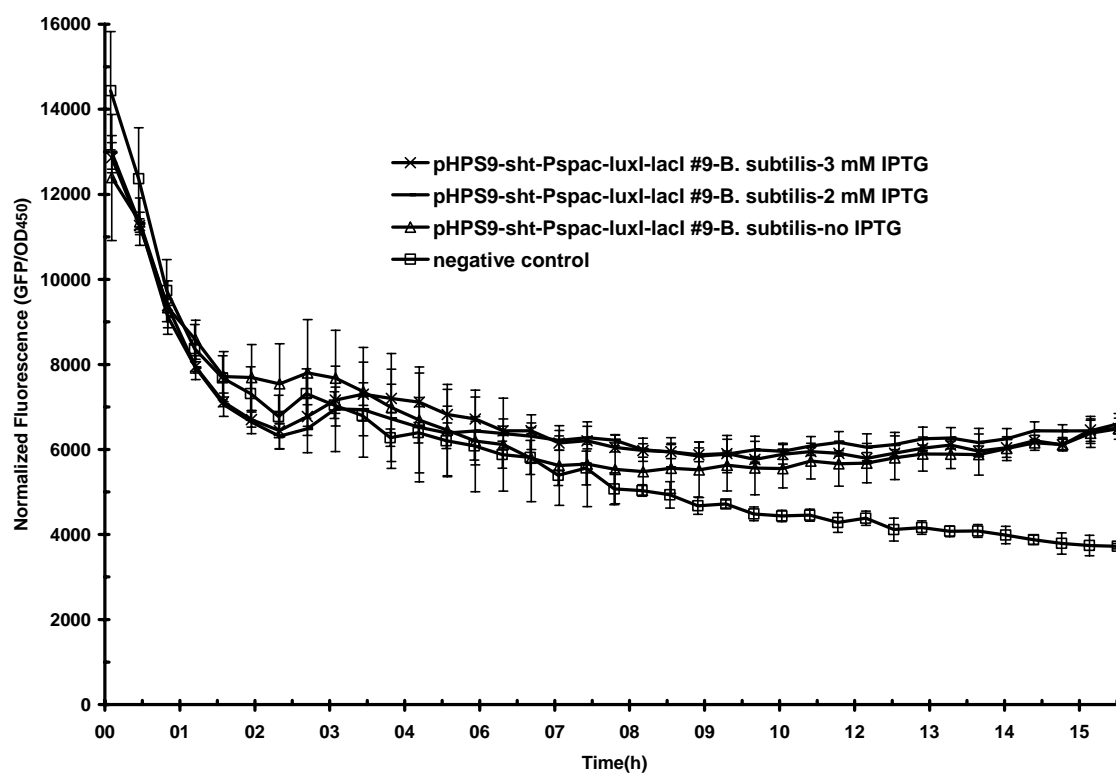


Figure 4-8 (B). Fluorescent OHHL detection from pHP-PL #9 (or pHPS9-sht-Pspac-luxI-lacI #9) in *B. subtilis* at 28°C with and without IPTG using the bioreporter *E. coli* MT102 with pJBA132 and Wallac Victor2 1420 Multilabel Counter. Results represent the mean fluorescence values ($n=3$) \pm SD (bars).

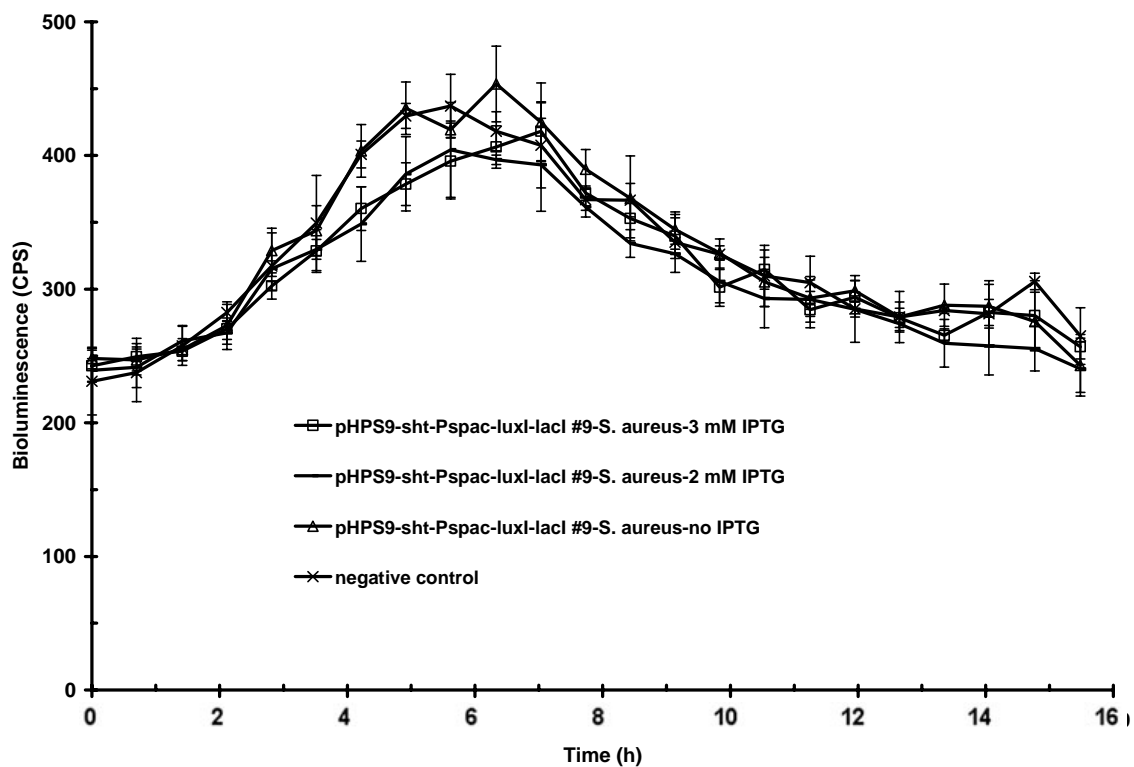


Figure 4-9 (A). Bioluminescent OHHL detection from pHP-PL #9 (or pHPS9-sht-Pspac-luxI-lacI #9) in *S. aureus* at 28°C with and without IPTG using the bioreporter *E. coli* OHHLux and Wallac 1450 Microbeta Plus Liquid Scintillation Counter. Results represent the mean bioluminescence values ($n=3$) \pm SD (bars).

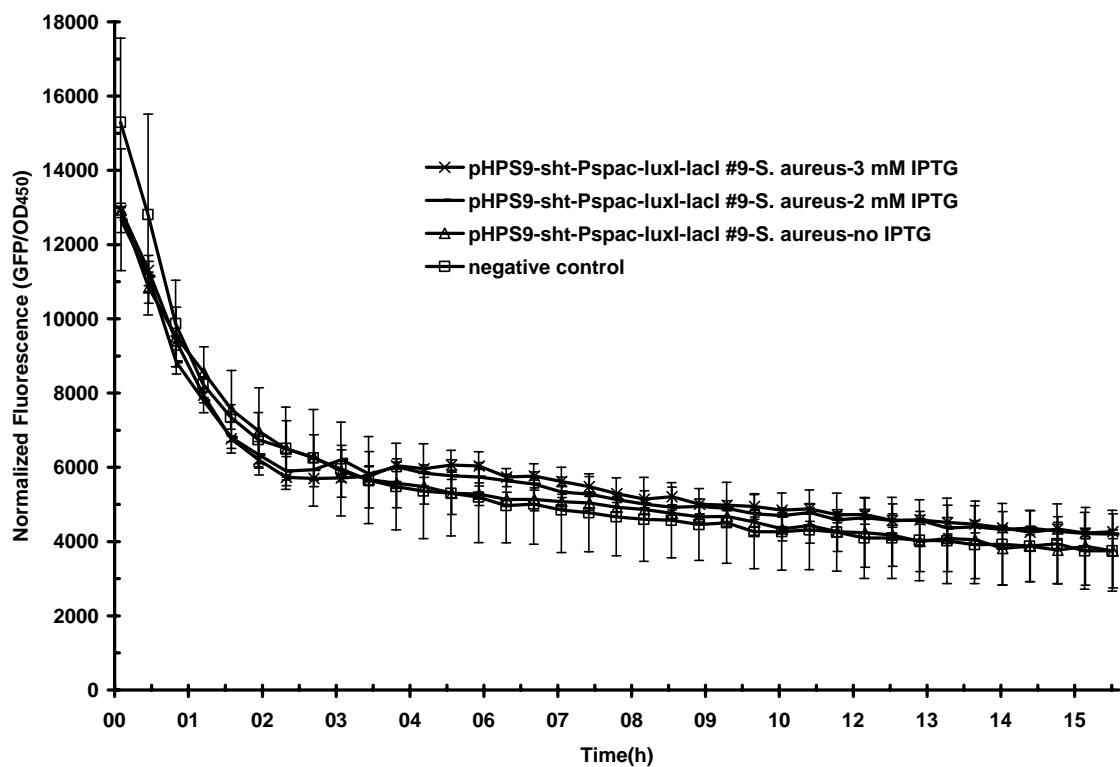


Figure 4-9 (B). Fluorescent OHHL detection from pHP-PL #9 (or pHPS9-sht-Pspac-luxI-lacI #9) in *S. aureus* at 28°C with and without IPTG using the bioreporter *E. coli* MT102 with pJBA132 and Wallac Victor2 1420 Multilabel Counter. Results represent the mean fluorescence values ($n=3$) \pm SD (bars).

Table 4-3. Comparison of bioluminescence and fluorescence from pDG-L #28 in *E. coli* and pHP-PL #9 in *B. subtilis*. Bioluminescence was detected using the bioreporter *E. coli* OHHLux and Wallac 1450 Microbeta Plus Liquid Scintillation Counter. Fluorescence was detected using the bioreporter *E. coli* MT102 harboring pJBA132 and Wallac Victor2 1420 Multilabel Counter. (MI = maximum induction; the highest amount of light from a sample divided by the negative control value at the same time point, T = Time period in h to obtain MI)

	pDG-L #28 in <i>E. coli</i>		pHP-PL #9 in <i>B. subtilis</i>	
	MI	T	MI	T
Bioluminescence	604X	7	3.12X	5.5
Fluorescence	20X	16	1.74X	16

The *Pspac* promoter of pHP-PL #9 was also evaluated using the Overnight Express Autoinduction System 1 (Novagen, Darmstadt, Germany) instead of IPTG. This system is a mixture of optimized media components which is used by combining with a glucose-free complex medium like LB. Lactose in the resulting medium induces protein expression after bacteria reach high densities. It replaces IPTG for protein expression induction in IPTG-inducible hosts. *Escherichia coli*, *B. subtilis* and *S. aureus* with pHP-PL #9 were tested for OHHL production using this system. Bioluminescent and fluorescent bioreporters were *E. coli* OHHLux and *E. coli* MT102 carrying pJBA132, respectively, which were grown in LB. The negative control for the *S. aureus* sample was *S. aureus* RN4220 which was grown in the Novagen System medium. Its supernatant was combined with the bioreporter and tested. The negative control for *E. coli* and *B. subtilis* samples was the bioluminescent or fluorescent bioreporter combined with dH₂O instead of the sample supernatant.

High levels of bioluminescence and fluorescence were obtained from *E. coli* and *B. subtilis* containing pHP-PL #9 (Figures 4-10 and 4-11) while there was no light produced by *S. aureus* carrying pHP-PL #9 (Figure 4-12) with the Overnight Express Autoinduction System 1 (Novagen, Darmstadt, Germany). Results were compared to those obtained from the previous experiment with the strains with no induction (Figures 4-7 and 4-8, Table 4-4). Since *E. coli* harboring pHP-PL #9 was not tested for IPTG induction, results from IPTG induction of *E. coli* with pDG-L #28 were used for comparison. pHP-PL #9 and pDG-L #28 carry *luxI* CDS under the control of the same promoter and RBS and they both have Gram-negative pBR322 origin of replication, pMB1. The maximum bioluminescence and fluorescence from pHP-PL #9 in *E. coli* and *B. subtilis* with the Overnight Express Autoinduction System 1 (Novagen, Darmstadt, Germany) were not significantly different from those produced by pDG-L #28 in *E. coli* and pHP-PL #9 in *B. subtilis* under no induction (Table 4-4). Therefore, the Overnight Express Autoinduction System 1 (Novagen, Darmstadt, Germany) does not have an inducing effect on *Pspac*.

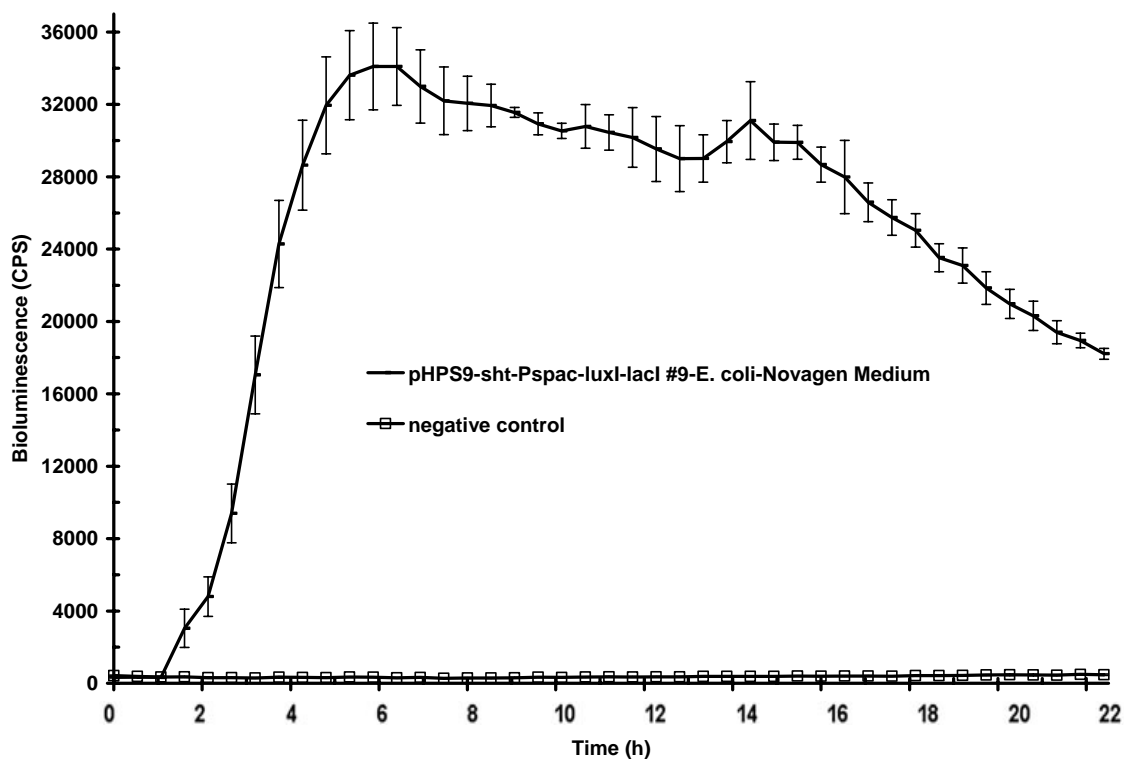


Figure 4-10 (A). Bioluminescent OHHL detection from pHP-PL #9 (or pHPS9-sht-Pspac-luxI-lacI #9) in *E. coli* in Overnight Express Autoinduction System 1 (Novagen, Darmstadt, Germany) at 28°C using the bioreporter *E. coli* OHHLux and Wallac 1450 Microbeta Plus Liquid Scintillation Counter. Results represent the mean bioluminescence values ($n=3$) \pm SD (bars).

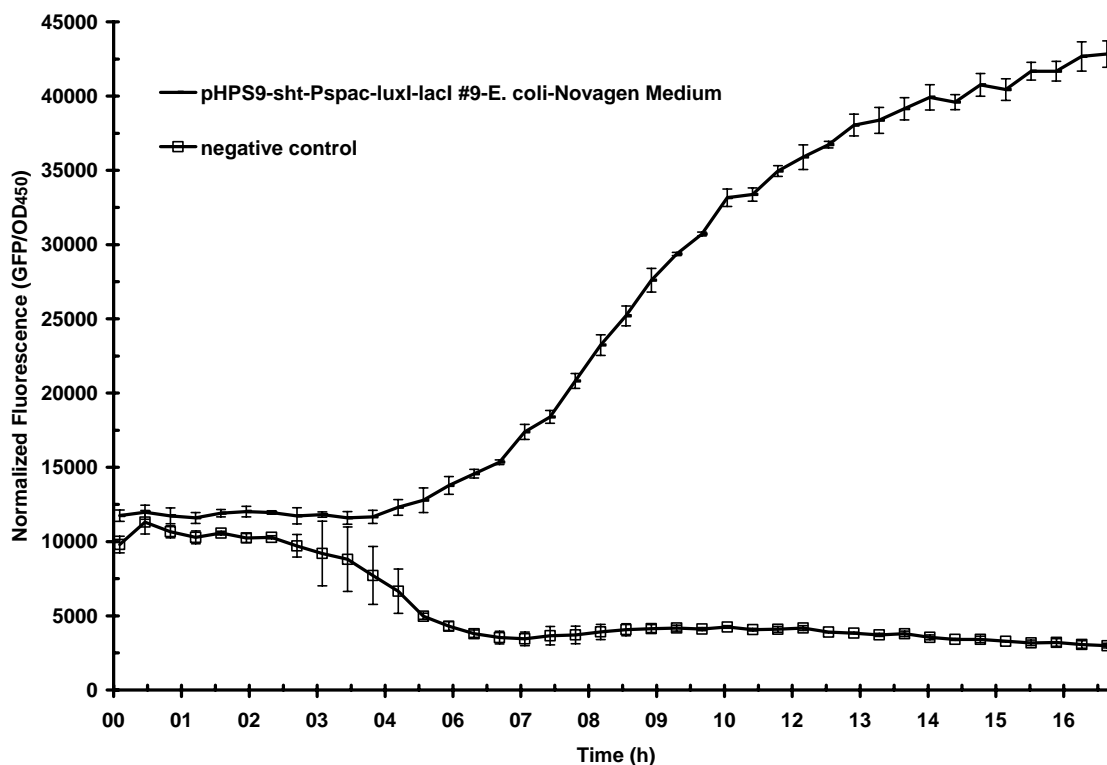


Figure 4-10 (B). Fluorescent OHHL detection from pHP-PL #9 (or pHP-PL #9) in *E. coli* in Overnight Express Autoinduction System 1 (Novagen, Darmstadt, Germany) at 28°C using the bioreporter *E. coli* MT102 with pJBA132 and Wallac Victor2 1420 Multilabel Counter. Results represent the mean fluorescence values ($n=3$) \pm SD (bars).

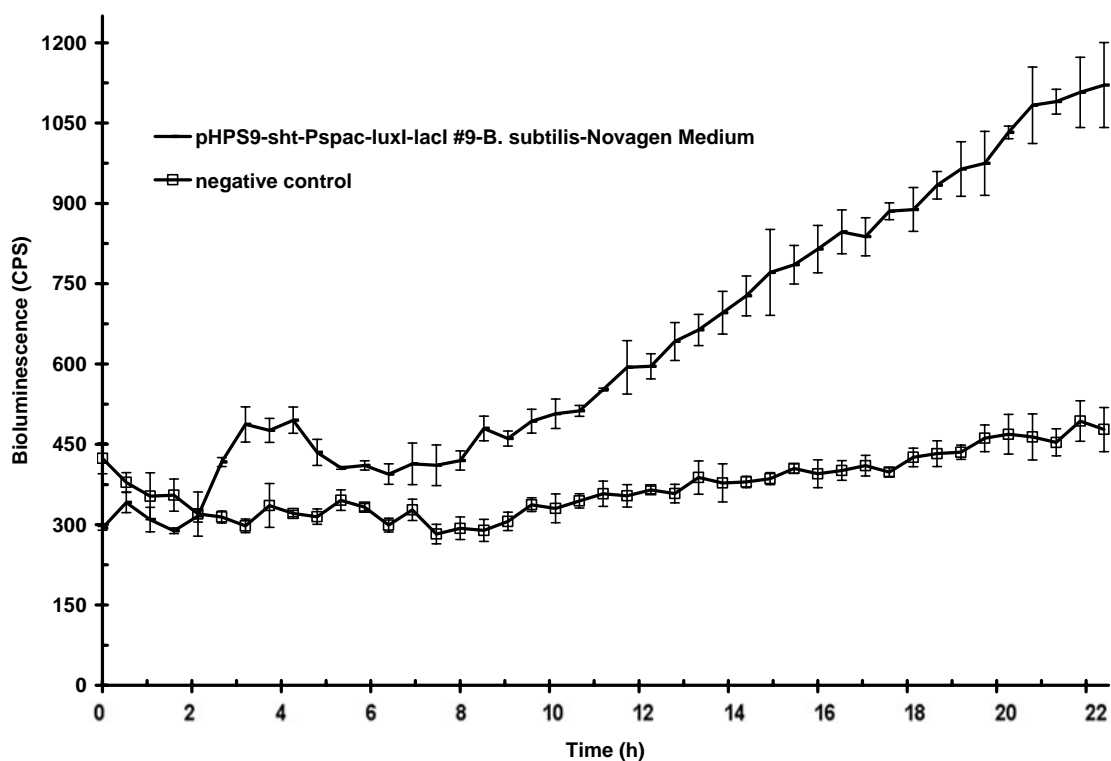


Figure 4-11 (A). Bioluminescent OHHL detection from pHP-PL #9 (or pHPS9-sht-Pspac-luxI-lacI #9) in *B. subtilis* in Overnight Express Autoinduction System 1 (Novagen, Darmstadt, Germany) at 28°C using the bioreporter *E. coli* OHHLux and Wallac 1450 Microbeta Plus Liquid Scintillation Counter. Results represent the mean bioluminescence values ($n=3$) \pm SD (bars).

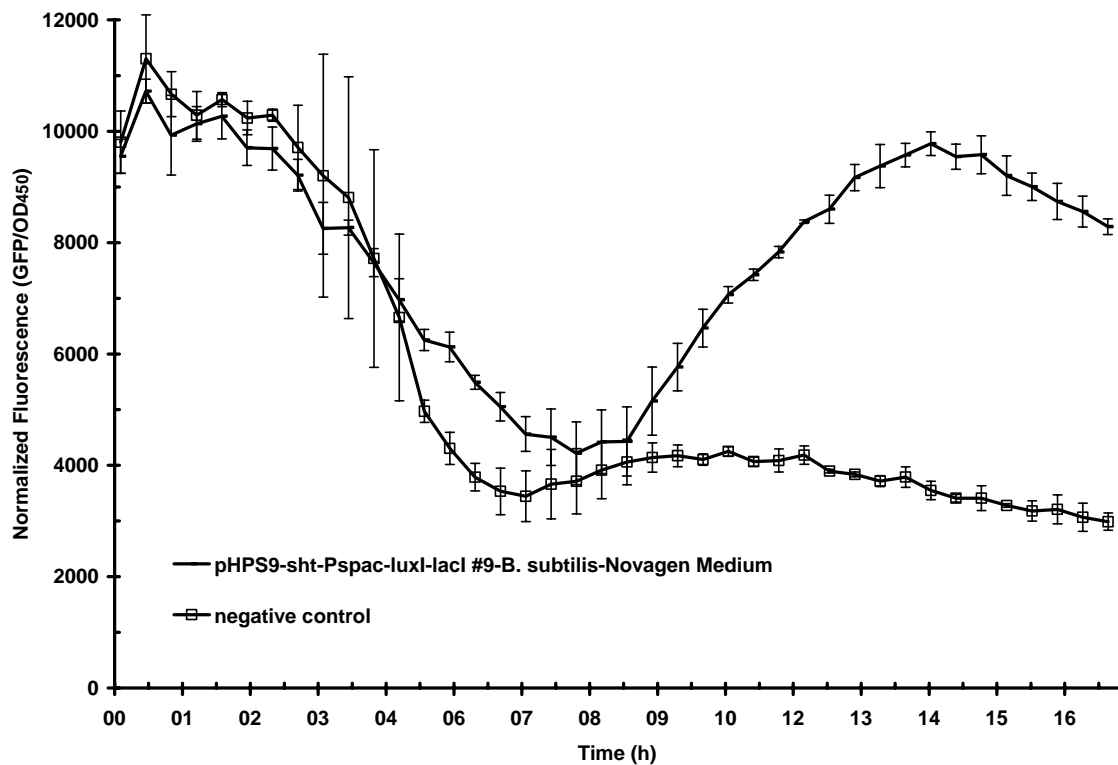


Figure 4-11 (B). Fluorescent OHHL detection from pHPL-PL #9 (or pHPS9-sht-Pspac-luxI-lacI #9) in *B. subtilis* in Overnight Express Autoinduction System 1 (Novagen, Darmstadt, Germany) at 28°C using the bioreporter *E. coli* MT102 with pJBA132 and Wallac Victor2 1420 Multilabel Counter. Results represent the mean fluorescence values ($n=3$) \pm SD (bars).

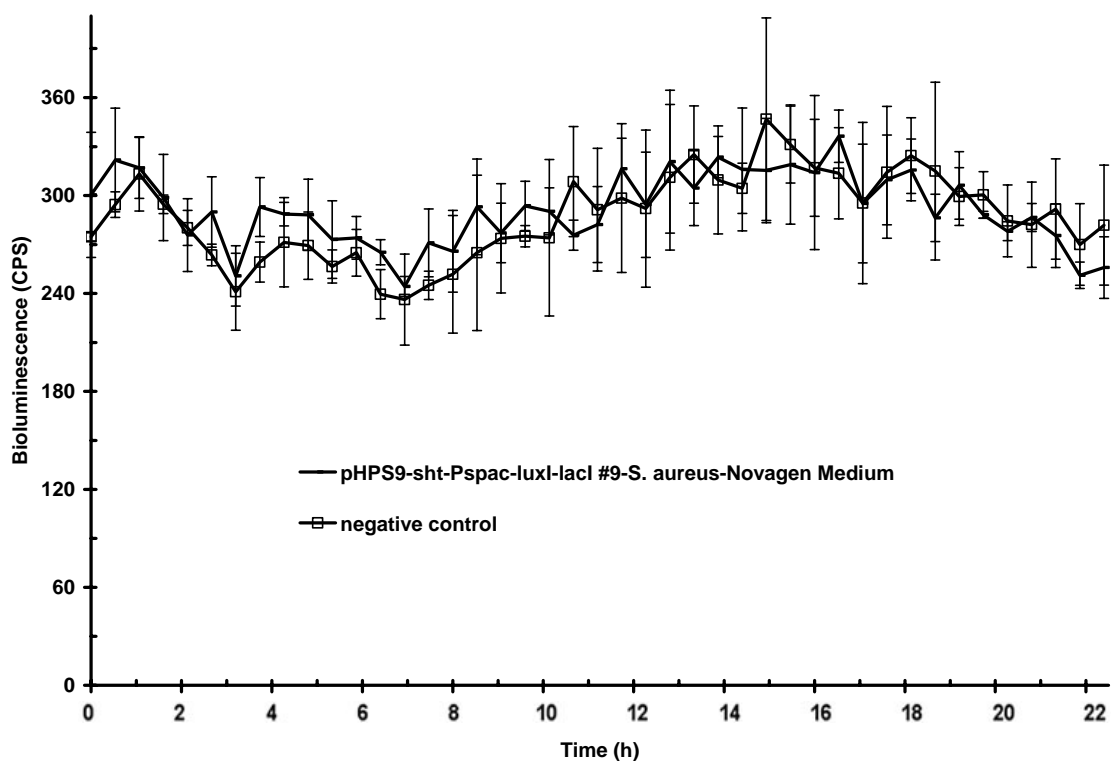


Figure 4-12 (A). Bioluminescent OHHL detection from pHP-PL #9 (or pHPS9-sht-Pspac-luxI-lacI #9) in *S. aureus* in Overnight Express Autoinduction System 1 (Novagen, Darmstadt, Germany) at 28°C using the bioreporter *E. coli* OHHLux and Wallac 1450 Microbeta Plus Liquid Scintillation Counter. Results represent the mean bioluminescence values ($n=3$) \pm SD (bars).

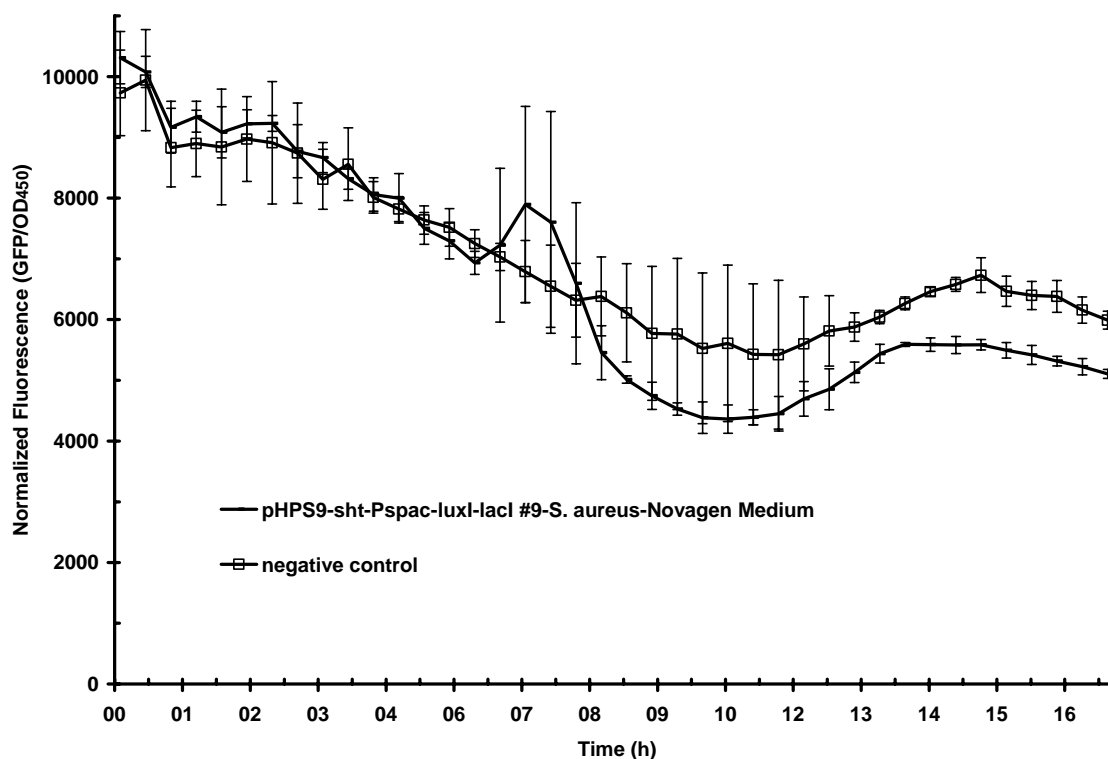


Figure 4-12 (B). Fluorescent OHHL detection from pHP-PL #9 (or pHPS9-sht-Pspac-luxI-lacI #9) in *S. aureus* in Overnight Express Autoinduction System 1 (Novagen, Darmstadt, Germany) at 28°C using the bioreporter *E. coli* MT102 with pJBA132 and Wallac Victor2 1420 Multilabel Counter. Results represent the mean fluorescence values ($n=3$) \pm SD (bars).

Table 4-4. Overnight Express Autoinduction System 1 (Novagen, Darmstadt, Germany) effect on bioluminescence and fluorescence from constructs using IPTG-inducible *Pspac*. Bioluminescence was detected using the bioreporter *E. coli* OHHLux and Wallac 1450 Microbeta Plus Liquid Scintillation Counter. Fluorescence was detected using the bioreporter *E. coli* MT102 harboring pJBA132 and Wallac Victor2 1420 Multilabel Counter. (LB = in LB, OEAS = in Overnight Express Autoinduction System 1, MI = maximum induction-the highest amount of light from a sample divided by the negative control value at the same time point, * = Time period in h to obtain MI)

	pDG-L #28 in <i>E. coli</i>- LB	pHP-PL #9 in <i>E. coli</i>- OEAS	pHP-PL #9 in <i>B. subtilis</i>-LB	pHP-PL #9 in <i>B. subtilis</i>- OEAS
Bioluminescence	604X _{(7)*}	114X _{(7.5)*}	3.12X _{(5.5)*}	2.4X _{(21.5)*}
Fluorescence	20X _{(16)*}	14X _{(17.5)*}	1.74X _{(16)*}	2.83X _{(16)*}

The *luxI* transcript detection from pHP-PL #9 and pDG-L #28 using real-time quantitative reverse transcriptase PCR

To determine the reason for generation of light by *E. coli* and *B. subtilis* which contained pHP-PL #9 but not by *S. aureus* carrying pHP-PL #9, efficiency of the promoter *Pspac* was controlled. Transcription of *luxI* from pHP-PL #9 in *E. coli*, *B. subtilis* and *S. aureus* and pDG-L #28 in *E. coli* was tested using real-time qRT-PCR. The wild type *S. aureus* RN4220 was the negative control for the experiment. RNAs extracted from mid-log phase cultures were subjected to real-time qRT-PCR with primers and a labeled probe which are specific to *luxI*. The same amount of RNA (125 ng) was used for each sample which was prepared in triplicate. An additional reverse transcriptase-free reaction was also tested for each sample to control DNA contamination. Opticon Monitor

Analysis Software Version 1.08 was used for data analysis. The baseline was measured between cycles 3 and 7.

Figure 4-13 shows results as plots of fluorescence versus the number of cycles for each sample. The threshold cycle (C_T) for each sample was determined by calculating the mean of triplicate measurements (Table 4-5). There was negligible level of DNA contamination from the samples as shown by the reverse transcriptase-free reaction results with the C_T difference of ≥ 7 between the triplicate sample average and the control values (Figure 4-13 and Table 4-5). The aim of this experiment was to detect the presence or absence of *luxI* transcripts and to compare them with one another. Therefore, the amounts of transcripts were not determined. Figure 4-13 and Table 4-5 show that all samples except for the negative control produced the *luxI* transcript. Comparison of C_T values show that the order of samples, starting with the one with the highest amount of transcript to the one with the lowest amount, is pHP-PL #9 in *B. subtilis*>pDG-L #28 in *E. coli*>pHP-PL #9 in *S. aureus*>pHP-PL #9 in *E. coli*. Although pHP-PL #9 in *S. aureus* can not generate light, it produces the transcript of *luxI*. All other samples which were transcript positive were also light positive unlike the *S. aureus* sample.

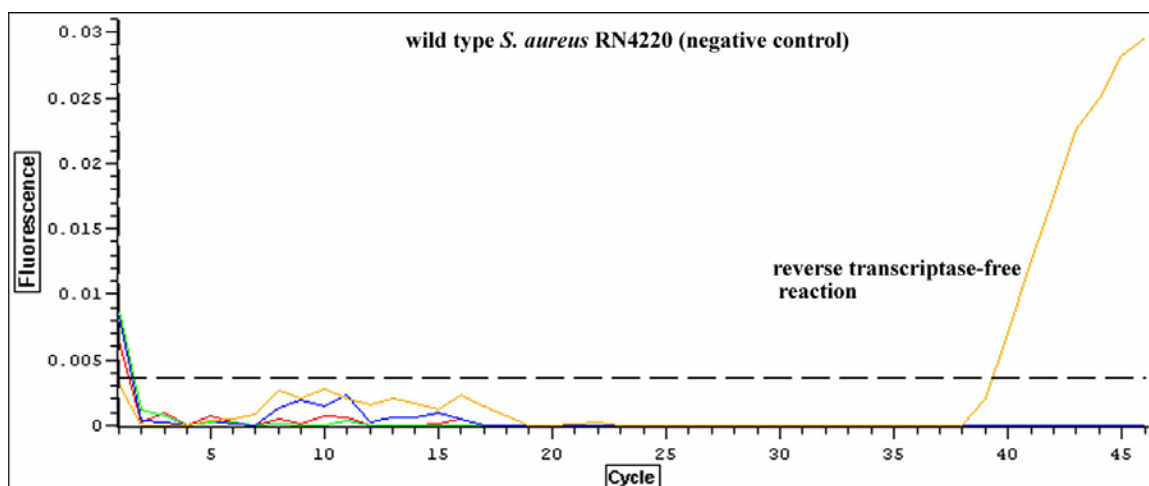


Figure 4-13 (A). Real-time qRT-PCR plots for *luxI* transcription from wild-type *S. aureus* (negative control). Reverse transcriptase-free control (n=1, yellow) was included to check DNA contamination. The horizontal line shows the baseline. The point at which the plot crosses the baseline is C_T .

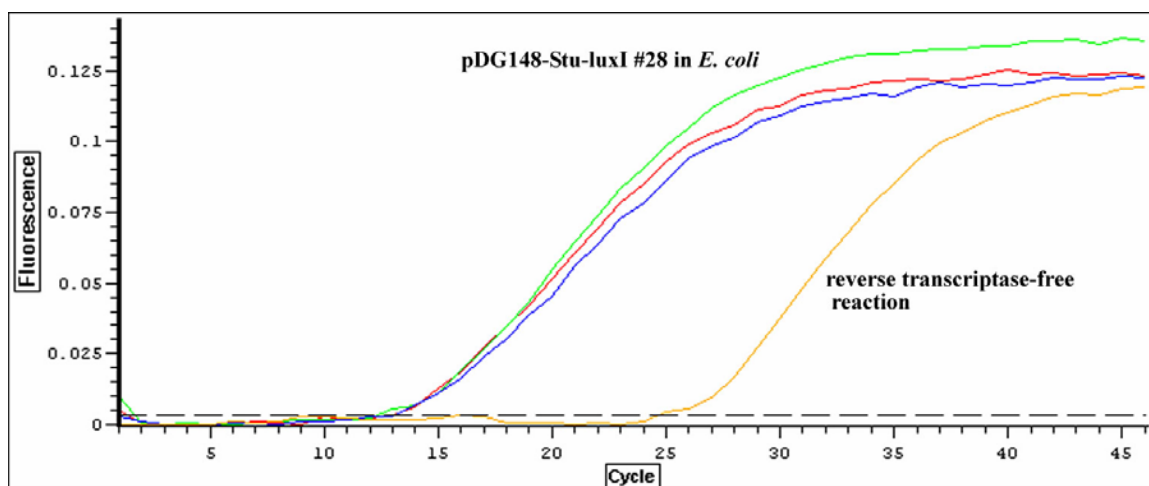


Figure 4-13 (B). Real-time qRT-PCR plots for *luxI* transcription from pDG-L #28 (or pDG148-Stu-luxI #28) in *E. coli* (n=3). Reverse transcriptase-free control (n=1, yellow) was included to check DNA contamination. The horizontal line shows the baseline. The point at which the plot crosses the baseline is C_T .

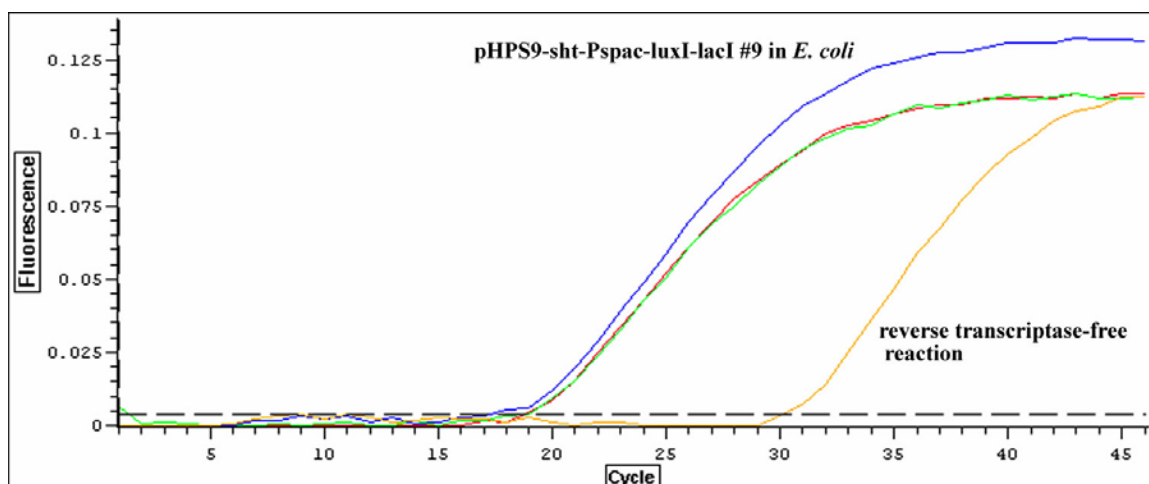


Figure 4-13 (C). Real-time qRT-PCR plots for *luxI* transcription from pHP-PL #9 (or pHPS9-sht-Pspac-luxI-lacI #9) in *E. coli* (n=3). Reverse transcriptase-free control (n=1, yellow) was included to check DNA contamination. The horizontal line shows the baseline. The point at which the plot crosses the baseline is C_T .

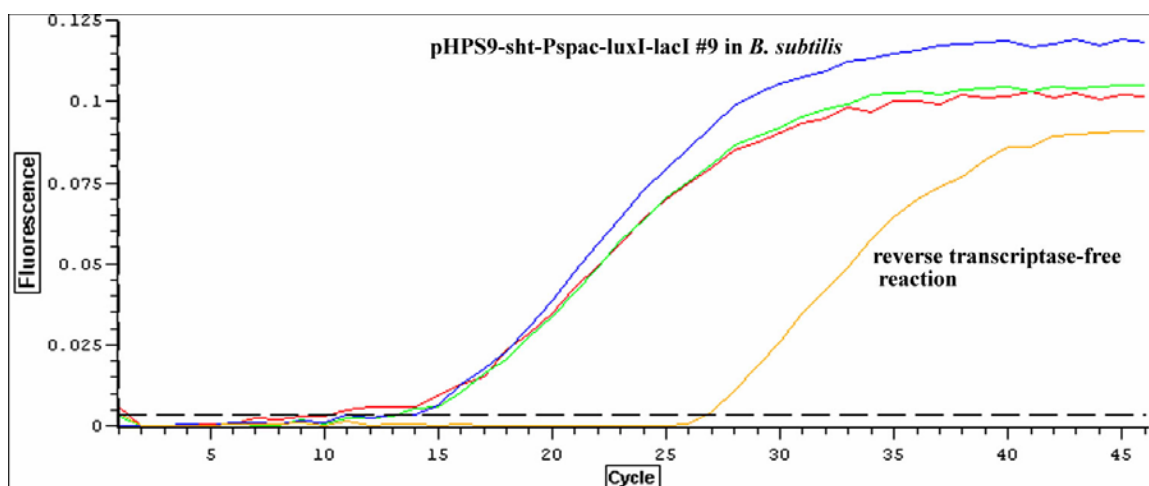


Figure 4-13 (D). Real-time qRT-PCR plots for *luxI* transcription from pHP-PL #9 (or pHPS9-sht-Pspac-luxI-lacI #9) in *B. subtilis* (n=3). Reverse transcriptase-free control (n=1, yellow) was included to check DNA contamination. The horizontal line shows the baseline. The point at which the plot crosses the baseline is C_T .

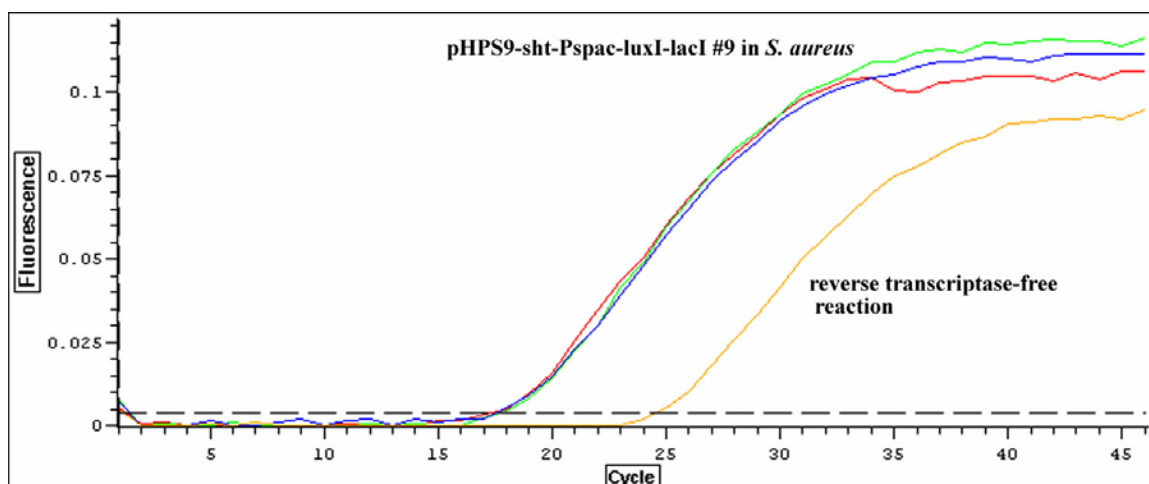


Figure 4-13 (E). Real-time qRT-PCR plots for *luxI* transcription from pHP-PL #9 (or pHPS9-sht-Pspac-luxI-lacI #9) in *S. aureus* (n=3). Reverse transcriptase-free control (n=1, yellow) was included to check DNA contamination. The horizontal line shows the baseline. The point at which the plot crosses the baseline is C_T .

Table 4-5. Real-time qRT-PCR C_T values for *luxI* transcription from pDG-L #28 in *E. coli* and pHP-PL #9 in *E. coli*, *B. subtilis*, and *S. aureus*. ($C_{T(ave)}$ = the average of triplicate C_T measurements, control C_T = the reverse transcriptase-free control for DNA contamination)

Sample	$C_{T(ave)}$	Control C_T	Light production
<i>S. aureus</i> RN4220 (the negative control)	None	39.3	No
pDG-L #28 in <i>E. coli</i>	12.9	24.8	Yes
pHP-PL #9 in <i>E. coli</i>	18.2	30.1	Yes
pHP-PL #9 in <i>B. subtilis</i>	12.6	26.8	Yes
pHP-PL #9 in <i>S. aureus</i>	17.4	24.5	No

***luxI* translation product detection from pHP-PL #9 and pDG-L #28 using SDS-PAGE and Western Blotting**

To determine whether LuxI is produced, soluble and insoluble protein extracts from *E. coli*, *B. subtilis* and *S. aureus* with pHP-PL #9 and *E. coli* containing pDG-L #28 were controlled with SDS-PAGE and Western Blotting. SDS-PAGE was used to determine protein yields. Western Blotting was performed using the LuxI antibody. The wild type *S. aureus* RN4220 was the negative control.

The *B. subtilis* soluble and *E. coli* insoluble protein yields were very low after the first extraction (Figure 4-14 (A)). Since LuxI protein was detected in soluble fractions of *E. coli* strains, another extraction was not performed for insoluble fractions. However, there was no LuxI in *B. subtilis* samples (Figure 4-15 (A)). Therefore, another extraction was done with French Press to increase protein yield. After verification of the high yield with SDS-PAGE (Figure 4-14 (A)), the extract was used for Western Blotting.

Protein yields from extractions were high enough to be visible on gels except for the *E. coli* insoluble fractions as shown by SDS-PAGE results (Figure 4-14). Western Blotting showed the presence of the LuxI protein only in soluble fractions of *E. coli* strains carrying pHP-PL #9 or pDG-L #28 (Figure 4-15). There was no LuxI detection in soluble and insoluble fractions of *B. subtilis* and *S. aureus* harboring pHP-PL #9 (Figure 4-15).

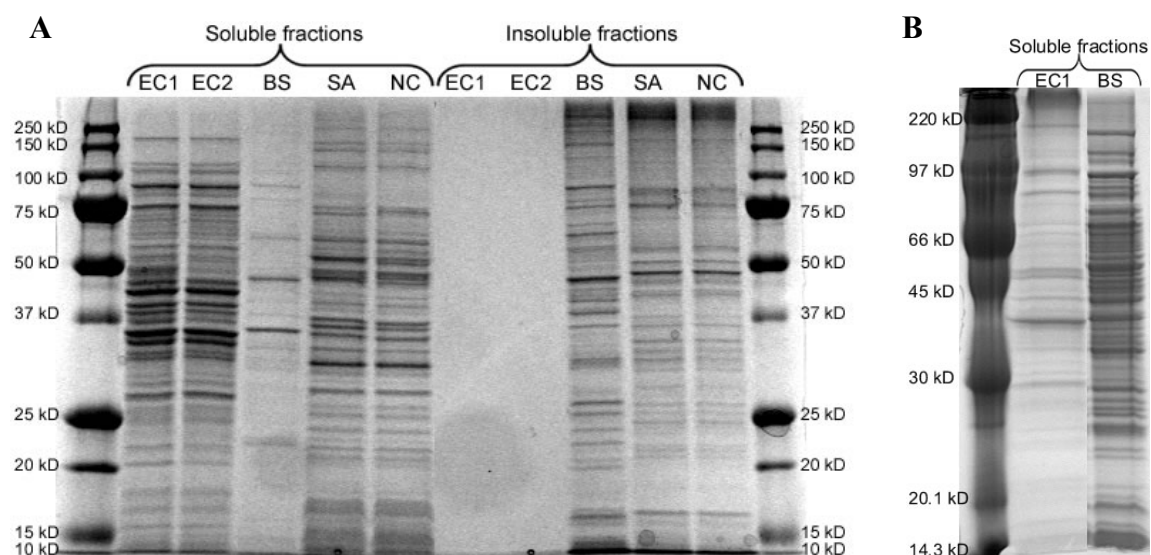


Figure 4-14. SDS-PAGE of total protein extracts from *E. coli*, *B. subtilis* and *S. aureus* with pHP-PL #9; and *E. coli* containing pDG-L #28. (A) First extraction proteins (B) First extraction EC1 protein and second extraction BS protein. (EC1 = *E. coli* containing pDG-L #28; EC2 = *E. coli* with pHP-PL #9; BS = *B. subtilis* harboring pHP-PL #9; SA = *S. aureus* carrying pHP-PL #9; NC = wild-type *S. aureus*)

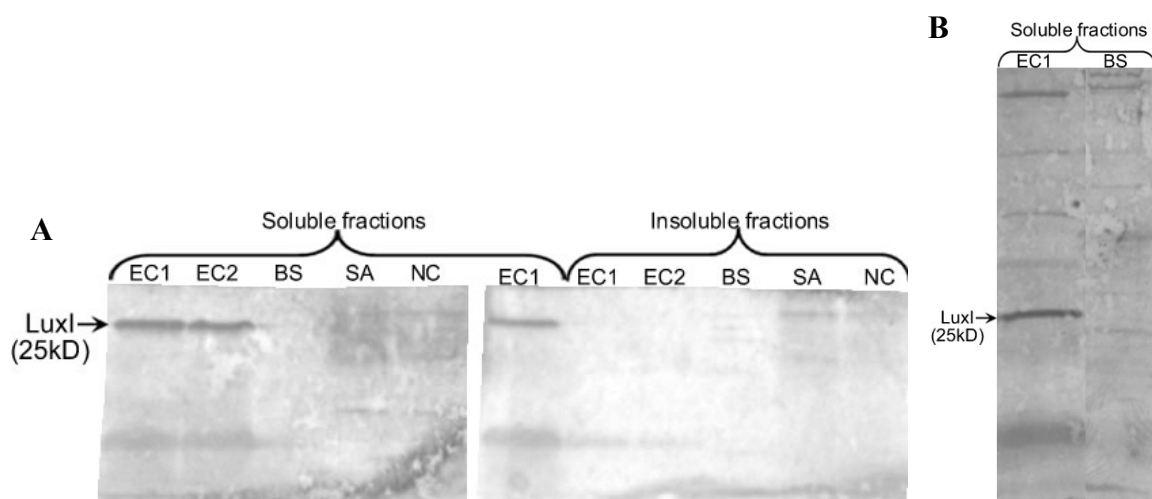


Figure 4-15. Western blotting for LuxI detection from *E. coli*, *B. subtilis* and *S. aureus* with pHP-PL #9; and *E. coli* containing pDG-L #28. (A) First extraction proteins (B) First extraction EC1 protein and second extraction BS protein. (EC1 = *E. coli* containing pDG-L #28; EC2 = *E. coli* with pHP-PL #9; BS = *B. subtilis* harboring pHP-PL #9; SA = *S. aureus* carrying pHP-PL #9; NC = wild-type *S. aureus*)

Detection and analysis of kanamycin resistance provided by pHP-PK #31 in *S. aureus*

Although both *E. coli* and *B. subtilis* containing pHP-PL #9 are capable of producing light, *S. aureus* carrying pHP-PL #9 is not. *S. aureus* with pHP-PL #9 was shown to produce the *luxI* transcript at a level which is close to that of *B. subtilis* containing pHP-PL #9 and higher than that of *E. coli* harboring pHP-PL #9. However, the LuxI protein could be detected only in *E. coli* with pHP-PL #9 but not in *S. aureus* and *B. subtilis* carrying pHP-PL #9 using the LuxI antibody. Therefore, RBS efficiency of pHP-PL #9 in *S. aureus* was tested by replacing the *luxI* CDS with the CDS of *kan^r* which is a

native gene of *S. aureus*. Utilization of a native gene eliminates the codon preference problem during the expression of transcript.

Table 4-6 shows the comparison of kanamycin resistance patterns detected with pHP-PK #31 in *S. aureus* to those of the other plasmids and constructs which have the *kan^r* gene under the control of various promoters and RBSs in *S. aureus*. Figure 4-16 shows the plates with various kanamycin concentrations (10-70 µg/ml) which were streaked with *S. aureus* carrying pHP-PK #31 and *S. aureus* containing pUB110 for comparison.

Table 4-6. Kanamycin resistance patterns provided by pHP-PK #31 in *S. aureus*. Patterns were compared to those of other constructs which contained *kan^r* under the control of different promoters and RBSs in *S. aureus*. (R = Resistant, S = Sensitive.)

	Kanamycin concentration (µg/ml)									
	2.5	5	10	15	20	25	30	35	45	50-70
pHP-PK #31	R	R	R	R	R	R	R	R	R	R
Wild-type <i>S. aureus</i> RN4220	R	R	S	S	S	S	S	S	S	S
pUB110	R	R	R	R	R	R	R	R	R	S
pHP-K #4	R	R	R	R	S	S	S	S	S	S

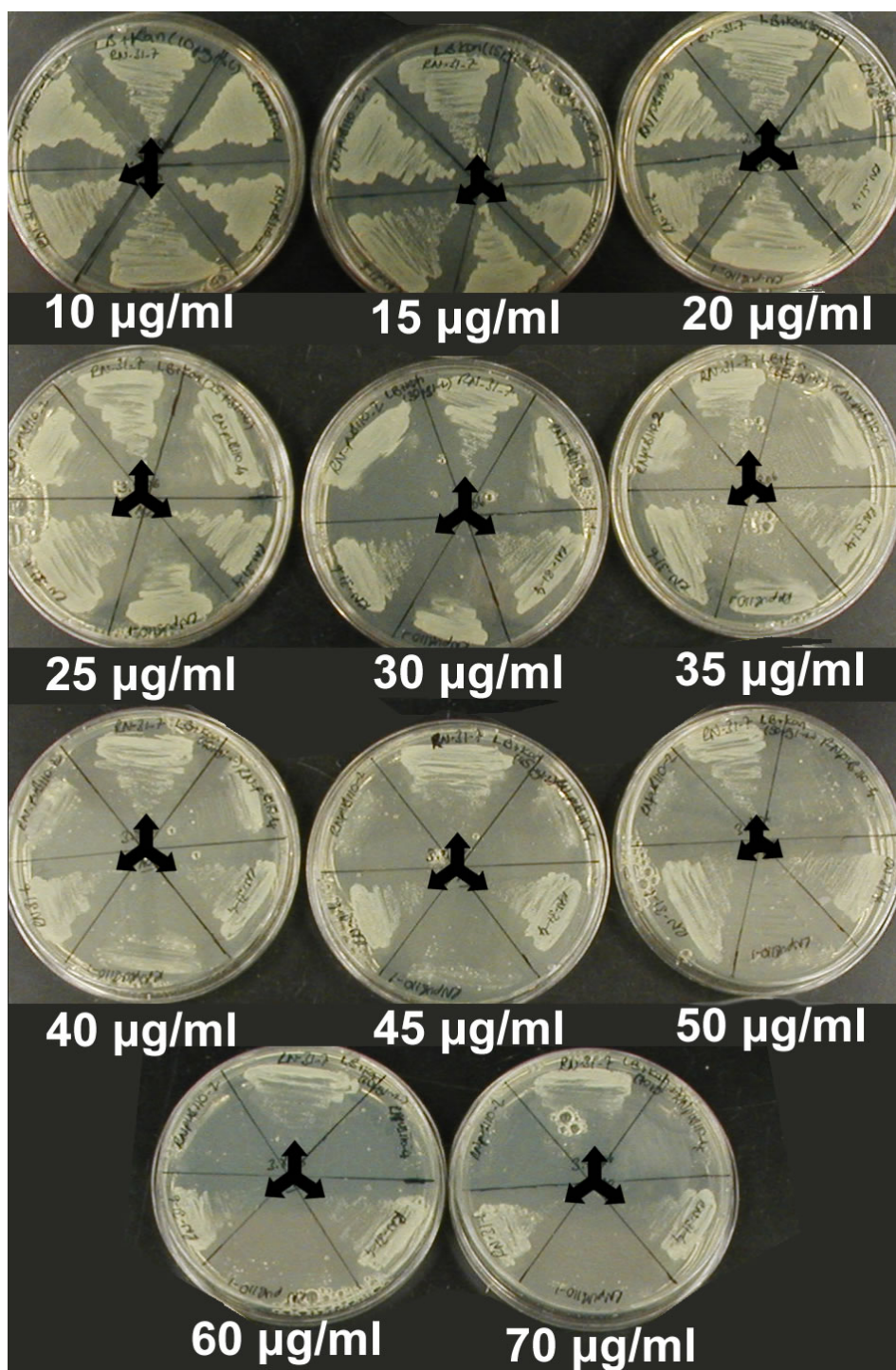


Figure 4-16. Kanamycin resistance patterns provided by pHP-PK #31 in *S. aureus* compared to those from pUB110 in *S. aureus*. Arrows point to colonies of *S. aureus* carrying pHP-PK #31. Other colonies are of *S. aureus* containing pUB110.

Both Figure 4-16 and Table 4-6 show that pHP-PK #31 in *S. aureus* provided the highest level of kanamycin resistance among all plasmids in *S. aureus*. Plasmids used for comparison carry *kan^r* CDS under the control of various RBS and promoters and in vectors with different copy numbers so the RBS efficiency is not the only reason for difference between patterns of kanamycin resistance. However, it was found previously that pHP-PK #31 in *S. aureus* produces RNA amounts which are the same as or higher than those of strains which can produce light using the same construct. Therefore, kanamycin resistance patterns provided by pHP-PK #31 in *S. aureus* provide evidence that the RNA produced can be translated to protein amounts which are even higher than those produced by pUB110 from which *kan^r* CDS originates as long as a *S. aureus*-native gene is used. This at least shows that there is no problem with utilization of pHP-PK #31 RBS in *S. aureus*.

Bioluminescent and fluorescent detection of OHHL from pHP-POL #5 in *E. coli*, *B. subtilis*, and *S. aureus* using Wallac Victor2 1420 Multilabel and 1450 Microbeta Plus Liquid Scintillation Counters

While the *luxI* transcript was obtained from pHP-PL #9 in *S. aureus*, LuxI protein was not detected. RBS of the construct was shown to work by exchanging *luxI* with a native *S. aureus* gene, *kan^r*. To determine if the problem for *luxI* translation in *S. aureus* is codon preference, the codons of *luxI* CDS were adapted to the codon bias of *S. aureus* phage P68. Although *S. aureus* RN4220 was the strain used for pHP-PL #9 expression, it was not selected for codon adaptation since its genome sequence is not known. P68 is not only the phage which *luxI* was planned to clone into but was also demonstrated to carry

genes most of which have high translation efficiency (616). Therefore, P68-optimized *luxI* replaced original *luxI* in pHP-PL #9, resulting in the construction of pHP-POL #5.

pHP-POL #5 was tested for OHHL production in *E. coli*, *B. subtilis*, and *S. aureus* using bioluminescent bioreporter *E. coli* OHHLux and fluorescent bioreporter *E. coli* MT102 with pJBA132. *Staphylococcus aureus* RN4220 was the negative control for *S. aureus* sample while the bioreporter combined with dH₂O instead of supernatant was used as the negative control for *E. coli* and *B. subtilis* samples. All samples and controls were prepared in triplicate. Wallac Victor2 1420 Multilabel Counter performed fluorescence and absorbance measurements while Wallac 1450 Microbeta Plus Liquid Scintillation Counter detected only bioluminescence. The Wallac Victor2 1420 Multilabel Counter measurements were normalized by dividing GFP data by OD₄₅₀ values. Bioluminescence or fluorescence values at each time point represent the mean value of triplicate measurements. All measurements were carried out at 28°C.

Results are shown in Figures 4-17 through 4-19. Although bioluminescence and fluorescence were obtained from pHP-POL #5 in *E. coli* and *B. subtilis*, pHP-POL #5 in *S. aureus* did not produce any light. However, comparison of maximum induction values obtained from *E. coli* and *B. subtilis* samples to those from *E. coli* and *B. subtilis* carrying non-optimized *luxI* (Table 4-7) shows that optimization of *luxI* decreased the amount of light from *E. coli* significantly, while the increase in light from *B. subtilis* was not significant. Therefore, lack of light from *S. aureus* containing pHP-POL #5 can not be used to eliminate the possibility of codon preference problem since it is not certain whether the optimization of *luxI* was successful.

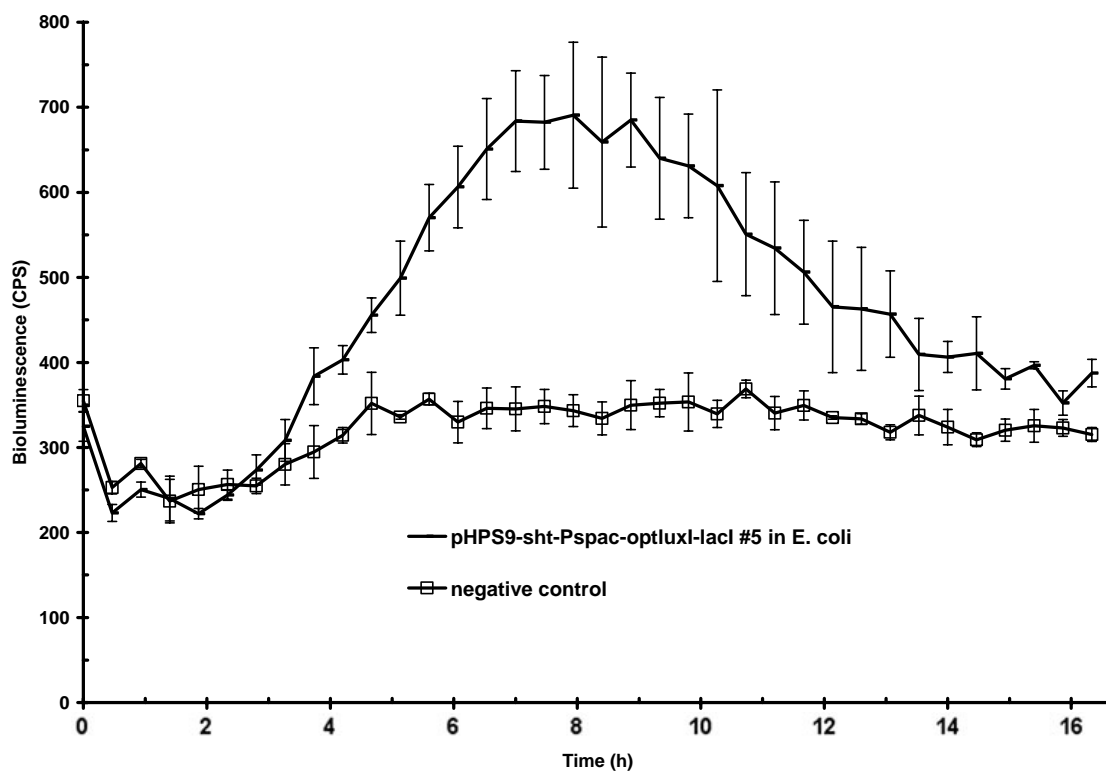


Figure 4-17 (A). Bioluminescent OHHL detection of from pHP-POL #5 (or pHP59-sht-Pspac-optluxI-lacI #5) in *E. coli* at 28°C using the bioreporter *E. coli* OHHLux and Wallac 1450 Microbeta Plus Liquid Scintillation Counter. Results represent the mean bioluminescence values ($n=3$) \pm SD (bars).

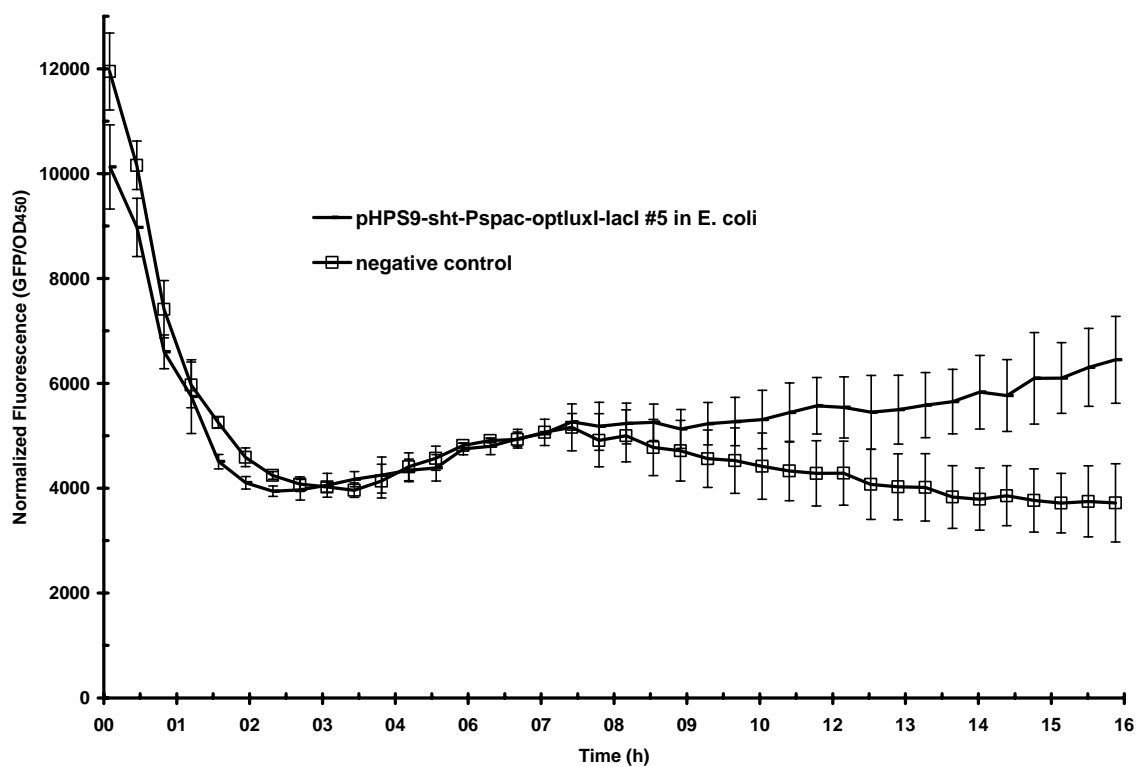


Figure 4-17 (B). Fluorescent OHHL detection from pHP-POL #5 (or pHPS9-sht-Pspac-optluxI-lacI #5) in *E. coli* at 28°C using the bioreporter *E. coli* MT102 with pJBA132 and Wallac Victor2 1420 Multilabel Counter. Results represent the mean fluorescence values ($n=3$) \pm SD (bars).

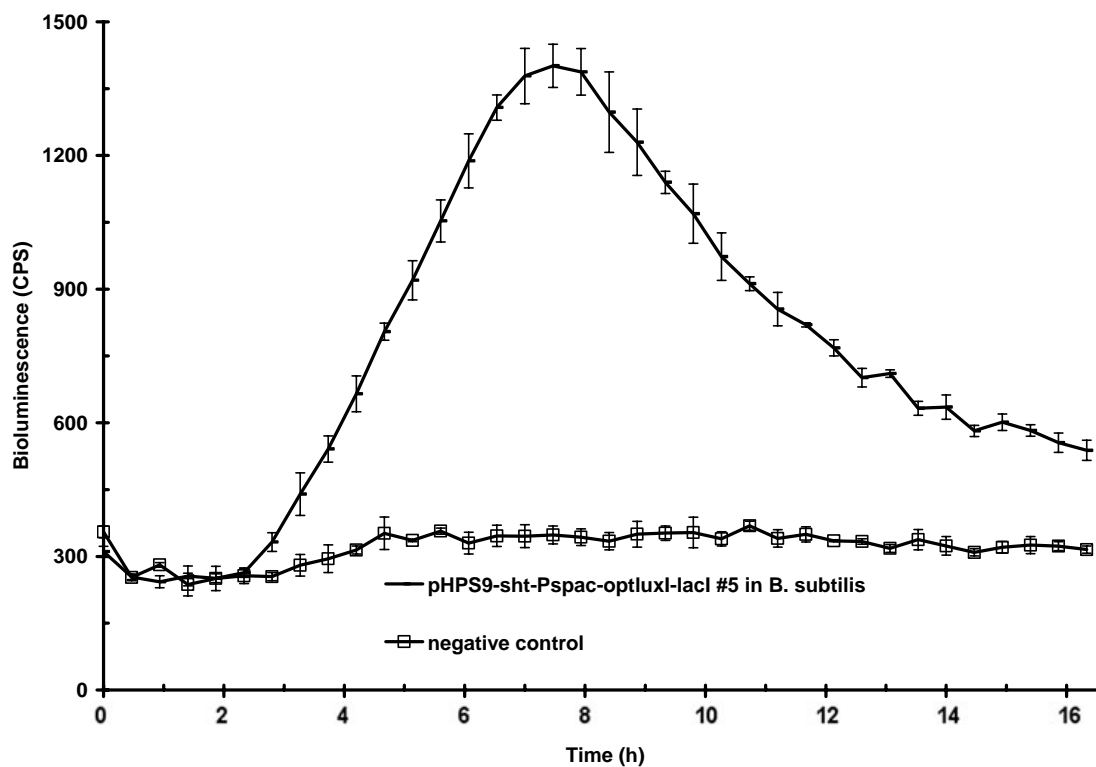


Figure 4-18 (A). Bioluminescent OHHL detection from pHP-POL #5 (or pHPS9-sht-Pspac-optluxI-lacI #5) in *B. subtilis* at 28°C using the bioreporter *E. coli* OHHLux and Wallac 1450 Microbeta Plus Liquid Scintillation Counter. Results represent the mean bioluminescence values ($n=3$) \pm SD (bars).

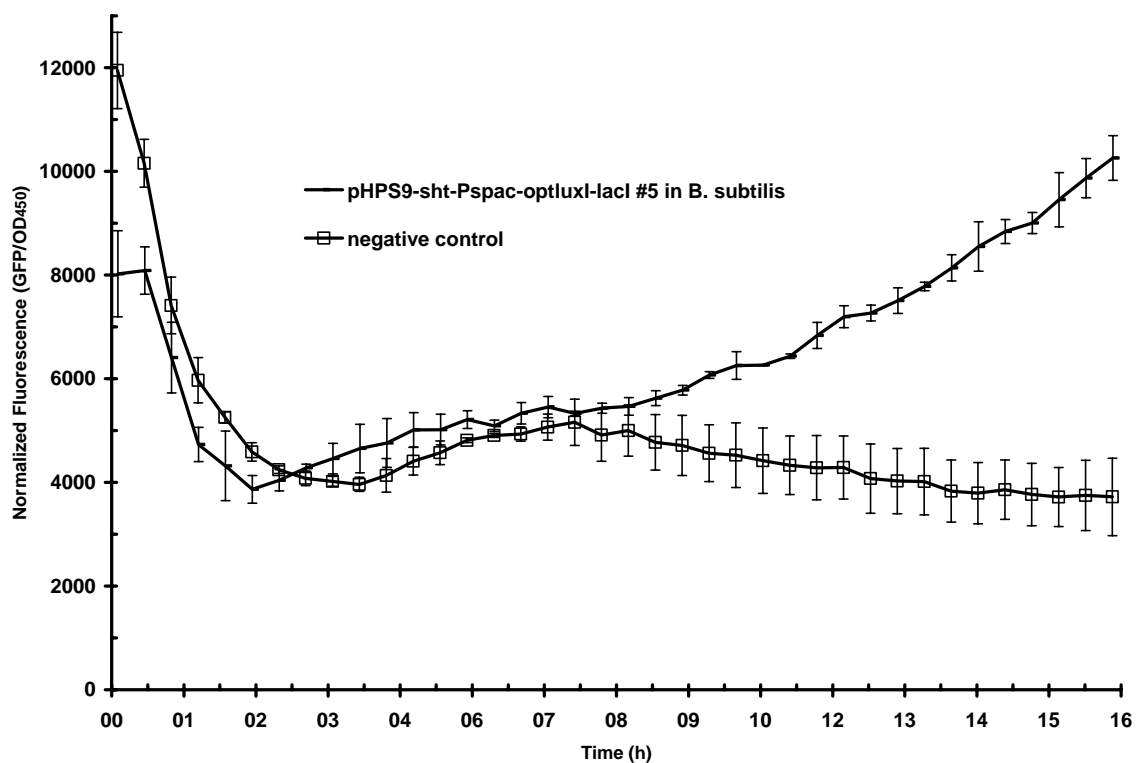


Figure 4-18 (B). Fluorescent OHHL detection from pHP-POL #5 (or pHPS9-sht-Pspac-optluxI-lacI #5) in *B. subtilis* at 28°C using the bioreporter *E. coli* MT102 with pJBA132 and Wallac Victor2 1420 Multilabel Counter. Results represent the mean fluorescence values ($n=3$) \pm SD (bars).

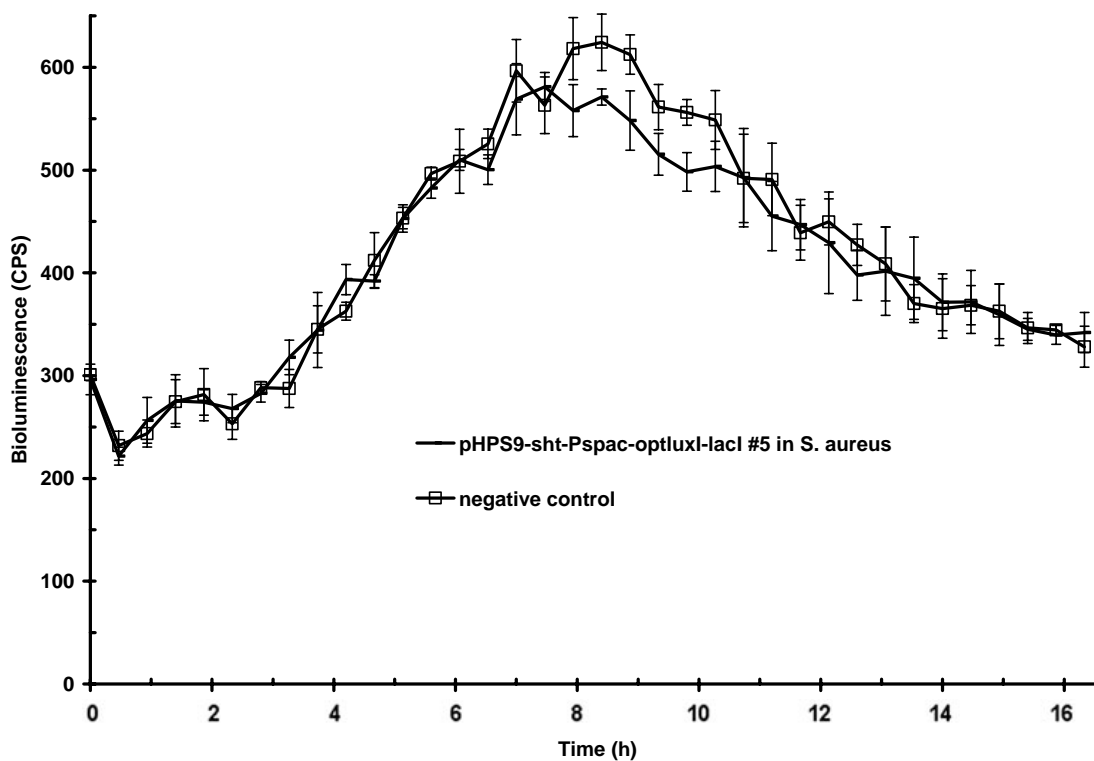


Figure 4-19 (A). Bioluminescent OHHL detection from pHP-POL #5 (or pHPS9-sht-Pspac-optluxI-lacI #5) in *S. aureus* at 28°C using the bioreporter *E. coli* OHHLux and Wallac 1450 Microbeta Plus Liquid Scintillation Counter. Results represent the mean bioluminescence values ($n=3$) \pm SD (bars).

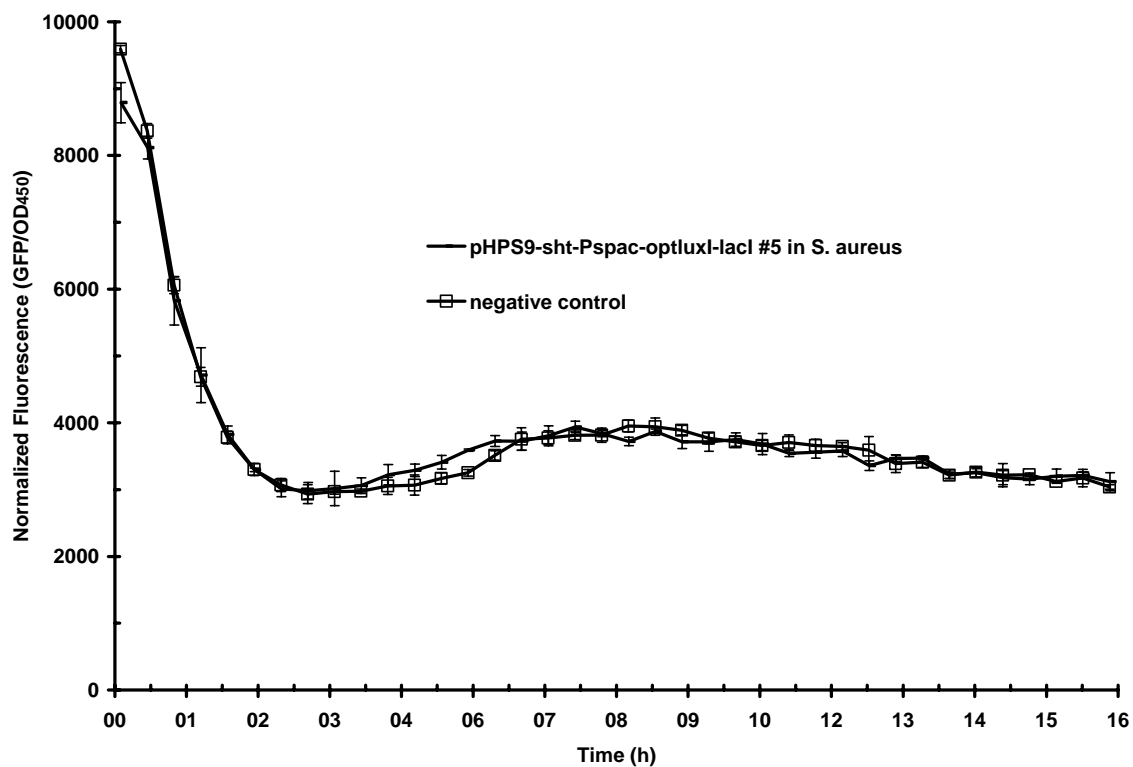


Figure 4-19 (B). Fluorescent OHHL detection from pHP-POL #5 (or pHPS9-sht-Pspac-optluxI-lacI #5) in *S. aureus* at 28°C using the bioreporter *E. coli* MT102 with pJBA132 and Wallac Victor2 1420 Multilabel Counter. Results represent the mean fluorescence values ($n=3$) \pm SD (bars).

Table 4-7. Comparison of bioluminescence and fluorescence from constructs that carry non-optimized or optimized *luxI* for adaptation to the codon bias of *S. aureus* phage P68. Bioluminescence was detected using the bioreporter *E. coli* OHHLux and Wallac 1450 Microbeta Plus Liquid Scintillation Counter. Fluorescence was detected using the bioreporter *E. coli* MT102 harboring pJBA132 and Wallac Victor2 1420 Multilabel Counter. (MI = maximum induction-the highest amount of light from a sample divided by the negative control value at the same time point, * = Time period in h to obtain MI)

	pDG-L #28 in <i>E. coli</i>	pHP-PL #9 in <i>E. coli</i>	pHP-PL #9 in <i>B. subtilis</i>	pHP-POL #5 in <i>E. coli</i>	pHP-POL #5 in <i>B. subtilis</i>
Bioluminescence	604X _{(7)*}	114X _{(7.5)*}	3.12X _{(5.5)*}	2X _{(8)*}	4X _{(8)*}
Fluorescence	20X _{(16)*}	14X _{(17.5)*}	1.74X _{(16)*}	1.7X _{(16.5)*}	2.8X _{(16.5)*}

Invitro packaging of *S. aureus* phage P68 genome

Staphylococcus aureus phage P68 was selected for *luxI* cloning to construct the recombinant phage for the *S. aureus* monitoring system. An invitro packaging method was developed by using only the P68 genome. The genome purified was packaged using MaxPlax Lambda Packaging Extracts (Epicentre Biotechnologies, Madison, WI). The phage obtained tested positive for infection of the host strain *S. aureus* RN451. *Staphylococcus aureus* phage P68 genome can be packaged invitro using MaxPlax Lambda Packaging Extracts (Epicentre Biotechnologies, Madison, WI).

Summary of results obtained with plasmids used to determine the *luxI* expression efficiency in *S. aureus*; and in *E. coli* and *B. subtilis* as controls

Table 4-8 shows a summary of results obtained with all constructs which were used to determine *luxI* expression efficiency in *S. aureus* and also in *E. coli* and *B. subtilis* for comparison purposes.

Table 4-8. A summary of results from all constructs used to determine *luxI* expression efficiency in *S. aureus*; and in *E. coli* and *B. subtilis* as controls. (x = not tested)

Plasmid	in <i>E. coli</i>	in <i>B. subtilis</i>	in <i>S. aureus</i>
pMO-L #7	no light production	x	x
pMK-L #13.3	x	x	no light production
pHP-L #7	light production	x	no light production
pHP-PL #9	light production	light production	no light production
	<i>luxI</i> transcript detected	<i>luxI</i> transcript detected	<i>luxI</i> transcript detected
	LuxI detected	LuxI not detected	LuxI not detected
	RBS = x	RBS = x	RBS working
	decrease in light when optimized <i>luxI</i> exchanged with <i>luxI</i>	no significant increase in light when optimized <i>luxI</i> exchanged with <i>luxI</i>	no light when optimized <i>luxI</i> exchanged with <i>luxI</i>

CHAPTER V

DISCUSSION AND CONCLUSIONS

CONSTRUCTION OF *S. AUREUS* BIOREPORTER

The expression of *luxI* gene in *S. aureus* was examined in this work. The gene was cloned into *E. coli*, *B. subtilis*, and *S. aureus* under the control of various RBSs and promoters specific to Gram-positive bacteria. After the trial of several constructs, significant light was generated with *E. coli* using the pDG148-Stu RBS and promoter. The same construct provided a moderate level of light in *B. subtilis* compared to that of *E. coli*. However, there was no light from *S. aureus*. The reason for this was investigated by measuring the *luxI* transcript and protein using real-time qRT-PCR and Western blotting, respectively. Although the presence of *luxI* transcript was shown in *E. coli*, *B. subtilis*, and *S. aureus* carrying the construct, the protein was detected only in *E. coli*. The adaptation of *luxI* codons for *S. aureus* phage P68 genome codon utilization to increase LuxI production in *S. aureus* was not successful in generating light from *S. aureus* harboring the construct.

First, *luxI* was cloned into EZ::TN pMOD-2<MCS> plasmid (Epicentre Biotechnologies, Madison, WI) between two MEs. MEs are EZ::TN transposase (Invitrogen, Carlsbad, CA) recognition sites for transposition of the region between MEs to occur. The original plan was to clone *luxI* into *S. aureus* phage Twort using transposition since its genome sequence was not known at this point. The RBS of *luxI* which is from Gram-negative *V. fischeri* was changed into a Gram-positive RBS (615).

The Gram-negative RBS is too weak for Gram-positive ribosomes since Gram-positive bacteria do not possess ribosomal protein S1 which is found in *E. coli* (615). S1 is thought to provide the positioning which is necessary for SD (Shine-Dalgarno) sequence of RBS to interact with the initiation codon signals on the 3' end of the 16S rRNA, part of ribosomal 30S subunit, by binding to RNA non-specifically (617). Therefore, Gram-positive SD sites need to be in more extensive complementarity with the 3' end of the 16S rRNA compared to Gram-negative bacteria. This causes Gram-positive ribosomes to show RBS selectivity. The SD sequence was placed 7 bps upstream of the *luxI* CDS, which is typical for *S. aureus* (615). *luxI* with the Gram-positive RBS was placed under the control of *S. aureus* phage Φ 85 X8 promoter (605) into pMOD-2<MCS> vector. The resulting construct, pMO-L #7, did not produce light in *E. coli* although X8 was found to be a promoter stronger than *E. coli* λ P_{Tac} and P_L promoters (605).

The X8 promoter-*S. aureus* RBS-*luxI* CDS fragment was integrated into pMK4 which is a Gram-positive and -negative shuttle vector and cloned into *S. aureus* to test the expression of *luxI* in *S. aureus* under the control of same RBS and promoter. There was no generation of light from *S. aureus* as well. The source of X8 promoter which was amplified from the phage Φ 85 genome was the X8 sequence described by Carbonelli et al. (605). Although its sequence was different from Carbonelli et al. (605), the putative promoter region was conserved. Therefore, the fragment obtained was used as the promoter region for constructs. The genome of phage Φ 85 was sequenced later in 2005 (606). The X8 sequence from the Carbonelli et al. article (605) and the sequence used in this study were aligned with the phage genome sequence by using BLAST engine for local alignment (Figure 5-1).

Query	42691	AATTCGGTAACGATGATGAAAGAGTTAAATTCGGAATGGAATTAAACAATAAAATTTT	42750
Sbjct	408	AATTCGGTAACGATGATGAAAGAGTTAAATTCGGAATGGAATTAAACAATAAAATTTT	349
Query	42751	TGGAGGATGACACAAATGAATAATCGCGAAAAAATCGAACAGTCCGTTATTAGTGCTAGT	42810
Sbjct	348	TGGAGGATGACACAAATGAATAATCGCGAAAAAATCGAACAGTCCGTTATTAGTGCTAGT	289
Query	42811	GCGTATAACGGTAATGACACAGAGGGGTTGCTAAAAGAGATTGAGGACGTGTATAAGAAA	42870
Sbjct	288	GCGTATAACGGTAATGACACAGAGGGGTTGCTAAAAGAGATTGAGGACGTGTATAAGAAA	229
Query	42871	GCGCAAGCGTTTGATGAAATACTTGAGGGAATGACAAATGCTATTCAACATTCAAGTTAAA	42930
Sbjct	228	GCGCAAGCGTTTGATGAAATACTTGAGGGAATGACAAATGCTATTCAACATTCAAGTTAAA	169
Query	42931	GAAGGTATTGAACTTGATGAAGCAGTAGGGATTATGGCAGGTCAAGTTGTCTATAAATAT	42990
Sbjct	168	GAAGGTATTGAACTTGATGAAGCAGTAGGGATTATGGCAGGTCAAGTTGTCTATAAATAT	109
Query	42991	GAGGAGGAATAGGAAAATGACTAACACATTACAAGTAAACTATTATCAAAAAATGCTAG	43050
Sbjct	108	GAGGAGGAATAGGAAAATGACTAACACATTACAAGTAAACTATTATCAAAAAATGCTAG	49
Query	43051	AATGCCCGAACGAAATCATAAGACGGATGCAGGTTATGACATATTCTC	43098
Sbjct	48	AATGCCCGAACGAAATCATAAGACGGATGCAGGTTATGACATATTCTC	1

Figure 5-1 (A). The aligning of phage Φ 85 genome sequence (the sense strand) and the X8 promoter sequence (the sense strand) used in construction of pMO-L #7 using BLAST. Vertical lines show identical bases. (Query = phage genome sequence, subject = X8 promoter sequence)

Query	42691	AATTCGGTAACGATGATGAAAGAGTTAAATTCGGAATGGAATTAAACAATAAAATTTT	42750
Sbjct	355	AATTCGGTAACGATGATGAAAGCGTTAAATTCGGAATGGAATTAAACAATAAAATTTT	296
Query	42751	TGGAGGATGACACAAATGAATAATCGCGAAAAAATCGAACAGTCCGTTATTAGTGCTAGT	42810
Sbjct	295	TGGAGGATGACACAAATGAATAATCGCGAAAAAATCGAACAGTCCGTTATTAGTGCTAGT	236
Query	42811	GCGTATAACGGTAATGACACAGAGGGGTTGCTAAAAGAGATTGAGGACGTGTATAAGAAA	42870
Sbjct	235	GCGTATAACGGTAATGACACAGAGGGGTTGCTAAAAGAGATTGAGGACGTGTATAAGAAA	176
Query	42871	G	42871
Sbjct	175	G	175
Query	42901	ATGACAAATGCTATTCAACATTCAAGTAAAGAGGTATTGAACTTGATGA	42950
Sbjct	149	ATGACAAATGCTATTCAACATTCAAGTAAAGAGGTATTGAACTTAATGA	100
Query	43006	AATGACTAACACATTACAAGTAAACTATTAT-----CAAAAAATGCTAGAATGC	43055
Sbjct	104	AATGACTAACACATTACAAGTAAACTATTATGACATATTATCAAAAAATGCTAGAATCG	45
Query	43056	CCGAACGAAATCATAAGACGGATGCAGGTTATGACATATTCTCA	43099
Sbjct	44	CCGAACGAAATCATAAGACGGATGCAGGTTATGACATATTCTCA	1

Figure 5-1 (B). The aligning of phage Φ 85 genome sequence (the sense strand) and the X8 promoter sequence (the sense strand) described by Carbonelli et al. (605) using BLAST. Vertical lines show identical bases and horizontal lines show missing nucleotides. (Query = phage genome sequence, subject = X8 promoter sequence)

While the X8 promoter sequence used for constructs match the phage genome sequence completely, this is not the case for the X8 promoter sequence reported by Carbonelli et al. (605). Out of a total 366 bps of the promoter sequence, 1-104th, 100-149th, and 175-355th bps match with different parts of the phage genome. The other sites of the promoter are extra regions which do not exist in the genome sequence. The X8 promoter was found experimentally by Carbonelli et al. (605) by placing DNA fragments obtained from digestion of various *S. aureus* phage genomes in place of the ampicillin resistance gene promoter. It was determined to belong to phage Φ85 using hybridization. The authors stated that it provides high ampicillin resistance and contains putative promoter motifs such as -10 and -35 regions. Based on these, the authors claimed that X8 possesses a real, strong promoter. However, the X8 sequence seems to be a combination of different regions some of which are not found in the phage Φ85 genome. Although the promoter motifs mentioned in the article are found in the X8 fragment of 175-355th bps which matches with the phage genome, these are putatively determined motifs. It is possible that the promoter sequence used for the constructs did not have the regions which acted as the promoter in the Carbonelli et al. study (605).

Expression of *luxI* in *E. coli* and *S. aureus* was tested using another promoter, P59 of pHPS9 plasmid. P59 is a Gram-positive promoter from *L. lactis*. *luxI* was cloned into pHPS9 in front of P59 under the control of same Gram-positive RBS used for previous constructs. With this construct, light was obtained from *E. coli* although there was no light from *S. aureus*. To determine if the lack of light from *S. aureus* is caused by a problem at the OHHL or LuxI production level, LCMS was used. OHHL production from *E. coli* and *S. aureus* harboring the construct was determined by LCMS. While *E.*

coli was found to produce it (however without certainty), there was no OHHL from *S. aureus*. The *luxI* CDS was replaced with *S. aureus kan^r* CDS from pDG148-Stu (same as the *kan^r* CDS from pUB110) to examine the efficiency of the construct for the insert production. It was named pHP-K #4. Kanamycin resistance provided by the insert under the control of same RBS and promoter and in the same plasmid used for *luxI* was determined. Results were compared to those of other constructs carrying *kan^r* CDS from this study (Table 4-2). pHP-K #4 in *S. aureus* provided the lowest kanamycin resistance compared to the other plasmids in *S. aureus*. *kan^r* CDS is under the control of various RBSs and promoters and in plasmids with different copy numbers with these constructs (Table 5-1).

Table 5-1. Comparison of copy numbers, RBSs, and promoters of constructs used for determination of *S. aureus* kanamycin resistance patterns.

Construct	Kan ^r	Plasmid copy no	RBS used for <i>kan^r</i>	Promoter used for <i>kan^r</i>
pHP-K #4	15 µg/ml	unknown in <i>S. aureus</i> , 5 in <i>B. subtilis</i> (pTA1060 ori) (610)	RBS for <i>luxI</i> expression in previous constructs (615)	P59 from pHPS9
pUB110	35 µg/ml	10 in <i>S. aureus</i> , 50 in <i>B. subtilis</i> (619, 621)	original <i>S. aureus kan^r</i>	original <i>S. aureus kan^r</i>
pHP-PK #31	70 µg/ml	unknown in <i>S. aureus</i> , 5 in <i>B. subtilis</i> (pTA1060 ori) (610)	pDG148-Stu Gram-positive (611)	Pspac from pDG148-Stu, hybrid of the <i>B. subtilis</i> phage SPO-1 promoter and the <i>lac</i> operator (611, 622)

Although pHP-K #4 copy number in *S. aureus* is not known, it is the same as the pHP-PK #31 copy number since both plasmids carry the same Gram-positive origin of replication. pHP-PK #31 provided much higher Kan^r. The plasmid copy number does not seem to be the reason for weak Kan^r level. Promoters and RBSs used for constructs are all different from one another. Therefore, the reason for the low efficiency of pHP-K #4 in *S. aureus* can be either one of these or a combination of them. pHP-K #4 in *E. coli* was found to produce the highest Kan^r level compared to other constructs, unlike *S. aureus* (Table 4-2). Since all constructs has the same ori, pMB1, for *E. coli*, the copy number for all of them is the same (15-20/chromosome) (610, ATCC). The different responses of the constructs in *E. coli* may be originating from either the promoter or RBS, or both. This difference between Kan^r from *E. coli* and *S. aureus* provided by the same construct was expected. *E. coli* ribosomes can use mRNA from a range of Gram-positive and -negative organisms while Gram-positive ribosomes show RBS selectivity as explained previously (617). Studies have shown that the same promoters show different transcription levels in *E. coli* and *S. aureus* (618-620). Also, constructs have higher copy numbers in *E. coli*. Other reasons may be mRNA or protein stability or codon utilization differences between two species.

luxI was cloned into a Gram-positive and -negative shuttle expression vector, pDG148-Stu in front of the Gram-positive promoter *Pspac* and RBS of the plasmid (611). *Pspac* is a hybrid promoter of the *B. subtilis* phage SPO-1 and the *lac* operator (611, 622). The plasmid also carries *E. coli lacI* repressor CDS under the control of penicillinase RBS and promoter of *B. licheniformis* to be expressed in *B. subtilis* (622). Therefore, *Pspac* which is repressed by LacI is induced when IPTG is added since IPTG

represses *lacI*. The IPTG-inducible promoter of the plasmid allows utilization of only SDS-PAGE to detect LuxI production. The resulting plasmid, pDG-L #28, could not be electroporated into *S. aureus*. To decrease the size of the plasmid, *lacI* and *luxI* under the control of *Pspac* and RBS were integrated into a shortened version of pHPS9. This smaller construct, pHP-PL #9, could be transferred into *S. aureus* and *B. subtilis*. The expression obtained with this plasmid was constitutive. IPTG (or IPTG substitute, Overnight Express Autoinduction System 1 of Novagen (Darmstadt, Germany) had no inducing effect on the promoter for both *E. coli* and *B. subtilis*. Therefore, further experiments were performed without IPTG addition. For *lac* repressor-operator system to be functional, both *lac* repressor and operator need to work properly (622). The binding site of the repressor not only contains the *lac* operator but also a part of the *lacZ*. The replacement of this region with a foreign gene may decrease the affinity of the repressor for the operator. Inability of the *lac* repressor to work leads to constitutive expression (622, 623). When the *lac* operator does not function, IPTG can not induce the promoter (622).

Light was obtained from *E. coli* and *B. subtilis* but not from *S. aureus* with pHP-PL #9. pDG-L #28 in *E. coli* generated light as well. However, the amount of light produced by *E. coli* with both constructs was much higher than *B. subtilis* light levels, pointing to the fact that the constructs work more efficiently in *E. coli*.

To determine the reason for the absence of light from *S. aureus*, *luxI* transcript and protein product were examined. *luxI* transcript was found in all strains with the constructs including *S. aureus* using the real time qRT-PCR (Table 4-5 and Figure 4-13). The amount of RNA (total) used for the experiment was the same (125 ng) for all strains.

All extractions were performed using the mid-log phase cultures. Since the aim was to detect only the presence or absence of *luxI* transcript, its amount was not determined. The transcript amounts from different constructs were compared with one another. The order of the strains from the one with the highest amount of transcript to the one with the lowest is *B. subtilis* with pHP-PL #9>*E. coli* with pDG-L #28>*S. aureus* with pHP-PL #9>*E. coli* with pHP-PL #9. Production of LuxI was checked by Western Blotting using an antibody which targeted a certain region of the LuxI sequence. The antibody detected LuxI in *E. coli* strains carrying pHP-PL #9 or pDG-L #28 but not in *B. subtilis* and *S. aureus* harboring pHP-PL #9 (Figure 4-15).

Since *luxI* transcript was detected from *S. aureus* but not LuxI, the efficiency of the construct for a native *S. aureus* gene CDS was tested to eliminate the codon preference problem. *luxI* CDS in pHP-PL #9 was replaced by the *S. aureus kan^r* CDS. Resistance to kanamycin provided by this construct, pHP-PK #31, was compared to those by other constructs in *S. aureus*. pHP-PK #31 was resistant up to 70 µg/ml kanamycin while pHP-K #4 was kan^r up to 15 µg/ml and pUB110 (the source of *kan^r* CDS) up to 45 µg/ml (Figure 4-16 and Table 4-6). pHP-PK #31 kanamycin resistance level was high unlike the other constructs (624-626). All constructs contained the same *kan^r* CDS under the control of different RBSs and promoters with different copy numbers in *S. aureus* (Table 5-1), so differences between Kan^r levels demonstrate efficiencies of all these features combined for the production of a native gene. Results show the capability of pHP-PK #31 to produce high amounts of the gene product in *S. aureus*, provided that the gene CDS is native to *S. aureus*.

luxI CDS was adapted to the codon bias of *S. aureus* phage P68 to eliminate potential problems which may be caused by codon preference. Phage P68 was used because it was the phage which was selected to use for construction of the recombinant phage with *luxI* and its genes have high translation efficiency (616). Optimized *luxI* gene replaced *luxI* in pHP-PL #9. The new construct, pHP-POL #5, was tested for light generation. *Escherichia coli* and *B. subtilis* harboring the construct produced light while *S. aureus* did not (Figures 4-17 through 4-19). However, light generated by *E. coli* decreased significantly and light from *B. subtilis* was not increased significantly compared to non-optimized *luxI* light levels (Table 4-7), which may point to an unsuccessful optimization process. Therefore, optimization results can not be used to assess the effect of codon preference on *luxI* expression in *S. aureus*.

luxI transcript production from pHP-PL #9 showed that the promoter *Pspac* worked efficiently in all strains including *S. aureus*. LuxI was detected from *E. coli* carrying pHP-PL #9 or pDG-L #28 which produces light but not from *S. aureus* harboring pHP-PL #9 which is light negative. Although *B. subtilis* with pHP-PL #9 generates light, there was no LuxI detection from this strain. This shows that there may be a problem with the protein detection method. Therefore, the absence of LuxI from *S. aureus* does not mean that it does not produce LuxI. The problem may be posttranslational modification of the protein in Gram-positive *B. subtilis* and *S. aureus*, which may be occurring in a different way or not be occurring at all in Gram-negative *V. fischeri* (source of *luxI*) and *E. coli* (627). The other possibility is an insufficient amount of protein from the strain to produce a band during Western blotting (628). Although *B. subtilis* produces light, its level is very low compared to *E. coli* strain light levels (~5-193

times lower) (Table 4-4) and there is no light detection from *S. aureus*. Therefore, the western blotting results are inconclusive for *B. subtilis* and *S. aureus*. The high-level of resistance obtained from *kan^r* CDS in *S. aureus* which replaced *luxI* CDS in pHP-PL #9 showed that this construct worked efficiently for genes which are not foreign to the host organism. However, this does not indicate that the RBS of the construct is strong since the promoter itself can be strong enough to cause such a Kan^r level.

In an attempt to increase translation, the *luxI* CDS codon preference was adapted to *S. aureus* codon usage. Determination of the codon usage for an organism to which a gene will be adapted is performed by using the organism's genome sequence. This eliminated *S. aureus* RN4220 whose sequence is unknown as the organism to which *luxI* codons will be adapted. P68, the phage to be used for *luxI* cloning, was selected instead. Most of the P68 genes (70%) were found to have high translation efficiency (616). The codon usage of P68 was expected to be adapted to its host's translation mechanism since it does not encode its own tRNAs (629). Indeed P68 codon usage was found to be positively correlated with the host, *S. aureus* Mu50, tRNA copy numbers (616). Although the *S. aureus* strain used in this study was different from the strain RN4220, the results should be applicable to all *S. aureus* strains. Genes within a species are very homogenous in codon usage (630). However, optimization did not increase light from *B. subtilis* significantly. *Staphylococcus aureus* and *B. subtilis* are phylogenetically very close (631-633). Almost half of the *S. aureus* proteins, most of which are essential for vegetative growth, are very similar to those of *B. subtilis* and *B. halodurans* (634). Furthermore, *S. aureus* genes have been shown to be translated in *B. subtilis* efficiently (635). Therefore, it is possible that light levels from *B. subtilis* with the optimized *luxI* point to an

unsuccessful optimization which may or may not be caused by the use of P68 codon usage for the optimization. However, *B. subtilis* and *S. aureus* are different organisms and thus results may also mean that the problem is not at the translational level.

Results from all of the experiments suggest that the problem is either at the LuxI protein level, translational or post-translational, or at the level of LuxI product, OHHL. The stability of mRNA is one of the factors for translation efficiency (636, 637). mRNA stability changes depending on the half-life which can be in the range of seconds to 20 min. After that, they are degraded by ribonucleases (RNases) (636, 637). mRNA with a short half life decreases the amount of translation. Factors affecting mRNA stability are folding, protection by ribosomes and polyadenylation (636, 637). Protein instability is also important in determining translational efficiency. Proteins are degraded by cellular proteases after translation (638, 639). Stability depends on the protein amino acid sequence. Certain amino acids located in certain places of the protein sequence affect stability (636). One example is the type of amino acid found in the N-terminus. Although the amino terminal amino acid is always methionine, it may be removed leaving another amino acid as the first one (636). There may be removals or additions of other amino acids as well. These post-translational modifications may place a particular amino acid in the amino terminus, which decreases protein half life (636). Arginine is such an example. If it is used as the first amino acid, the half life of protein is decreased to two minutes from hours. The third problem may be over-expression or incorrect folding of the protein which leads to aggregation and thus formation of inclusion bodies in the cell (636, 637). These are insoluble and not functional. There may also be some post-translational

modifications on the protein which is specific to *S. aureus*. These modifications may result in production of a nonfunctional LuxI protein.

The cause for the lack of light from *S. aureus* with the non-optimized or optimized *luxI* may be related with OHHL production. There are different AHL-inactivation mechanisms developed by various prokaryotic and eukaryotic organisms. *Bacillus* species including *B. thuringiensis*, *B. cereus* and *B. mycoides* were shown to produce AHL lactonases (475, 476, 640). AHL lactonases inactivate AHLs by hydrolyzing their lactone ring. AHL lactonase homologues were found in other species as well such as *A. tumefaciens* (641) and *Arthrobacter* sp. (642). Although AHL lactonase has not been reported from *S. aureus* so far, future studies may show otherwise. AHL antagonists which were detected in various Gram-negative bacteria are another AHL inactivation mechanism (131, 142, 227, 643-646). They compete with the AHL to bind to regulatory proteins, which blocks the quorum sensing response. The halogenated furanones from marine red algae *Delisea pulchra* have been documented to inhibit luminescence and virulence in *V. harveyi* by displacing OHHL from LuxR transcription factor (647-649). AHL was found to be metabolized by *Variovorax paradoxus* as the sole source of energy and nitrogen (650). Other possible mechanisms include AHL synthesis inhibition as a result of antimicrobial triclosan suppression of the reaction which is catalyzed by enoyl-acyl carrier protein reductase and autoinducer synthase targeting (651). *Staphylococcus aureus* may be found to possess one or more of these mechanisms in the future.

CHAPTER VI

MATERIALS AND METHODS

CONSTRUCTION OF *SALMONELLA* BIOREPORTER

Bacterial strains, plasmids, and bacteriophage

Bacterial strains, plasmids, and bacteriophage used in this study are shown in Tables 6-1, 6-2, and 6-3, respectively.

Growth and storage conditions

Escherichia coli, *Salmonella*, and *Klebsiella* strains were grown overnight in LB at 37°C at 220 rpm unless stated otherwise. *Agrobacterium tumefaciens* strains were grown overnight in LB at 30°C at 220 rpm unless stated otherwise. LB contains 10 g tryptone, 5 g yeast extract, 10 g NaCl (pH 7.5). Media were sterilized by autoclaving at 121°C and 15 psi for 20 min. Agar plates were prepared by adding 15 g/L of agar into the medium before autoclaving. Overnight cultures of the bacterial strains were stored at -80°C in 25% glycerol.

Table 6-1. Bacterial strains used in this study.

Species	Strain	Description and/or Genotype	Reference and/or Source
<i>V. fischeri</i>	NCMB 1281	Type strain	ATCC 7744, 602
<i>E. coli</i>	DH5 α	General cloning , blue/white screening without IPTG; F ⁻ ϕ 80 <i>lacZ</i> Δ M15 Δ (<i>lacZYA-argF</i>)U169 <i>recA1 endA1 hsdR</i> 17(<i>r_k⁻, m_k⁺</i>) <i>phoA supE44 thi-1 gyrA96 relA1</i>	Invitrogen, Carlsbad, CA
<i>E. coli</i>	TOP10	Chemically competent, general cloning, blue/white screening without IPTG; F ⁻ <i>mcrA</i> Δ (<i>mrr-hsdRMS-mcrBC</i>) Φ 80 <i>lacZ</i> Δ M15 Δ <i>lacX74 recA1 araD139</i> Δ (<i>ara-leu</i>)7697 <i>galU galK rpsL</i> (Str ^R) <i>endA1 nupG</i>	Invitrogen, Carlsbad, CA
<i>E. coli</i>	RoLux	OHHL bioluminescent bioreporter, phage λ sensitive; STBL4 (EZ::TN <i>luxRoCDABE</i>)	603
<i>E. coli</i>	OHHLux	OHHL bioluminescent bioreporter, phage λ resistant; EZ::TN pMOD (Epicentre Biotechnologies, Madison, WI)- <i>V. fischeri luxR-P_{luxI}-P. luminescens luxCDABE-rrnB</i> T ₁ T ₂ , Kan ^r	63
<i>E. coli</i> carrying pJBA132	MT102	OHHL fluorescent bioreporter; pME6031- <i>luxR-P_{luxI}</i> -RBSII- <i>gfp</i> (ASV)-T ₀ -T ₁ , Tc ^r	604
<i>S. choleraesuis</i>	VCS 275		Lab stock
<i>K. pneumoniae</i>	NCTC 418, DSM 2026, NCIB 418	Wild-type prototroph	ATCC 15380, 652
<i>K. pneumoniae</i>			Lab stock
<i>K. oxytoca</i>	M5a1	Wild-type prototroph, lacks the normal polysaccharide capsule so amenable to genetic analysis, dinitrogen-fixer	Salmonella Genetic Stock Centre, Un. of Calgary, 653

Table 6-1. Continued.

Species	Strain	Description and/or Genotype	Reference and/or Source
<i>K. oxytoca</i>	VJSK009	M5a1 mutant carrying a modified <i>hsdI</i> allele, host restriction deficient	Salmonella Genetic Stock Centre, Un. of Calgary
<i>A. tumefaciens</i>	A136	AHL bioreporter. Ti plasmidless, <i>traR</i> overexpression plasmid (pCF218) and <i>traI-lacZ</i> (pCF372), Tet ^r , Sp ^r	654
<i>A. tumefaciens</i>	KYC6	AHL overproducer. <i>traM</i> null mutant, <i>traR</i> overexpression plasmid PCF218, Tet ^r , Kan ^r	654

Table 6-2. Plasmids used in this study.

Plasmid	Description	Function	Reference and/or Source
pCR2.1-TOPO	3931 bp, <i>LacZ</i> α , MCS, pUC origin, Kan ^r , Amp ^r	5 min-cloning of <i>Taq</i> polymerase-amplified PCR products	Invitrogen, Carlsbad, CA
pCR2.1-P _L #1	3982 bp, P _L with 5' <i>SpeI</i> and 3' <i>SalI</i> sites	Cloning of P _L , <i>Salmonella</i> phage P22 early left promoter	This work
pCR2.1-luxISalm #2.8	4539 bp, <i>luxI</i> CDS with the Gram-negative RBS carrying 5' <i>SalI</i> and 3' <i>XhoI</i> sites	Cloning of <i>luxI</i> CDS under the control of the Gram-negative RBS for expression in <i>Salmonella</i>	This work
pCR2.1-T1T2 #2.5	4369 bp, T ₁ T ₂ with 5' <i>XhoI</i> and 3' <i>XbaI</i> sites	Cloning of rRNB ribosomal terminator T ₁ T ₂	This work
pCR2.1-P _L -luxI #2	4541 bp, P _L - <i>luxI</i> CDS with the Gram-negative RBS	Cloning of <i>luxI</i> CDS with the Gram-negative RBS in front of P _L	This work
pCR2.1-P _L -luxI-T1T2 #3 (also referred to as pCR-L #3 in text and tables)*	4964 bp, P _L - <i>luxI</i> CDS with the Gram-negative RBS-T ₁ T ₂ , pUC origin, Kan ^r , Amp ^r	Testing OHHL production from <i>luxI</i> under the control of Gram-negative RBS and <i>Salmonella</i> phage P22 promoter P _L , early left promoter, inside <i>S. choleraesuis</i>	This work
pCR2.1-HA1 #2	4243 bp, the <i>Salmonella</i> phage P22 genome site between 22,406 th and 22,711 th bps with 5' <i>KpnI</i> and 3' <i>SpeI</i> sites	Cloning of homology arm #1, the <i>Salmonella</i> phage P22 genome region from 22,406 th to 22,711 th nucleotide	This work
pCR2.1-HA2 #2	4262bp, P22 genome site from 22,712 th to 23,030 th bps with 5' <i>XbaI</i> and 3' <i>ApaI</i> sites	Cloning of the homology arm #2, the <i>Salmonella</i> phage P22 genome region from 22,712 th to 23,030 th nucleotide	This work
pCR2.1-HA1-P _L -luxI-T1T2 #1	5217 bp, the homology arm #1-P _L - <i>luxI</i> CDS with the Gram-negative RBS-T ₁ T ₂	Cloning of the homology arm #1, <i>Salmonella</i> phage P22 genome region from 22,406 th to 22,711 th nucleotide, into pCR2.1-P _L -luxI-T1T2 #3 (or pCR-L #3)	This work

Table 6-2. Continued.

Plasmid	Description	Function	Reference and/or Source
pCR2.1-HA1-P _L -luxI-T1T2-HA2 #5 (also referred to as pCR-HAL #5 in text and tables)*	5466 bp, the homology arm #1-P _L - <i>luxI</i> CDS with the Gram-negative RBS-T ₁ T ₂ -the homology arm #2, pUC origin, Kan ^r , Amp ^r	Cloning of the <i>luxI</i> CDS under the control of Gram-negative RBS and <i>Salmonella</i> phage P22 promoter P _L , early left promoter, into the P22 genome and the packaging of the resulting genome with homologous recombination	This work

(*See Table A in the appendix for a complete list of alternative names used for plasmids.)

Table 6-3. Bacteriophage used in this study.

Phage	Host	Description	Reference and/or Source
P22	<i>Salmonella</i>	Podoviridae, 60 nm diameter, short/non-contractile tail (20 nm), temperate (high multiplicity of infection leading to lysogenization; single infections leading to lysis), single linear ds DNA genome (41,724 bp), transducing phage for <i>Salmonella</i> Groups B and D,	ATCC 19585-B1, 655-657
P22luxI #3	<i>Salmonella</i>	Recombinant P22 carrying <i>luxI</i> under the control of Gram-negative RBS and <i>Salmonella</i> phage P22 promoter P _L , early left promoter	This work
P22luxI #7	<i>Salmonella</i>	Recombinant P22 carrying <i>luxI</i> under the control of Gram-negative RBS and <i>Salmonella</i> phage P22 promoter P _L ,	This work
P22luxI 10 ⁻⁴	<i>Salmonella</i>	Recombinant P22 carrying <i>luxI</i> under the control of Gram-negative RBS and <i>Salmonella</i> phage P22 promoter P _L	This work
P22luxI HR	<i>Salmonella</i>	Recombinant P22 carrying <i>luxI</i> under the control of Gram-negative RBS and <i>Salmonella</i> phage P22 promoter P _L ,	This work

Molecular biology techniques

All molecular biology techniques were carried out according to Molecular Cloning: A Laboratory Manual (612) unless stated otherwise. Manufacturer's instructions were followed for kits. All restriction enzymes were from Promega (Madison, WI). Electrophoresis was done using TBE buffer (0.045 M Tris-Borate, 0.001 M EDTA, pH 8.0). All PCR reactions were carried out using PCR Ready-To-Go beads (Amersham Biosciences, Buckinghamshire, England) according to manufacturer's instructions with a PTC-225 DNA Engine Tetrad Peltier Thermal Cycler (MJ Research, Inc., Waltham, MA, Inc.). All primers were from Sigma Genosys (The Woodlands, TX) or Operon Biotechnologies, Inc. (Huntsville, AL). A list of primers is given in Table 6-4. Lyophilized primers were suspended in sterile dH₂O to obtain a stock solution of 1 nmol/μl. The stock solution was diluted with sterile dH₂O to working solution of 5 pmol/μl concentration. All PCR and sequencing reactions were performed using working solutions. DNA quantifications were done using a DyNA 200 Fluorometer (GE Healthcare, Buckinghamshire, UK).

DNA sequencing

Sequencing reactions were carried out by the Molecular Biology Resource Facility at The University of Tennessee, Knoxville with an ABI Prism 3100 Genetic Analyzer and a 3730 DNA Analyzer (Applied Biosystems, Foster City, CA). M13 reverse and forward primers (Invitrogen, Carlsbad, CA) were used in sequencing reactions of genes which were cloned into pCR2.1-TOPO or pCR2.1 (Invitrogen,

Carlsbad, CA). Sequencing of genes cloned into other plasmids was performed with primers which were used for cloning.

Electroporation of *S. choleraesuis*

The method of O'Callaghan and Charbit (658) was used for preparation of electrically competent cells and electroporation of *S. choleraesuis*. Briefly, mid-log phase cultures were washed with sterile ice-cold dH₂O twice and sterile ice-cold 10% glycerol twice. Cells were resuspended in 10% glycerol in 40 µl aliquots and used for electroporation by mixing with 1 µl DNA in a 2-mm gap electroporation cuvette with a time constant of 5 ms, 200 ohms resistance, 25 µF capacitance, and 2.5 kV at 4°C.

Table 6-4. List of primers used in this study.

Name	Sequence (5'-3')	References
P _L SpeI forward	ACTAGTTTGACCATTTAATTAAGAA	This work
P _L Sall reverse	GTCGACTGATGGCTAAAATTTAAG	This work
luxISalmSall forward	GTCGACTAAGGAGGTCACCCATGACTATAA TGATAAAAA	This work
luxISalmXhoI reverse	CTCGAGTTAATTTAAGACTGCTT	This work
T1T2XhoI forward	CTCGAGAAGAGTTTGTAGAAACGCAA	This work
T1T2XbaI reverse	TCTAGATCTGTTTTGGCGGATGAG	This work
HRA1KpnI forward	GGTACCTCTTCTCGATAATATCTTCA	This work
HRA1SpeI reverse	ACTAGTCGATTCATGACAT	This work
HRA2XbaI forward	TCTAGATGAGATAGTCCAGATGGGCGT	This work
HRA2ApaI reverse	GGGCCCCCAAATTGATTACGCGGACCAC	This work

Electroporation of *Klebsiella* strains

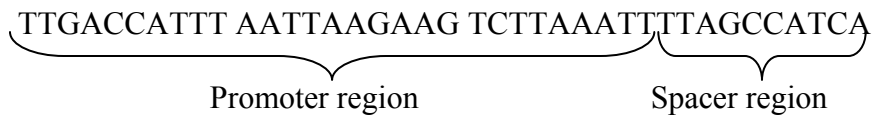
The method of Fournet-Fayard et al. (659) was used for preparation of electrically competent cells and electroporation of *Klebsiella* strains. Briefly, the cultures were grown in LB and EDTA until OD₆₀₀ of 0.2. Then these cultures were washed with sterile ice-cold 10% glycerol once. Cells were resuspended in 10% glycerol in 40 µl aliquots and used for electroporation. Electroporation was performed by mixing 40 µl electrocompetent cells with 1 µl DNA in a 1-mm gap electroporation cuvette. Cells and DNA were electroporated at 4°C, 200 ohms resistance, 25 µF capacitance (optimum time constant of 4.5 ms), and 1.8 kV.

Plasmid purification using rapid boiling mini-prep method

One ml of an overnight culture was centrifuged at 10,000 x g for 5 min at room temperature in a microcentrifuge. The pellet was resuspended in 40 µl of STET buffer (50 mM EDTA, 50 mM Tris pH 8.0, 5% Triton, 8% sucrose). Four µl of freshly prepared lysozyme solution (10 mg/ml in 20% sucrose, 50 mM Tris pH 8.0) were added to the suspension. The tube was placed in a boiling water bath for 1 min, and centrifuged at 14,000 x g for 10 min at room temperature. The pellet was removed with a sterile toothpick and then 150 µl of 0.3 M KAc, pH 8.0 and 500 µl ice-cold ethanol were added to the supernatant. After mixing by inversion, the solution was stored on ice for 10 min, centrifuged at 14,000 x g for 15 min at 4°C, and supernatant was discarded. The DNA pellet was washed with 500 µl of 70% ethanol. The pellet was dried at room temperature, resuspended in enzyme digestion buffer, and used for digestion.

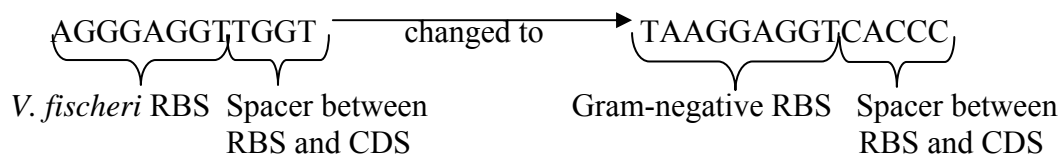
Construction of pCR2.1-P_L-luxI-T1T2 #3 (or pCR-L #3)

The plasmid pCR2.1-P_L-luxI-T1T2 #3 (or pCR-L #3) was constructed by placing *luxI* under the control of a *Salmonella* phage promoter to test *luxI* expression in *Salmonella* and to clone it into the phage. Since *Salmonella* phage P22 was selected to use to construct the recombinant phage carrying *luxI*, P22 early left promoter, P_L, (655, 656) was chosen as the promoter. A 10-bp spacer region was placed between the promoter and the RBS since transcription is started approximately 7 bp downstream of the promoter. Promoter and spacer sequences are shown below:



Promoter and spacer sequences were amplified using P_LSpeI forward and P_LSalI reverse primers following a PCR protocol which contained a step of 94°C for 5 min followed by 40 cycles of 94°C for 30 sec, 45°C for 30 sec, and 72°C for 4 sec, and then a final step of 72°C for 15 min. The PCR product was confirmed based on size by running it on a 0.5% agarose gel with EtBr in 0.5xTBE and UV illumination of the gel. The amplicon with the 5' SpeI and 3' SalI sites was cloned into the TOPO TA cloning vector pCR2.1 and *E. coli* TOP10 cells (Invitrogen, Carlsbad, CA). Transformants were screened using *Eco*RI digestion and sequencing. The construct pCR2.1-P_L #1 was selected.

The RBS of *luxI* was changed from the original to a Gram-negative consensus sequence after examination of various RBSs from *Salmonella* and phage P22 genes (PubMed Nos: AF217253, L06296, L07556, L19603, D90203, M11047, L26246; 660-664):



The RBS change of *luxI* was carried out by amplification from pMO-L #7 using luxISalmSalI forward and luxISalmXhoI reverse primers. The PCR protocol consisted of a first step of 94°C for 5 min and then 35 cycles of 94°C for 30 sec, 42°C for 30 sec, and 72°C for 38 sec, and finally a step of 72°C for 15 min. The product was run on a 0.5% agarose gel with EtBr in 0.5xTBE. UV light screening of the gel verified the amplicon, based on size. The PCR product carrying the changed RBS and the 5' *SalI* and 3' *XhoI* sites was cut out of the gel and purified using QIAquick Gel Extraction Kit (Qiagen Inc., Valencia, CA). The purified product was cloned into the TOPO TA cloning vector pCR2.1 into *E. coli* TOP10 cells (Invitrogen, Carlsbad, CA). After transformant screening with *EcoRI* analysis and sequencing, the construct picked was named pCR2.1-luxISalm #2.8.

rRNB ribosomal terminator T₁T₂ of pKK223-3 plasmid (Pharmacia, Uppsala, Sweden) was used as the transcription termination site for *luxI* expression in *Salmonella*. It was amplified from pMO-L #7 using T1T2XhoI forward and T1T2XbaI reverse primers. The PCR protocol was a step of 94°C for 5 min followed by 35 cycles of 94°C for 30 sec, 54°C for 30 sec, and 72°C for 28 sec, and a final step of 72°C for 15 min. Confirmation and cloning of the PCR product, and transformant screening were performed the same way as that of *luxI* described previously. The plasmid selected was called pCR2.1-T1T2 #2.5.

pCR2.1-P_L #1 and pCR2.1-luxISalm #2.8 were digested with *SalI* and *XhoI* in the presence of 1X buffer D (Promega, Madison, WI) at 37°C to place *luxI* under the P_L control into pCR2.1-P_L #1. Digests were run on a 0.5% agarose gel with EtBr in 0.5xTBE. UV illumination was used to spot the *luxI* fragment from pCR2.1-luxISalm #2.8 and digested pCR2.1-P_L #1 plasmid on the gel. The *luxI* fragment and pCR2.1-P_L #1 were cut out of the gel and purified using the QIAquick Gel Extraction Kit (Qiagen Inc., Valencia, CA). *luxI* was integrated into pCR2.1-P_L #1 using the DNA Ligation Kit<Mighty Mix> (Takara Bio Inc., Shiga, Japan). Reactions which contained 122 ng vector and 196 ng insert (1:10 ratio); and 94 ng vector and 220 ng insert (1:15 ratio) were incubated overnight at 16°C. Then, ligation reactions were transformed into chemically competent *E. coli* TOP10 cells (Invitrogen, Carlsbad, CA). Transformants were screened using *EcoRI* restriction analysis and sequencing. The construct pCR2.1-P_L-luxI #2 was chosen to use for the future experiments.

To add a transcription termination site after the *luxI* gene, pCR2.1-T1T2 #2.5 and pCR2.1-P_L-luxI #2 were cut with *XhoI* and *XbaI* using 1X buffer D (Promega, Madison, WI) at 37°C. The pCR2.1-T1T2 #2.5 digest was run on a 0.5% agarose gel with EtBr in 0.5xTBE while the pCR2.1-P_L-luxI #2 digest was purified directly from the reaction with the QIAquick Gel Extraction Kit (Qiagen Inc., Valencia, CA). T₁T₂ fragment spotted on the gel based on size under UV light was cut and purified using the same kit. Ligation of 165 ng T₁T₂ to 170 ng pCR2.1-P_L-luxI #2 was performed with the DNA Ligation Kit<Mighty Mix> (Takara Bio Inc., Shiga, Japan) at 16°C overnight. *SalI/XbaI* digestion and sequencing were used to screen transformants. The construct with the correct insert was named pCR2.1-P_L-luxI-T1T2 #3 (or pCR-L #3; see Table A in the appendix for a

complete list of alternative names used for plasmids). The construct diagram is shown in Figure 6-1.

Transfer of pCR-L #3 into *Salmonella*

pCR-L #3 was electroporated into electrically competent *S. choleraesuis*. Plasmids were purified from overnight cultures of transformants using the Wizard Plus Midi-Preps DNA Purification Systems (Promega, Madison, WI) according to manufacturer instructions, and screened by sequencing. The *S. choleraesuis* strain containing pCR-L #3 was tested for OHHL production.

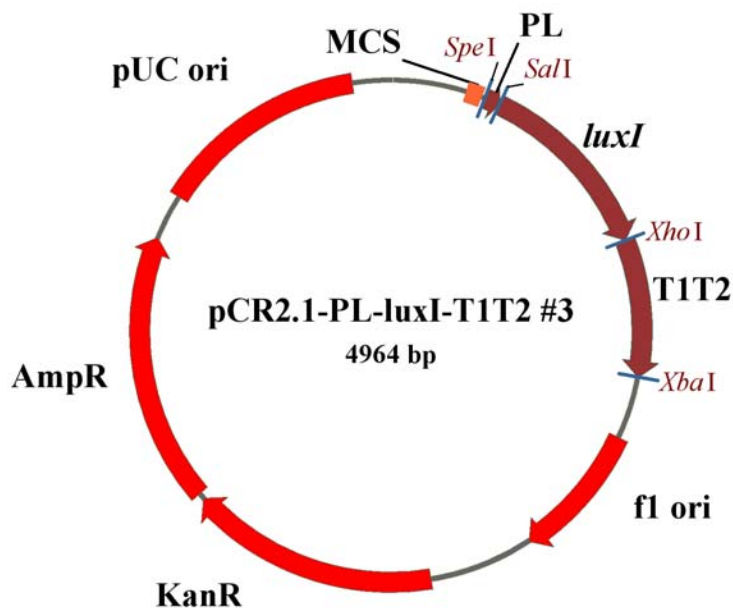


Figure 6-1. pCR2.1-P_L-luxI-T1T2 #3 (or pCR-L #3) plasmid. *luxI* is under the control of a Gram-negative RBS and a *Salmonella* phage P22 promoter P_L. (MCS=multiple cloning site of *Hind*III/*Kpn*I/*Sac*I/*Bam*HI/*Spe*I/*Eco*RI)

Bioluminescent and fluorescent detection of OHHL from pCR-L #3 in *S. choleraesuis* using Wallac Victor2 1420 Multilabel and 1450 Microbeta Plus Liquid Scintillation Counters

Overnight cultures of the bioluminescent bioreporter *E. coli* OHHLux, the fluorescent bioreporter *E. coli* MT102 with pJBA132, the negative control (wild type *S. choleraesuis* strain), and *S. choleraesuis* harboring pCR-L #3 were prepared by growth of cells in LB with antibiotics at 37°C with 220 rpm. Cultures of *S. choleraesuis* strains were inoculated into fresh LB without antibiotics (100 µl into 10 ml LB) and grown at 37°C until mid-log phase (OD₆₀₀=0.9). Supernatants were collected, passed through 0.22 µm filters and used for the assay. Overnight cultures of bioreporters were washed with LB, resuspended in LB with antibiotics to OD₆₀₀=0.1 and used for the assay. Costar 96-well black microtiter plates with a black or clear bottom (Corning Inc. Life Sciences, Lowell, MA) were used for measurements with a Wallac 1450 Microbeta Plus Liquid Scintillation or Victor2 1420 Multilabel Counter (PerkinElmer Life and Analytical Sciences, Waltham, MA), respectively. Samples and controls were prepared in triplicate. Each preparation contained 100 µl supernatant of the sample or control and 100 µl bioreporter solution. Also, measurements from bioreporters alone were performed to test background bioluminescence and fluorescence. These were in triplicate as well and each contained 100 µl bioreporter and 100 µl dH₂O. The assay methodology is summarized in Figure 3-2. The protocol followed by the Wallac Victor2 1420 Multilabel Counter was shaking for 10 sec, absorbance measurement at 450 nm, shaking for 10 sec, bioluminescence measurement (CPS), shaking for 10 sec, fluorescence measurement (GFP), and incubation for 20 min repeated overnight at 28°C. Measurements were

normalized by dividing CPS and GFP by OD₄₅₀ values. The average of normalized values in triplicate was calculated. The Wallac 1450 Microbeta Plus Liquid Scintillation Counter protocol was bioluminescence measurement (CPS) followed by incubation for 20 min repeated overnight at 28°C. The mean of CPS values in triplicate was calculated for each sample.

Construction of homologous recombination plasmid, pCR2.1-HA1-P_L-luxI-T1T2-HA2 #5 (or pCR-HAL #5)

To integrate the P_L-*luxI*-T₁T₂ fragment from pCR-L #3 into the phage P22 genome and to package the resulting genome with *luxI*, homologous recombination method was used. The insertion site in the genome was between the 22,711th and 22,712th nucleotides; and ORF-201 and ORF-80 genes (phage genome PubMed No: AF217253; 655). Homology regions selected from the genome were the 306-bp sequence before the insertion site (from 22,406th to 22,711th nucleotide) and the 319-bp sequence after the insertion site (from 22,712th to 23,030th nucleotide). The region before the insertion site was named homology arm #1 and the region after the insertion site was called homology arm #2. They are shown below:

Homology arm #1 (primer sites in bold):

tcttctcgataatatcttcaaggtgggcaatTTTTgctctatatctgacatgtccactccttgcataaagttcttgtggtgaaaagt
ggcactcaccgacaagcaagaaatgttctgtcatgagtacctcatcgatttaaagccacgcaagcggcgatttgggcggagat
atctaagattgctatcacactgccaagaaaaatgtcaaaaccttacgtccagccaaggattattgttctgtaaactaaagcaatg
atctggttggtataaatgtgacacat**gtcatgaatcgactagt**

Homology arm #2 (primer sites in bold):

tgagatagttccagatgggcgtgctcggcatcatcaccacaaccggagccaacaatggcagagattattcccatgactgaaga
acagaaattccagtttagagatttacaagctgggtcatgaaccagaacgcagccgcagaggaagcatttcaattcattggcactgac
gagctgaagcttgagctattcaaaattcacttccagtcaggcggagcaaattcggatatcacgacccgcactatcgaagcgggtgc
gtaaatcgaggggaagcgttagacctgttactaccggagcatgatgtgggtccgcgtaatcaatttgg

Homology arms were amplified from phage P22 genome which was extracted using Wizard Lambda Preps DNA Purification System (Promega, Madison, WI). HRA1KpnI forward and HRA1SpeI reverse primers were utilized for homology arm #1 amplification with the PCR protocol of a first step of 94°C for 5 min followed by 40 cycles of 94°C for 30 sec, 51°C for 30 sec, and 72°C for 20 sec, and then a step of 72°C for 15 min. Homology arm #2 was amplified using HRA2XbaI forward and HRA2ApaI reverse primers and the PCR protocol which contained a step of 94°C for 5 min and then 40 cycles of 94°C for 30 sec, 62°C for 30 sec, and 72°C for 20 sec, and a final step of 72°C for 15 min. Products were confirmed by running 15 µl of each reaction on a 0.5% agarose gel with EtBr in 0.5xTBE and screening the gel with UV light to control the product size. The remaining 10 µl of each PCR product was cloned into the TOPO TA cloning vector pCR2.1 and then into *E. coli* TOP10 cells (Invitrogen, Carlsbad, CA). Transformants were screened with EcoRI analysis and sequencing. The construct carrying homology arm #1 was called pCR2.1-HA1 #2 and the one containing homology arm #2 was named pCR2.1-HA2 #2.

Homology arms were inserted into pCR-L #3 to construct a plasmid to use for homologous recombination. Homology arm #1 was placed before the P_L-*luxI*-T₁T₂ fragment and homology arm #2 was placed after the fragment. First, homology arm #1 was cloned into the plasmid at the *KpnI* and *SpeI* sites. For this, pCR2.1-HA1 #2 and

pCR-L #3 were digested with *KpnI* and *SpeI* with 1X multicore buffer (Promega, Madison, WI) at 37°C. Digestion products were run on a 0.5% agarose gel with EtBr in 0.5xTBE and then screened with UV illumination. This spotted the homology arm #1 fragment from pCR2.1-HA1 #2 and the digested pCR-L #3 on the gel based on size. Homology arm #1 and pCR-L #3 were cut out of the gel and purified using the QIAquick Gel Extraction Kit (Qiagen Inc., Valencia, CA). The DNA Ligation Kit<Mighty Mix> (Takara Bio Inc., Shiga, Japan) was used to integrate 69 ng homology arm into 111 ng pCR-L #3. The reaction was incubated at 16°C for 30 min and then transformed into chemically competent *E. coli* TOP10 cells (Invitrogen, Carlsbad, CA). Transformants were screened using *XhoI/KpnI* digestion and sequencing. Results showed that construct pCR2.1-HA1-P_L-luxI-T1T2 #1 carried the correct insert.

To clone homology arm #2 into pCR2.1-HA1-P_L-luxI-T1T2 #1 at the *XbaI* and *ApaI* sites, pCR2.1-HA2 #2 and pCR2.1-HA1-P_L-luxI-T1T2 #1 were digested with these enzymes in the presence of 1X multicore buffer (Promega, Madison, WI) at 37°C. Digests were run on a 0.5% agarose gel with EtBr in 0.5xTBE. UV light screening showed homology arm #2 fragment from pCR2.1-HA2 #2 and the digested pCR2.1-HA1-P_L-luxI-T1T2 #1 on the gel based on size. Homology arm #2 and pCR2.1-HA1-P_L-luxI-T1T2 #1 were cut out of the gel and purified using the QIAquick Gel Extraction Kit (Qiagen Inc., Valencia, CA). The homology arm fragment (96 ng) was ligated to pCR2.1-HA1-P_L-luxI-T1T2 #1 (160 ng) using the DNA Ligation Kit<Mighty Mix> (Takara Bio Inc., Shiga, Japan) at 16°C for 30 min. The reaction was chemically transformed into competent *E. coli* TOP10 cells (Invitrogen, Carlsbad, CA). Transformant screening was carried out with *XhoI/ApaI* restriction analysis and sequencing. The construct picked was

called pCR2.1-HA1-PL-luxI-T1T2-HA2 #5 (or pCR-HAL #5; see Table A in the appendix for a complete list of alternative names used for plasmids). A diagram of the plasmid is shown in Figure 6-2.

Transfer of pCR-HAL #5 into *S. choleraesuis*

pCR-HAL #5 was electroporated into electrically competent *S. choleraesuis*. Plasmids were purified from the overnight cultures of transformants using the Wizard Plus Midi-Preps DNA Purification Systems (Promega, Madison, WI) and run on a 0.5% agarose gel with EtBr in 0.5xTBE and sequenced. The *S. choleraesuis* strain determined to have pCR-HAL #5 was used for homologous recombination.

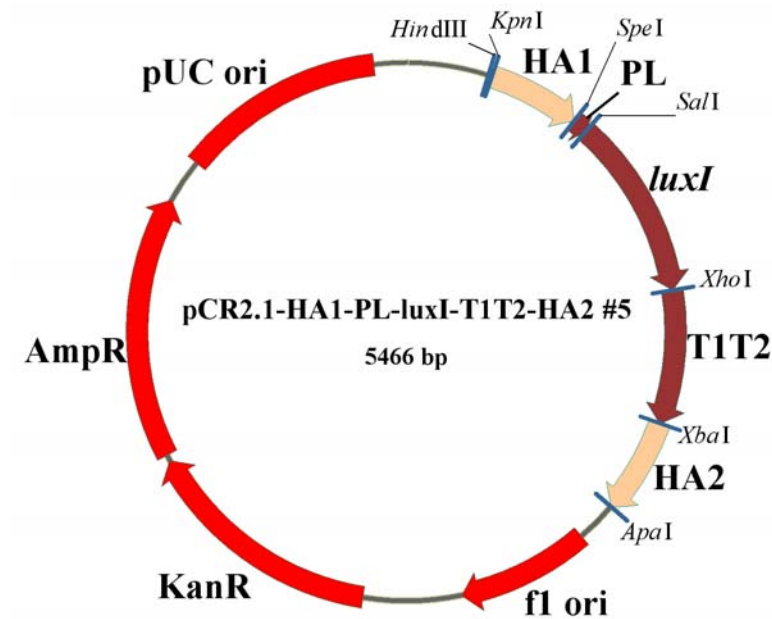


Figure 6-2. pCR2.1-HA1-PL-luxI-T1T2-HA2 #5 (or pCR-HAL #5) plasmid used for homologous recombination

Cloning of P_L , *luxI*, and T_1T_2 into *Salmonella* phage P22 using homologous recombination

Salmonella choleraesuis strain carrying pCR-HAL #5 was used to clone P_L , *luxI*, and T_1T_2 into phage P22. The homologous recombination method of Oda et al. (665) was used with some modifications. The overnight culture of *S. choleraesuis* with pCR-HAL #5 was diluted 10X in fresh LB with antibiotic and grown at 37°C with 220 rpm until reaching $OD_{600}=0.1$. Then, 4 ml of the culture were infected with 1.4×10^7 plaque forming units (pfu) P22 in 640 μ l. The infected culture was incubated for 5 h at 37°C with 220 rpm. To lyse bacterial cells, 50 μ l of chloroform were added to the culture and mixed, and then centrifuged at 8,000 x g for 10 min. The supernatant which contained the phage was collected and 50 μ l of chloroform were added. The lysate was diluted with SM buffer (50 mM Tris-HCL pH 7.5, 100 mM NaCl, 8 mM $MgSO_4$, 0.01% gelatin) to obtain 10^{-1} , 10^{-2} , 10^{-3} , and 10^{-4} dilutions. Each dilution (100 μ l) was mixed with the overnight culture of *S. choleraesuis* harboring pCR-HAL #5 (5 μ l) and top agar (2.5 ml LB, 0.5% agar) and poured onto an LB plate. Plates were incubated overnight at 37°C.

Propagation of phage from homologous recombination

Two plaques were picked from the 10^{-4} homologous recombination phage dilution plate. Each was placed into 250 μ l SM buffer (50 mM Tris-HCL pH 7.5, 100 mM NaCl, 8 mM $MgSO_4$, 0.01% gelatin) containing 12 μ l of chloroform. Suspensions were shaken gently at room temperature for 2 h. The remainder of plaques on the plate was collected by scraping the top agar off of the plate surface. The top agar containing plaques was suspended in 2 ml LB containing 40 μ l of chloroform and shaken gently at room

temperature for 1.5 h. Supernatants of 2 plaques and the top agar collected after centrifugation at 8,000 x g for 10 min were added into 2 h-*S. choleraesuis* cultures (4 ml each) and a 2 h-*S. choleraesuis* with pCR-HAL #5 culture (4 ml), respectively. One ml of undiluted homologous recombination lysate was also added to a 2 h-*S. choleraesuis* with pCR-HAL #5 culture (4 ml). Cultures with phage were incubated overnight at 37°C with 220 rpm. Lysates were centrifuged at 8,000 x g for 10 min. Supernatants containing the phage were stored at 4°C with chloroform. Lysates of 2 individual plaques picked from the 10⁻⁴ dilution plate were named P22luxI #3 and #7. The lysate obtained from the 10⁻⁴ dilution plate was called P22luxI 10⁻⁴. The homologous recombination lysate was named P22luxI HR.

Phage propagation for preparation of phage lysate stocks

Routine propagation of phage to renew lysate stocks were performed in serial propagations using *S. choleraesuis* or *S. choleraesuis* harboring pCR-HAL #5 as the host. The host culture was prepared by inoculation of fresh LB with the overnight culture followed by incubation at 37°C at 220 rpm for 2-3 h. The phage lysate was mixed with this culture and incubated overnight at 37°C with 220 rpm. The lysate supernatant was subjected to the same protocol. This process was repeated 3 times in series. The final lysate obtained was filtered through a 0.22 µm filter and stored at 4°C.

Bioluminescent detection of OHHL from P22luxI phage propagated with *S. choleraesuis* or *S. choleraesuis* with pCR-HAL #5 using Wallac Victor2 1420 Multilabel and 1450 Microbeta Plus Liquid Scintillation Counters

Bioluminescent bioreporters *E. coli* OHHLux and *S. choleraesuis* were grown overnight in LB (with antibiotic for the bioreporter) at 37°C with 220 rpm. *Salmonella choleraesuis* was diluted 10 times in fresh LB and shaken at 37°C with 220 rpm until mid-log phase. The bioreporter overnight culture and the *S. choleraesuis* mid-log phase culture were washed with LB. The bioreporter culture was diluted to OD₆₀₀=0.1 in LB without antibiotic. The *S. choleraesuis* culture was resuspended in the same volume of LB. The Costar 96-well black microtiter plates with a black bottom (Corning Inc. Life Sciences, Lowell, MA) were used for measurement of samples. Each sample contained 50 µl bioreporter (~5x10⁹ cfu), 50 µl *S. choleraesuis* (~4.3x10⁸ cfu), and 100 µl P22luxI lysate. The P22luxI phage were #3, #7, 10⁻⁴, and HR. Two types of lysates were tested for each phage. One was the stock propagated using *S. choleraesuis* as the host and the other was the stock propagated using *S. choleraesuis* harboring pCR-HAL #5 as the host. The amount of each phage in a plate well is shown in Table 6-5. Each sample was prepared in triplicate. The methodology for the assay is shown in Figure 6-3. The protocol for Wallac Victor2 1420 Multilabel Counter measurements was shaking for 20 sec, bioluminescence measurement (CPS), shaking for 10 sec, and incubation for 20 min repeated overnight at 28°C. The Wallac 1450 Microbeta Plus Liquid Scintillation Counter followed the protocol of bioluminescence measurement (CPS) and then incubation for 20 min repeated overnight at 28°C. The average of triplicate CPS values was calculated for each sample.

Table 6-5. P22luxI amounts (per each plate well) for bioluminescence detection from P22luxI propagated with *S. choleraesuis* or *S. choleraesuis* carrying pCR-HAL #5. Wells also included the bioreporter *E. coli* OHHLux and the host *S. choleraesuis*.

	Propagated with <i>S. choleraesuis</i>	Propagated with <i>S. choleraesuis</i> carrying pCR-HAL #5
#3	$\sim 7 \times 10^8$ pfu	$\sim 1.3 \times 10^9$ pfu
#7	$\sim 1.3 \times 10^9$ pfu	$\sim 8 \times 10^8$ pfu
10⁻⁴	$\sim 10^9$ pfu	$\sim 10^9$ pfu
HR	$\sim 9.5 \times 10^8$ pfu	$\sim 7.7 \times 10^8$ pfu

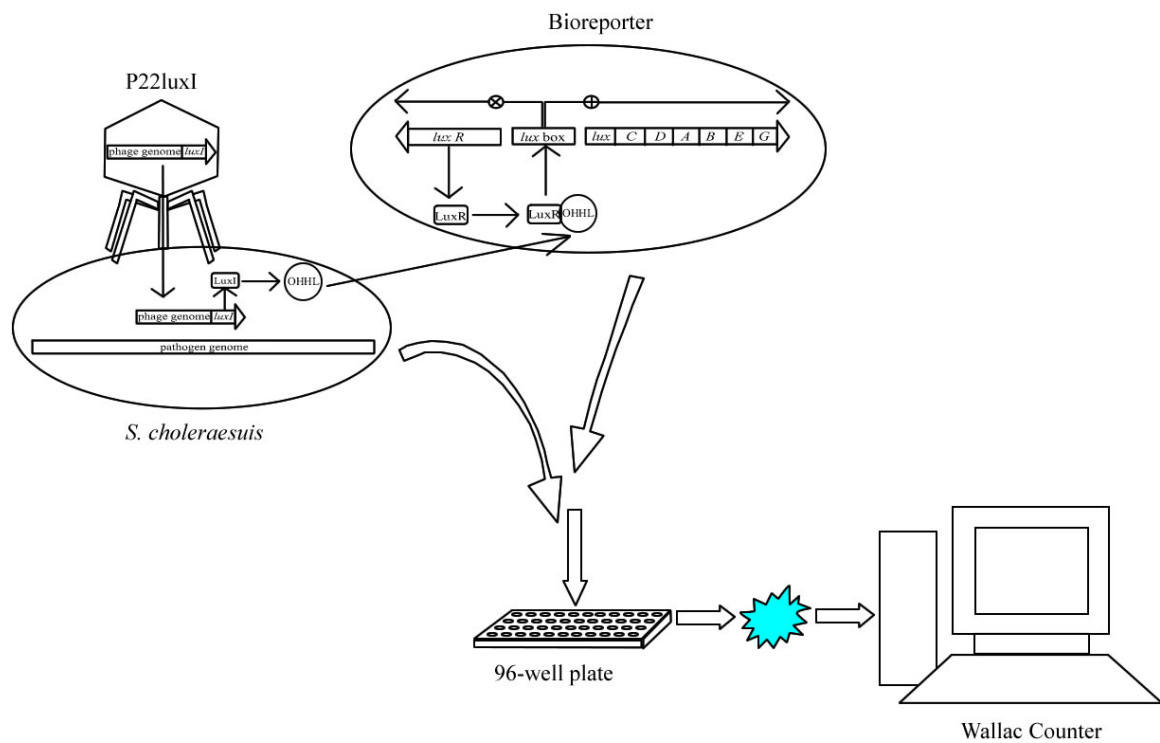


Figure 6-3. Methodology for bioluminescent OHHL detection of from recombinant P22luxI phage.

Screening of P22luxI #3 and #7 phage by PCR

The presence of *luxI* in P22luxI #3 and #7 phage which were propagated using *S. choleraesuis* and *S. choleraesuis* carrying pCR-HAL #5 were checked by PCR. For this, plaques of each phage type were prepared by pouring a mixture of *S. choleraesuis* culture, the phage lysate which was filtered through 0.22 µm filters after the propagation (see above) and checked for bacterial contamination (see below), and top agar (2.5 ml LB, 0.5% agar) onto an LB plate. Plates were incubated overnight at 37°C. The tip of a sterile toothpick was touched to a plaque and then washed with sterile dH₂O into a sterile tube. This was performed for a plaque of each phage type. Plaque suspensions in the tubes were heated for 2 min in a boiling water bath, cooled to room temperature, and used as templates for PCR reactions to amplify *luxI* with luxISalmSalI forward and luxISalmXhoI reverse primers. The PCR protocol consisted of a step of 94°C for 5 min followed by 35 cycles of 94°C for 30 sec, 42°C for 30 sec, and 72°C for 38 sec, and finally a step of 72°C for 15 min. PCR products were run on a 0.5% agarose gel with EtBr in 0.5xTBE. The gel was screened by UV illumination to detect *luxI* amplicons based on size.

Testing bioluminescent bioreporter *E. coli* OHHLux for infection by P22 and P22luxI #3 and #7 phage on an LB plate

An overnight culture of bioluminescent bioreporter *E. coli* OHHLux and top agar (2.5 ml LB, 0.5% agar) were mixed and poured onto an LB plate. Drops of P22 and

P22luxI #3 and #7 phage stocks (a few μl each) were placed onto the plate and incubated overnight at 37°C.

Detection of bioluminescence from the bioluminescent bioreporter *E. coli* OHHLux and P22luxI mixture using Wallac Victor2 1420 Multilabel and 1450 Microbeta Plus Liquid Scintillation Counters

The bioluminescent bioreporter *E. coli* OHHLux overnight culture was washed in LB and then diluted to $\text{OD}_{600}=0.1$ in LB without antibiotic to use for the assay. The overnight culture of *S. choleraesuis* (100 μl) was inoculated into fresh LB (10 ml) and grown at 37°C with 220 rpm until mid-log phase. The mid-log phase culture was resuspended in the same volume of SM buffer (50 mM Tris-HCL pH 7.5, 100 mM NaCl, 8 mM MgSO_4 , 0.01% gelatin) after washing to use for P22luxI #3 assay. For the P22luxI #7 assay, the mid-log phase culture was washed with and resuspended in same volume of LB. Samples prepared in triplicate were placed into Costar 96-well black microtiter plates with a black bottom (Corning Inc. Life Sciences, Lowell, MA). Samples used for the P22luxI #7 and #3 assays and their amounts are shown in Tables 6-6 and 6-7. The assay methodology is shown in Figure 6-3. The Wallac Victor2 1420 Multilabel Counter measurement followed the protocol of shaking for 20 sec, bioluminescence measurement (CPS), shaking for 10 sec, and incubation for 20 min repeated overnight at 28°C. The Wallac 1450 Microbeta Plus Liquid Scintillation Counter measurements contained a bioluminescence measurement (CPS) and then incubation for 20 min repeated overnight at 28°C. The mean of CPS values in triplicate was calculated for each sample and used for the chart constructions.

Table 6-6. Samples and amounts (per each plate well) used for bioluminescence detection from *E. coli* OHHLux and P22luxI #7. Each row represents a sample.

P22luxI #7	<i>S. choleraesuis</i>	<i>E. coli</i> OHHLux bioreporter
100 µl (~8.2x10 ⁸ pfu)	50 µl (~10 ⁹ cfu)	50 µl (~6x10 ⁹ cfu)
100 µl (~8.2x10 ⁸ pfu)	exchanged with 50 µl LB	50 µl (~6x10 ⁹ cfu)

Table 6-7. Samples and amounts (per each plate well) used for bioluminescence detection from *E. coli* OHHLux and P22luxI #3. Each row represents a sample.

P22luxI #3	<i>S. choleraesuis</i>	<i>E. coli</i> OHHLux bioreporter	
100 µl (~1.3x10 ⁹ pfu)	50 µl (~10 ⁹ cfu)	50 µl (~6x10 ⁹ cfu)	+50 µl LB
100 µl (~1.3x10 ⁹ pfu)	exchanged with 50 µl SM buffer	50 µl (~6x10 ⁹ cfu)	+50 µl LB
100 µl (~1.3x10 ⁹ pfu)	50 µl (~10 ⁹ cfu)	exchanged with 50 µl LB	+50 µl LB
exchanged with 100 µl SM buffer	50 µl (~10 ⁹ cfu)	50 µl (~6x10 ⁹ cfu)	+50 µl LB
100 µl (~1.3x10 ⁹ pfu)	exchanged with 50 µl SM buffer	exchanged with 50 µl LB	+50 µl LB
exchanged with 100 µl SM buffer	50 µl (~10 ⁹ cfu)	exchanged with 50 µl LB	+50 µl LB
exchanged with 100 µl SM buffer	exchanged with 50 µl SM buffer	50 µl (~6x10 ⁹ cfu)	+50 µl LB

Control of phage stocks for contamination

Lysate stocks of P22luxI #3 and #7 phage were tested for bacterial contamination. One-hundred μl of each phage lysate (1.3×10^9 pfu P22luxI #3; 8.2×10^8 pfu P22luxI #7) were spreaded onto a sterile LB plate. Plates were incubated overnight at 37°C and checked for bacterial growth the next day. Furthermore, 520 μl of each phage stock (1.9×10^{10} pfu P22luxI #3; 1.4×10^{10} pfu P22luxI #7) were incubated with 10 ml sterile LB at 37°C with 220 rpm for 6 d. Suspensions were checked for bacterial growth after incubation.

Measurements from mixtures of bioluminescent bioreporter *E. coli* OHHLux and P22luxI #3 phage to determine the source of bioluminescence using Wallac 1450 Microbeta Plus Liquid Scintillation Counter

The overnight culture of the bioluminescent bioreporter *E. coli* OHHLux which was washed with LB was diluted to $\text{OD}_{600}=0.1$ in LB without antibiotic. Various dilutions of this culture were prepared using LB. The lysate stock of P22luxI #3 phage was diluted serially using SM buffer (50 mM Tris-HCL pH 7.5, 100 mM NaCl, 8 mM MgSO_4 , 0.01% gelatin). Samples containing different dilutions of the phage combined with a constant amount of bioreporter and samples of a constant amount of phage mixed with different dilutions of bioreporter were prepared. Control samples were a mixture of P22luxI #3 phage and bioreporter without dilution, P22luxI #3 phage alone, bioreporter alone, a mixture of wild type phage P22 and bioreporter, and P22 phage alone. Samples

and controls were prepared in triplicate and placed into Costar 96-well black microtiter plates with a black bottom (Corning Inc. Life Sciences, Lowell, MA). Samples and controls used and their amounts are shown in Tables 6-8 and 6-9. The Wallac 1450 Microbeta Plus Liquid Scintillation Counter protocol consisted of a bioluminescence measurement (CPS) and then incubation for 20 min repeated overnight at 28°C. The mean CPS value was calculated for each sample prepared in triplicate.

Test of pseudolysogeny

This experiment was performed to determine whether a pseudolysogenic interaction existed between the bioluminescent bioreporter *E. coli* OHHLux and P22luxI phage. Two cultures with OD₆₀₀ = 0.1 were prepared by diluting the bioreporter overnight culture in LB. One culture was infected with P22luxI #3 phage. The other culture was used as the negative control. The culture with the phage contained ~10¹¹ cfu/ml bioreporter and ~6x10⁹ pfu/ml phage and the negative control culture had ~10¹¹ cfu/ml bioreporter. Cultures were incubated at 37°C with 220 rpm and measured for bioluminescence at certain time points using DeltaTox luminometer with ATP Mode Testing (Strategic Diagnostics Inc., Newark, DE). Bioluminescence from the bioreporter culture with the phage was compared to that of the negative control. When bioluminescence from the bioreporter-phage sample started to increase (~4 times higher than that of the control; Table 6-10), incubation was terminated.

Table 6-8. Samples and amounts (per each plate well) used to determine the source of bioluminescence from the *E. coli* OHHLux and P22luxI mixture. Each row represents a sample.

P22luxI #3	<i>E. coli</i> OHHLux bioreporter	
100 µl (~1.9x10 ⁹ pfu)-diluted 2x	50 µl (~6x10 ⁹ cfu)	+50 µl LB
100 µl (~9.3x10 ⁸ pfu)-diluted 4x	50 µl (~6x10 ⁹ cfu)	+50 µl LB
100 µl (~4.6x10 ⁸ pfu)-diluted 8x	50 µl (~6x10 ⁹ cfu)	+50 µl LB
100 µl (~3.7x10 ⁸ pfu)-diluted 10x	50 µl (~6x10 ⁹ cfu)	+50 µl LB
100 µl (~1.2x10 ⁸ pfu)-diluted 32x	50 µl (~6x10 ⁹ cfu)	+50 µl LB
100 µl (~3.7x10 ⁷ pfu)-diluted 100x	50 µl (~6x10 ⁹ cfu)	+50 µl LB
100 µl (~3.7x10 ⁹ pfu)	50 µl (~3x10 ⁹ cfu)-diluted 2x	+50 µl LB
100 µl (~3.7x10 ⁹ pfu)	50 µl (~1.5x10 ⁹ cfu)-diluted 4x	+50 µl LB
100 µl (~3.7x10 ⁹ pfu)	50 µl (~7.7x10 ⁸ cfu)-diluted 8x	+50 µl LB
100 µl (~3.7x10 ⁹ pfu)	50 µl (~2x10 ⁸ cfu)-diluted 32x	+50 µl LB

Table 6-9. Controls and amounts (per each plate well) used to determine the source of bioluminescence from the *E. coli* OHHLux and P22luxI mixture. Each row represents a sample.

P22luxI #3 = 100 µl (~3.7x10 ⁹ pfu)	Bioreporter = 50 µl (~6x10 ⁹ cfu)	+50 µl LB
P22 = 100 µl (~4x10 ⁹ pfu)	Bioreporter = 50 µl (~6x10 ⁹ cfu)	+50 µl LB
P22luxI #3 = 100 µl (~3.7x10 ⁹ pfu)	X	+100 µl LB
P22 = 100 µl (~4x10 ⁹ pfu)	X	+100 µl LB
100 µl SM buffer	Bioreporter = 50 µl (~6x10 ⁹ cfu)	+50 µl LB

Table 6-10. Bioluminescence detection from *E. coli* OHHLux during its incubation with P22luxI and negative control, *E. coli* OHHLux using DeltaTox luminometer (Strategic Diagnostics Inc., Newark, DE)

Time period (min)	Bioluminescence in photon counts	
	<i>E. coli</i> OHHLux	<i>E. coli</i> OHHLux + P22luxI #3
140	1,184,157	1,082,840
200	1,125,739	1,712,733
245	2,914,816	4,933,702
300	2,654,806	11,130,231

The culture of bioreporter containing phage was divided into two. Both were centrifuged at 10,000 x g for 10 min. Supernatant was discarded to remove phage particles. Pellets which contained bacterial cells were resuspended in fresh LB and vortexed vigorously for 5 min to remove phage particles which may be adsorbed to bacterial cells. One of the suspensions was centrifuged at 10,000 x g for 10 min. The resulting pellet was subjected to plasmid purification using Wizard Midi-Prep Plasmid Purification Kit (Promega, Madison, WI). The other suspension was centrifuged at 16,000 x g for 2 min and used for genomic DNA purification with Wizard Genomic DNA Purification Kit (Promega, Madison, WI). Plasmid and genomic DNA were used as templates in PCR reactions with luxISalmSalI forward and luxISalmXhoI reverse primers to detect *luxI*. The PCR protocol followed a step of 94°C for 5 min and then 35 cycles of 94°C for 30 sec, 42°C for 30 sec, and 72°C for 38 sec, and a final step of 72°C for 15 min. The PCR products were run on a 0.5% agarose gel with EtBr in 0.5xTBE. The gel was screened with UV light to spot the *luxI* amplicons based on size.

Qualitative detection of OHHL from P22luxI and *S. choleraesuis* mixture using AHL bioreporter *A. tumefaciens* A136

Since the bioluminescent bioreporter *E. coli* OHHLux produces bioluminescence in the presence of P22luxI without *S. choleraesuis*, it can not be used to test P22luxI for *S. choleraesuis* detection. Therefore, another AHL bioreporter, *A. tumefaciens* A136, was employed for this test. Although *A. tumefaciens* A136 can not quantify OHHL, it can detect the presence of it. Cultures of bacterial strains grown overnight were used for the assay. LB agars were spreaded with freshly prepared X-gal (40 mg/ml in dimethyl

formamide), 50 µl for each plate. One half of a plate was used for the test of each sample. *Agrobacterium tumefaciens* A136 was streaked across one half of an LB plate at two places, the top and the bottom. The culture or the culture-phage mixture to be tested was streaked onto the plate in between the two lines of bioreporter at exactly 0.5 cm distance vertically from each bioreporter line. Each *A. tumefaciens* A136 line consisted of 4 µl of an overnight culture of the strain. A diagram of the assay is shown in Figure 6-4. Samples and controls and their amounts are shown in Table 6-11.

This experiment was used to determine the efficiency of P22luxI phage for detection of *S. choleraesuis*. Also, the bioluminescent bioreporter *E. coli* OHHLux and bioreporter *A. tumefaciens* A136 were tested for OHHL production in the presence of P22luxI without *S. choleraesuis*. Positive controls included *A. tumefaciens* KYC6 which is an AHL overproducer and *S. choleraesuis* containing pCR-HAL #5. Negative control was *S. choleraesuis* mixed with the wild type P22 phage. Plates were checked after 32 h of incubation at room temperature and 36 h of incubation at 4°C.

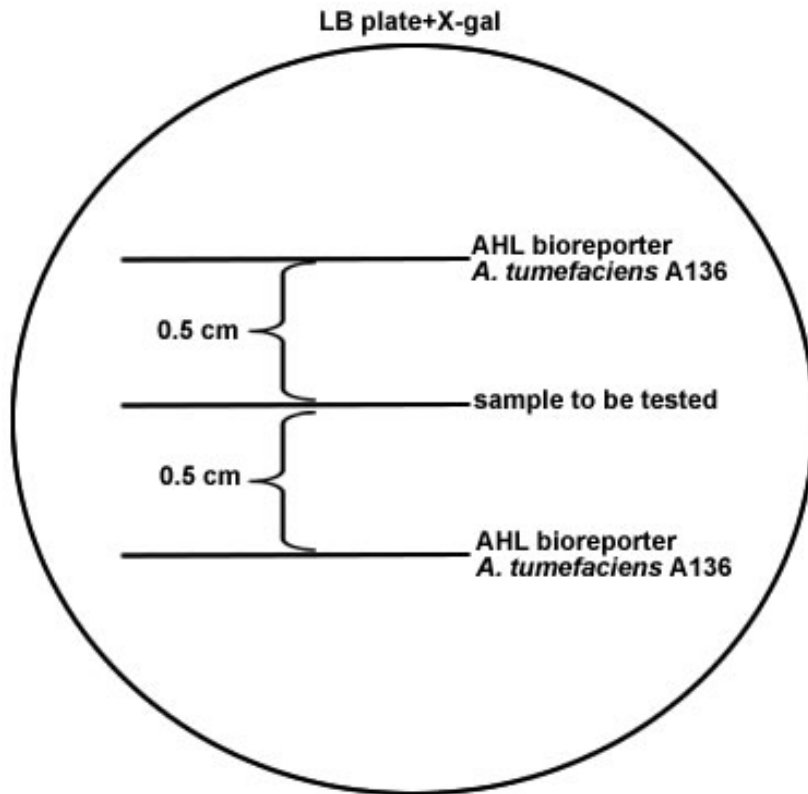


Figure 6-4. Assay diagram for qualitative detection of OHHL using AHL bioreporter *A. tumefaciens* A136.

Table 6-11. Samples, controls, and amounts (per each sample or control) used for OHHL detection from P22luxI and *S. choleraesuis* using AHL bioreporter *A. tumefaciens* A136. Each row represents a sample.

<i>S. choleraesuis</i> = 2 μ l ($\sim 6 \times 10^{10}$ cfu)	P22luxI #3 = 2 μ l ($\sim 7.4 \times 10^7$ pfu)
<i>S. choleraesuis</i> = 2 μ l ($\sim 6 \times 10^{10}$ cfu)	P22luxI #7 = 2 μ l ($\sim 5.4 \times 10^7$ pfu)
<i>E. coli</i> OHHLux bioreporter = 2 μ l ($\sim 4.8 \times 10^9$ cfu)	P22luxI #3 = 2 μ l ($\sim 7.4 \times 10^7$ pfu)
<i>E. coli</i> OHHLux bioreporter = 2 μ l ($\sim 4.8 \times 10^9$ cfu)	P22luxI #7 = 2 μ l ($\sim 5.4 \times 10^7$ pfu)
<i>A. tumefaciens</i> A136 = 4 μ l	P22luxI #3 = 2 μ l ($\sim 7.4 \times 10^7$ pfu)
<i>A. tumefaciens</i> A136 = 4 μ l	P22luxI #7 = 2 μ l ($\sim 5.4 \times 10^7$ pfu)
<i>A. tumefaciens</i> KYC6 = 4 μ l	X
<i>S. choleraesuis</i> with pCR-HAL #5 = 4 μ l	X
<i>S. choleraesuis</i> = 2 μ l ($\sim 6 \times 10^{10}$ cfu)	P22 = 2 μ l ($\sim 2.5 \times 10^7$ pfu)

Construction of *Klebsiella* bioluminescent bioreporters

The bioluminescent bioreporter *E. coli* OHHLux can not be used for monitoring *Salmonella* since it produces bioluminescence in the presence of P22luxI phage without *S. choleraesuis*. *Agrobacterium tumefaciens* A136 AHL bioreporter was used successfully to detect *S. choleraesuis* with the assistance of P22luxI. However, it provides a qualitative detection so it can not be used for optimization of the system. Therefore, to construct a new bioluminescent bioreporter, the plasmid carried by *E. coli* OHHLux was transferred into various *Klebsiella* strains.

The plasmid of *E. coli* OHHLux was constructed by placing a fusion of the *luxCDABE* genes from *P. luminescens*, the *luxR* gene and *luxI* promoter from *V. fischeri*, *rrnB* T1T2 transcriptional terminator, and a kanamycin resistance gene into an EZ::TN pMOD cloning vector (Epicentre Biotechnologies, Madison, WI) (63). The plasmid was purified from the strain using Wizard Plus Midi-Preps DNA Purification Systems (Promega, Madison, WI), and electroporated into electrically competent cells of *K. oxytoca* M5a1, *K. oxytoca* VJSK009, *K. pneumoniae* NCTC 418, and *K. pneumoniae* strains. Transformants were obtained from only *K. oxytoca* VJSK009 and *K. pneumoniae* NCTC 418. Plasmids of transformants were purified from overnight cultures with Wizard Plus Midi-Preps DNA Purification Systems (Promega, Madison, WI) and controlled by *EcoRI* (Promega, Madison, WI) digestion and sequencing for verification. One transformant carrying the plasmid was selected for each *Klebsiella* strain and used for bioluminescence tests of *S. choleraesuis* and P22luxI.

Bioluminescent detection of OHHL from *S. choleraesuis* and P22luxI phage using *Klebsiella* bioluminescent bioreporters and a Wallac 1450 Microbeta Plus Liquid Scintillation Counter

Overnight cultures of *K. oxytoca* VJSK009 and *K. pneumoniae* NCTC 418 harboring the plasmid from the bioluminescent bioreporter *E. coli* OHHLux and *S. choleraesuis* were prepared. *Klebsiella* cultures which were washed in LB were diluted to OD₆₀₀=0.1 in LB without antibiotic. The *S. choleraesuis* culture was diluted 10X in fresh LB and grown at 37°C with 220 rpm until mid-log phase, and resuspended in the same volume LB. The Costar 96-well black microtiter plates with black bottom (Corning Inc. Life Sciences, Lowell, MA) were used for samples and controls, prepared in triplicate. Samples and controls, and their amounts are shown in Tables 6-12, 6-13, and 6-14. The assay methodology is shown in Figure 6-3. Wallac 1450 Microbeta Plus Liquid Scintillation Counter measurements included a bioluminescence measurement (CPS) and then incubation for 20 min repeated overnight at 28°C. Average CPS values in triplicate was calculated for each sample.

Table 6-12. Samples and amounts (per each plate well) used for bioluminescence detection from P22luxI and its host *S. choleraesuis* using the *K. pneumoniae* bioreporter. Each row represents a sample.

P22luxI	<i>S. choleraesuis</i>	<i>K. pneumoniae</i> bioreporter
(#3) 100 µl (~5x10 ⁸ -5x10 ⁹ pfu)	50 µl (~7x10 ⁸ cfu)	50 µl (~5x10 ¹⁰ cfu)
(#7) 100 µl (~4x10 ⁸ pfu)	50 µl (~7x10 ⁸ cfu)	50 µl (~5x10 ¹⁰ cfu)
(#3) 100 µl (~5x10 ⁸ -5x10 ⁹ pfu)	exchanged with 50 µl LB	50 µl (~5x10 ¹⁰ cfu)
(#7) 100 µl (~4x10 ⁸ pfu)	exchanged with 50 µl LB	50 µl (~5x10 ¹⁰ cfu)

Table 6-13. Samples and amounts (per each plate well) used for bioluminescence detection from P22luxI and its host *S. choleraesuis* using the *K. oxytoca* bioreporter. Each row represents a sample.

P22luxI	<i>S. choleraesuis</i>	<i>K. oxytoca</i> bioreporter
(#3) 100 µl (~5x10 ⁸ -5x10 ⁹ pfu)	50 µl (~7x10 ⁸ cfu)	50 µl (~1.3x10 ¹⁰ cfu)
(#7) 100 µl (~4x10 ⁸ pfu)	50 µl (~7x10 ⁸ cfu)	50 µl (~1.3x10 ¹⁰ cfu)
(#3) 100 µl (~5x10 ⁸ -5x10 ⁹ pfu)	exchanged with 50 µl LB	50 µl (~1.3x10 ¹⁰ cfu)
(#7) 100 µl (~4x10 ⁸ pfu)	exchanged with 50 µl LB	50 µl (~1.3x10 ¹⁰ cfu)

Table 6-14. Negative controls and amounts (per each plate well) used for bioluminescence detection P22luxI and its host *S. choleraesuis* using *Klebsiella* bioreporters. Each row represents a sample.

100 µl P22 (~4x10 ⁹ pfu)	50 µl <i>S. choleraesuis</i> (~7x10 ⁸ cfu)	50 µl <i>K. pneumoniae</i> (~5x10 ¹⁰ cfu)
100 µl P22 (~4x10 ⁹ pfu)	50 µl <i>S. choleraesuis</i> (~7x10 ⁸ cfu)	50 µl <i>K. oxytoca</i> (~1.3x10 ¹⁰ cfu)
100 µl SM buffer	50 µl <i>S. choleraesuis</i> (~7x10 ⁸ cfu)	50 µl <i>K. pneumoniae</i> (~5x10 ¹⁰ cfu)
100 µl SM buffer	50 µl <i>S. choleraesuis</i> (~7x10 ⁸ cfu)	50 µl <i>K. oxytoca</i> (~1.3x10 ¹⁰ cfu)
100 µl P22luxI #3 (~5x10 ⁸ -5x10 ⁹ pfu)	50 µl <i>S. choleraesuis</i> (~7x10 ⁸ cfu)	50 µl LB
100 µl P22luxI #7 (~4x10 ⁸ pfu)	50 µl <i>S. choleraesuis</i> (~7x10 ⁸ cfu)	50 µl LB
100 µl SM buffer	50 µl LB	50 µl <i>K. pneumoniae</i> (~5x10 ¹⁰ cfu)
100 µl SM buffer	50 µl LB	50 µl <i>K. oxytoca</i> (~1.3x10 ¹⁰ cfu)
100 µl SM buffer	50 µl <i>S. choleraesuis</i> (~7x10 ⁸ cfu)	50 µl LB
100 µl P22luxI #3 (~5x10 ⁸ -5x10 ⁹ pfu)	100 µl LB	
100 µl P22luxI #7 (~4x10 ⁸ pfu)	100 µl LB	

Bioluminescent detection of OHHL from P22luxI genome and bioluminescent bioreporters using a Wallac 1450 Microbeta Plus Liquid Scintillation Counter

Bioluminescence measurements were performed to test the possibility that the P22luxI genome is taken by the bioreporter cells without infection, leading to bioluminescence generation from bioreporter and phage mixtures. Overnight cultures of *K. oxytoca* VJSK009, *K. pneumoniae* NCTC 418, and *E. coli* OHHLux bioluminescent bioreporters were washed in LB, and diluted to OD₆₀₀=0.1 in LB without antibiotic. Samples and controls were set up in triplicate. Costar 96-well black microtiter plates with black bottom (Corning Inc. Life Sciences, Lowell, MA) were used for the assay. Samples and controls, and their amounts are shown in Tables 6-15 and 6-16. Two different concentrations of the phage genome were used for each P22luxI with 4.6 ng corresponding to 10⁸ pfu and 46 ng corresponding to 10⁹ pfu. Phage genomes were extracted using Wizard Lambda Preps DNA Purification System (Promega, Madison, WI). Phage-bioreporter mixtures were used as positive controls. Also, bioreporters alone and bioreporter-P22 mixtures were used as negative controls in addition to those in Table 6-16. A bioluminescence measurement (CPS) followed by incubation for 20 min which was repeated overnight to 52 h at 28°C was performed by Wallac 1450 Microbeta Plus Liquid Scintillation Counter. The mean of CPS values in triplicate was calculated for each sample.

Table 6-15. Samples and amounts (per each plate well) used for bioluminescence detection from P22luxI genome and *K. oxytoca*, *K. pneumoniae*, or *E. coli* OHHLux bioreporters. Each row represents a sample.

P22luxI or P22 phage; or their genome	Bioreporter	
#3 = 100 μ l ($\sim 5 \times 10^8$ - 5×10^9 pfu)	50 μ l ($\sim 5 \times 10^{10}$ cfu)	50 μ l LB
#3 genome = 4.6 ng in 100 μ l SM buffer	50 μ l ($\sim 5 \times 10^{10}$ cfu)	50 μ l LB
#3 genome = 46 ng in 100 μ l SM buffer	50 μ l ($\sim 5 \times 10^{10}$ cfu)	50 μ l LB
#7 = 100 μ l ($\sim 4 \times 10^8$ pfu)	50 μ l ($\sim 5 \times 10^{10}$ cfu)	50 μ l LB
#7 genome = 4.6 ng in 100 μ l SM buffer	50 μ l ($\sim 5 \times 10^{10}$ cfu)	50 μ l LB
#7 genome = 46 ng in 100 μ l SM buffer	50 μ l ($\sim 5 \times 10^{10}$ cfu)	50 μ l LB
P22 = 100 μ l ($\sim 4 \times 10^9$ pfu)	50 μ l ($\sim 5 \times 10^{10}$ cfu)	50 μ l LB
exchanged with 100 μ l SM buffer	50 μ l ($\sim 5 \times 10^{10}$ cfu)	50 μ l LB

Table 6-16. Negative controls and amounts (per each plate well) used for bioluminescence detection from P22luxI genome and *K. oxytoca*, *K. pneumoniae*, or *E. coli* OHHLux bioreporters. Each row represents a sample.

P22luxI or its genome	
#3 = 100 μ l ($\sim 5 \times 10^8$ - 5×10^9 pfu)	+ 100 μ l LB
#3 genome = 4.6 ng in 100 μ l SM buffer	+ 100 μ l LB
#3 genome = 46 ng in 100 μ l SM buffer	+ 100 μ l LB
#7 = 100 μ l ($\sim 4 \times 10^8$ pfu)	+ 100 μ l LB
#7 genome = 4.6 ng in 100 μ l SM buffer	+ 100 μ l LB
#7 genome = 46 ng in 100 μ l SM buffer	+ 100 μ l LB

Statistical calculations

Bioluminescence and fluorescence values were normalized by dividing the CPS and GFP values obtained, respectively, by absorbance values at OD₄₅₀ of the bioreporter culture measured at the same time point where available. The average of triplicate measurements was calculated for each time point. Normalized values were used if the absorbance of the bioreporter culture was measured. Error bars were determined by calculating the standard deviation of triplicate bioluminescence or fluorescence values at each time point as follows: The average of triplicate measurements (normalized where available) for a time point was subtracted from each measurement (normalized where available) at that time point. The squares of the differences were calculated. The average of all three squared differences was determined. The square root of the value found was used as the standard deviation for the average value at each time point. Significance levels were determined by comparing average bioluminescence or fluorescence values of a sample to those of the negative control using Student's *t*-test ($P < 0.05$). Maximum induction value of a sample for an assay was calculated by dividing the highest amount of light obtained from the sample during the assay by the amount of light from the negative control at the same time point.

CHAPTER VII

RESULTS

CONSTRUCTION OF *SALMONELLA* BIOREPORTER

Bioluminescent and fluorescent detection of OHHL from pCR-L #3 in *S. choleraesuis* using Wallac Victor2 1420 Multilabel and 1450 Microbeta Plus Liquid Scintillation Counters

The plasmid pCR-L #3 was constructed and transferred to *S. choleraesuis* to test *luxI* expression in *Salmonella* with a *Salmonella* phage promoter to detect promoter efficiency. The aim was to finally clone the *luxI* into a *Salmonella* phage under this promoter. Therefore, *S. choleraesuis* harboring pCR-L #3 was tested for bioluminescence and fluorescence using the bioluminescent bioreporter *E. coli* OHHLux, the fluorescent bioreporter *E. coli* MT102 with pJBA132, and the wild type *S. choleraesuis* strain as the negative control. Also, measurements from bioreporters alone were done to determine background bioluminescence and fluorescence. Samples and controls were in triplicate. Wallac Victor2 1420 Multilabel Counter (PerkinElmer Life and Analytical Sciences, Waltham, MA) bioluminescence and fluorescence measurements were normalized by dividing CPS and GFP by OD₄₅₀ values. The mean of triplicate values obtained was calculated for each sample. The mean of Wallac 1450 Microbeta Plus Liquid Scintillation Counter (PerkinElmer Life and Analytical Sciences, Waltham, MA) bioluminescence measurements in triplicate was calculated for each sample. Measurements were carried out at 28°C.

High levels of bioluminescence and fluorescence were obtained from pCR-L #3 in *S. choleraesuis* (Figure 7-1). Table 7-1 shows the maximum inductions obtained from each assay. Bioluminescence and fluorescence levels obtained from the construct were 15 to 33 times higher than those of the negative control.

Cloning of P_L , *luxI*, and T_1T_2 into *Salmonella* phage P22 using homologous recombination

luxI under the control of the Gram-negative RBS, and P22 promoter P_L followed by transcription termination site T_1T_2 was cloned into phage P22 using the homologous recombination method (665) with some modifications. The integration site was after the 22,711th nucleotide of the genome and between ORF-201 and ORF-80 genes (phage genome PubMed No: AF217253; 655). Homology regions of the genome which were used for homologous recombination were the 306-bp sequence before and the 319-bp sequence after the insertion site. *Salmonella choleraesuis* harboring pCR-HAL #5 which carries homology arms was infected with P22 for homologous recombination to take place. Resulting plaques were screened by plating dilutions of the lysate with the culture of *S. choleraesuis* containing pCR-HAL #5. Isolated plaques could be visualized only on the 10^{-4} phage dilution plate. The morphology of all ~200 plaques obtained on the plate differed from wild type P22 plaque morphology. A wild type plaque occupied a large area with a clear halo around the center where there was bacterial growth. The plaques obtained from the homologous recombination formed much smaller (~1 mm), clear areas on the plate.

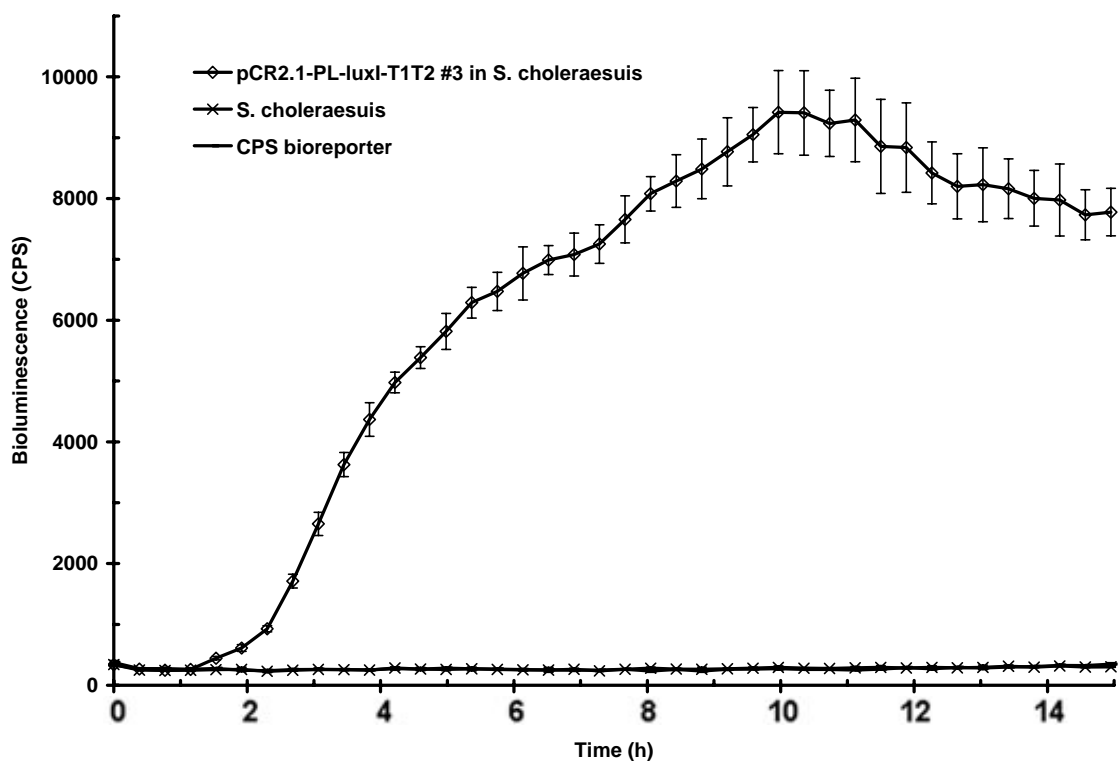


Figure 7-1 (A). Bioluminescent OHHL detection from pCR-L #3 (or pCR2.1-P_L-luxI-T1T2 #3) in *S. choleraesuis* at 28°C using the bioreporter *E. coli* OHHLux and Wallac 1450 Microbeta Plus Liquid Scintillation Counter. Results represent the mean bioluminescence values (n=3) ± SD (bars).

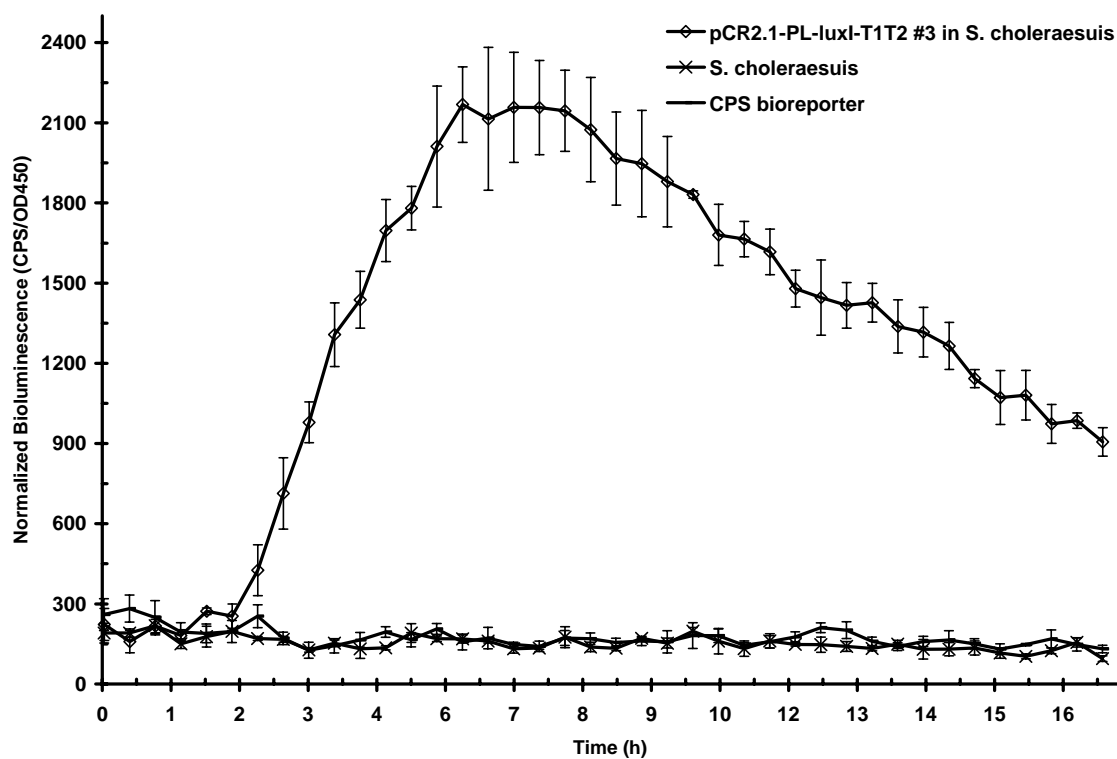


Figure 7-1 (B). Bioluminescent OHHL detection from pCR-L #3 (or pCR2.1-P_L-luxI-T1T2 #3) in *S. choleraesuis* at 28°C using the bioreporter *E. coli* OHHLux and Wallac Victor2 1420 Multilabel Counter. Results represent the mean bioluminescence values (n=3) ± SD (bars).

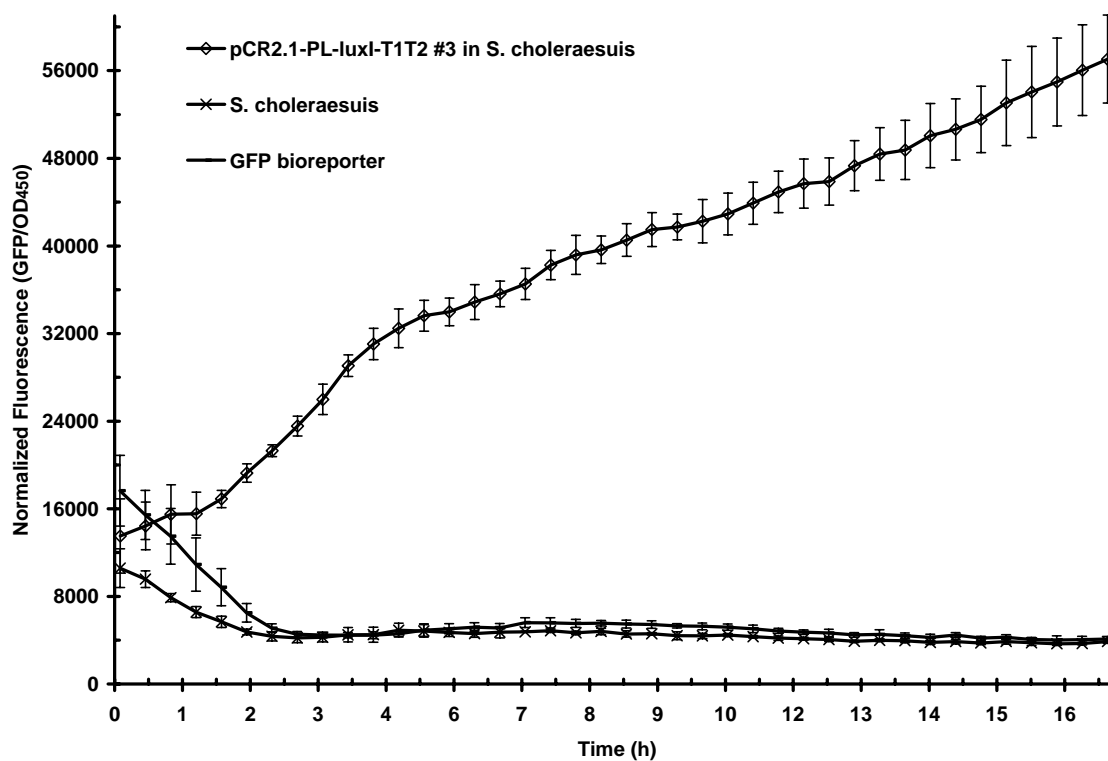


Figure 7-1 (C). Fluorescent OHHL detection from pCR-L #3 (or pCR2.1-P_L-luxI-T1T2 #3) in *S. choleraesuis* at 28°C using the bioreporter *E. coli* MT102 with pJBA132 and Wallac Victor2 1420 Multilabel Counter. Results represent the mean fluorescence values (n=3) ± SD (bars).

Table 7-1. Bioluminescence and fluorescence from pCR-L #3 in *S. choleraesuis*. Bioluminescence was detected using the bioreporter *E. coli* OHHLux and Wallac 1450 Microbeta Plus Liquid Scintillation Counter. Fluorescence was detected using the bioreporter *E. coli* MT102 harboring pJBA132 and Wallac Victor2 1420 Multilabel Counter. (MI = maximum induction; the highest amount of light from a sample divided by the negative control value at the same time point, T = Time period in h to obtain MI)

	pCR-L #3 in <i>S. choleraesuis</i>	
	MI	T
Bioluminescence-Wallac 1450	33.5X	10.5
Bioluminescence-Wallac Victor2	16.4X	7
Fluorescence-Wallac Victor2	15.2X	17

Bioluminescent detection of OHHL from P22luxI phage propagated with *S. choleraesuis* or *S. choleraesuis* with pCR-HAL #5 using Wallac Victor2 1420 Multilabel and 1450 Microbeta Plus Liquid Scintillation Counters

The P22luxI phage #3, #7, 10^{-4} , and HR obtained from homologous recombination were tested for OHHL production using the bioluminescent bioreporter *E. coli* OHHLux and Wallac Victor2 1420 Multilabel and 1450 Microbeta Plus Liquid Scintillation Counters. Samples were prepared in triplicate. Each sample contained $\sim 5 \times 10^9$ cfu bioreporter, $\sim 4.3 \times 10^8$ cfu *S. choleraesuis*, and P22luxI lysate. There were two varieties of each phage type: the one propagated with *S. choleraesuis* and the one propagated with *S. choleraesuis* carrying pCR-HAL #5 as the host. The amount of each phage in a plate well is shown in Table 6-5. Measurements were performed at 28°C.

High levels of bioluminescence from all phage propagated using *S. choleraesuis* with pCR-HAL #5 were detected (Figure 7-2). Maximum bioluminescence values

obtained from these phage compared with the background (time 0) are shown in Table 7-2. There was no bioluminescence produced by any of the phage which were propagated with *S. choleraesuis* (Figure 7-2). Phage P22luxI #3 and #7 were selected for further experiments. They were propagated using *S. choleraesuis* harboring pCR-HAL #5 when needed since they lose the capability of bioluminescence production when propagated with the wild type *S. choleraesuis*.

Screening of P22luxI #3 and #7 phage by PCR

The phage P22luxI #3 and #7 propagated with *S. choleraesuis* and *S. choleraesuis* harboring pCR-HAL #5 were controlled for the presence of *luxI* by PCR. Plaques of the phage suspended in sterile dH₂O were boiled and used as the template for PCR with luxISalmSalI forward and luxISalmXhoI reverse primers. PCR products were screened by running on a gel. *luxI* was obtained only from phage that were propagated with *S. choleraesuis* containing pCR-HAL #5 (.Figure 7-3).

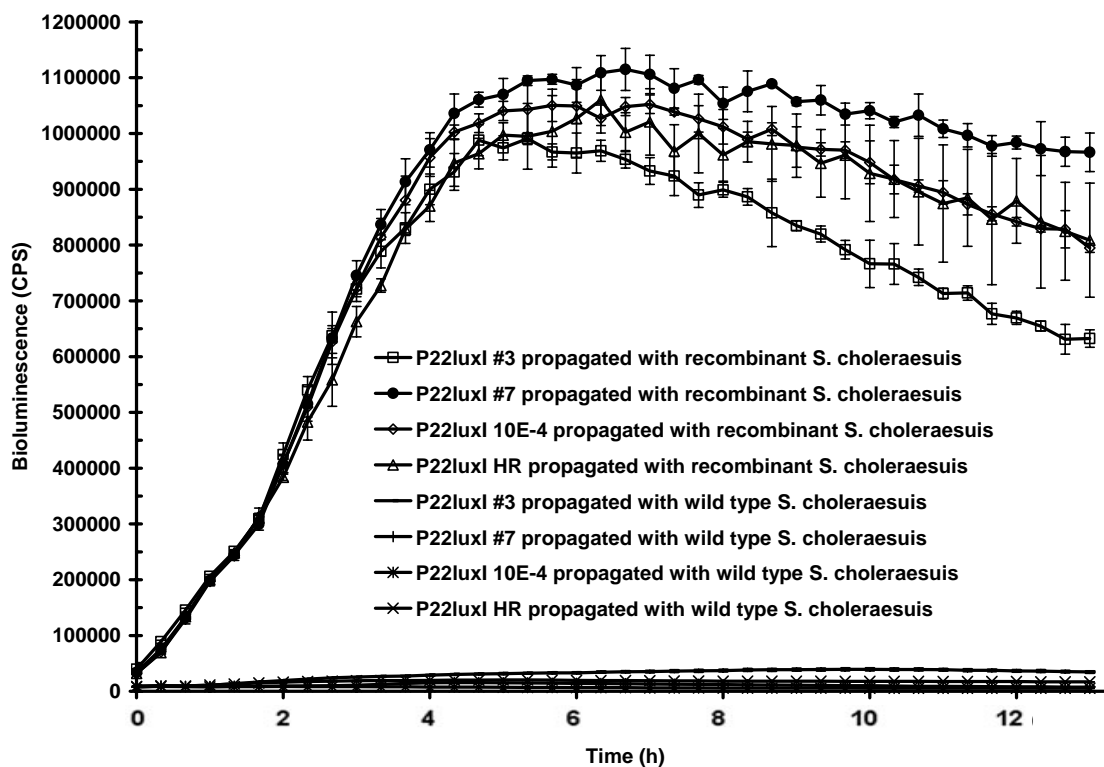


Figure 7-2 (A). Bioluminescent OHHL detection from P22luxI #3, #7, 10^{-4} , and HR using the bioreporter *E. coli* OHHLux, the host *S. choleraesuis*, and Wallac 1450 Microbeta Plus Liquid Scintillation Counter. Results represent the mean bioluminescence values ($n=3$) \pm SD (bars). (Recombinant *S. choleraesuis* = *S. choleraesuis* with pCR-HAL #5)

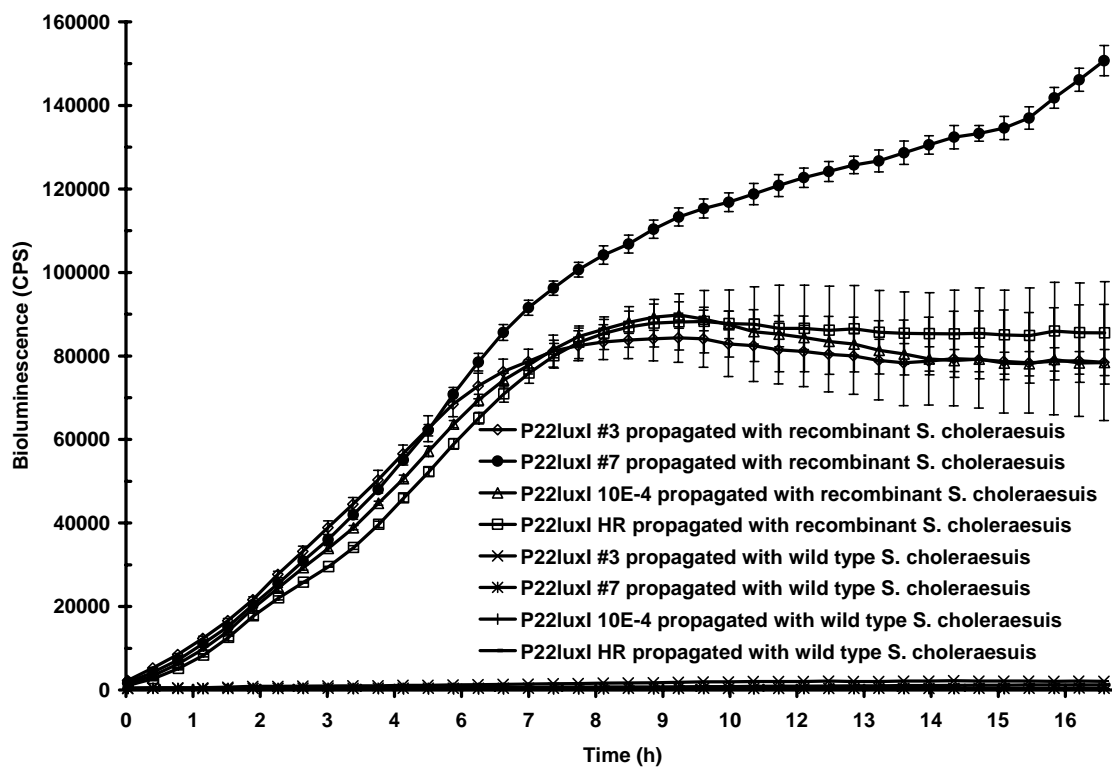


Figure 7-2 (B). Bioluminescent OHHL detection from P22luxI #3, #7, 10^{-4} , and HR using the bioreporter *E. coli* OHHLux, the host *S. choleraesuis*, and Wallace Victor2 1420 Multilabel Counter. Results represent the mean bioluminescence values ($n=3$) \pm SD (bars). (Recombinant *S. choleraesuis* = *S. choleraesuis* with pCR-HAL #5)

Table 7-2. Bioluminescence from P22luxI #3, #7, 10^{-4} , and HR propagated using *S. choleraesuis* containing pCR-HAL #5. Detection was performed using *E. coli* OHHLux as the bioreporter and *S. choleraesuis* as the host. (MI = maximum induction-the highest amount of light from a sample divided by the time 0 value of the same sample, * = Time period in h to obtain MI, Wallac 1450 = Wallac 1450 Microbeta Plus Liquid Scintillation Counter, Wallac Victor2 = Wallac Victor2 1420 Multilabel Counter)

	MI by P22luxI phage propagated using <i>S. choleraesuis</i> carrying pCR-HAL #5			
	#3	#7	10^{-4}	HR
Bioluminescence-Wallac 1450	25X _{*(5)}	33X _{*(6.5)}	33X _{*(7)}	33X _{*(6)}
Bioluminescence-Wallac Victor2	37X _{*(10)}	80X _{*(17.5)}	60X _{*(10)}	80X _{*(10.5)}

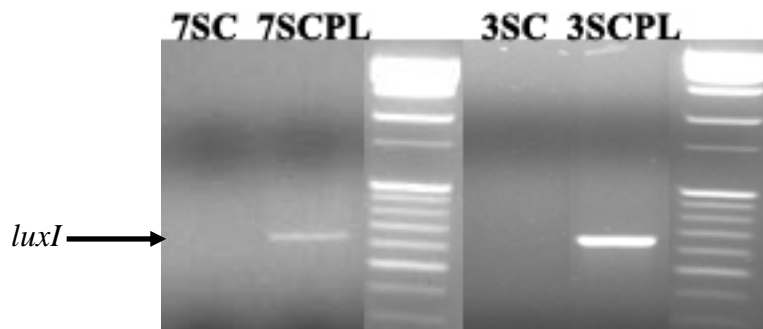


Figure 7-3. Products from PCR to check the presence of *luxI* in P22luxI #3 and #7 propagated using *S. choleraesuis* or *S. choleraesuis* carrying pCR-HAL #5. (7SC=P22luxI #7 propagated using *S. choleraesuis*, 7SCPL=P22luxI #7 propagated using *S. choleraesuis* with pCR-HAL #5, 3SC = P22luxI #3 propagated using *S. choleraesuis*, 3SCPL = P22luxI #3 propagated using *S. choleraesuis* with pCR-HAL #5)

Testing the bioluminescent bioreporter *E. coli* OHHLux for infection by P22 and P22luxI #3 and #7 phage on an LB plate

The P22 and P22luxI #3 and #7 phage stock drops were put on a bioluminescent bioreporter *E. coli* OHHLux LB plate to test the bioreporter infection by the phage. After overnight incubation at 37°C, no lysis was detected with any of the phage drops.

Detection of bioluminescence from the bioluminescent bioreporter *E. coli* OHHLux and P22luxI mixture using Wallac Victor2 1420 Multilabel and 1450 Microbeta Plus Liquid Scintillation Counters

Bioluminescence from the bioreporter *E. coli* OHHLux combined with P22luxI #3 or #7 was tested using Wallac Counters. Control samples were also prepared for comparison. The control for P22luxI #7 was a mixture of phage, bioreporter, and *S. choleraesuis*. P22luxI #3 controls consisted of a mixture of phage, bioreporter, and *S. choleraesuis*; a mixture of phage and *S. choleraesuis*; a mixture of bioreporter and *S. choleraesuis*; phage alone; bioreporter alone; and *S. choleraesuis* alone. Samples and their amounts for the P22luxI #7 and #3 assays are shown in Tables 6-6 and 6-7, respectively. Measurements were performed at 28°C.

Results of P22luxI #3 and #7 assays are shown in Figure 7-4. There was no bioluminescence from controls, phage-*S. choleraesuis*, bioreporter-*S. choleraesuis*, phage, bioreporter, and *S. choleraesuis* as expected. However, high levels of bioluminescence were produced by samples which contain the P22luxI #3 or #7 and the bioreporter. These were even higher than amounts obtained from control samples which consisted of P22luxI #3 or #7, bioreporter, and *S. choleraesuis*.

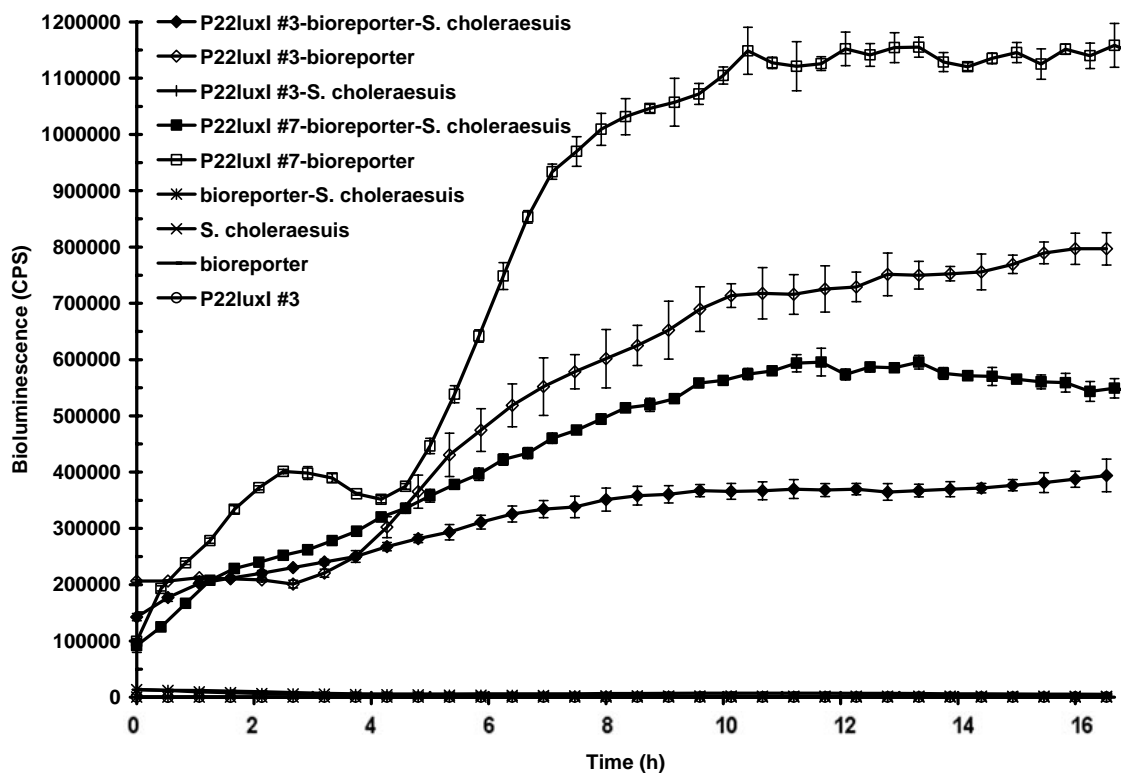


Figure 7-4 (A). Bioluminescent OHHL detection from P22luxI and the bioreporter *E. coli* OHHLux using Wallac 1450 Microbeta Plus Liquid Scintillation Counter. Results represent the mean bioluminescence values ($n=3$) \pm SD (bars).

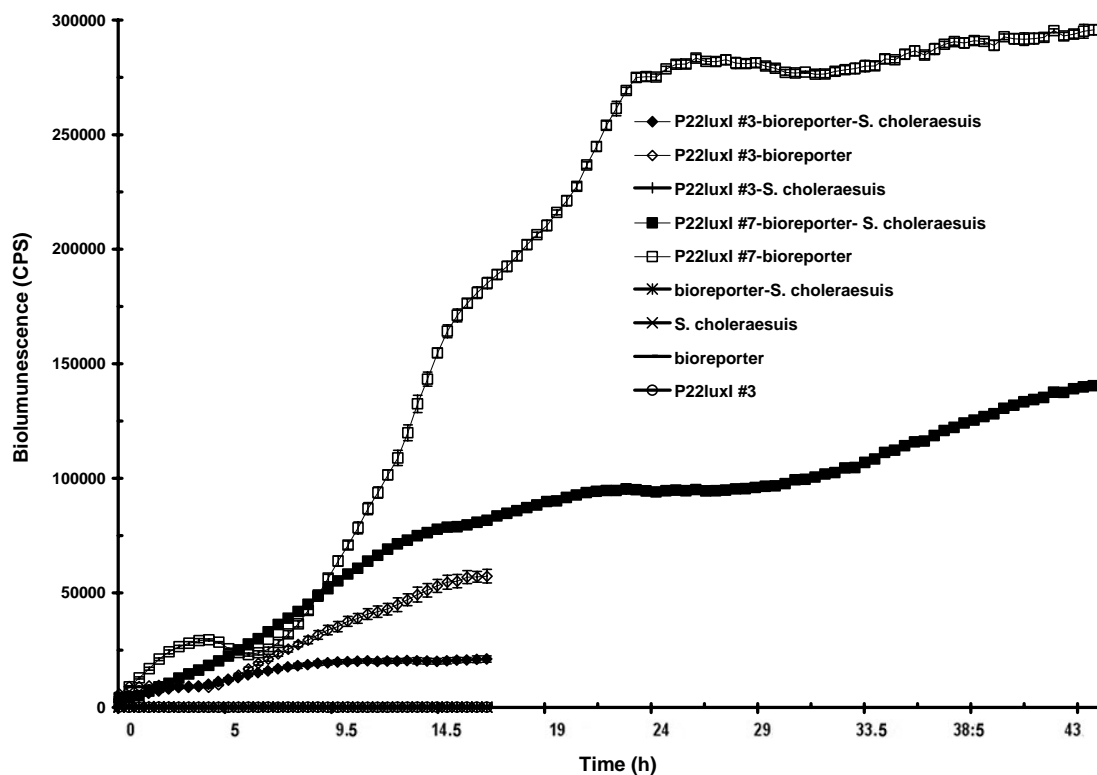


Figure 7-4 (B). Bioluminescent OHHL detection from P22luxI and the bioreporter *E. coli* OHHLux using Wallac Victor2 1420 Multilabel Counter. Results represent the mean bioluminescence values ($n=3$) \pm SD (bars).

Control of phage stocks for contamination

Lysate stocks of P22luxI #3 and #7 phage were checked for bacterial contamination which may cause bioluminescence production from mixtures of bioreporter and phage. Each phage stock (100 μ l; 1.3×10^9 pfu P22luxI #3; 8.2×10^8 pfu P22luxI #7) was spreaded onto a sterile LB plate. Plates were incubated overnight at 37°C. Also, an aliquot from the lysate of each phage (520 μ l- 1.9×10^{10} pfu P22luxI #3; 1.4×10^{10} pfu P22luxI #7) was incubated with 10 ml sterile LB at 37°C with 220 rpm for 6 d. There was no growth in both media after incubation.

Measurements from the mixtures of bioluminescent bioreporter *E. coli* OHHLux and P22luxI #3 phage to determine the source of bioluminescence using Wallac 1450 Microbeta Plus Liquid Scintillation Counter

To determine the source of bioluminescence from the mixture of bioluminescent bioreporter *E. coli* OHHLux and phage P22luxI, samples of various phage P22luxI #3 dilutions mixed with a constant amount of bioreporter and samples of a constant amount of phage P22luxI #3 combined with various dilutions of bioreporter were prepared. Bioluminescence from these samples was measured using Wallac 1450 Microbeta Plus Liquid Scintillation Counter. Bioreporter dilutions were prepared with LB and phage dilutions with SM buffer (50 mM Tris-HCL pH 7.5, 100 mM NaCl, 8 mM MgSO₄, 0.01% gelatin). Control samples consisted of a mixture of P22luxI #3 phage and bioreporter without dilution, P22luxI #3 phage alone, bioreporter alone, a mixture of wild type phage P22 and bioreporter, and P22 phage alone. Samples and controls were prepared in triplicate. Samples and controls including the amounts are shown in Tables 6-

8 and 6-9, respectively. Measurements were performed overnight at 28°C. The average of CPS values from each sample prepared in triplicate was calculated.

Table 7-3 shows the comparison of the bioluminescence values reached at the end of the assay shown in Figure 7-5. Dilutions of the bioreporter did not affect the output of bioluminescence considerably. Bioluminescence with all bioreporter dilutions reached levels which were not significantly different from the level obtained with the undiluted bioreporter. However, dilutions in phage decreased the amount of bioluminescence significantly. The decrease bioluminescence was correlated with the increase in phage dilution. As expected, there was no bioluminescence from controls, P22-bioreporter, P22luxI #3, P22, and bioreporter.

Table 7-3. Comparison of bioluminescence from P22luxI and *E. coli* OHHLux dilutions determined to find the source of light from the P22luxI and *E. coli* OHHLux mixture. A constant amount of *E. coli* OHHLux was used with P22luxI dilutions and a constant amount of P22luxI was used with *E. coli* OHHLux dilutions. The final induction was calculated by dividing the final value from a sample by the negative control value at the same time point.

dilution	Final induction by P22luxI #3 dilutions	Final induction by bioreporter dilutions	Final induction by P22luxI #3-bioreporter with no dilution
2X	10.6X	19.3X	23.5X
4X	6.6X	20.8X	
8X	4.6X	22.3X	
10X	2.2X	--	
32X	1.1X	20.3X	
100X	0.3X	--	

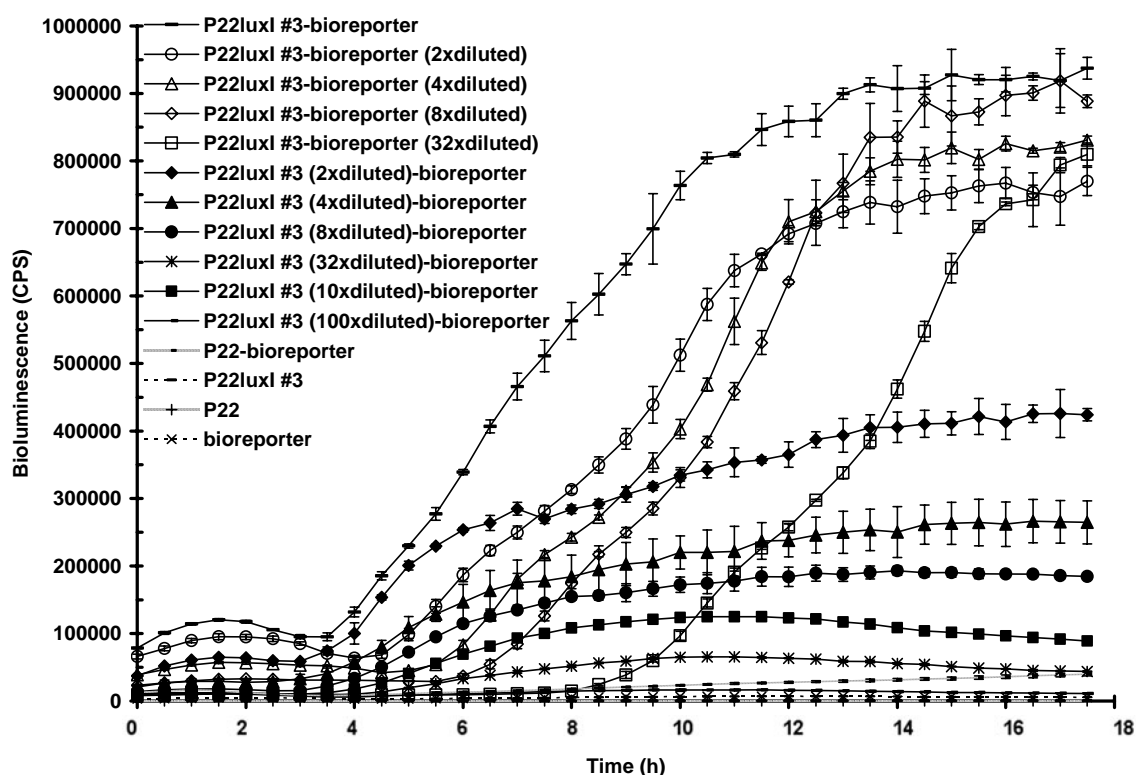


Figure 7-5. Bioluminescence detection to find the source of light from the P22luxI and *E. coli* OHHLux mixture. A constant amount of *E. coli* OHHLux was used with P22luxI dilutions and a constant amount of P22luxI was used with *E. coli* OHHLux dilutions. Results represent the mean bioluminescence values ($n=3$) \pm SD (bars).

Test of pseudolysogeny

Bioluminescence obtained from the bioluminescent bioreporter *E. coli* OHHLux and P22luxI phage mixture decreased with dilutions of phage. Test of phage lysate for bacterial contamination detected no bacterial cells. It was also determined previously that there was no plaque formation on plates containing the bioreporter culture infected with the phage, implicating no lysis or lysogeny. Therefore, the possibility of a pseudolysogenic interaction between the bioreporter and phage was evaluated. A culture of bioreporter infected with P22luxI #3 was incubated until the detection of bioluminescence. Then, bacterial cells were separated from phage particles by collecting the pellet after centrifugation. The resuspended pellet was vortexed vigorously for 5 min to remove phage particles which may be found adsorbed to bacterial cell surfaces. After another centrifugation, bacterial cells were suspended in LB and used for separate plasmid and genomic DNA purifications. Purifications were controlled for the presence of *luxI* by PCR using luxISalmSalI forward and luxISalmXhoI reverse primers. PCR products were screened by running on a gel and followed by UV illumination. *luxI* was detected in both plasmid and genome purifications (Figure 7-6) and the amount was higher in plasmid purifications.

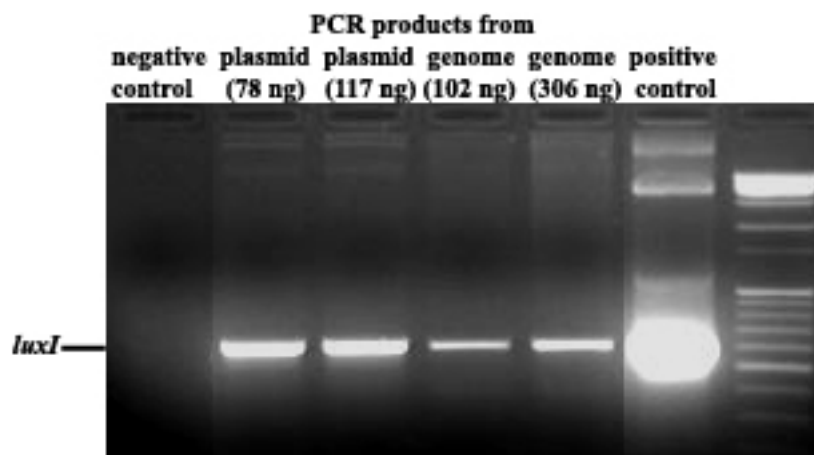


Figure 7-6. Products from PCR to check the presence of *luxI* in genome and plasmid purifications of *E. coli* OHHLux after incubation with P22luxI. (Negative control = P22 genome, positive control = pCR-L #3, genome = genome from *E. coli* OHHLux after incubation with P22luxI, plasmid = plasmid from *E. coli* OHHLux after incubation with P22luxI)

Qualitative detection of OHHL from P22luxI and *S. choleraesuis* mixture using AHL bioreporter *A. tumefaciens* A136

The bioluminescent bioreporter *E. coli* OHHLux was found to produce bioluminescence in the presence of P22luxI without *S. choleraesuis*. Therefore, to determine the efficiency of P22luxI for *S. choleraesuis* detection, another AHL bioreporter, *A. tumefaciens* A136, was used. *Agrobacterium tumefaciens* A136 can detect the presence of OHHL; however, it is not as sensitive as *E. coli* OHHLux for OHHL quantification.

Overnight cultures of bacterial strains were used for the experiment. The sample to be tested was placed in between two lines of *A. tumefaciens* A136 on an LB plate

spread with X-gal. The line of sample was adjusted to be at exactly 0.5 cm distance vertically from each bioreporter line. Each line of bioreporter contained 4 µl overnight culture of the strain. A diagram of the assay is shown in Figure 6-4. Samples and controls, and their amounts are shown in Table 6-11. *Agrobacterium tumefaciens* KYC6 which is an AHL overproducer and *S. choleraesuis* containing pCR-HAL #5 were used as positive controls. *Salmonella choleraesuis* mixed with the wild type P22 phage was the negative control. Plates were incubated for 32 h at room temperature and then 36 h at 4°C.

Agrobacterium tumefaciens A136 carries a *traI-lacZ* fusion. When OHHL is produced by the sample, it diffuses across the plate and reaches the strain. This results in activation of the *traI-lacZ* fusion, causing expression of β-galactosidase activity. This expression converts the color of *A. tumefaciens* A136 colonies on the plate from white to blue. Therefore, no change in white color of *A. tumefaciens* A136 colonies demonstrates the absence of OHHL from the sample while a change to a blue color shows the release of OHHL from the sample.

As expected, there was OHHL production by positive controls and no OHHL from the negative control (Figure 7-7). *Agrobacterium tumefaciens* A136 bioreporter did not generate OHHL in the presence of only P22luxI, making it a suitable bioreporter to determine P22luxI efficiency for *S. choleraesuis* detection. High amounts of OHHL were released from mixtures of *S. choleraesuis* and P22luxI #3 or #7 as demonstrated by the dense blue color of bioreporter colonies. This demonstrates that P22luxI #3 and #7 can be used effectively to monitor *S. choleraesuis*

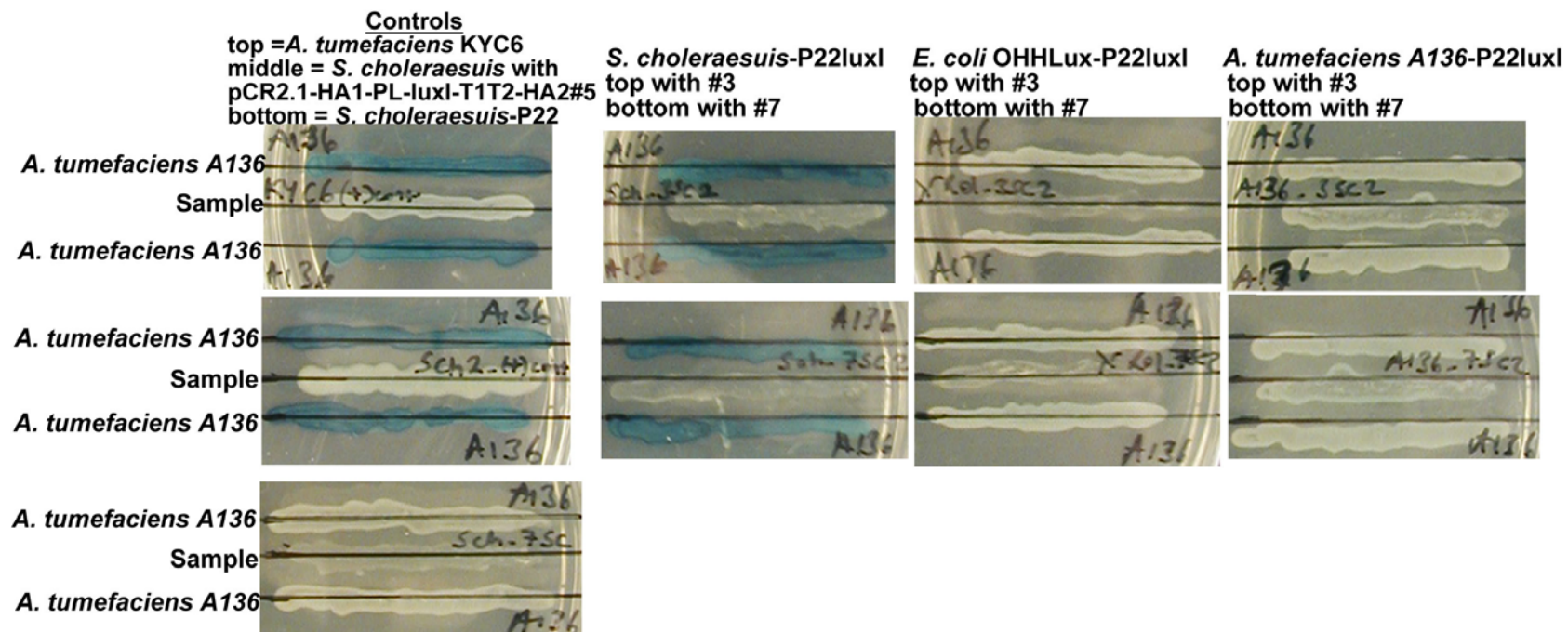


Figure 7-7. Qualitative OHHL detection using AHL bioreporter *A. tumefaciens* A136. Sample names are shown on top of pictures. (top = top picture, middle = middle picture, bottom = bottom picture, #3 = P22luxI #3, #7 = P22luxI #7)

However, there was no OHHL produced by the combination of the bioluminescent bioreporter *E. coli* OHHLux and P22luxI although the same combination was found to produce bioluminescence using Wallac Victor2 1420 Multilabel and 1450 Microbeta Plus Liquid Scintillation Counters. This may suggest a possible pseudolysogenic interaction between *E. coli* OHHLux and P22luxI, which is discussed in more detail in the discussion section (see chapter 8).

Bioluminescent detection of OHHL from *S. choleraesuis* and P22luxI phage using *Klebsiella* bioluminescent bioreporters and a Wallac 1450 Microbeta Plus Liquid Scintillation Counter

The bioreporter *E. coli* OHHLux produces bioluminescence when combined with P22luxI phage and thus can not be used for *Salmonella* monitoring. *Agrobacterium tumefaciens* A136 AHL bioreporter can not replace *E. coli* OHHLux since it is not as sensitive as the bioluminescent *E. coli* OHHLux for OHHL quantification.

To construct another OHHL bioreporter to use with P22luxI phage, *E. coli* OHHLux plasmid (63) was transferred into *K. oxytoca* VJSK009 and *K. pneumoniae* NCTC 418 strains. *Klebsiella* strains carrying the plasmid were tested for *S. choleraesuis* detection using P22luxI #3 and #7 phage and Wallac 1450 Microbeta Plus Liquid Scintillation Counter. They were also tested for infection by P22luxI phage. Costar 96-well black microtiter plates with black bottom (Corning Inc. Life Sciences, Lowell, MA) were used for the assay. Samples and controls, prepared in triplicate, and their amounts

are shown in Tables 6-12 through 6-14. The experiment was performed at 28°C. The mean of CPS values in triplicate for each sample was calculated.

Results are shown in Figures 7-8 and 7-9. Both *Klebsiella* bioreporters produced bioluminescence in the presence of P22luxI #3 or #7 without *S. choleraesuis* like *E. coli* OHHLux bioreporter. Levels of bioluminescence were not significantly different from those which were obtained with the presence of *S. choleraesuis*. Also, background levels from the negative controls, the bioreporter, the bioreporter-*S. choleraesuis* mixture, and the bioreporter-*S. choleraesuis*-P22 mixture were very high. Bioluminescence from these controls reached amounts as high as those from the bioreporter-*S. choleraesuis*-P22luxI and bioreporter-P22luxI combinations in some cases. There was no bioluminescence from negative controls, *S. choleraesuis*, P22luxI, and *S. choleraesuis*-P22luxI mixture. Since light was obtained from the *Klebsiella* bioreporters in the presence of P22luxI without its host, these results may be pointing to the possible infection of *Klebsiella* strains by P22luxI like *E. coli* OHHLux bioreporter. This will be discussed in more detail in discussion section (see chapter 8).

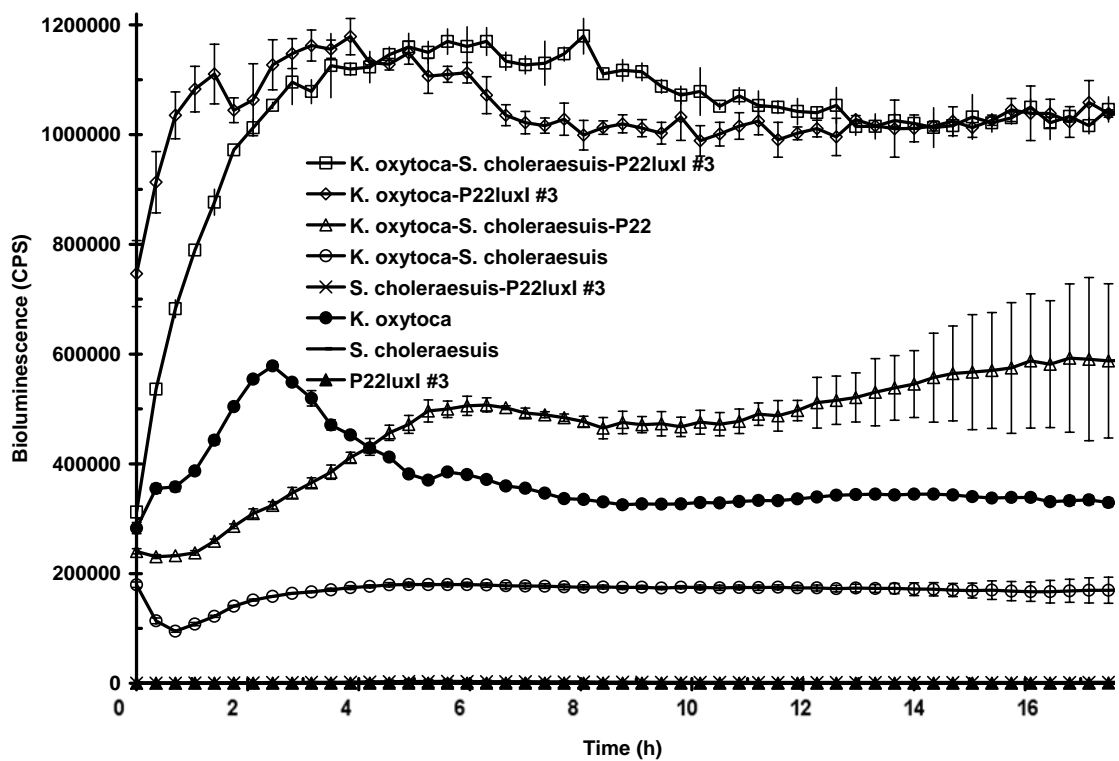


Figure 7-8 (A). Bioluminescent OHHL detection from P22luxI #3 using the host *S. choleraesuis* and the *K. oxytoca* bioreporter. Results represent the mean bioluminescence values ($n=3$) \pm SD (bars).

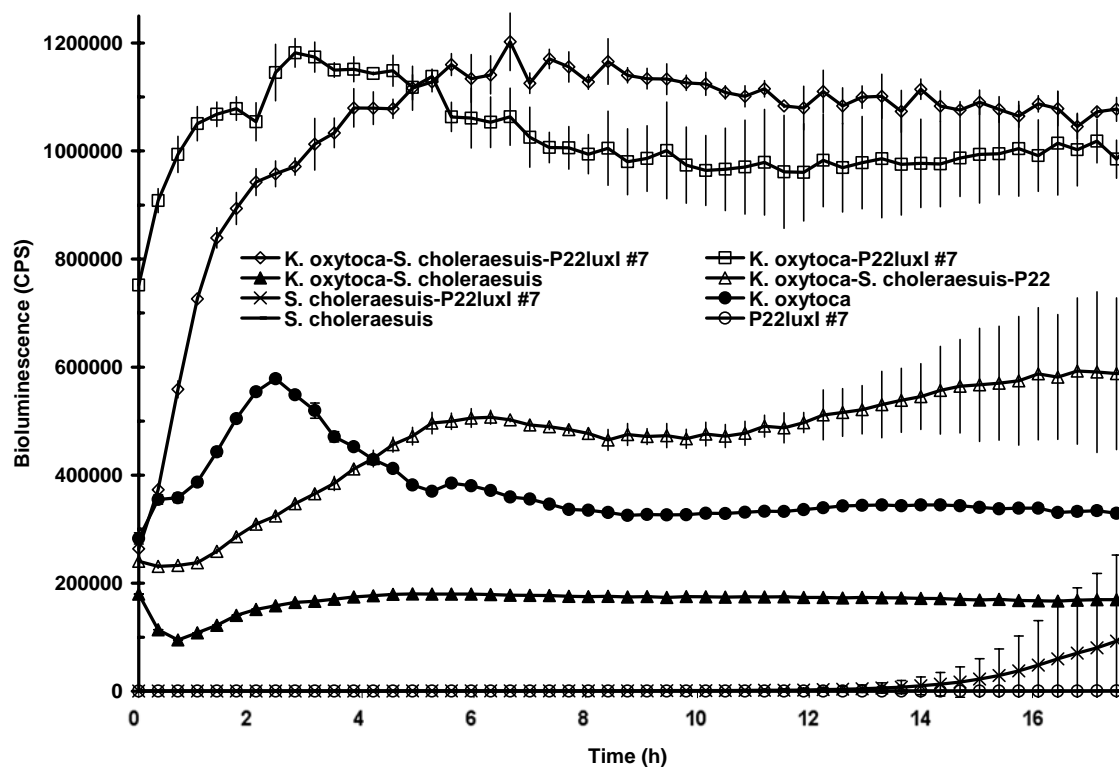


Figure 7-8 (B). Bioluminescent OHHL detection from P22luxI #7 using the host *S. choleraesuis* and the *K. oxytoca* bioreporter. Results represent the mean bioluminescence values ($n=3$) \pm SD (bars).

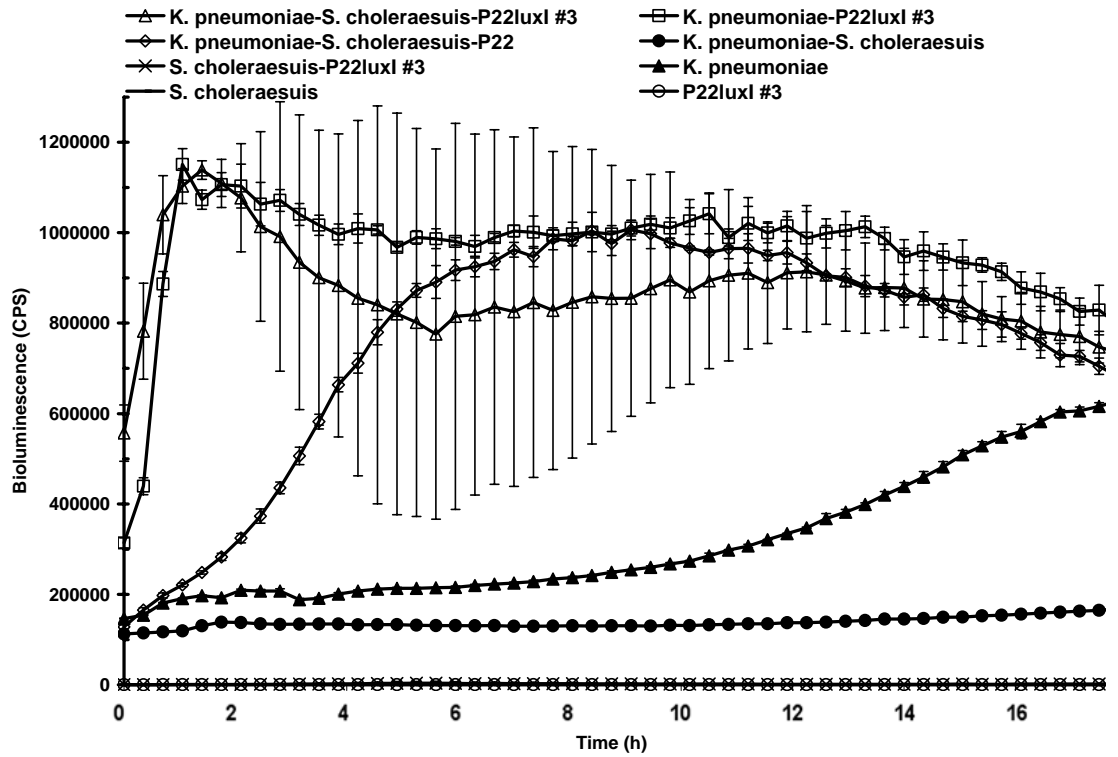


Figure 7-9 (A). Bioluminescent OHHL detection from P22luxI #3 using the host *S. choleraesuis* and the *K. pneumoniae* bioreporter. Results represent the mean bioluminescence values ($n=3$) \pm SD (bars).

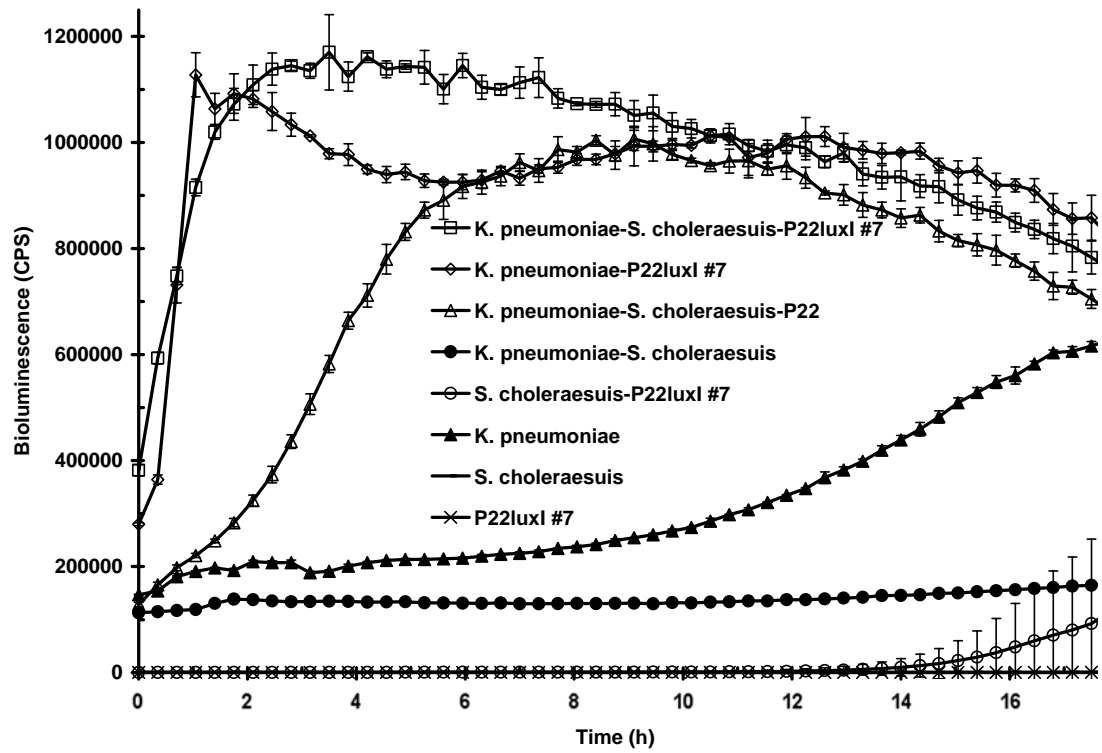


Figure 7-9 (B). Bioluminescent OHHL detection from P22luxI #7 using the host *S. choleraesuis* and the *K. pneumoniae* bioreporter. Results represent the mean bioluminescence values ($n=3 \pm \text{SD}$ (bars)).

Bioluminescent detection of OHHL from P22luxI genome and bioluminescent bioreporters using a Wallac 1450 Microbeta Plus Liquid Scintillation Counter

This test was carried out to determine if bioluminescence from the bioreporter and P22luxI mixtures is caused by the pick-up of the phage genome by the bioreporter cells instead of an infection. *Klebsiella oxytoca* VJSK009, *K. pneumoniae* NCTC 418, and *E. coli* OHHLux bioluminescent bioreporters were combined with the phage genome and then measured for bioluminescence. Samples and negative controls with their amounts are shown in Tables 6-15 and 6-16, respectively. The phage genome of 4.6 ng corresponds to 10^8 pfu and 46 ng corresponds to 10^9 pfu. The positive control was the phage-bioreporter mixture. Two more negative controls, the bioreporter alone and the bioreporter-P22 mixture were used in addition to those above. Costar 96-well black microtiter plates with black bottom (Corning Inc. Life Sciences, Lowell, MA) were employed for the assay performed at 28°C. Average CPS value for each sample in triplicate was calculated.

Results are presented in Figures 7-10 through 7-12. There was high amount of bioluminescence from the positive control and bioreporter-P22luxI, but no bioluminescence from negative controls, P22luxI alone and P22luxI genome alone, as expected. There was background bioluminescence from bioreporter-P22 samples. Their peak bioluminescence values were 4.5X, 4X, and 145X higher than those from the bioreporter samples for *K. pneumoniae*, *K. oxytoca*, and *E. coli* OHHLux, respectively. Bioluminescence from the bioreporter-phage genome was lower than the bioreporter-P22 bioluminescence for all bioreporter types. It was also not significantly different from that of the bioreporter sample for *Klebsiella* strains. The same result was obtained for *E. coli*

OHHLux in the case of the P22luxI #3 genome and the P22luxI #7 genome of 4.6 ng. However, bioluminescence from *E. coli* OHHLux-P22luxI #7 genome of 46 ng was 12X higher than that of *E. coli* OHHLux at its peak value. Nevertheless, values from this sample never exceeded values from the bioreporter-P22 sample. Furthermore, bioluminescence from *E. coli* OHHLux-P22luxI #7 phage was much higher with a maximum value which was 391X higher than the bioreporter value.

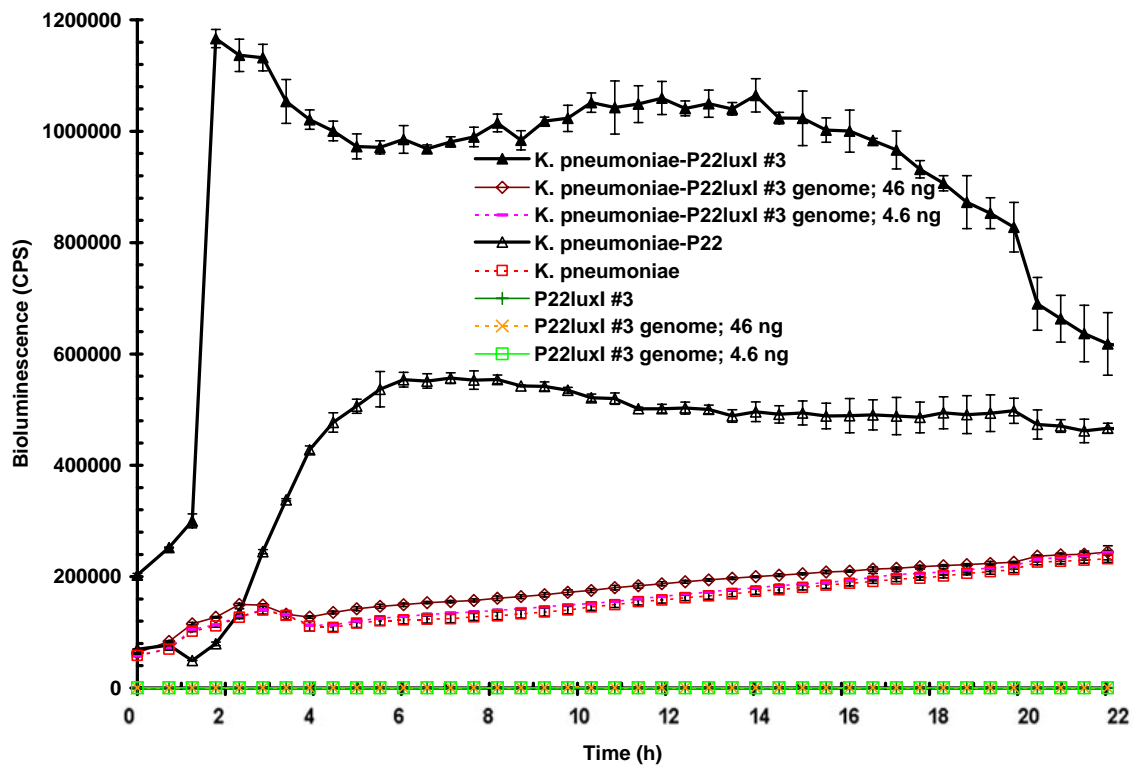


Figure 7-10 (A). Bioluminescent OHHL detection from P22luxI #3 genome using the *K. pneumoniae* bioreporter and Wallac 1450 Microbeta Plus Liquid Scintillation Counter. Results represent the mean bioluminescence values ($n=3$) \pm SD (bars).

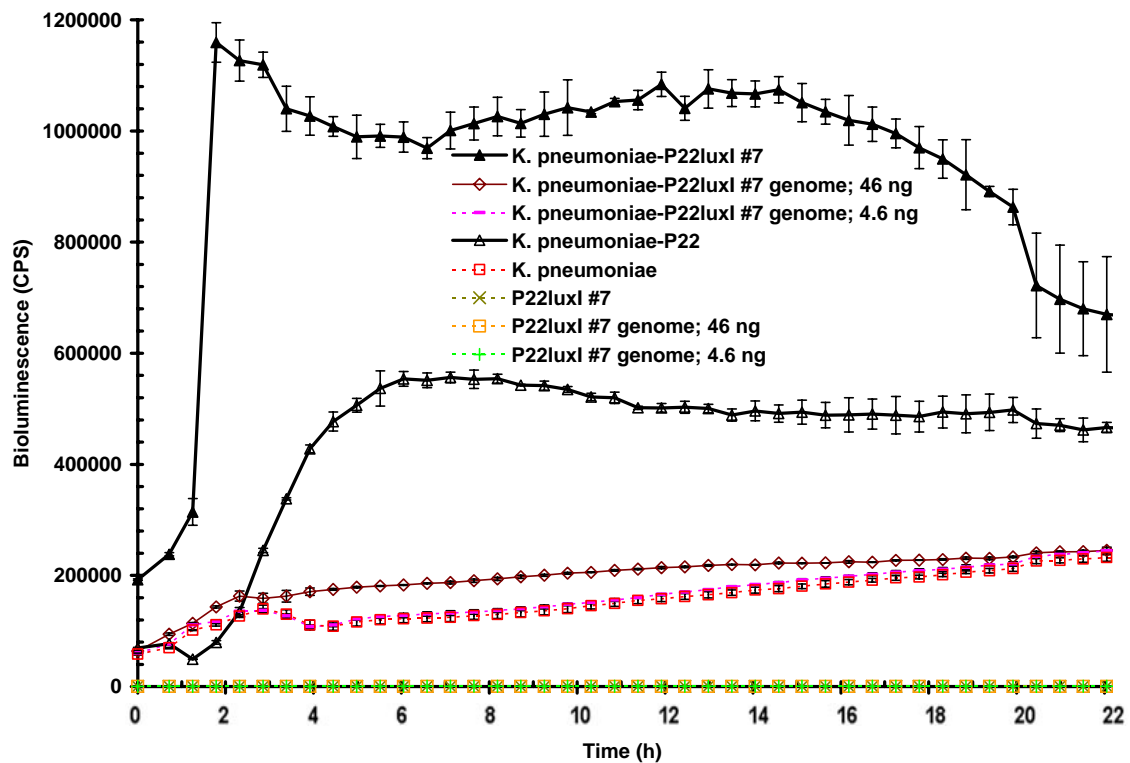


Figure 7-10 (B). Bioluminescent OHHL detection from P22luxI #7 genome using the *K. pneumoniae* bioreporter and Wallac 1450 Microbeta Plus Liquid Scintillation Counter. Results represent the mean bioluminescence values ($n=3$) \pm SD (bars).

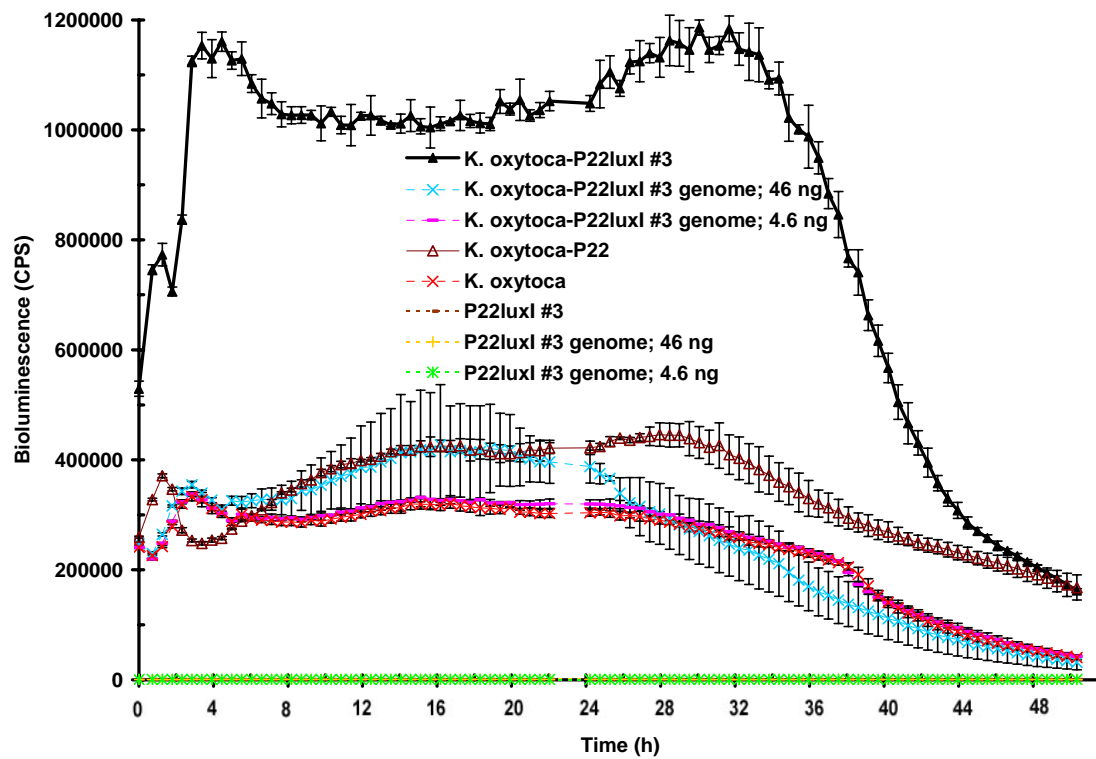


Figure 7-11 (A). Bioluminescent OHHL detection from P22luxI #3 genome using the *K. oxytoca* bioreporter and Wallac 1450 Microbeta Plus Liquid Scintillation Counter. Results represent the mean bioluminescence values ($n=3$) \pm SD (bars).

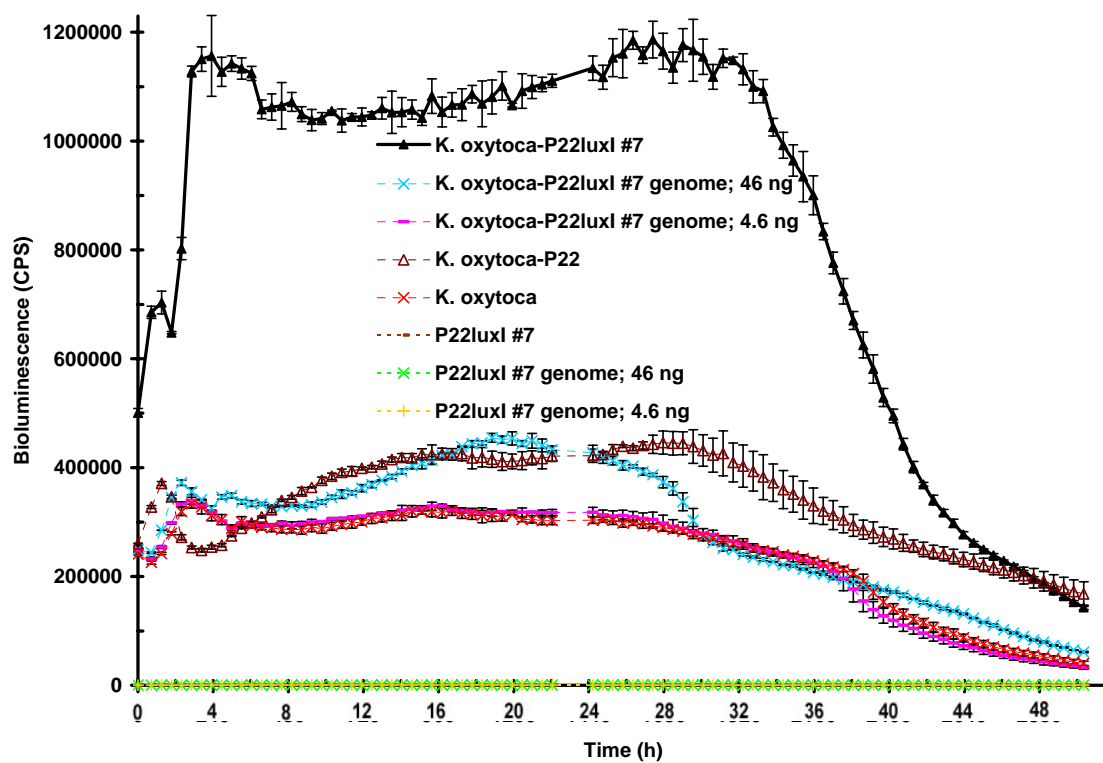


Figure 7-11 (B). Bioluminescent OHHL detection from P22luxI #7 genome using the *K. oxytoca* bioreporter and Wallac 1450 Microbeta Plus Liquid Scintillation Counter. Results represent the mean bioluminescence values ($n=3$) \pm SD (bars).

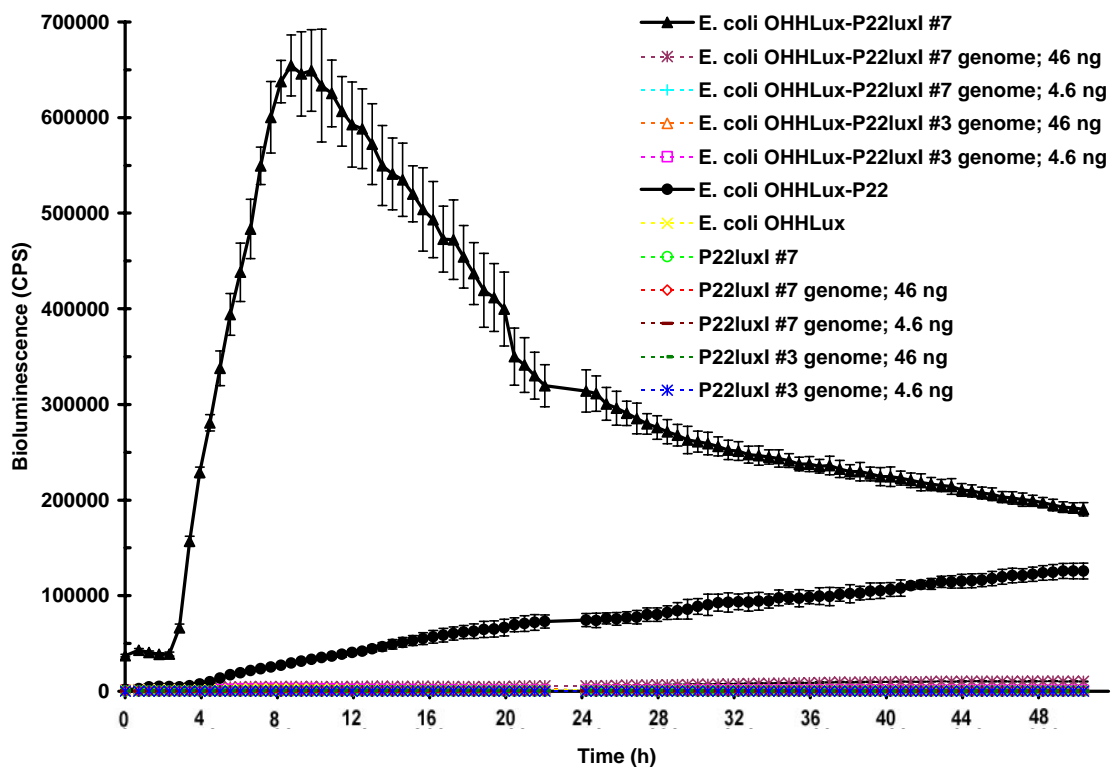


Figure 7-12. Bioluminescent OHHL detection from P22luxI genome using the *E. coli* OHHLux bioreporter and Wallac 1450 Microbeta Plus Liquid Scintillation Counter. Results represent the mean bioluminescence values ($n=3$) \pm SD (bars).

CHAPTER VIII

DISCUSSION AND CONCLUSIONS

CONSTRUCTION OF *SALMONELLA* BIOREPORTER

The *luxI* gene which was placed under the control of a *Salmonella* phage promoter and a Gram-negative RBS was cloned into *S. choleraesuis*. The promoter was phage P22 early left promoter, P_L, (655, 656) since *luxI* was planned to clone into phage P22. RBS sequence was selected after examination of various RBSs from *Salmonella* and phage P22 genes. Also, the rRNB ribosomal terminator T₁T₂ of pKK223-3 plasmid (Pharmacia, Uppsala, Sweden) was used as the transcription termination site. The plasmid, pCR-L #3 produced high levels of bioluminescence and fluorescence in *S. choleraesuis*. *luxI*, under the control of same promoter and RBS, was integrated into the P22 genome between ORF-201 and ORF-80 using homologous recombination (phage genome PubMed No: AF217253; 655).

Bioluminescence and fluorescence tests showed that the recombinant phage produced light only when propagated using *S. choleraesuis* harboring pCR-HAL #5, the homologous recombination plasmid. When recombinant phage were propagated with the wild type *S. choleraesuis* as the host, they lost the capability of light production. *luxI* was detected by PCR in the recombinant phage propagated using *S. choleraesuis* carrying pCR-HAL #5 but not in those propagated using the wild type strain. The recombinant phage, P22luxI, may be genetically unstable. Although *luxI* was placed in between genes, its insertion place is in an important region related with head formation and lysis (656).

luxI presence may be creating a disadvantage for the phage, which may lead to takeover by the wild type phage or loss of the *luxI* insert when *S. choleraesuis* is used as the host. The reason for retaining *luxI* by the phage when *S. choleraesuis* with pCR-HAL #5 is used as the propagation host may be the replication mechanism of P22. Homologous recombination is an essential mechanism for replication of the P22 genome in the host cell (656). The linear P22 genome is circularized early after infection by homologous recombination between terminal repeats at the two genome ends. The circularized genome is replicated via a rolling circle mechanism. Also, replicated P22 DNA molecules need to be circularized by homologous recombination to be inserted into the host chromosome for the lysogenic cycle (656). Homologous recombination can be performed by host *rec* gene products but P22 also has its own genes to perform recombination (656). Therefore, when the phage genome is inserted into a host cell containing *luxI* between the phage genome homology arms, high homologous recombination activity which takes place in the cell and the recombination machinery of the phage may result in an elevated level of *luxI* integration into the genome.

The bioluminescent bioreporter *E. coli* OHHLux and P22luxI phage produced light in the absence of *S. choleraesuis*. Tests performed with serial dilutions of the bioreporter mixed with a constant amount of P22luxI; and serial dilutions of P22luxI combined with a constant amount of the bioreporter showed P22luxI as the source of the problem. Previous tests did not detect plaque formation on bioreporter plates by P22luxI or the wild type P22, suggesting no lysis or lysogeny. Also, phage lysate stocks were determined to be contamination free. The possibility of the phage genome take-up by the bioreporter which may cause light production by bioreporter-P22luxI mixtures was

controlled. There was no light generated by the phage genome and the bioreporter combination.

Results above may be pointing to infection of the bioreporter by P22luxI although P22 is known to infect only *Salmonella* strains. The receptor site for P22 adsorption is a specific type of O antigen, a component of the outer membrane lipopolysaccharide. This O antigen type is found only in *Salmonella* serogroups A, B, and D1 (656, 666, 667). However, P22 is a “lambdoid” phage with the same genetic organization of the *E. coli* phage λ (656). P22 and λ contain homologous sequences and can recombine forming viable hybrids. This may suggest a possibility of *E. coli* bioreporter infection by P22luxI whose wild type is a close relative of an *E. coli* phage. Indeed, *E. coli* K-12 which was engineered to carry the *Salmonella* O-antigen-encoding *rfb* cluster was shown to be infected by P22 (667). This strain acted as a host for P22 infection and replication. Propagation of P22 on this strain resulted in phage concentrations which were close to those obtained using *Salmonella* as the host. *Escherichia coli* can be infected by P22 as long as it carries receptors for phage adsorption.

If the bioreporter *E. coli* OHHLux is infected by P22luxI, this is not a lytic or lysogenic infection since no lysis was obtained on bioreporter plates by P22luxI or P22. Also, if it was a lytic or lysogenic interaction, the high amount of light which was sustained for long periods of time would not be obtained from bioreporter-P22luxI mixtures. Since bioreporter cells would be lysed by the phage, light would not be generated. P22 is known to infect *Salmonella* by following one of three pathways: lytic, lysogenic, and pseudolysogenic (668). Pseudolysogeny is a state where the phage genome which does not integrate into the host chromosome replicates continuously

without lysing the host cell. It was suggested to be an environmental condition which occurs as a result of infection of starved bacterial cells (669, 670). The infecting phage does not enter a lytic or a lysogenic cycle since bacterial cells do not have enough resources to provide for the phage. The Wallace bioluminescence and fluorescence measurement conditions may leave bioreporter cells starved. Each well which was set up for these assays contained a very small volume of fresh LB (100 µl) which was used to suspend bioreporter cells and spent LB (100 µl) which came from the phage lysate. These are nutrient-poor conditions which may cause starvation of bioreporter cells. Starvation may be causing some changes in the *E. coli* cell membrane, which makes it susceptible to P22 infection. It was found that *E. coli* O157:H7 loses O antigenicity under starvation conditions (671). P22luxI may be infecting these starved susceptible bioreporter cells following a pseudolysogenic cycle under the particular conditions of light measurement assays.

To test pseudolysogeny, the bioreporter was infected with P22luxI and incubated until light production started. Then, bioreporter cells were collected from the culture. The genome and the plasmid of bioreporter cells were purified separately and checked for the presence of *luxI* to determine the presence of P22luxI genome. *luxI* was expected to be found in plasmid purifications since a pseudolysogenic phage genome acts like a plasmid. It was detected in both preparations but the amount of the *luxI* PCR product from the plasmid purification was much higher than that of the PCR product from the genome preparation. *luxI* presence in the genome may be caused by a contamination of the preparation by plasmids which were not eliminated completely during the purification. Another possibility is integration of a small part of phage genome molecules into the host

cell chromosome. Results from this experiment suggest a pseudolysogenic interaction between P22luxI and the bioreporter. However, it is also possible that the phage which adsorbed to the bioreporter cell surface could not be removed totally and *luxI* was amplified from the genomes of these phage.

Another result which may be supporting a pseudolysogenic interaction between P22luxI and the bioreporter during Wallac light measurement assays is the one obtained using the AHL bioreporter *A. tumefaciens* A136. The same combination which generated light during Wallac measurements did not produce OHHL during *A. tumefaciens* A136 experiments. Since these experiments were done on LB plates, conditions were not starving for the bioreporter. This supports a possible pseudolysogenic infection of the bioreporter by P22luxI which occurs only under nutrient-poor conditions.

The P22luxI-*S. choleraesuis* mixture was shown to produce OHHL which was detected by the AHL bioreporter, *A. tumefaciens* A136. Therefore, P22luxI can be used for *Salmonella* monitoring as long as the bioreporter itself does not produce light only in the presence of P22luxI. *Agrobacterium tumefaciens* A136 is not sensitive enough to be used to quantify the amount of OHHL produced, which makes it an unsuitable bioreporter for construction of a self-sustained, continuous, and real-time monitoring system. In an attempt to construct a new bioluminescent bioreporter to use with P22luxI, the plasmid of *E. coli* OHHLux bioreporter was transferred into *K. oxytoca* and *K. pneumoniae* strains. Since ColE1 which is the *ori* of the bioreporter plasmid works only in *E. coli*, *Salmonella*, and *Klebsiella* strains, *Klebsiella* strains were chosen to transfer the plasmid into. *Klebsiella* bioreporters produced bioluminescence in the presence of P22luxI without *S. choleraesuis* like *E. coli* OHHLux bioreporter. *Salmonella*, *E. coli*,

and *Klebsiella* all belong to *Enterobacteriaceae*. The outer membrane of *Enterobacteriaceae* is primarily composed of lipopolysaccharides (672) which contain the adsorption site, O-antigen, for P22 (656, 666, 667). P22luxI may be infecting all enterobacteria whose outer membrane composition may be affected by the starving conditions of the assays. A new bioluminescent bioreporter which does not produce light when mixed with P22luxI should be constructed to develop a *Salmonella* monitoring system using P22luxI. A bacterial strain other than enterobacteria such as *A. tumefaciens* which did not generate light in the presence of P22luxI needs to be employed for the construction of this bioreporter. This new bioreporter can be used for optimization and the sensitivity and specificity determination of the system. Tests which will be performed on artificially contaminated food should finalize the development of the *Salmonella* monitoring system.

LIST OF REFERENCES

LIST OF REFERENCES

1. Lukinmaa, S., et al., *Application of molecular genetic methods in diagnostics and epidemiology of food-borne bacterial pathogens*. Apmis, 2004. **112**(11-12): p. 908-29.
2. Theron, J. and T.E. Cloete, *Emerging waterborne infections: contributing factors, agents, and detection tools*. Crit Rev Microbiol, 2002. **28**(1): p. 1-26.
3. Savichtcheva, O. and S. Okabe, *Alternative indicators of fecal pollution: relations with pathogens and conventional indicators, current methodologies for direct pathogen monitoring and future application perspectives*. Water Res, 2006. **40**(13): p. 2463-76.
4. Gilbride, K.A., D.Y. Lee, and L.A. Beaudette, *Molecular techniques in wastewater: Understanding microbial communities, detecting pathogens, and real-time process control*. J Microbiol Methods, 2006. **66**(1): p. 1-20.
5. Simpson, J.M., J.W. Santo Domingo, and D.J. Reasoner, *Microbial source tracking: state of the science*. Environ Sci Technol, 2002. **36**(24): p. 5279-88.
6. Gracias, K.S. and J.L. McKillip, *A review of conventional detection and enumeration methods for pathogenic bacteria in food*. Can J Microbiol, 2004. **50**(11): p. 883-90.
7. Kuske, C.R., *Current and emerging technologies for the study of bacteria in the outdoor air*. Curr Opin Biotechnol, 2006. **17**(3): p. 291-6.
8. Fenollar, F. and D. Raoult, *Molecular genetic methods for the diagnosis of fastidious microorganisms*. Apmis, 2004. **112**(11-12): p. 785-807.
9. Mothershed, E.A. and A.M. Whitney, *Nucleic acid-based methods for the detection of bacterial pathogens: present and future considerations for the clinical laboratory*. Clin Chim Acta, 2006. **363**(1-2): p. 206-20.
10. Rompre, A., et al., *Detection and enumeration of coliforms in drinking water: current methods and emerging approaches*. J Microbiol Methods, 2002. **49**(1): p. 31-54.
11. Petrenko, V.A. and I.B. Sorokulova, *Detection of biological threats. A challenge for directed molecular evolution*. J Microbiol Methods, 2004. **58**(2): p. 147-68.
12. Churchill, R.L., H. Lee, and J.C. Hall, *Detection of Listeria monocytogenes and the toxin listeriolysin O in food*. J Microbiol Methods, 2006. **64**(2): p. 141-70.
13. Belkin, S., *Microbial whole-cell sensing systems of environmental pollutants*. Curr Opin Microbiol, 2003. **6**(3): p. 206-12.
14. D'Souza, S.F., *Microbial biosensors*. Biosens Bioelectron, 2001. **16**(6): p. 337-53.
15. Kohler, S., S. Belkin, and R.D. Schmid, *Reporter gene bioassays in environmental analysis*. Fresenius J Anal Chem, 2000. **366**(6-7): p. 769-79.
16. Roda, A., et al., *Biotechnological applications of bioluminescence and chemiluminescence*. Trends Biotechnol, 2004. **22**(6): p. 295-303.
17. Ren, S., *Assessing wastewater toxicity to activated sludge: recent research and developments*. Environ Int, 2004. **30**(8): p. 1151-64.

18. Leveau, J.H. and S.E. Lindow, *Bioreporters in microbial ecology*. Curr Opin Microbiol, 2002. **5**(3): p. 259-65.
19. Sayler, G.S., J.T. Fleming, and D.E. Nivens, *Gene expression monitoring in soils by mRNA analysis and gene lux fusions*. Curr Opin Biotechnol, 2001. **12**(5): p. 455-60.
20. Roda, A., et al., *Bio- and chemiluminescence in bioanalysis*. Fresenius J Anal Chem, 2000. **366**(6-7): p. 752-9.
21. Burlage, R.S. and C.T. Kuo, *Living biosensors for the management and manipulation of microbial consortia*. Annu Rev Microbiol, 1994. **48**: p. 291-309.
22. Jansson, J.K., *Marker and reporter genes: illuminating tools for environmental microbiologists*. Curr Opin Microbiol, 2003. **6**(3): p. 310-6.
23. Burlage, R.S., G.S. Sayler, and F. Larimer, *Monitoring of naphthalene catabolism by bioluminescence with nah-lux transcriptional fusions*. J Bacteriol, 1990. **172**(9): p. 4749-57.
24. Heitzer, A., et al., *Optical biosensor for environmental on-line monitoring of naphthalene and salicylate bioavailability with an immobilized bioluminescent catabolic reporter bacterium*. Appl Environ Microbiol, 1994. **60**(5): p. 1487-94.
25. Ripp, S., et al., *Bioluminescent most-probable-number monitoring of a genetically engineered bacterium during a long-term contained field release*. Appl Microbiol Biotechnol, 2000. **53**(6): p. 736-41.
26. King, J.M.H., et al., *Rapid, sensitive bioluminescent reporter technology for naphthalene exposure and biodegradation*. Science, 1990. **249**: p. 778-81.
27. Heitzer, A., et al., *Physiological considerations of environmental applications of lux reporter fusions*. J. Microbiol. Methods, 1998. **33**: p. 45-57.
28. Webb, O.F., et al., *Kinetics and response of a Pseudomonas fluorescence HK44 biosensor*. Biotechnol. Bioeng., 1997. **54**: p. 491-502.
29. Matrubutham, U., J.E. Thonnard, and G.S. Sayler, *Bioluminescence induction response and survival of the bioreporter bacterium Pseudomonas fluorescens HK44 in nutrient-deprived conditions*. Appl Microbiol Biotechnol, 1997. **47**: p. 604-9.
30. Layton, A.C., et al., *Construction of a bioluminescent reporter strain To detect polychlorinated biphenyls*. Appl Environ Microbiol, 1998. **64**(12): p. 5023-6.
31. Applegate, B.M., S.R. Kehrmeyer, and G.S. Sayler, *A chromosomally based tod-luxCDABE whole-cell reporter for benzene, toluene, ethylbenzene, and xylene (BTEX) sensing*. Appl Environ Microbiol, 1998. **64**(7): p. 2730-5.
32. Shingleton, J.T., et al., *Induction of the tod operon by trichloroethylene in Pseudomonas putida TVA8*. Appl Environ Microbiol, 1998. **64**(12): p. 5049-52.
33. Ripp, S., et al., *Controlled field release of a bioluminescent genetically engineered microorganism for bioremediation process monitoring and control*. Environ. Sci. Technol., 2000. **34**: p. 846-53.
34. Sayler, G.S., et al., *Field application of a genetically engineered microorganism for polycyclic aromatic hydrocarbon bioremediation process monitoring and control*, in *Novel Approaches for Bioremediation of Organic Pollution*, R. Fass, Y. Flashner, and S. Reuveny, Editors. 1999, Kluwer Academic/Plenum Press: New York. p. 241-54.

35. Hay, A.G., et al., *A bioluminescent whole-cell reporter for detection of 2, 4-dichlorophenoxyacetic acid and 2,4-dichlorophenol in soil*. Appl Environ Microbiol, 2000. **66**(10): p. 4589-94.
36. Abd-El-Haleem, D., et al., *A luxCDABE-based bioluminescent bioreporter for the detection of phenol*. J Ind Microbiol Biotechnol, 2002. **29**(5): p. 233-7.
37. Kelly, C.J., et al., *Bioluminescent reporter bacterium for toxicity monitoring in biological wastewater treatment systems*. Water Environ Res, 1999. **71**: p. 31-5.
38. Nivens, D.E., et al., *Bioluminescent bioreporter integrated circuits: potentially small, rugged and inexpensive whole-cell biosensors for remote environmental monitoring*. J Appl Microbiol, 2004. **96**(1): p. 33-46.
39. Santamaria, J. and G.A. Toranzos, *Enteric pathogens and soil: a short review*. Int Microbiol, 2003. **6**(1): p. 5-9.
40. Guan, T.Y. and R.A. Holley, *Pathogen survival in swine manure environments and transmission of human enteric illness--a review*. J Environ Qual, 2003. **32**(2): p. 383-92.
41. Mead, P.S., et al., *Food-related illness and death in the United States*. Emerg Infect Dis, 1999. **5**(5): p. 607-25.
42. Adak, G.K., S.M. Long, and S.J. O'Brien, *Trends in indigenous foodborne disease and deaths, England and Wales: 1992 to 2000*. Gut, 2002. **51**(6): p. 832-41.
43. Bures, S., et al., *Computer keyboards and faucet handles as reservoirs of nosocomial pathogens in the intensive care unit*. Am J Infect Control, 2000. **28**(6): p. 465-71.
44. Hurst, C.J., et al., *Manual of Environmental Microbiology, second ed.* 2002, Washington, D. C.: ASM Press.
45. Sharma, S., P. Sachdeva, and J.S. Virdi, *Emerging water-borne pathogens*. Appl Microbiol Biotechnol, 2003. **61**(5-6): p. 424-8.
46. Polo, F., et al., *Relationship between presence of Salmonella and indicators of faecal pollution in aquatic habitats*. FEMS Microbiol Lett, 1998. **160**(2): p. 253-6.
47. Sahlstrom, L., et al., *Bacterial pathogen incidences in sludge from Swedish sewage treatment plants*. Water Res, 2004. **38**(8): p. 1989-94.
48. Grant, S.B., et al., *Prevalence of enterohemorrhagic Escherichia coli in raw and treated municipal sewage*. Appl Environ Microbiol, 1996. **62**(9): p. 3466-9.
49. Gagliardi, J.V. and J.S. Karns, *Leaching of Escherichia coli O157:H7 in diverse soils under various agricultural management practices*. Appl Environ Microbiol, 2000. **66**(3): p. 877-83.
50. Brooks, J.P., et al., *A national study on the residential impact of biological aerosols from the land application of biosolids*. J Appl Microbiol, 2005. **99**(2): p. 310-22.
51. Tanner, B.D., et al., *Bioaerosol emission rate and plume characteristics during land application of liquid class B biosolids*. Environ Sci Technol, 2005. **39**(6): p. 1584-90.
52. Paez-Rubio, T., et al., *Source bioaerosol concentration and rRNA gene-based identification of microorganisms aerosolized at a flood irrigation wastewater reuse site*. Appl Environ Microbiol, 2005. **71**(2): p. 804-10.

53. Lewis, D.L., et al., *Interactions of pathogens and irritant chemicals in land-applied sewage sludges (biosolids)*. BMC Public Health, 2002. **2**: p. 11.
54. Edmiston, C.E., Jr., et al., *Airborne particulates in the OR environment*. Aorn J, 1999. **69**(6): p. 1169-72, 1175-7, 1179 passim.
55. Getchell-White, S.I., L.G. Donowitz, and D.H. Groschel, *The inanimate environment of an intensive care unit as a potential source of nosocomial bacteria: evidence for long survival of Acinetobacter calcoaceticus*. Infect Control Hosp Epidemiol, 1989. **10**(9): p. 402-7.
56. Smith, S.M., R.H. Eng, and F.T. Padberg, Jr., *Survival of nosocomial pathogenic bacteria at ambient temperature*. J Med, 1996. **27**(5-6): p. 293-302.
57. Neely, A.N. and M.P. Maley, *Survival of enterococci and staphylococci on hospital fabrics and plastic*. J Clin Microbiol, 2000. **38**(2): p. 724-6.
58. LaRocco, M.T. and D.L. Pierson, *Deep space exploration: will we be ready?* ASM News, 1999. **65**(12): p. 817-21.
59. Pierson, D.L., et al., *Epidemiology of Staphylococcus aureus during space flight*. FEMS Immunol Med Microbiol, 1996. **16**(3-4): p. 273-81.
60. Taylor, G.R., *Recovery of medically important microorganisms from Apollo astronauts*. Aerosp Med, 1974. **45**(8): p. 824-8.
61. Sonnenfeld, G., *Extreme environments and the immune system: effects of spaceflight on immune responses*. J Allergy Clin Immunol, 2001. **107**(1): p. 19-20.
62. Gu, J.D., et al., *The role of microbial biofilms in deterioration of space station candidate materials*. Int Biodeterior Biodegradation, 1998. **41**(1): p. 25-33.
63. Ripp, S., et al., *Linking bacteriophage infection to quorum sensing signalling and bioluminescent bioreporter monitoring for direct detection of bacterial agents*. J Appl Microbiol, 2006. **100**(3): p. 488-99.
64. Fuqua, W.C., S.C. Winans, and E.P. Greenberg, *Quorum sensing in bacteria: the LuxR-LuxI family of cell density-responsive transcriptional regulators*. J Bacteriol, 1994. **176**(2): p. 269-75.
65. Nealson, K.H. and J.W. Hastings, *Bacterial bioluminescence: its control and ecological significance*. Microbiol Rev, 1979. **43**(4): p. 496-518.
66. Nealson, K.H., T. Platt, and J.W. Hastings, *Cellular control of the synthesis and activity of the bacterial luminescent system*. J Bacteriol, 1970. **104**(1): p. 313-22.
67. Eberhard, A., *Inhibition and activation of bacterial luciferase synthesis*. J Bacteriol, 1972. **109**(3): p. 1101-5.
68. Miller, M.B. and B.L. Bassler, *Quorum sensing in bacteria*. Annu Rev Microbiol, 2001. **55**: p. 165-99.
69. Camara, M., P. Williams, and A. Hardman, *Controlling infection by tuning in and turning down the volume of bacterial small-talk*. Lancet Infect Dis, 2002. **2**(11): p. 667-76.
70. Daniels, R., J. Vanderleyden, and J. Michiels, *Quorum sensing and swarming migration in bacteria*. FEMS Microbiol Rev, 2004. **28**(3): p. 261-89.
71. Reading, N.C. and V. Sperandio, *Quorum sensing: the many languages of bacteria*. FEMS Microbiol Lett, 2006. **254**(1): p. 1-11.

72. Parsek, M.R. and E.P. Greenberg, *Sociomicrobiology: the connections between quorum sensing and biofilms*. Trends Microbiol, 2005. **13**(1): p. 27-33.
73. Henke, J.M. and B.L. Bassler, *Bacterial social engagements*. Trends Cell Biol, 2004. **14**(11): p. 648-56.
74. Federle, M.J. and B.L. Bassler, *Interspecies communication in bacteria*. J Clin Invest, 2003. **112**(9): p. 1291-9.
75. Taga, M.E. and B.L. Bassler, *Chemical communication among bacteria*. Proc Natl Acad Sci U S A, 2003. **100 Suppl 2**: p. 14549-54.
76. Shiner, E.K., K.P. Rumbaugh, and S.C. Williams, *Inter-kingdom signaling: deciphering the language of acyl homoserine lactones*. FEMS Microbiol Rev, 2005. **29**(5): p. 935-47.
77. Raffa, R.B., et al., *Bacterial communication ("quorum sensing") via ligands and receptors: a novel pharmacologic target for the design of antibiotic drugs*. J Pharmacol Exp Ther, 2005. **312**(2): p. 417-23.
78. Ruby, E.G., *The Euprymna scolopes-Vibrio fischeri symbiosis: a biomedical model for the study of bacterial colonization of animal tissue*. J Mol Microbiol Biotechnol, 1999. **1**(1): p. 13-21.
79. Visick, K.L. and M.J. McFall-Ngai, *An exclusive contract: specificity in the Vibrio fischeri-Euprymna scolopes partnership*. J Bacteriol, 2000. **182**(7): p. 1779-87.
80. Nyholm, S.V. and M.J. McFall-Ngai, *The winnowing: establishing the squid-vibrio symbiosis*. Nat Rev Microbiol, 2004. **2**(8): p. 632-42.
81. Nyholm, S.V. and M.J. McFall-Ngai, *Sampling the light-organ microenvironment of Euprymna scolopes: description of a population of host cells in association with the bacterial symbiont Vibrio fischeri*. Biol Bull, 1998. **195**(2): p. 89-97.
82. Graf, J. and E.G. Ruby, *Host-derived amino acids support the proliferation of symbiotic bacteria*. Proc Natl Acad Sci U S A, 1998. **95**(4): p. 1818-22.
83. McFall-Ngai, M.J. and E.G. Ruby, *Symbiont recognition and subsequent morphogenesis as early events in an animal-bacterial mutualism*. Science, 1991. **254**(5037): p. 1491-4.
84. Ruby, E.G., *Lessons from a cooperative, bacterial-animal association: the Vibrio fischeri-Euprymna scolopes light organ symbiosis*. Annu Rev Microbiol, 1996. **50**: p. 591-624.
85. Ruby, E.G. and M.J. McFall-Ngai, *A squid that glows in the night: development of an animal-bacterial mutualism*. J Bacteriol, 1992. **174**(15): p. 4865-70.
86. Engebrecht, J. and M. Silverman, *Identification of genes and gene products necessary for bacterial bioluminescence*. Proc Natl Acad Sci U S A, 1984. **81**(13): p. 4154-8.
87. Engebrecht, J., K. Nealson, and M. Silverman, *Bacterial bioluminescence: isolation and genetic analysis of functions from Vibrio fischeri*. Cell, 1983. **32**(3): p. 773-81.
88. Visick, K.L., et al., *Vibrio fischeri lux genes play an important role in colonization and development of the host light organ*. J Bacteriol, 2000. **182**(16): p. 4578-86.

89. Boettcher, K.J. and E.G. Ruby, *Detection and quantification of Vibrio fischeri autoinducer from symbiotic squid light organs*. J Bacteriol, 1995. **177**(4): p. 1053-8.
90. Lee, K.H. and E.G. Ruby, *Effect of the Squid Host on the Abundance and Distribution of Symbiotic Vibrio fischeri in Nature*. Appl Environ Microbiol, 1994. **60**(5): p. 1565-1571.
91. Meighen, E.A., *Molecular biology of bacterial bioluminescence*. Microbiol Rev, 1991. **55**(1): p. 123-42.
92. Meighen, E.A., *Bacterial bioluminescence: organization, regulation, and application of the lux genes*. Faseb J, 1993. **7**(11): p. 1016-22.
93. Lee, J., et al., *The mechanism of bacterial bioluminescence*, in *Chemistry and biochemistry of flavoenzymes*, F. Müller, Editor. 1991, CRC Press: Boca Raton. p. 109-151.
94. Baldwin, T.O. and M.M. Ziegler, *The biochemistry and molecular biology of bacterial bioluminescence*, in *Chemistry and biochemistry of flavoenzymes*, F. Müller, Editor. 1992, CRC Press: Boca Raton. p. 467-530.
95. Meighen, E.A., *Genetics of bacterial bioluminescence*. Annu Rev Genet, 1994. **28**: p. 117-39.
96. Tu, S.C. and H.I. Mager, *Biochemistry of bacterial bioluminescence*. Photochem Photobiol, 1995. **62**(4): p. 615-24.
97. Dunn, D.K., et al., *Conversion of aldehyde to acid in the bacterial bioluminescent reaction*. Biochemistry, 1973. **12**(24): p. 4911-8.
98. Hastings, J.W. and K.H. Nealson, *Bacterial bioluminescence*. Annu Rev Microbiol, 1977. **31**: p. 549-95.
99. Hastings, J.W., *Bacterial bioluminescence: an overview*. Methods in Enzymology, 1978. **57**: p. 125-135.
100. Boylan, M., A.F. Graham, and E.A. Meighen, *Functional identification of the fatty acid reductase components encoded in the luminescence operon of Vibrio fischeri*. J Bacteriol, 1985. **163**(3): p. 1186-90.
101. Boylan, M., et al., *Lux C, D and E genes of the Vibrio fischeri luminescence operon code for the reductase, transferase, and synthetase enzymes involved in aldehyde biosynthesis*. Photochem Photobiol, 1989. **49**(5): p. 681-8.
102. Zenno, S. and K. Saigo, *Identification of the genes encoding NAD(P)H-flavin oxidoreductases that are similar in sequence to Escherichia coli Fre in four species of luminous bacteria: Photorhabdus luminescens, Vibrio fischeri, Vibrio harveyi, and Vibrio orientalis*. J Bacteriol, 1994. **176**(12): p. 3544-51.
103. Engebrecht, J. and M. Silverman, *Nucleotide sequence of the regulatory locus controlling expression of bacterial genes for bioluminescence*. Nucleic Acids Res, 1987. **15**(24): p. 10455-67.
104. Swartzman, A., et al., *A new Vibrio fischeri lux gene precedes a bidirectional termination site for the lux operon*. J Bacteriol, 1990. **172**(12): p. 6797-802.
105. Ulitzur, S. and P.V. Dunlap, *Regulatory circuitry controlling luminescence autoinduction in Vibrio fischeri*. Photochemistry and Photobiology, 1995. **62**(4): p. 625-632.

106. Eberhard, A., et al., *Structural identification of autoinducer of Photobacterium fischeri luciferase*. Biochemistry, 1981. **20**(9): p. 2444-9.
107. Schaefer, A.L., et al., *Generation of cell-to-cell signals in quorum sensing: acyl homoserine lactone synthase activity of a purified Vibrio fischeri LuxI protein*. Proc Natl Acad Sci U S A, 1996. **93**(18): p. 9505-9.
108. Nealson, K.H., *Autoinduction of bacterial luciferase. Occurrence, mechanism and significance*. Arch Microbiol, 1977. **112**(1): p. 73-9.
109. Kaplan, H.B. and E.P. Greenberg, *Diffusion of autoinducer is involved in regulation of the Vibrio fischeri luminescence system*. J Bacteriol, 1985. **163**(3): p. 1210-4.
110. Eglund, K.A. and E.P. Greenberg, *Quorum sensing in Vibrio fischeri: analysis of the LuxR DNA binding region by alanine-scanning mutagenesis*. J Bacteriol, 2001. **183**(1): p. 382-6.
111. Trott, A.E. and A.M. Stevens, *Amino acid residues in LuxR critical for its mechanism of transcriptional activation during quorum sensing in Vibrio fischeri*. J Bacteriol, 2001. **183**(1): p. 387-92.
112. Choi, S.H. and E.P. Greenberg, *The C-terminal region of the Vibrio fischeri LuxR protein contains an inducer-independent lux gene activating domain*. Proc Natl Acad Sci U S A, 1991. **88**(24): p. 11115-9.
113. Choi, S.H. and E.P. Greenberg, *Genetic evidence for multimerization of LuxR, the transcriptional activator of Vibrio fischeri luminescence*. Mol. Mar. Biol. Biotechnol., 1992. **1**: p. 408-413.
114. Choi, S.H. and E.P. Greenberg, *Genetic dissection of DNA binding and luminescence gene activation by the Vibrio fischeri LuxR protein*. J Bacteriol, 1992. **174**(12): p. 4064-9.
115. Fuqua, C., S.C. Winans, and E.P. Greenberg, *Census and consensus in bacterial ecosystems: the LuxR-LuxI family of quorum-sensing transcriptional regulators*. Annu Rev Microbiol, 1996. **50**: p. 727-51.
116. Shadel, G.S., R. Young, and T.O. Baldwin, *Use of regulated cell lysis in a lethal genetic selection in Escherichia coli: identification of the autoinducer-binding region of the LuxR protein from Vibrio fischeri ATCC 7744*. J Bacteriol, 1990. **172**(7): p. 3980-7.
117. Slock, J., et al., *Critical regions of the Vibrio fischeri luxR protein defined by mutational analysis*. J Bacteriol, 1990. **172**(7): p. 3974-9.
118. Hanzelka, B.L. and E.P. Greenberg, *Evidence that the N-terminal region of the Vibrio fischeri LuxR protein constitutes an autoinducer-binding domain*. J Bacteriol, 1995. **177**(3): p. 815-7.
119. Stevens, A.M., K.M. Dolan, and E.P. Greenberg, *Synergistic binding of the Vibrio fischeri LuxR transcriptional activator domain and RNA polymerase to the lux promoter region*. Proc Natl Acad Sci U S A, 1994. **91**(26): p. 12619-23.
120. Devine, J.H., C. Countryman, and T.O. Baldwin, *Nucleotide sequence of the luxR and luxI genes and structure of the primary regulatory region of the lux regulon of Vibrio fischeri ATCC 7744*. Biochemistry, 1988. **27**: p. 837-42.

121. Devine, J.H., G.S. Shadel, and T.O. Baldwin, *Identification of the operator of the lux regulon from the Vibrio fischeri strain ATCC7744*. Proc Natl Acad Sci U S A, 1989. **86**(15): p. 5688-92.
122. Eglund, K.A. and E.P. Greenberg, *Quorum sensing in Vibrio fischeri: elements of the luxI promoter*. Mol Microbiol, 1999. **31**(4): p. 1197-204.
123. Shadel, G.S. and T.O. Baldwin, *Identification of a distantly located regulatory element in the luxD gene required for negative autoregulation of the Vibrio fischeri luxR gene*. J Biol Chem, 1992. **267**(11): p. 7690-5.
124. Eberhard, A., et al., *Synthesis of the lux gene autoinducer in Vibrio fischeri is positively autoregulated*. Arch. Microbiol., 1991. **155**: p. 294-97.
125. Shadel, G.S. and T.O. Baldwin, *The Vibrio fischeri LuxR protein is capable of bidirectional stimulation of transcription and both positive and negative regulation of the luxR gene*. J Bacteriol, 1991. **173**(2): p. 568-74.
126. Shadel, G.S. and T.O. Baldwin, *Positive autoregulation of the Vibrio fischeri luxR gene. LuxR and autoinducer activate cAMP-catabolite gene activator protein complex-independent and -dependent luxR transcription*. J Biol Chem, 1992. **267**(11): p. 7696-702.
127. Dunlap, P.V. and J.M. Ray, *Requirement for autoinducer in transcriptional negative autoregulation of the Vibrio fischeri luxR gene in Escherichia coli*. J Bacteriol, 1989. **171**(6): p. 3549-52.
128. Eglund, K.A. and E.P. Greenberg, *Conversion of the Vibrio fischeri transcriptional activator, LuxR, to a repressor*. J Bacteriol, 2000. **182**(3): p. 805-11.
129. Kuo, A., N.V. Blough, and P.V. Dunlap, *Multiple N-acyl-L-homoserine lactone autoinducers of luminescence in the marine symbiotic bacterium Vibrio fischeri*. J Bacteriol, 1994. **176**(24): p. 7558-65.
130. Gilson, L., A. Kuo, and P.V. Dunlap, *AinS and a new family of autoinducer synthesis proteins*. J Bacteriol, 1995. **177**(23): p. 6946-51.
131. Kuo, A., S.M. Callahan, and P.V. Dunlap, *Modulation of luminescence operon expression by N-octanoyl-L-homoserine lactone in ainS mutants of Vibrio fischeri*. J Bacteriol, 1996. **178**(4): p. 971-6.
132. Callahan, S.M. and P.V. Dunlap, *LuxR- and acyl-homoserine-lactone-controlled non-lux genes define a quorum-sensing regulon in Vibrio fischeri*. J Bacteriol, 2000. **182**(10): p. 2811-22.
133. Hanzelka, B.L., et al., *Acylhomoserine lactone synthase activity of the Vibrio fischeri AinS protein*. J Bacteriol, 1999. **181**(18): p. 5766-70.
134. Lupp, C. and E.G. Ruby, *Vibrio fischeri LuxS and AinS: comparative study of two signal synthases*. J Bacteriol, 2004. **186**(12): p. 3873-81.
135. Ruby, E.G., et al., *Complete genome sequence of Vibrio fischeri: a symbiotic bacterium with pathogenic congeners*. Proc Natl Acad Sci U S A, 2005. **102**(8): p. 3004-9.
136. Fidopiastis, P.M., et al., *LitR, a new transcriptional activator in Vibrio fischeri, regulates luminescence and symbiotic light organ colonization*. Mol Microbiol, 2002. **45**(1): p. 131-43.

137. Miyamoto, C.M., et al., *LuxO controls luxR expression in Vibrio harveyi: evidence for a common regulatory mechanism in Vibrio*. Mol Microbiol, 2003. **48**(2): p. 537-48.
138. Lupp, C., et al., *The Vibrio fischeri quorum-sensing systems ain and lux sequentially induce luminescence gene expression and are important for persistence in the squid host*. Mol Microbiol, 2003. **50**(1): p. 319-31.
139. Lupp, C. and E.G. Ruby, *Vibrio fischeri uses two quorum-sensing systems for the regulation of early and late colonization factors*. J Bacteriol, 2005. **187**(11): p. 3620-9.
140. Miyamoto, C.M., Y.H. Lin, and E.A. Meighen, *Control of bioluminescence in Vibrio fischeri by the LuxO signal response regulator*. Mol Microbiol, 2000. **36**(3): p. 594-607.
141. Eberhard, A., et al., *Analogues of the autoinducer of bioluminescence in Vibrio fischeri*. Arch Microbiol, 1986. **146**(1): p. 35-40.
142. McClean, K.H., et al., *Quorum sensing and Chromobacterium violaceum: exploitation of violacein production and inhibition for the detection of N-acylhomoserine lactones*. Microbiology, 1997. **143** (Pt 12): p. 3703-11.
143. Shaw, P.D., et al., *Detecting and characterizing N-acyl-homoserine lactone signal molecules by thin-layer chromatography*. Proc Natl Acad Sci U S A, 1997. **94**(12): p. 6036-41.
144. Winson, M.K., et al., *Construction and analysis of luxCDABE-based plasmid sensors for investigating N-acyl homoserine lactone-mediated quorum sensing*. FEMS Microbiol Lett, 1998. **163**(2): p. 185-92.
145. Swift, S., et al., *A novel strategy for the isolation of luxI homologues: evidence for the widespread distribution of a LuxR:LuxI superfamily in enteric bacteria*. Mol Microbiol, 1993. **10**(3): p. 511-20.
146. Blosser, R.S. and K.M. Gray, *Extraction of violacein from Chromobacterium violaceum provides a new quantitative bioassay for N-acyl homoserine lactone autoinducers*. J Microbiol Methods, 2000. **40**(1): p. 47-55.
147. Charlton, T.S., et al., *A novel and sensitive method for the quantification of N-3-oxoacyl homoserine lactones using gas chromatography-mass spectrometry: application to a model bacterial biofilm*. Environ Microbiol, 2000. **2**(5): p. 530-41.
148. Andersen, J.B., et al., *gfp-based N-acyl homoserine-lactone sensor systems for detection of bacterial communication*. Appl Environ Microbiol, 2001. **67**(2): p. 575-85.
149. Fuqua, C. and A. Eberhard, *Signal generation in autoinduction systems: synthesis of acylated homoserine lactones by LuxI-type proteins*, in *Cell-Cell Signalling in Bacteria*, S.C. Winans, Editor. 1999, ASM Press: Washington, DC. p. 211-30.
150. Winson, M.K., et al., *Multiple N-acyl-L-homoserine lactone signal molecules regulate production of virulence determinants and secondary metabolites in Pseudomonas aeruginosa*. Proc Natl Acad Sci U S A, 1995. **92**(20): p. 9427-31.
151. Schaefer, A.L., et al., *Long-chain acyl-homoserine lactone quorum-sensing regulation of Rhodobacter capsulatus gene transfer agent production*. J Bacteriol, 2002. **184**(23): p. 6515-21.

152. Marketon, M.M., et al., *Characterization of the Sinorhizobium meliloti sinR/sinI locus and the production of novel N-acyl homoserine lactones*. J Bacteriol, 2002. **184**(20): p. 5686-95.
153. Gray, K.M., et al., *Cell-to-cell signaling in the symbiotic nitrogen-fixing bacterium Rhizobium leguminosarum: autoinduction of a stationary phase and rhizosphere-expressed genes*. J Bacteriol, 1996. **178**(2): p. 372-6.
154. Schripsema, J., et al., *Bacteriocin small of Rhizobium leguminosarum belongs to the class of N-acyl-L-homoserine lactone molecules, known as autoinducers and as quorum sensing co-transcription factors*. J Bacteriol, 1996. **178**(2): p. 366-71.
155. Puskas, A., et al., *A quorum-sensing system in the free-living photosynthetic bacterium Rhodobacter sphaeroides*. J Bacteriol, 1997. **179**(23): p. 7530-7.
156. Swift, S., P. Williams, and G.S.A.B. Stewart, *N-acylhomoserine lactones and quorum sensing in the proteobacteria*, in *Cell-Cell Signalling in Bacteria*, G.M. Dunny and S.C. Winans, Editors. 1999, ASM Press: Washington, DC. p. 291-313.
157. Swift, S., et al., *Quorum sensing in Aeromonas hydrophila and Aeromonas salmonicida: identification of the LuxRI homologs AhyRI and AsaRI and their cognate N-acylhomoserine lactone signal molecules*. J Bacteriol, 1997. **179**(17): p. 5271-81.
158. Swift, S., et al., *Quorum sensing-dependent regulation and blockade of exoprotease production in Aeromonas hydrophila*. Infect Immun, 1999. **67**(10): p. 5192-9.
159. More, M.I., et al., *Enzymatic synthesis of a quorum-sensing autoinducer through use of defined substrates*. Science, 1996. **272**(5268): p. 1655-8.
160. Piper, K.R., S. Beck von Bodman, and S.K. Farrand, *Conjugation factor of Agrobacterium tumefaciens regulates Ti plasmid transfer by autoinduction*. Nature, 1993. **362**(6419): p. 448-50.
161. Zhang, L., et al., *Agrobacterium conjugation and gene regulation by N-acyl-L-homoserine lactones*. Nature, 1993. **362**(6419): p. 446-8.
162. Fuqua, C., M. Burbea, and S.C. Winans, *Activity of the Agrobacterium Ti plasmid conjugal transfer regulator TraR is inhibited by the product of the traM gene*. J Bacteriol, 1995. **177**(5): p. 1367-73.
163. Fuqua, W.C. and S.C. Winans, *A LuxR-LuxI type regulatory system activates Agrobacterium Ti plasmid conjugal transfer in the presence of a plant tumor metabolite*. J Bacteriol, 1994. **176**(10): p. 2796-806.
164. Hwang, I., D.M. Cook, and S.K. Farrand, *A new regulatory element modulates homoserine lactone-mediated autoinduction of Ti plasmid conjugal transfer*. J Bacteriol, 1995. **177**(2): p. 449-58.
165. Hwang, I., et al., *TraI, a LuxI homologue, is responsible for production of conjugation factor, the Ti plasmid N-acylhomoserine lactone autoinducer*. Proc Natl Acad Sci U S A, 1994. **91**(11): p. 4639-43.
166. Lewenza, S., et al., *Quorum sensing in Burkholderia cepacia: identification of the LuxRI homologs CepRI*. J Bacteriol, 1999. **181**(3): p. 748-56.
167. Chernin, L.S., et al., *Chitinolytic activity in Chromobacterium violaceum: substrate analysis and regulation by quorum sensing*. J Bacteriol, 1998. **180**(17): p. 4435-41.

168. Bainton, N.J., et al., *A general role for the lux autoinducer in bacterial cell signalling: control of antibiotic biosynthesis in Erwinia*. Gene, 1992. **116**(1): p. 87-91.
169. Jones, S., et al., *The lux autoinducer regulates the production of exoenzyme virulence determinants in Erwinia carotovora and Pseudomonas aeruginosa*. Embo J, 1993. **12**(6): p. 2477-82.
170. Pirhonen, M., et al., *A small diffusible signal molecule is responsible for the global control of virulence and exoenzyme production in the plant pathogen Erwinia carotovora*. Embo J, 1993. **12**(6): p. 2467-76.
171. Bainton, N.J., et al., *N-(3-oxohexanoyl)-L-homoserine lactone regulates carbapenem antibiotic production in Erwinia carotovora*. Biochem J, 1992. **288** (Pt 3): p. 997-1004.
172. Chatterjee, A., et al., *Inactivation of rsmA leads to overproduction of extracellular pectinases, cellulases, and proteases in Erwinia carotovora subsp. carotovora in the absence of the starvation/cell density-sensing signal, N-(3-oxohexanoyl)-L-homoserine lactone*. Appl Environ Microbiol, 1995. **61**(5): p. 1959-67.
173. Cui, Y., et al., *Identification of a global repressor gene, rsmA, of Erwinia carotovora subsp. carotovora that controls extracellular enzymes, N-(3-oxohexanoyl)-L-homoserine lactone, and pathogenicity in soft-rotting Erwinia spp.* J Bacteriol, 1995. **177**(17): p. 5108-15.
174. McGowan, S., et al., *Carbapenem antibiotic production in Erwinia carotovora is regulated by CarR, a homologue of the LuxR transcriptional activator*. Microbiology, 1995. **141** (Pt 3): p. 541-50.
175. Nasser, W., et al., *Characterization of the Erwinia chrysanthemi expI-expR locus directing the synthesis of two N-acyl-homoserine lactone signal molecules*. Mol Microbiol, 1998. **29**(6): p. 1391-405.
176. Reverchon, S., et al., *Integration of the quorum-sensing system in the regulatory networks controlling virulence factor synthesis in Erwinia chrysanthemi*. Mol Microbiol, 1998. **29**(6): p. 1407-18.
177. Beck von Bodman, S. and S.K. Farrand, *Capsular polysaccharide biosynthesis and pathogenicity in Erwinia stewartii require induction by an N-acylhomoserine lactone autoinducer*. J Bacteriol, 1995. **177**(17): p. 5000-8.
178. Garcia-Lara, J., L.H. Shang, and L.I. Rothfield, *An extracellular factor regulates expression of sdiA, a transcriptional activator of cell division genes in Escherichia coli*. J Bacteriol, 1996. **178**(10): p. 2742-8.
179. Sitnikov, D.M., J.B. Schineller, and T.O. Baldwin, *Control of cell division in Escherichia coli: regulation of transcription of ftsQA involves both rpoS and SdiA-mediated autoinduction*. Proc Natl Acad Sci U S A, 1996. **93**(1): p. 336-41.
180. Withers, H.L. and K. Nordstrom, *Quorum-sensing acts at initiation of chromosomal replication in Escherichia coli*. Proc Natl Acad Sci U S A, 1998. **95**(26): p. 15694-9.
181. Wang, X.D., P.A. de Boer, and L.I. Rothfield, *A factor that positively regulates cell division by activating transcription of the major cluster of essential cell division genes of Escherichia coli*. Embo J, 1991. **10**(11): p. 3363-72.

182. von Bodman, S.B., D.R. Majerczak, and D.L. Coplin, *A negative regulator mediates quorum-sensing control of exopolysaccharide production in Pantoea stewartii subsp. stewartii*. Proc Natl Acad Sci U S A, 1998. **95**(13): p. 7687-92.
183. Pierson, L.S., 3rd, V.D. Keppenne, and D.W. Wood, *Phenazine antibiotic biosynthesis in Pseudomonas aureofaciens 30-84 is regulated by PhzR in response to cell density*. J Bacteriol, 1994. **176**(13): p. 3966-74.
184. Wood, D.W., et al., *N-acyl-homoserine lactone-mediated regulation of phenazine gene expression by Pseudomonas aureofaciens 30-84 in the wheat rhizosphere*. J Bacteriol, 1997. **179**(24): p. 7663-70.
185. Wood, D.W. and L.S. Pierson, 3rd, *The phzI gene of Pseudomonas aureofaciens 30-84 is responsible for the production of a diffusible signal required for phenazine antibiotic production*. Gene, 1996. **168**(1): p. 49-53.
186. Pearson, J.P., et al., *Structure of the autoinducer required for expression of Pseudomonas aeruginosa virulence genes*. Proc Natl Acad Sci U S A, 1994. **91**(1): p. 197-201.
187. Davies, D.G., et al., *The involvement of cell-to-cell signals in the development of a bacterial biofilm*. Science, 1998. **280**(5361): p. 295-8.
188. de Kievit, T.R. and B.H. Iglewski, *Bacterial quorum sensing in pathogenic relationships*. Infect Immun, 2000. **68**(9): p. 4839-49.
189. Gambello, M.J. and B.H. Iglewski, *Cloning and characterization of the Pseudomonas aeruginosa lasR gene, a transcriptional activator of elastase expression*. J Bacteriol, 1991. **173**(9): p. 3000-9.
190. Gambello, M.J., S. Kaye, and B.H. Iglewski, *LasR of Pseudomonas aeruginosa is a transcriptional activator of the alkaline protease gene (apr) and an enhancer of exotoxin A expression*. Infect Immun, 1993. **61**(4): p. 1180-4.
191. Passador, L., et al., *Expression of Pseudomonas aeruginosa virulence genes requires cell-to-cell communication*. Science, 1993. **260**(5111): p. 1127-30.
192. Pearson, J.P., et al., *A second N-acylhomoserine lactone signal produced by Pseudomonas aeruginosa*. Proc Natl Acad Sci U S A, 1995. **92**(5): p. 1490-4.
193. Latifi, A., et al., *A hierarchical quorum-sensing cascade in Pseudomonas aeruginosa links the transcriptional activators LasR and RhIR (VsmR) to expression of the stationary-phase sigma factor RpoS*. Mol Microbiol, 1996. **21**(6): p. 1137-46.
194. Brint, J.M. and D.E. Ohman, *Synthesis of multiple exoproducts in Pseudomonas aeruginosa is under the control of RhIR-RhII, another set of regulators in strain PAO1 with homology to the autoinducer-responsive LuxR-LuxI family*. J Bacteriol, 1995. **177**(24): p. 7155-63.
195. Latifi, A., et al., *Multiple homologues of LuxR and LuxI control expression of virulence determinants and secondary metabolites through quorum sensing in Pseudomonas aeruginosa PAO1*. Mol Microbiol, 1995. **17**(2): p. 333-43.
196. Ochsner, U.A., et al., *Isolation and characterization of a regulatory gene affecting rhamnolipid biosurfactant synthesis in Pseudomonas aeruginosa*. J Bacteriol, 1994. **176**(7): p. 2044-54.

197. Ochsner, U.A. and J. Reiser, *Autoinducer-mediated regulation of rhamnolipid biosurfactant synthesis in Pseudomonas aeruginosa*. Proc Natl Acad Sci U S A, 1995. **92**(14): p. 6424-8.
198. Flavier, A.B., et al., *Hierarchical autoinduction in Ralstonia solanacearum: control of acyl-homoserine lactone production by a novel autoregulatory system responsive to 3-hydroxypalmitic acid methyl ester*. J Bacteriol, 1997. **179**(22): p. 7089-97.
199. Cubo, M.T., et al., *Molecular characterization and regulation of the rhizosphere-expressed genes rhiABCR that can influence nodulation by Rhizobium leguminosarum biovar viciae*. J Bacteriol, 1992. **174**(12): p. 4026-35.
200. Rodelas, B., et al., *Analysis of quorum-sensing-dependent control of rhizosphere-expressed (rhi) genes in Rhizobium leguminosarum bv. viciae*. J Bacteriol, 1999. **181**(12): p. 3816-23.
201. Lithgow, J.K., et al., *The regulatory locus cinRI in Rhizobium leguminosarum controls a network of quorum-sensing loci*. Mol Microbiol, 2000. **37**(1): p. 81-97.
202. van Brussel, A.A., et al., *Bacteriocin small of fast-growing rhizobia is chloroform soluble and is not required for effective nodulation*. J Bacteriol, 1985. **162**(3): p. 1079-82.
203. Ahmer, B.M., et al., *Salmonella typhimurium encodes an SdiA homolog, a putative quorum sensor of the LuxR family, that regulates genes on the virulence plasmid*. J Bacteriol, 1998. **180**(5): p. 1185-93.
204. Eberl, L., et al., *Involvement of N-acyl-L-homoserine lactone autoinducers in controlling the multicellular behaviour of Serratia liquefaciens*. Mol Microbiol, 1996. **20**(1): p. 127-36.
205. Givskov, M., L. Eberl, and S. Molin, *Control of exoenzyme production, motility and cell differentiation in Serratia liquefaciens*. FEMS Microbiol Lett, 1997. **148**: p. 115-22.
206. Milton, D.L., et al., *Quorum sensing in Vibrio anguillarum: characterization of the vanI/vanR locus and identification of the autoinducer N-(3-oxodecanoyl)-L-homoserine lactone*. J Bacteriol, 1997. **179**(9): p. 3004-12.
207. Bassler, B.L., et al., *Intercellular signalling in Vibrio harveyi: sequence and function of genes regulating expression of luminescence*. Mol Microbiol, 1993. **9**(4): p. 773-86.
208. Bassler, B.L., M. Wright, and M.R. Silverman, *Sequence and function of LuxO, a negative regulator of luminescence in Vibrio harveyi*. Mol Microbiol, 1994. **12**(3): p. 403-12.
209. Cao, J.G. and E.A. Meighen, *Purification and structural identification of an autoinducer for the luminescence system of Vibrio harveyi*. J Biol Chem, 1989. **264**(36): p. 21670-6.
210. Martin, M., R. Showalter, and M. Silverman, *Identification of a locus controlling expression of luminescence genes in Vibrio harveyi*. J Bacteriol, 1989. **171**(5): p. 2406-14.
211. Sun, W., et al., *Biosynthesis of poly-3-hydroxybutyrate in the luminescent bacterium, Vibrio harveyi, and regulation by the lux autoinducer, N-(3-hydroxybutanoyl)homoserine lactone*. J Biol Chem, 1994. **269**(32): p. 20785-90.

212. Bassler, B.L., M. Wright, and M.R. Silverman, *Multiple signalling systems controlling expression of luminescence in Vibrio harveyi: sequence and function of genes encoding a second sensory pathway*. Mol Microbiol, 1994. **13**(2): p. 273-86.
213. Throup, J.P., et al., *Characterisation of the yenI/yenR locus from Yersinia enterocolitica mediating the synthesis of two N-acylhomoserine lactone signal molecules*. Mol Microbiol, 1995. **17**(2): p. 345-56.
214. Atkinson, S., et al., *A hierarchical quorum-sensing system in Yersinia pseudotuberculosis is involved in the regulation of motility and clumping*. Mol Microbiol, 1999. **33**(6): p. 1267-77.
215. Hanzelka, B.L. and E.P. Greenberg, *Quorum sensing in Vibrio fischeri: evidence that S-adenosylmethionine is the amino acid substrate for autoinducer synthesis*. J Bacteriol, 1996. **178**(17): p. 5291-4.
216. Jiang, Y., et al., *In vitro biosynthesis of the Pseudomonas aeruginosa quorum-sensing signal molecule N-butanoyl-L-homoserine lactone*. Mol Microbiol, 1998. **28**(1): p. 193-203.
217. Hoang, T.T., et al., *Construction and use of low-copy number T7 expression vectors for purification of problem proteins: purification of mycobacterium tuberculosis RmlD and pseudomonas aeruginosa LasI and RhII proteins, and functional analysis of purified RhII*. Gene, 1999. **237**(2): p. 361-71.
218. Parsek, M.R., et al., *Acyl homoserine-lactone quorum-sensing signal generation*. Proc Natl Acad Sci U S A, 1999. **96**(8): p. 4360-5.
219. Val, D.L. and J.E. Cronan, Jr., *In vivo evidence that S-adenosylmethionine and fatty acid synthesis intermediates are the substrates for the LuxI family of autoinducer synthases*. J Bacteriol, 1998. **180**(10): p. 2644-51.
220. Hoang, T.T. and H.P. Schweizer, *Characterization of Pseudomonas aeruginosa enoyl-acyl carrier protein reductase (FabI): a target for the antimicrobial triclosan and its role in acylated homoserine lactone synthesis*. J Bacteriol, 1999. **181**(17): p. 5489-97.
221. Greene, R.C., *Biosynthesis of methionine*, in *Escherichia coli and Salmonella: Cellular and Molecular Biology*, F.C. Neidhardt, Editor. 1996, ASM Press: Washington, DC. p. 542-60.
222. Watson, W.T., et al., *Structural basis and specificity of acyl-homoserine lactone signal production in bacterial quorum sensing*. Mol Cell, 2002. **9**(3): p. 685-94.
223. Swift, S., et al., *Quorum sensing: a population-density component in the determination of bacterial phenotype*. Trends Biochem Sci, 1996. **21**(6): p. 214-9.
224. Swift, S., et al., *Quorum sensing as a population-density-dependent determinant of bacterial physiology*. Adv Microb Physiol, 2001. **45**: p. 199-270.
225. Parsek, M.R., A.L. Schaefer, and E.P. Greenberg, *Analysis of random and site-directed mutations in rhII, a Pseudomonas aeruginosa gene encoding an acylhomoserine lactone synthase*. Mol Microbiol, 1997. **26**(2): p. 301-10.
226. Hanzelka, B.L., et al., *Mutational analysis of the Vibrio fischeri LuxI polypeptide: critical regions of an autoinducer synthase*. J Bacteriol, 1997. **179**(15): p. 4882-7.

227. Zhu, J., et al., *Analogues of the autoinducer 3-oxooctanoyl-homoserine lactone strongly inhibit activity of the TraR protein of Agrobacterium tumefaciens*. J Bacteriol, 1998. **180**(20): p. 5398-405.
228. Schaefer, A.L., et al., *Quorum sensing in Vibrio fischeri: probing autoinducer-LuxR interactions with autoinducer analogs*. J Bacteriol, 1996. **178**(10): p. 2897-901.
229. Gould, T.A., H.P. Schweizer, and M.E. Churchill, *Structure of the Pseudomonas aeruginosa acyl-homoserine lactone synthase LasI*. Mol Microbiol, 2004. **53**(4): p. 1135-46.
230. Zhang, R.G., et al., *Structure of a bacterial quorum-sensing transcription factor complexed with pheromone and DNA*. Nature, 2002. **417**(6892): p. 971-4.
231. Zhu, J. and S.C. Winans, *The quorum-sensing transcriptional regulator TraR requires its cognate signaling ligand for protein folding, protease resistance, and dimerization*. Proc Natl Acad Sci U S A, 2001. **98**(4): p. 1507-12.
232. Vannini, A., et al., *The crystal structure of the quorum sensing protein TraR bound to its autoinducer and target DNA*. Embo J, 2002. **21**(17): p. 4393-401.
233. Pearson, J.P., C. Van Delden, and B.H. Iglewski, *Active efflux and diffusion are involved in transport of Pseudomonas aeruginosa cell-to-cell signals*. J Bacteriol, 1999. **181**(4): p. 1203-10.
234. Evans, K., et al., *Influence of the MexAB-OprM multidrug efflux system on quorum sensing in Pseudomonas aeruginosa*. J Bacteriol, 1998. **180**(20): p. 5443-7.
235. Hellingwerf, K.J., et al., *Current topics in signal transduction in bacteria*. Antonie Van Leeuwenhoek, 1998. **74**(4): p. 211-27.
236. Fuqua, C., M.R. Parsek, and E.P. Greenberg, *Regulation of gene expression by cell-to-cell communication: acyl-homoserine lactone quorum sensing*. Annu Rev Genet, 2001. **35**: p. 439-68.
237. Chirala, S.S., et al., *Animal fatty acid synthase: functional mapping and cloning and expression of the domain I constituent activities*. Proc Natl Acad Sci U S A, 1997. **94**(11): p. 5588-93.
238. Tsay, J.T., et al., *Isolation and characterization of the beta-ketoacyl-acyl carrier protein synthase III gene (fabH) from Escherichia coli K-12*. J Biol Chem, 1992. **267**(10): p. 6807-14.
239. Clough, R.C., et al., *Purification and characterization of 3-ketoacyl-acyl carrier protein synthase III from spinach. A condensing enzyme utilizing acetyl-coenzyme A to initiate fatty acid synthesis*. J Biol Chem, 1992. **267**(29): p. 20992-8.
240. Waller, R.F., et al., *Nuclear-encoded proteins target to the plastid in Toxoplasma gondii and Plasmodium falciparum*. Proc Natl Acad Sci U S A, 1998. **95**(21): p. 12352-7.
241. Magnuson, K., et al., *Regulation of fatty acid biosynthesis in Escherichia coli*. Microbiol Rev, 1993. **57**(3): p. 522-42.
242. Zhang, Y.M., et al., *The application of computational methods to explore the diversity and structure of bacterial fatty acid synthase*. J Lipid Res, 2003. **44**(1): p. 1-10.

243. Cronan, J.E., Jr. and E.P. Gelmann, *An estimate of the minimum amount of unsaturated fatty acid required for growth of Escherichia coli*. J Biol Chem, 1973. **248**(4): p. 1188-95.
244. Cronan, J.E., Jr., *Thermal regulation of the membrane lipid composition of Escherichia coli. Evidence for the direct control of fatty acid synthesis*. J Biol Chem, 1975. **250**(17): p. 7074-7.
245. Ulrich, A.K., et al., *Genetic and biochemical analyses of Escherichia coli mutants altered in the temperature-dependent regulation of membrane lipid composition*. J Bacteriol, 1983. **154**(1): p. 221-30.
246. Cronan, J.E., Jr. and C.O. Rock, *Biosynthesis of membrane lipids*, in *Escherichia coli and Salmonella: Cellular and Molecular Biology*, F.C. Neidhardt, Editor. 1996, ASM Press: Washington, DC. p. 612-36.
247. Sanyal, I., S.L. Lee, and D.H. Flint, *Biosynthesis of pimeloyl-CoA, a biotin precursor in Escherichia coli, follows a modified fatty acid synthesis pathway: ¹³C-labeling studies*. J. Amer. Chem. Soc., 1994. **116**: p. 2637-8.
248. Jordan, S.W. and J.E. Cronan, Jr., *A new metabolic link. The acyl carrier protein of lipid synthesis donates lipoic acid to the pyruvate dehydrogenase complex in Escherichia coli and mitochondria*. J Biol Chem, 1997. **272**(29): p. 17903-6.
249. Rehm, B.H., T.A. Mitsky, and A. Steinbuchel, *Role of fatty acid de novo biosynthesis in polyhydroxyalkanoic acid (PHA) and rhamnolipid synthesis by pseudomonads: establishment of the transacylase (PhaG)-mediated pathway for PHA biosynthesis in Escherichia coli*. Appl Environ Microbiol, 2001. **67**(7): p. 3102-9.
250. Stanley, P., V. Koronakis, and C. Hughes, *Acylation of Escherichia coli hemolysin: a unique protein lipidation mechanism underlying toxin function*. Microbiol Mol Biol Rev, 1998. **62**(2): p. 309-33.
251. Rock, C.O. and J.E. Cronan, *Escherichia coli as a model for the regulation of dissociable (type II) fatty acid biosynthesis*. Biochim Biophys Acta, 1996. **1302**(1): p. 1-16.
252. Kaneda, T., *Iso- and anteiso-fatty acids in bacteria: biosynthesis, function, and taxonomic significance*. Microbiol Rev, 1991. **55**(2): p. 288-302.
253. Zhang, Y.M., et al., *Identification and analysis of the acyl carrier protein (ACP) docking site on beta-ketoacyl-ACP synthase III*. J Biol Chem, 2001. **276**(11): p. 8231-8.
254. Davis, M.S., J. Solbiati, and J.E. Cronan, Jr., *Overproduction of acetyl-CoA carboxylase activity increases the rate of fatty acid biosynthesis in Escherichia coli*. J Biol Chem, 2000. **275**(37): p. 28593-8.
255. Bilder, P., et al., *The structure of the carboxyltransferase component of acetyl-coA carboxylase reveals a zinc-binding motif unique to the bacterial enzyme*. Biochemistry, 2006. **45**(6): p. 1712-22.
256. Serre, L., et al., *The Escherichia coli malonyl-CoA:acyl carrier protein transacylase at 1.5-A resolution. Crystal structure of a fatty acid synthase component*. J Biol Chem, 1995. **270**(22): p. 12961-4.

257. Qiu, X., et al., *Crystal structure of beta-ketoacyl-acyl carrier protein synthase III. A key condensing enzyme in bacterial fatty acid biosynthesis*. J Biol Chem, 1999. **274**(51): p. 36465-71.
258. Davies, C., et al., *The 1.8 Å crystal structure and active-site architecture of beta-ketoacyl-acyl carrier protein synthase III (FabH) from escherichia coli*. Structure, 2000. **8**(2): p. 185-95.
259. Jackowski, S., et al., *Acetoacetyl-acyl carrier protein synthase. A target for the antibiotic thiolactomycin*. J Biol Chem, 1989. **264**(13): p. 7624-9.
260. Revill, W.P., et al., *Beta-ketoacyl acyl carrier protein synthase III (FabH) is essential for fatty acid biosynthesis in Streptomyces coelicolor A3(2)*. J Bacteriol, 2001. **183**(11): p. 3526-30.
261. Lai, C.Y. and J.E. Cronan, *Beta-ketoacyl-acyl carrier protein synthase III (FabH) is essential for bacterial fatty acid synthesis*. J Biol Chem, 2003. **278**(51): p. 51494-503.
262. Heath, R.J. and C.O. Rock, *Inhibition of beta-ketoacyl-acyl carrier protein synthase III (FabH) by acyl-acyl carrier protein in Escherichia coli*. J Biol Chem, 1996. **271**(18): p. 10996-1000.
263. Jackowski, S. and C.O. Rock, *Acetoacetyl-acyl carrier protein synthase, a potential regulator of fatty acid biosynthesis in bacteria*. J Biol Chem, 1987. **262**(16): p. 7927-31.
264. Zhang, Y. and J.E. Cronan, Jr., *Transcriptional analysis of essential genes of the Escherichia coli fatty acid biosynthesis gene cluster by functional replacement with the analogous Salmonella typhimurium gene cluster*. J Bacteriol, 1998. **180**(13): p. 3295-303.
265. Price, A.C., et al., *Structure of beta-ketoacyl-[acyl carrier protein] reductase from Escherichia coli: negative cooperativity and its structural basis*. Biochemistry, 2001. **40**(43): p. 12772-81.
266. Heath, R.J. and C.O. Rock, *Roles of the FabA and FabZ beta-hydroxyacyl-acyl carrier protein dehydratases in Escherichia coli fatty acid biosynthesis*. J Biol Chem, 1996. **271**(44): p. 27795-801.
267. Clark, D.P., et al., *Beta-hydroxydecanoyl thio ester dehydrase does not catalyze a rate-limiting step in Escherichia coli unsaturated fatty acid synthesis*. Biochemistry, 1983. **22**(25): p. 5897-902.
268. Mohan, S., et al., *An Escherichia coli gene (FabZ) encoding (3R)-hydroxymyristoyl acyl carrier protein dehydrase. Relation to fabA and suppression of mutations in lipid A biosynthesis*. J Biol Chem, 1994. **269**(52): p. 32896-903.
269. Leesong, M., et al., *Structure of a dehydratase-isomerase from the bacterial pathway for biosynthesis of unsaturated fatty acids: two catalytic activities in one active site*. Structure, 1996. **4**(3): p. 253-64.
270. Birge, C.H. and P.R. Vagelos, *Acyl carrier protein. XVII. Purification and properties of -hydroxyacyl acyl carrier protein dehydrase*. J Biol Chem, 1972. **247**(16): p. 4930-8.

271. Heath, R.J. and C.O. Rock, *Enoyl-acyl carrier protein reductase (fabI) plays a determinant role in completing cycles of fatty acid elongation in Escherichia coli*. J Biol Chem, 1995. **270**(44): p. 26538-42.
272. Heath, R.J., et al., *The enoyl-[acyl-carrier-protein] reductases FabI and FabL from Bacillus subtilis*. J Biol Chem, 2000. **275**(51): p. 40128-33.
273. Heath, R.J. and C.O. Rock, *A triclosan-resistant bacterial enzyme*. Nature, 2000. **406**(6792): p. 145-6.
274. Bergler, H., et al., *Protein EnvM is the NADH-dependent enoyl-ACP reductase (FabI) of Escherichia coli*. J Biol Chem, 1994. **269**(8): p. 5493-6.
275. Olsen, J.G., et al., *The X-ray crystal structure of beta-ketoacyl [acyl carrier protein] synthase I*. FEBS Lett, 1999. **460**(1): p. 46-52.
276. Huang, W., et al., *Crystal structure of beta-ketoacyl-acyl carrier protein synthase II from E.coli reveals the molecular architecture of condensing enzymes*. Embo J, 1998. **17**(5): p. 1183-91.
277. Garwin, J.L., A.L. Klages, and J.E. Cronan, Jr., *Beta-ketoacyl-acyl carrier protein synthase II of Escherichia coli. Evidence for function in the thermal regulation of fatty acid synthesis*. J Biol Chem, 1980. **255**(8): p. 3263-5.
278. Garwin, J.L., A.L. Klages, and J.E. Cronan, Jr., *Structural, enzymatic, and genetic studies of beta-ketoacyl-acyl carrier protein synthases I and II of Escherichia coli*. J Biol Chem, 1980. **255**(24): p. 11949-56.
279. D'Agno, G., I.S. Rosenfeld, and P.R. Vagelos, *Multiple forms of beta-ketoacyl-acyl carrier protein synthetase in Escherichia coli*. J Biol Chem, 1975. **250**(14): p. 5289-94.
280. Moche, M., et al., *Structure of the complex between the antibiotic cerulenin and its target, beta-ketoacyl-acyl carrier protein synthase*. J Biol Chem, 1999. **274**(10): p. 6031-4.
281. Price, A.C., et al., *Inhibition of beta-ketoacyl-acyl carrier protein synthases by thiolactomycin and cerulenin. Structure and mechanism*. J Biol Chem, 2001. **276**(9): p. 6551-9.
282. Olsen, J.G., et al., *Structures of beta-ketoacyl-acyl carrier protein synthase I complexed with fatty acids elucidate its catalytic machinery*. Structure, 2001. **9**(3): p. 233-43.
283. Nishida, I., A. Kawaguchi, and M. Yamada, *Effect of thiolactomycin on the individual enzymes of the fatty acid synthase system in Escherichia coli*. J Biochem (Tokyo), 1986. **99**(5): p. 1447-54.
284. Tsay, J.T., C.O. Rock, and S. Jackowski, *Overproduction of beta-ketoacyl-acyl carrier protein synthase I imparts thiolactomycin resistance to Escherichia coli K-12*. J Bacteriol, 1992. **174**(2): p. 508-13.
285. Subrahmanyam, S. and J.E. Cronan, Jr., *Overproduction of a functional fatty acid biosynthetic enzyme blocks fatty acid synthesis in Escherichia coli*. J Bacteriol, 1998. **180**(17): p. 4596-602.
286. McGuire, K.A., et al., *beta-Ketoacyl-[acyl carrier protein] synthase I of Escherichia coli: aspects of the condensation mechanism revealed by analyses of mutations in the active site pocket*. Biochemistry, 2001. **40**(33): p. 9836-45.

287. Edwards, P., et al., *Cloning of the fabF gene in an expression vector and in vitro characterization of recombinant fabF and fabB encoded enzymes from Escherichia coli*. FEBS Lett, 1997. **402**(1): p. 62-6.
288. Kass, L.R. and K. Bloch, *On the enzymatic synthesis of unsaturated fatty acids in Escherichia coli*. Proc Natl Acad Sci U S A, 1967. **58**(3): p. 1168-73.
289. Birge, C.H., D.F. Silbert, and P.R. Vagelos, *A beta-hydroxydecanoyl-ACP dehydrase specific for saturated fatty acid biosynthesis in E. coli*. Biochem Biophys Res Commun, 1967. **29**(6): p. 808-14.
290. Kass, L.R., D.J. Brock, and K. Bloch, *Beta-hydroxydecanoyl thioester dehydrase. I. Purification and properties*. J Biol Chem, 1967. **242**(19): p. 4418-31.
291. Silbert, D.F. and P.R. Vagelos, *Fatty acid mutant of E. coli lacking a beta-hydroxydecanoyl thioester dehydrase*. Proc Natl Acad Sci U S A, 1967. **58**(4): p. 1579-86.
292. Clark, D.P. and J.E. Cronan, Jr., *Bacterial mutants for the study of lipid metabolism*. Methods Enzymol, 1981. **72**: p. 693-707.
293. Bloch, K., *Enzymatic synthesis of monounsaturated fatty acids*. Acc. Chem. Res., 1969. **2**: p. 193-202.
294. Brock, D.J., L.R. Kass, and K. Bloch, *Beta-hydroxydecanoyl thioester dehydrase. II. Mode of action*. J Biol Chem, 1967. **242**(19): p. 4432-40.
295. Cronan, J.E., Jr., C.H. Birge, and P.R. Vagelos, *Evidence for two genes specifically involved in unsaturated fatty acid biosynthesis in Escherichia coli*. J Bacteriol, 1969. **100**(2): p. 601-4.
296. DeMendoza, D. and J.E. Cronan, *Thermal regulation of membrane lipid fluidity in bacteria*. Trends Biochem Sci, 1983. **8**: p. 49-52.
297. Rosenfeld, I.S., G. D'Agnolo, and P.R. Vagelos, *Synthesis of unsaturated fatty acids and the lesion in fab B mutants*. J Biol Chem, 1973. **248**(7): p. 2452-60.
298. Jackson, M.B. and J.E. Cronan, Jr., *An estimate of the minimum amount of fluid lipid required for the growth of Escherichia coli*. Biochim Biophys Acta, 1978. **512**(3): p. 472-9.
299. Payne, D.J., et al., *Bacterial fatty-acid biosynthesis: a genomics-driven target for antibacterial drug discovery*. Drug Discov Today, 2001. **6**(10): p. 537-544.
300. Aguilar, P.S., J.E. Cronan, Jr., and D. de Mendoza, *A Bacillus subtilis gene induced by cold shock encodes a membrane phospholipid desaturase*. J Bacteriol, 1998. **180**(8): p. 2194-200.
301. Cybulski, L.E., et al., *Mechanism of membrane fluidity optimization: isothermal control of the Bacillus subtilis acyl-lipid desaturase*. Mol Microbiol, 2002. **45**(5): p. 1379-88.
302. Mansilla, M.C., et al., *Regulation of fatty acid desaturation in Bacillus subtilis*. Prostaglandins Leukot Essent Fatty Acids, 2003. **68**(2): p. 187-90.
303. Choi, K.H., R.J. Heath, and C.O. Rock, *beta-ketoacyl-acyl carrier protein synthase III (FabH) is a determining factor in branched-chain fatty acid biosynthesis*. J Bacteriol, 2000. **182**(2): p. 365-70.
304. Smirnova, N. and K.A. Reynolds, *Branched-chain fatty acid biosynthesis in Escherichia coli*. J Ind Microbiol Biotechnol, 2001. **27**(4): p. 246-51.

305. Kaneda, T., E.J. Smith, and D.N. Naik, *Fatty acid composition and primer specificity of de novo fatty acid synthetase in Bacillus globisporus, Bacillus insolitus, and Bacillus psychrophilus*. Can J Microbiol, 1983. **29**(12): p. 1634-41.
306. Han, L., S. Lobo, and K.A. Reynolds, *Characterization of beta-ketoacyl-acyl carrier protein synthase III from Streptomyces glaucescens and its role in initiation of fatty acid biosynthesis*. J Bacteriol, 1998. **180**(17): p. 4481-6.
307. Lu, Y.J., Y.M. Zhang, and C.O. Rock, *Product diversity and regulation of type II fatty acid synthases*. Biochem Cell Biol, 2004. **82**(1): p. 145-55.
308. Qiu, X., et al., *Refined structures of beta-ketoacyl-acyl carrier protein synthase III*. J Mol Biol, 2001. **307**(1): p. 341-56.
309. Kaneda, T., *Biosynthesis of branched chain fatty acids. II. Microbial synthesis of branched long chain fatty acids from certain short chain fatty acid substrates*. J Biol Chem, 1963. **238**: p. 1229-35.
310. Kaneda, T., *Incorporation of branched-chain C6-fatty acid isomers into the related long-chain fatty acids by growing cells of Bacillus subtilis*. Biochemistry, 1971. **10**(2): p. 340-7.
311. Kaneda, T., *Stereoselectivity in the 2-methylbutyrate incorporation into anteiso fatty acids in Bacillus subtilis mutants*. Biochim Biophys Acta, 1988. **960**(1): p. 10-8.
312. Oku, H. and T. Kaneda, *Biosynthesis of branched-chain fatty acids in Bacillus subtilis. A decarboxylase is essential for branched-chain fatty acid synthetase*. J Biol Chem, 1988. **263**(34): p. 18386-96.
313. Khandekar, S.S., et al., *Identification, substrate specificity, and inhibition of the Streptococcus pneumoniae beta-ketoacyl-acyl carrier protein synthase III (FabH)*. J Biol Chem, 2001. **276**(32): p. 30024-30.
314. Kaneda, T., *Biosynthesis of branched long-chain fatty acids from the related short-chain -keto acid substrates by a cell-free system of Bacillus subtilis*. Can J Microbiol, 1973. **19**(1): p. 87-96.
315. Naik, D.N. and T. Kaneda, *Biosynthesis of branched long-chain fatty acids by species of Bacillus: relative activity of three alpha-keto acid substrates and factors affecting chain length*. Can J Microbiol, 1974. **20**(12): p. 1701-8.
316. Young, K., et al., *Discovery of FabH/FabF inhibitors from natural products*. Antimicrob Agents Chemother, 2006. **50**(2): p. 519-26.
317. Qiu, X., et al., *Crystal structure and substrate specificity of the beta-ketoacyl-acyl carrier protein synthase III (FabH) from Staphylococcus aureus*. Protein Sci, 2005. **14**(8): p. 2087-94.
318. Butterworth, P.H. and K. Bloch, *Comparative aspects of fatty acid synthesis in Bacillus subtilis and Escherichia coli*. Eur J Biochem, 1970. **12**(3): p. 496-501.
319. Wang, G.F., et al., *The primary structure of branched-chain alpha-oxo acid dehydrogenase from Bacillus subtilis and its similarity to other alpha-oxo acid dehydrogenases*. Eur J Biochem, 1993. **213**(3): p. 1091-9.
320. Willecke, K. and A.B. Pardee, *Fatty acid-requiring mutant of bacillus subtilis defective in branched chain alpha-keto acid dehydrogenase*. J Biol Chem, 1971. **246**(17): p. 5264-72.

321. Heath, R.J. and C.O. Rock, *The Claisen condensation in biology*. Nat Prod Rep, 2002. **19**(5): p. 581-96.
322. Wang, H. and J.E. Cronan, *Functional replacement of the FabA and FabB proteins of Escherichia coli fatty acid synthesis by Enterococcus faecalis FabZ and FabF homologues*. J Biol Chem, 2004. **279**(33): p. 34489-95.
323. Price, A.C., C.O. Rock, and S.W. White, *The 1.3-Angstrom-resolution crystal structure of beta-ketoacyl-acyl carrier protein synthase II from Streptococcus pneumoniae*. J Bacteriol, 2003. **185**(14): p. 4136-43.
324. Moche, M., et al., *The crystal structure of beta-ketoacyl-acyl carrier protein synthase II from Synechocystis sp. at 1.54 Å resolution and its relationship to other condensing enzymes*. J Mol Biol, 2001. **305**(3): p. 491-503.
325. Roujeinikova, A., et al., *Inhibitor binding studies on enoyl reductase reveal conformational changes related to substrate recognition*. J Biol Chem, 1999. **274**(43): p. 30811-7.
326. Roujeinikova, A., et al., *Crystallographic analysis of triclosan bound to enoyl reductase*. J Mol Biol, 1999. **294**(2): p. 527-35.
327. Stewart, M.J., et al., *Structural basis and mechanism of enoyl reductase inhibition by triclosan*. J Mol Biol, 1999. **290**(4): p. 859-65.
328. Baldock, C., et al., *The X-ray structure of Escherichia coli enoyl reductase with bound NAD⁺ at 2.1 Å resolution*. J Mol Biol, 1998. **284**(5): p. 1529-46.
329. Baldock, C., et al., *A mechanism of drug action revealed by structural studies of enoyl reductase*. Science, 1996. **274**(5295): p. 2107-10.
330. Rozwarski, D.A., et al., *Modification of the NADH of the isoniazid target (InhA) from Mycobacterium tuberculosis*. Science, 1998. **279**(5347): p. 98-102.
331. Rozwarski, D.A., et al., *Crystal structure of the Mycobacterium tuberculosis enoyl-ACP reductase, InhA, in complex with NAD⁺ and a C16 fatty acyl substrate*. J Biol Chem, 1999. **274**(22): p. 15582-9.
332. Heath, R.J., et al., *Inhibition of the Staphylococcus aureus NADPH-dependent enoyl-acyl carrier protein reductase by triclosan and hexachlorophene*. J Biol Chem, 2000. **275**(7): p. 4654-9.
333. Ohlrogge, J., et al., *Alteration of acyl-acyl carrier protein pools and acetyl-CoA carboxylase expression in Escherichia coli by a plant medium chain acyl-acyl carrier protein thioesterase*. Arch Biochem Biophys, 1995. **317**(1): p. 185-90.
334. Tropf, S., et al., *Heterologously expressed acyl carrier protein domain of rat fatty acid synthase functions in Escherichia coli fatty acid synthase and Streptomyces coelicolor polyketide synthase systems*. Chem Biol, 1998. **5**(3): p. 135-46.
335. Reed, M.A., et al., *The type I rat fatty acid synthase ACP shows structural homology and analogous biochemical properties to type II ACPs*. Org Biomol Chem, 2003. **1**(3): p. 463-71.
336. Bateman, A., et al., *The Pfam protein families database*. Nucleic Acids Res, 2000. **28**(1): p. 263-6.
337. Holak, T.A., et al., *Three-dimensional structure of acyl carrier protein in solution determined by nuclear magnetic resonance and the combined use of dynamical simulated annealing and distance geometry*. Eur J Biochem, 1988. **175**(1): p. 9-15.

338. Flugel, R.S., et al., *Holo-(acyl carrier protein) synthase and phosphopantetheinyl transfer in Escherichia coli*. J Biol Chem, 2000. **275**(2): p. 959-68.
339. Holak, T.A., et al., *Three-dimensional structure of acyl carrier protein determined by NMR pseudoenergy and distance geometry calculations*. Biochemistry, 1988. **27**(16): p. 6135-42.
340. Kim, Y. and J.H. Prestegard, *A dynamic model for the structure of acyl carrier protein in solution*. Biochemistry, 1989. **28**(22): p. 8792-7.
341. Kim, Y., J.B. Ohlrogge, and J.H. Prestegard, *Motional effects on NMR structural data. Comparison of spinach and Escherichia coli acyl carrier proteins*. Biochem Pharmacol, 1990. **40**(1): p. 7-13.
342. Kim, Y. and J.H. Prestegard, *Refinement of the NMR structures for acyl carrier protein with scalar coupling data*. Proteins, 1990. **8**(4): p. 377-85.
343. Broun, P., et al., *Catalytic plasticity of fatty acid modification enzymes underlying chemical diversity of plant lipids*. Science, 1998. **282**(5392): p. 1315-7.
344. Xu, G.Y., et al., *Solution structure of B. subtilis acyl carrier protein*. Structure, 2001. **9**(4): p. 277-87.
345. Park, S.J., et al., *pH-induced conformational transition of H. pylori acyl carrier protein: insight into the unfolding of local structure*. J Biochem (Tokyo), 2004. **135**(3): p. 337-46.
346. Wong, H.C., et al., *The solution structure of acyl carrier protein from Mycobacterium tuberculosis*. J Biol Chem, 2002. **277**(18): p. 15874-80.
347. Findlow, S.C., et al., *Solution structure and dynamics of oxytetracycline polyketide synthase acyl carrier protein from Streptomyces rimosus*. Biochemistry, 2003. **42**(28): p. 8423-33.
348. Weber, T., et al., *Solution structure of PCP, a prototype for the peptidyl carrier domains of modular peptide synthetases*. Structure, 2000. **8**(4): p. 407-18.
349. Volkman, B.F., et al., *Biosynthesis of D-alanyl-lipoteichoic acid: the tertiary structure of apo-D-alanyl carrier protein*. Biochemistry, 2001. **40**(27): p. 7964-72.
350. Li, Q., et al., *Solution structure and backbone dynamics of the holo form of the frenolicin acyl carrier protein*. Biochemistry, 2003. **42**(16): p. 4648-57.
351. Crump, M.P., et al., *Solution structure of the actinorhodin polyketide synthase acyl carrier protein from Streptomyces coelicolor A3(2)*. Biochemistry, 1997. **36**(20): p. 6000-8.
352. Showalter, A.D., et al., *Differential conservation of transcriptional domains of mammalian Prophet of Pit-1 proteins revealed by structural studies of the bovine gene and comparative functional analysis of the protein*. Gene, 2002. **291**(1-2): p. 211-21.
353. Zhang, Y.M., et al., *Key residues responsible for acyl carrier protein and beta-ketoacyl-acyl carrier protein reductase (FabG) interaction*. J Biol Chem, 2003. **278**(52): p. 52935-43.
354. Kremer, L., et al., *Biochemical characterization of acyl carrier protein (AcpM) and malonyl-CoA:AcpM transacylase (mtFabD), two major components of Mycobacterium tuberculosis fatty acid synthase II*. J Biol Chem, 2001. **276**(30): p. 27967-74.

355. Schaeffer, M.L., et al., *Expression, purification, and characterization of the Mycobacterium tuberculosis acyl carrier protein, AcpM*. Biochim Biophys Acta, 2001. **1532**(1-2): p. 67-78.
356. Ritsema, T., et al., *Functional analysis of an interspecies chimera of acyl carrier proteins indicates a specialized domain for protein recognition*. Mol Gen Genet, 1998. **257**(6): p. 641-8.
357. Kutchma, A.J., T.T. Hoang, and H.P. Schweizer, *Characterization of a Pseudomonas aeruginosa fatty acid biosynthetic gene cluster: purification of acyl carrier protein (ACP) and malonyl-coenzyme A:ACP transacylase (FabD)*. J Bacteriol, 1999. **181**(17): p. 5498-504.
358. Harder, M.E., et al., *Mutants of Escherichia coli with temperature-sensitive malonyl coenzyme A-acyl carrier protein transacylase*. J Biol Chem, 1974. **249**(23): p. 7468-75.
359. Keatinge-Clay, A.T., et al., *Catalysis, specificity, and ACP docking site of Streptomyces coelicolor malonyl-CoA:ACP transacylase*. Structure, 2003. **11**(2): p. 147-54.
360. Lai, C.Y. and J.E. Cronan, *Isolation and characterization of beta-ketoacyl-acyl carrier protein reductase (fabG) mutants of Escherichia coli and Salmonella enterica serovar Typhimurium*. J Bacteriol, 2004. **186**(6): p. 1869-78.
361. Rawlings, M. and J.E. Cronan, Jr., *The gene encoding Escherichia coli acyl carrier protein lies within a cluster of fatty acid biosynthetic genes*. J Biol Chem, 1992. **267**(9): p. 5751-4.
362. McQueney, M.S., K.S. Anderson, and G.D. Markham, *Energetics of S-adenosylmethionine synthetase catalysis*. Biochemistry, 2000. **39**(15): p. 4443-54.
363. Komoto, J., et al., *Crystal structure of the S-adenosylmethionine synthetase ternary complex: a novel catalytic mechanism of S-adenosylmethionine synthesis from ATP and Met*. Biochemistry, 2004. **43**(7): p. 1821-31.
364. Markham, G.D., et al., *S-Adenosylmethionine synthetase from Escherichia coli*. J Biol Chem, 1980. **255**(19): p. 9082-92.
365. Markham, G.D., *Spatial proximity of two divalent metal ions at the active site of S-adenosylmethionine synthetase*. J Biol Chem, 1981. **256**(4): p. 1903-9.
366. Zhang, C., G.D. Markham, and R. LoBrutto, *Coordination of vanadyl(IV) cation in complexes of S-adenosylmethionine synthetase: multifrequency electron spin echo envelope modulation study*. Biochemistry, 1993. **32**(37): p. 9866-73.
367. Taylor, J.C., F. Takusagawa, and G.D. Markham, *The active site loop of S-adenosylmethionine synthetase modulates catalytic efficiency*. Biochemistry, 2002. **41**(30): p. 9358-69.
368. Taylor, J.C. and G.D. Markham, *The bifunctional active site of S-adenosylmethionine synthetase. Roles of the basic residues*. J Biol Chem, 2000. **275**(6): p. 4060-5.
369. McQueney, M.S. and G.D. Markham, *Investigation of monovalent cation activation of S-adenosylmethionine synthetase using mutagenesis and uranyl inhibition*. J Biol Chem, 1995. **270**(31): p. 18277-84.

370. Taylor, J.C. and G.D. Markham, *The bifunctional active site of S-adenosylmethionine synthetase. Roles of the active site aspartates.* J Biol Chem, 1999. **274**(46): p. 32909-14.
371. Reczkowski, R.S., J.C. Taylor, and G.D. Markham, *The active-site arginine of S-adenosylmethionine synthetase orients the reaction intermediate.* Biochemistry, 1998. **37**(39): p. 13499-506.
372. Markham, G.D., P.O. Norrby, and C.W. Bock, *S-adenosylmethionine conformations in solution and in protein complexes: conformational influences of the sulfonium group.* Biochemistry, 2002. **41**(24): p. 7636-46.
373. Schalk-Hihi, C. and G.D. Markham, *The conformations of a substrate and a product bound to the active site of S-adenosylmethionine synthetase.* Biochemistry, 1999. **38**(8): p. 2542-50.
374. Sufrin, J.R., D.A. Dunn, and G.R. Marshall, *Steric mapping of the L-methionine binding site of ATP:L-methionine S-adenosyltransferase.* Mol Pharmacol, 1981. **19**(2): p. 307-13.
375. Sufrin, J.R., J.B. Lombardini, and V. Alks, *Differential kinetic properties of L-2-amino-4-methylthio-cis-but-3-enoic acid, a methionine analog inhibitor of S-adenosylmethionine synthetase.* Biochim Biophys Acta, 1993. **1202**(1): p. 87-91.
376. Ma, Q.F., G.L. Kenyon, and G.D. Markham, *Specificity of S-adenosylmethionine synthetase for ATP analogues mono- and disubstituted in bridging positions of the polyphosphate chain.* Biochemistry, 1990. **29**(6): p. 1412-6.
377. Kappler, F., V.M. Vrudhula, and A. Hampton, *Toward the synthesis of isozyme-specific enzyme inhibitors. Potent inhibitors of rat methionine adenosyltransferases. Effect of one-atom elongation of the ribose-P alpha bridge in two covalent adducts of L-methionine and beta,gamma-imido-ATP.* J Med Chem, 1988. **31**(2): p. 384-9.
378. Kappler, F., V.M. Vrudhula, and A. Hampton, *Isozyme-specific enzyme inhibitors. 14. 5'(R)-C-[(L-homocystein-S-yl)methyl]adenosine 5'-(beta,gamma-imidotriphosphate), a potent inhibitor of rat methionine adenosyltransferases.* J Med Chem, 1987. **30**(9): p. 1599-603.
379. Cantoni, G.L., *S-Adenosylmethionine; a new intermediate formed enzymatically from L-methionine and adenosinetriphosphate.* J. Biol. Chem., 1953. **204**: p. 403-16.
380. Mudd, S.H., *Activation of methionine for transmethylation. VI. Enzyme-bound tripolyphosphate as an intermediate in the reaction catalyzed by the methionine-activating enzyme of Baker's yeast.* J Biol Chem, 1963. **238**: p. 2156-63.
381. Parry, R.J. and A. Minta, *Studies of enzyme stereochemistry. Elucidation of the stereochemistry of S-adenosylmethionine formation by yeast methionine adenosyltransferase.* J. Amer. Chem. Soc., 1982. **104**: p. 871-2.
382. Markham, G.D., et al., *A kinetic isotope effect study and transition state analysis of the S-adenosylmethionine synthetase reaction.* J Biol Chem, 1987. **262**(12): p. 5609-15.
383. Reczkowski, R.S. and G.D. Markham, *Slow binding inhibition of S-adenosylmethionine synthetase by imidophosphate analogues of an intermediate and product.* Biochemistry, 1999. **38**(28): p. 9063-8.

384. Takusagawa, F., S. Kamitori, and G.D. Markham, *Structure and function of S-adenosylmethionine synthetase: crystal structures of S-adenosylmethionine synthetase with ADP, BrADP, and PPi at 28 angstroms resolution*. Biochemistry, 1996. **35**(8): p. 2586-96.
385. Takusagawa, F., et al., *Crystal structure of S-adenosylmethionine synthetase*. J Biol Chem, 1996. **271**(1): p. 136-47.
386. Fu, Z., et al., *Flexible loop in the structure of S-adenosylmethionine synthetase crystallized in the tetragonal modification*. J Biomol Struct Dyn, 1996. **13**(5): p. 727-39.
387. Reczkowski, R.S. and G.D. Markham, *Structural and functional roles of cysteine 90 and cysteine 240 in S-adenosylmethionine synthetase*. J Biol Chem, 1995. **270**(31): p. 18484-90.
388. Newman, E.B., et al., *Lack of S-adenosylmethionine results in a cell division defect in Escherichia coli*. J Bacteriol, 1998. **180**(14): p. 3614-9.
389. Wei, Y. and E.B. Newman, *Studies on the role of the metK gene product of Escherichia coli K-12*. Mol Microbiol, 2002. **43**(6): p. 1651-6.
390. Cantoni, G.L. and J. Durell, *Activation of methionine for transmethylation. II. The methionine-activating enzyme; studies on the mechanism of the reaction*. J Biol Chem, 1957. **225**(2): p. 1033-48.
391. Greene, R.C., J.S. Hunter, and E.H. Coch, *Properties of metK mutants of Escherichia coli K-12*. J Bacteriol, 1973. **115**(1): p. 57-67.
392. Markham, G.D., J. DeParasis, and J. Gatmaitan, *The sequence of metK, the structural gene for S-adenosylmethionine synthetase in Escherichia coli*. J Biol Chem, 1984. **259**(23): p. 14505-7.
393. Hafner, E.W., C.W. Tabor, and H. Tabor, *Isolation of a metK mutant with a temperature-sensitive S-adenosylmethionine synthetase*. J Bacteriol, 1977. **132**(3): p. 832-40.
394. Boyle, S.M., et al., *Expression of the cloned genes encoding the putrescine biosynthetic enzymes and methionine adenosyltransferase of Escherichia coli (speA, speB, speC and metK)*. Gene, 1984. **30**(1-3): p. 129-36.
395. Dixon, M.M., et al., *The structure of the C-terminal domain of methionine synthase: presenting S-adenosylmethionine for reductive methylation of B12*. Structure, 1996. **4**(11): p. 1263-75.
396. Winzer, K., et al., *LuxS: its role in central metabolism and the in vitro synthesis of 4-hydroxy-5-methyl-3(2H)-furanone*. Microbiology, 2002. **148**(Pt 4): p. 909-22.
397. Cantoni, G.L., *Biological methylation: selected aspects*. Annu Rev Biochem, 1975. **44**: p. 435-51.
398. Kerr, S.J. and E. Borek, *Enzymic methylation of natural polynucleotides*, in *The Enzymes*, P.D. Boyer, Editor. 1973, Academic Press Inc.: New York. p. 167-195.
399. Hughes, J.A., L.R. Brown, and A.J. Ferro, *Expression of the cloned coliphage T3 S-adenosylmethionine hydrolase gene inhibits DNA methylation and polyamine biosynthesis in Escherichia coli*. J Bacteriol, 1987. **169**(8): p. 3625-32.
400. Posnick, L.M. and L.D. Samson, *Influence of S-adenosylmethionine pool size on spontaneous mutation, dam methylation, and cell growth of Escherichia coli*. J Bacteriol, 1999. **181**(21): p. 6756-62.

401. Chiang, P.K., et al., *S-Adenosylmethionine and methylation*. *Faseb J*, 1996. **10**(4): p. 471-80.
402. Sofia, H.J., et al., *Radical SAM, a novel protein superfamily linking unresolved steps in familiar biosynthetic pathways with radical mechanisms: functional characterization using new analysis and information visualization methods*. *Nucleic Acids Res*, 2001. **29**(5): p. 1097-106.
403. Pegg, A.E., *Polyamine metabolism and its importance in neoplastic growth and a target for chemotherapy*. *Cancer Res*, 1988. **48**(4): p. 759-74.
404. Sekowska, A., P. Bertin, and A. Danchin, *Characterization of polyamine synthesis pathway in Bacillus subtilis 168*. *Mol Microbiol*, 1998. **29**(3): p. 851-8.
405. Tabor, H., E.W. Hafner, and C.W. Tabor, *Construction of an Escherichia coli strain unable to synthesize putrescine, spermidine, or cadaverine: characterization of two genes controlling lysine decarboxylase*. *J Bacteriol*, 1980. **144**(3): p. 952-6.
406. Berkovitch, F., et al., *Crystal structure of biotin synthase, an S-adenosylmethionine-dependent radical enzyme*. *Science*, 2004. **303**(5654): p. 76-9.
407. Reichard, P., *The anaerobic ribonucleotide reductase from Escherichia coli*. *J Biol Chem*, 1993. **268**(12): p. 8383-6.
408. Boyer, H.W., *Restriction and modification of DNA: enzymes and substrates. Introductory remarks*. *Fed Proc*, 1974. **33**(5): p. 1125-7.
409. Linn, S., et al., *Host-controlled restriction and modification enzymes of Escherichia coli B*. *Fed Proc*, 1974. **33**(5): p. 1128-34.
410. Nathans, D. and H.O. Smith, *Restriction endonucleases in the analysis and restructuring of dna molecules*. *Annu Rev Biochem*, 1975. **44**: p. 273-93.
411. Roulland-Dussoix, D. and H.W. Boyer, *The Escherichia coli B restriction endonuclease*. *Biochim Biophys Acta*, 1969. **195**(1): p. 219-29.
412. Frey, P.A., M.D. Ballinger, and G.H. Reed, *S-adenosylmethionine: a 'poor man's coenzyme B12' in the reaction of lysine 2,3-aminomutase*. *Biochem Soc Trans*, 1998. **26**(3): p. 304-10.
413. Grundy, F.J. and T.M. Henkin, *The S box regulon: a new global transcription termination control system for methionine and cysteine biosynthesis genes in gram-positive bacteria*. *Mol Microbiol*, 1998. **30**(4): p. 737-49.
414. Grundy, F.J. and T.M. Henkin, *The T box and S box transcription termination control systems*. *Front Biosci*, 2003. **8**: p. d20-31.
415. Nakamori, S., et al., *Mechanism of L-methionine overproduction by Escherichia coli: the replacement of Ser-54 by Asn in the MetJ protein causes the derepression of L-methionine biosynthetic enzymes*. *Appl Microbiol Biotechnol*, 1999. **52**(2): p. 179-85.
416. Rodionov, D.A., et al., *Comparative genomics of the methionine metabolism in Gram-positive bacteria: a variety of regulatory systems*. *Nucleic Acids Res*, 2004. **32**(11): p. 3340-53.
417. McDaniel, B.A., et al., *Identification of a mutation in the Bacillus subtilis S-adenosylmethionine synthetase gene that results in derepression of S-box gene expression*. *J Bacteriol*, 2006. **188**(10): p. 3674-81.

418. Yocum, R.R., et al., *Cloning and characterization of the metE gene encoding S-adenosylmethionine synthetase from Bacillus subtilis*. J Bacteriol, 1996. **178**(15): p. 4604-10.
419. Kleerebezem, M., et al., *Quorum sensing by peptide pheromones and two-component signal-transduction systems in Gram-positive bacteria*. Mol Microbiol, 1997. **24**(5): p. 895-904.
420. Novick, R.P. and T.W. Muir, *Virulence gene regulation by peptides in staphylococci and other Gram-positive bacteria*. Curr Opin Microbiol, 1999. **2**(1): p. 40-5.
421. Dunny, G.M. and B.A. Leonard, *Cell-cell communication in gram-positive bacteria*. Annu Rev Microbiol, 1997. **51**: p. 527-64.
422. Lyon, G.J. and R.P. Novick, *Peptide signaling in Staphylococcus aureus and other Gram-positive bacteria*. Peptides, 2004. **25**(9): p. 1389-403.
423. Ji, G., R.C. Beavis, and R.P. Novick, *Cell density control of staphylococcal virulence mediated by an octapeptide pheromone*. Proc Natl Acad Sci U S A, 1995. **92**(26): p. 12055-9.
424. Ji, G., R. Beavis, and R.P. Novick, *Bacterial interference caused by autoinducing peptide variants*. Science, 1997. **276**(5321): p. 2027-30.
425. Otto, M., *Staphylococcus aureus and Staphylococcus epidermidis peptide pheromones produced by the accessory gene regulator agr system*. Peptides, 2001. **22**(10): p. 1603-8.
426. Booth, M.C., et al., *Accessory gene regulator controls Staphylococcus aureus virulence in endophthalmitis*. Invest Ophthalmol Vis Sci, 1995. **36**(9): p. 1828-36.
427. Janzon, L. and S. Arvidson, *The role of the delta-lysin gene (hld) in the regulation of virulence genes by the accessory gene regulator (agr) in Staphylococcus aureus*. Embo J, 1990. **9**(5): p. 1391-9.
428. Morfeldt, E., et al., *Activation of alpha-toxin translation in Staphylococcus aureus by the trans-encoded antisense RNA, RNAIII*. Embo J, 1995. **14**(18): p. 4569-77.
429. Van Wamel, W.J., et al., *Cloning and characterization of an accessory gene regulator (agr)-like locus from Staphylococcus epidermidis*. FEMS Microbiol Lett, 1998. **163**(1): p. 1-9.
430. Wesson, C.A., et al., *Staphylococcus aureus Agr and Sar global regulators influence internalization and induction of apoptosis*. Infect Immun, 1998. **66**(11): p. 5238-43.
431. Balaban, N. and R.P. Novick, *Autocrine regulation of toxin synthesis by Staphylococcus aureus*. Proc Natl Acad Sci U S A, 1995. **92**(5): p. 1619-23.
432. Mayville, P., et al., *Structure-activity analysis of synthetic autoinducing thiolactone peptides from Staphylococcus aureus responsible for virulence*. Proc Natl Acad Sci U S A, 1999. **96**(4): p. 1218-23.
433. Morfeldt, E., et al., *Cloning of a chromosomal locus (exp) which regulates the expression of several exoprotein genes in Staphylococcus aureus*. Mol Gen Genet, 1988. **211**(3): p. 435-40.
434. Novick, R.P., et al., *The agr P2 operon: an autocatalytic sensory transduction system in Staphylococcus aureus*. Mol Gen Genet, 1995. **248**(4): p. 446-58.

435. Peng, H.L., et al., *Cloning, characterization, and sequencing of an accessory gene regulator (agr) in Staphylococcus aureus*. J Bacteriol, 1988. **170**(9): p. 4365-72.
436. Lyon, G.J., et al., *Rational design of a global inhibitor of the virulence response in Staphylococcus aureus, based in part on localization of the site of inhibition to the receptor-histidine kinase, AgrC*. Proc Natl Acad Sci U S A, 2000. **97**(24): p. 13330-5.
437. McDowell, P., et al., *Structure, activity and evolution of the group I thiolactone peptide quorum-sensing system of Staphylococcus aureus*. Mol Microbiol, 2001. **41**(2): p. 503-12.
438. Otto, M., et al., *Structure of the pheromone peptide of the Staphylococcus epidermidis agr system*. FEBS Lett, 1998. **424**(1-2): p. 89-94.
439. Lyon, G.J., et al., *Reversible and specific extracellular antagonism of receptor-histidine kinase signaling*. J Biol Chem, 2002. **277**(8): p. 6247-53.
440. Magnuson, R., J. Solomon, and A.D. Grossman, *Biochemical and genetic characterization of a competence pheromone from B. subtilis*. Cell, 1994. **77**(2): p. 207-16.
441. Solomon, J.M., et al., *Convergent sensing pathways mediate response to two extracellular competence factors in Bacillus subtilis*. Genes Dev, 1995. **9**(5): p. 547-58.
442. Tortosa, P., et al., *Specificity and genetic polymorphism of the Bacillus competence quorum-sensing system*. J Bacteriol, 2001. **183**(2): p. 451-60.
443. Bacon Schneider, K., T.M. Palmer, and A.D. Grossman, *Characterization of comQ and comX, two genes required for production of ComX pheromone in Bacillus subtilis*. J Bacteriol, 2002. **184**(2): p. 410-9.
444. Solomon, J.M., B.A. Lazazzera, and A.D. Grossman, *Purification and characterization of an extracellular peptide factor that affects two different developmental pathways in Bacillus subtilis*. Genes Dev, 1996. **10**(16): p. 2014-24.
445. Lazazzera, B.A., J.M. Solomon, and A.D. Grossman, *An exported peptide functions intracellularly to contribute to cell density signaling in B. subtilis*. Cell, 1997. **89**(6): p. 917-25.
446. Benito, Y., et al., *Probing the structure of RNAIII, the Staphylococcus aureus agr regulatory RNA, and identification of the RNA domain involved in repression of protein A expression*. Rna, 2000. **6**(5): p. 668-79.
447. Tegmark, K., E. Morfeldt, and S. Arvidson, *Regulation of agr-dependent virulence genes in Staphylococcus aureus by RNAIII from coagulase-negative staphylococci*. J Bacteriol, 1998. **180**(12): p. 3181-6.
448. Morfeldt, E., K. Tegmark, and S. Arvidson, *Transcriptional control of the agr-dependent virulence gene regulator, RNAIII, in Staphylococcus aureus*. Mol Microbiol, 1996. **21**(6): p. 1227-37.
449. Saenz, H.L., et al., *Inducible expression and cellular location of AgrB, a protein involved in the maturation of the staphylococcal quorum-sensing pheromone*. Arch Microbiol, 2000. **174**(6): p. 452-5.

450. Zhang, L., J. Lin, and G. Ji, *Membrane anchoring of the AgrD N-terminal amphipathic region is required for its processing to produce a quorum-sensing pheromone in Staphylococcus aureus*. J Biol Chem, 2004. **279**(19): p. 19448-56.
451. Zhang, L., et al., *Transmembrane topology of AgrB, the protein involved in the post-translational modification of AgrD in Staphylococcus aureus*. J Biol Chem, 2002. **277**(38): p. 34736-42.
452. Lina, G., et al., *Transmembrane topology and histidine protein kinase activity of AgrC, the agr signal receptor in Staphylococcus aureus*. Mol Microbiol, 1998. **28**(3): p. 655-62.
453. Koenig, R.L., et al., *Staphylococcus aureus AgrA binding to the RNAIII-agr regulatory region*. J Bacteriol, 2004. **186**(22): p. 7549-55.
454. Recsei, P., et al., *Regulation of exoprotein gene expression in Staphylococcus aureus by agar*. Mol Gen Genet, 1986. **202**(1): p. 58-61.
455. Novick, R.P., et al., *Synthesis of staphylococcal virulence factors is controlled by a regulatory RNA molecule*. EMBO J., 1993. **12**: p. 3967-75.
456. Huntzinger, E., et al., *Staphylococcus aureus RNAIII and the endoribonuclease III coordinately regulate spa gene expression*. Embo J, 2005. **24**(4): p. 824-35.
457. Saravia-Otten, P., H.P. Muller, and S. Arvidson, *Transcription of Staphylococcus aureus fibronectin binding protein genes is negatively regulated by agr and an agr-independent mechanism*. J Bacteriol, 1997. **179**(17): p. 5259-63.
458. Bunce, C., et al., *Murine model of cutaneous infection with gram-positive cocci*. Infect Immun, 1992. **60**(7): p. 2636-40.
459. Abdelnour, A., et al., *The accessory gene regulator (agr) controls Staphylococcus aureus virulence in a murine arthritis model*. Infect Immun, 1993. **61**(9): p. 3879-85.
460. Cheung, A.L., et al., *Diminished virulence of a sar-/agr- mutant of Staphylococcus aureus in the rabbit model of endocarditis*. J Clin Invest, 1994. **94**(5): p. 1815-22.
461. Dufour, P., et al., *High genetic variability of the agr locus in Staphylococcus species*. J Bacteriol, 2002. **184**(4): p. 1180-6.
462. Jarraud, S., et al., *Exfoliatin-producing strains define a fourth agr specificity group in Staphylococcus aureus*. J Bacteriol, 2000. **182**(22): p. 6517-22.
463. Lyon, G.J., et al., *Key determinants of receptor activation in the agr autoinducing peptides of Staphylococcus aureus*. Biochemistry, 2002. **41**(31): p. 10095-104.
464. Turgay, K., et al., *Competence in Bacillus subtilis is controlled by regulated proteolysis of a transcription factor*. Embo J, 1998. **17**(22): p. 6730-8.
465. Turgay, K., et al., *Biochemical characterization of a molecular switch involving the heat shock protein ClpC, which controls the activity of ComK, the competence transcription factor of Bacillus subtilis*. Genes Dev, 1997. **11**(1): p. 119-28.
466. van Sinderen, D., et al., *comK encodes the competence transcription factor, the key regulatory protein for competence development in Bacillus subtilis*. Mol Microbiol, 1995. **15**(3): p. 455-62.
467. Nakano, M.M. and P. Zuber, *The primary role of comA in establishment of the competent state in Bacillus subtilis is to activate expression of srfA*. J Bacteriol, 1991. **173**(22): p. 7269-74.

468. Perego, M., *A peptide export-import control circuit modulating bacterial development regulates protein phosphatases of the phosphorelay*. Proc Natl Acad Sci U S A, 1997. **94**(16): p. 8612-7.
469. Lazazzera, B.A., et al., *An autoregulatory circuit affecting peptide signaling in Bacillus subtilis*. J Bacteriol, 1999. **181**(17): p. 5193-200.
470. Core, L. and M. Perego, *TPR-mediated interaction of RapC with ComA inhibits response regulator-DNA binding for competence development in Bacillus subtilis*. Mol Microbiol, 2003. **49**(6): p. 1509-22.
471. Hoch, J.A., *Regulation of the phosphorelay and the initiation of sporulation in Bacillus subtilis*. Annu Rev Microbiol, 1993. **47**: p. 441-65.
472. Perego, M., et al., *Multiple protein-aspartate phosphatases provide a mechanism for the integration of diverse signals in the control of development in B. subtilis*. Cell, 1994. **79**(6): p. 1047-55.
473. Pottathil, M. and B.A. Lazazzera, *The extracellular Phr peptide-Rap phosphatase signaling circuit of Bacillus subtilis*. Front Biosci, 2003. **8**: p. d32-45.
474. Reimann, C., et al., *Genetically programmed autoinducer destruction reduces virulence gene expression and swarming motility in Pseudomonas aeruginosa PAOI*. Microbiology, 2002. **148**(Pt 4): p. 923-32.
475. Dong, Y.H., et al., *Quenching quorum-sensing-dependent bacterial infection by an N-acyl homoserine lactonase*. Nature, 2001. **411**(6839): p. 813-7.
476. Dong, Y.H., et al., *AiiA, an enzyme that inactivates the acylhomoserine lactone quorum-sensing signal and attenuates the virulence of Erwinia carotovora*. Proc Natl Acad Sci U S A, 2000. **97**(7): p. 3526-31.
477. Surette, M.G., M.B. Miller, and B.L. Bassler, *Quorum sensing in Escherichia coli, Salmonella typhimurium, and Vibrio harveyi: a new family of genes responsible for autoinducer production*. Proc Natl Acad Sci U S A, 1999. **96**(4): p. 1639-44.
478. Surette, M.G. and B.L. Bassler, *Quorum sensing in Escherichia coli and Salmonella typhimurium*. Proc Natl Acad Sci U S A, 1998. **95**(12): p. 7046-50.
479. Waters, C.M. and B.L. Bassler, *Quorum sensing: cell-to-cell communication in bacteria*. Annu Rev Cell Dev Biol, 2005. **21**: p. 319-46.
480. Taga, M.E., J.L. Semmelhack, and B.L. Bassler, *The LuxS-dependent autoinducer AI-2 controls the expression of an ABC transporter that functions in AI-2 uptake in Salmonella typhimurium*. Mol Microbiol, 2001. **42**(3): p. 777-93.
481. Taga, M.E., S.T. Miller, and B.L. Bassler, *Lsr-mediated transport and processing of AI-2 in Salmonella typhimurium*. Mol Microbiol, 2003. **50**(4): p. 1411-27.
482. Xavier, K.B. and B.L. Bassler, *Regulation of uptake and processing of the quorum-sensing autoinducer AI-2 in Escherichia coli*. J Bacteriol, 2005. **187**(1): p. 238-48.
483. Surette, M.G. and B.L. Bassler, *Regulation of autoinducer production in Salmonella typhimurium*. Mol Microbiol, 1999. **31**(2): p. 585-95.
484. DeLisa, M.P., J.J. Valdes, and W.E. Bentley, *Mapping stress-induced changes in autoinducer AI-2 production in chemostat-cultivated Escherichia coli K-12*. J Bacteriol, 2001. **183**(9): p. 2918-28.

485. Rahmati, S., et al., *Control of the AcrAB multidrug efflux pump by quorum-sensing regulator SdiA*. Mol Microbiol, 2002. **43**(3): p. 677-85.
486. Michael, B., et al., *SdiA of Salmonella enterica is a LuxR homolog that detects mixed microbial communities*. J Bacteriol, 2001. **183**(19): p. 5733-42.
487. Cirillo, D.M., et al., *Identification of a domain in Rck, a product of the Salmonella typhimurium virulence plasmid, required for both serum resistance and cell invasion*. Infect Immun, 1996. **64**(6): p. 2019-23.
488. Rychlik, I., et al., *Identification of Salmonella enterica serovar Typhimurium genes associated with growth suppression in stationary-phase nutrient broth cultures and in the chicken intestine*. Arch Microbiol, 2002. **178**(6): p. 411-20.
489. Volf, J., et al., *Role of SdiA in Salmonella enterica serovar Typhimurium physiology and virulence*. Arch Microbiol, 2002. **178**(2): p. 94-101.
490. Kanamaru, K., et al., *SdiA, an Escherichia coli homologue of quorum-sensing regulators, controls the expression of virulence factors in enterohaemorrhagic Escherichia coli O157:H7*. Mol Microbiol, 2000. **38**(4): p. 805-16.
491. Sperandio, V., et al., *Quorum sensing controls expression of the type III secretion gene transcription and protein secretion in enterohemorrhagic and enteropathogenic Escherichia coli*. Proc Natl Acad Sci U S A, 1999. **96**(26): p. 15196-201.
492. Wei, Y., A.C. Vollmer, and R.A. LaRossa, *In vivo titration of mitomycin C action by four Escherichia coli genomic regions on multicopy plasmids*. J Bacteriol, 2001. **183**(7): p. 2259-64.
493. Miller, S.T., et al., *Salmonella typhimurium recognizes a chemically distinct form of the bacterial quorum-sensing signal AI-2*. Mol Cell, 2004. **15**(5): p. 677-87.
494. Smith, J.N. and B.M. Ahmer, *Detection of other microbial species by Salmonella: expression of the SdiA regulon*. J Bacteriol, 2003. **185**(4): p. 1357-66.
495. Guttman, B., R. Raya, and E. Kutter, *Basic phage biology*, in *Bacteriophages: Biology and Applications*, E. Kutter and A. Sulakvelidze, Editors. 2005, CRC Press: Boca Raton. p. 29-66.
496. Ackermann, H.W., *Bacteriophage classification*, in *Bacteriophages: Biology and Applications*, E. Kutter and A. Sulakvelidze, Editors. 2005, CRC Press: Boca Raton. p. 67-90.
497. Ackermann, H.W., L. Berthiaume, and M. Tremblay, *A summary of virus classification*, in *Virus Life in Diagrams*, H.W. Ackermann, L. Berthiaume, and M. Tremblay, Editors. 1998, CRC Press: Boca Raton. p. 3-5.
498. Ackermann, H.W., L. Berthiaume, and M. Tremblay, *DNA viruses*, in *Virus Life in Diagrams*, H.W. Ackermann, L. Berthiaume, and M. Tremblay, Editors. 1998, CRC Press: Boca Raton. p. 27-114.
499. Ackermann, H.W. and M.S. Dubow, *The viruses. Descriptions of taxa.*, in *Virus Taxonomy: Classification and Nomenclature of Viruses*, F.A. Murphy, et al., Editors. 1995, Springer-Verlag: Wien. p. 49-63.
500. Ackermann, H.W. and M.S. Dubow, *General properties of tailed phages*, in *Viruses of Prokaryotes: Natural Groups of Bacteriophages*, H.W. Ackermann and M.S. Dubow, Editors. 1987, CRC Press: Boca Raton. p. 1-54.

501. Calendar, R. and R. Inman, *Phage biology*, in *Phages: Their Role in Bacterial Pathogenesis and Biotechnology*, M.K. Waldor, D.I. Friedman, and S.L. Adhya, Editors. 2005, ASM Press: Washington, D. C. p. 18-36.
502. Little, J.W., *Lysogeny, prophage induction, and lysogenic conversion*, in *Phages: Their Role in Bacterial Pathogenesis and Biotechnology*, M.K. Waldor, D.I. Friedman, and S.L. Adhya, Editors. 2005, ASM Press: Washington, D. C. p. 37-54.
503. Ackermann, H.W., L. Berthiaume, and M. Tremblay, *The replication cycle*, in *Virus Life in Diagrams*, H.W. Ackermann, L. Berthiaume, and M. Tremblay, Editors. 1998, CRC Press: Boca Raton. p. 7-9.
504. Kutter, E., R. Raya, and K. Carlson, *Molecular mechanisms of phage infection*, in *Bacteriophages: Biology and Applications*, E. Kutter and A. Sulakvelidze, Editors. 2005, CRC Press: Boca Raton. p. 165-222.
505. Young, R., *Phage lysis*, in *Phages: Their Role in Bacterial Pathogenesis and Biotechnology*, M.K. Waldor, D.I. Friedman, and S.L. Adhya, Editors. 2005, ASM Press: Washington, D. C. p. 92-127.
506. Mattila, L., et al., *Reactive arthritis following an outbreak of Salmonella Bovismorbificans infection*. J Infect, 1998. **36**(3): p. 289-95.
507. Helms, M., et al., *Short and long term mortality associated with foodborne bacterial gastrointestinal infections: registry based study*. Bmj, 2003. **326**(7385): p. 357.
508. Leder, K., M.I. Sinclair, and J.J. McNeil, *Water and the environment: a natural resource or a limited luxury?* Med. J. Aust., 2002. **177**: p. 609-13.
509. Emmerson, A.M., *Emerging waterborne infections in health-care settings*. Emerg Infect Dis, 2001. **7**(2): p. 272-6.
510. Brown, J.S., et al., *Comparative assessment of the toxicity of a papermill effluent by respirometry and luminescence-based bacterial assay*. Chemosphere, 1996. **32**: p. 1553-1561.
511. Tauriainen, S., et al., *Luminescent bacterial sensor for cadmium and lead*. Biosens Bioelectron, 1998. **13**(9): p. 931-8.
512. Corbisier, P., et al., *luxAB gene fusions with the arsenic and cadmium resistance operons of Staphylococcus aureus plasmid pI258*. FEMS Microbiol Lett, 1993. **110**(2): p. 231-8.
513. Korpela, M. and M. Karp, *Stable-light producing Escherichia coli*. Biotechnol. Lett., 1988. **10**: p. 383-88.
514. Peitzsch, N., G. Eberz, and D.H. Nies, *Alcaligenes eutrophus as a bacterial chromate sensor*. Appl Environ Microbiol, 1998. **64**(2): p. 453-8.
515. Tibazarwa, C., et al., *A microbial biosensor to predict bioavailable nickel in soil and its transfer to plants*. Environ Pollut, 2001. **113**(1): p. 19-26.
516. Ramanathan, S., et al., *Sensing antimonite and arsenite at the subattomole level with genetically engineered bioluminescent bacteria*. Anal Chem, 1997. **69**(16): p. 3380-4.
517. Preston, S., et al., *Biosensing the acute toxicity of metal interactions: are they additive, synergistic, or antagonistic?* Environ. Toxicol. Chem., 2000. **19**: p. 775-80.

518. McGrath, S.P., et al., *Assesment of the toxicity of metals in soils amended with sewage sludge using a chemical speciation technique and a lux-based biosensor*. Environ. Toxicol. Chem., 1999. **18**: p. 659-63.
519. Guzzo, J., A. Guzzo, and M.S. DuBow, *Characterization of the effects of aluminum on luciferase biosensors for the detection of ecotoxicity*. Toxicol Lett, 1992. **64-65 Spec No**: p. 687-93.
520. Ji, G., et al., *Bacterial molecular genetics and enzymatic transformations of arsenate, arsenite, and chromate*, in *Biohydrometallurgical Techniques*, A.E. Torma, M.L. Apel, and C.L. Brierly, Editors. 1983, The Minerals, Metals and Materials Society: Warrendale, Pa. p. 529-39.
521. Cai, J. and M.S. DuBow, *Use of a luminescent bacterial biosensor for biomonitoring and characterization of arsenic toxicity of chromated copper arsenate (CCA)*. Biodegradation, 1997. **8**(2): p. 105-11.
522. Holmes, D.S., S.K. Dubey, and S. Gangolli, *Development of biosensors for the detection of mercury and copper ions*. Environ. Geochem. Health, 1994. **16**: p. 229-33.
523. Khang, Y.H., Z.K. Yang, and R.S. Burlage, *Measurement of iron-dependence of *pupA* promoter activity by a *pup-lux* bioreporter*. J. Microbiol. Biotechnol., 1997. **7**: p. 352-55.
524. Condee, C.W. and A.O. Summers, *A *mer-lux* transcriptional fusion for real-time examination of in vivo gene expression kinetics and promoter response to altered superhelicity*. J Bacteriol, 1992. **174**(24): p. 8094-101.
525. Barkay, T., et al., *Luminescence facilitated detection of bioavailable mercury in natural waters*. Methods Mol Biol, 1998. **102**: p. 231-46.
526. Rouch, D.A., J. Parkhill, and N.L. Brown, *Induction of bacterial mercury- and copper-responsive promoters: functional differences between inducible systems and implications for their use in gene-fusions for in vivo metal biosensors*. J. Indust. Microbiol., 1995. **14**: p. 249-53.
527. Selifonova, O., R. Burlage, and T. Barkay, *Bioluminescent sensors for detection of bioavailable Hg(II) in the environment*. Appl Environ Microbiol, 1993. **59**(9): p. 3083-90.
528. Tescione, L. and G. Belfort, *Construction and evaluation of a metal ion biosensor*. Biotechnol. Bioeng., 1993. **42**: p. 945-52.
529. Geiselhart, L., M. Osgood, and D.S. Holmes, *Construction and evaluation of a self-luminescent biosensor*. Ann N Y Acad Sci, 1991. **646**: p. 53-60.
530. Rasmussen, L.D., R.R. Turner, and T. Barkay, *Cell-density-dependent sensitivity of a *mer-lux* bioassay*. Appl Environ Microbiol, 1997. **63**(8): p. 3291-3.
531. Prest, A.G., et al., *The construction and application of a lux-based nitrate biosensor*. Lett Appl Microbiol, 1997. **24**(5): p. 355-60.
532. Erbe, J.L., et al., *Cyanobacteria carrying an *smt-lux* transcriptional fusion as biosensors for the detection of heavy metal cations*. J Ind Microbiol, 1996. **17**(2): p. 80-3.
533. Costanzo, M.A., J. Guzzo, and M.S. DuBow, *Luciferase-based measurement of water contaminants*. Methods Mol Biol, 1998. **102**: p. 201-17.

534. Corbisier, P., et al., *Whole cell- and protein-based biosensors for the detection of bioavailable heavy metals in environmental samples*. Anal. Chim. Acta, 1999. **387**: p. 235-244.
535. Ren, S. and P.D. Frymier, *The use of a genetically engineered Pseudomonas species (Shk1) as a bioluminescent reporter for heavy metal toxicity screening in wastewater treatment plant influent*. Water Environ Res, 2003. **75**(1): p. 21-9.
536. Lampinen, J., et al., *Use of Escherichia coli cloned with genes encoding bacterial luciferase for evaluation of chemical toxicity*. Tox. Asses., 1990. **5**: p. 337-50.
537. Min, J., C.H. Pham, and M.B. Gu, *Specific responses of bacterial cells to dioxins*. Environ Toxicol Chem, 2003. **22**(2): p. 233-8.
538. Gu, M.B., J. Min, and E.J. Kim, *Toxicity monitoring and classification of endocrine disrupting chemicals (EDCs) using recombinant bioluminescent bacteria*. Chemosphere, 2002. **46**(2): p. 289-94.
539. Cox, C.D., et al., *An intermediate-scale lysimeter facility for subsurface bioremediation*. Bioremediation J., 2000. **4**: p. 69-79.
540. Neilson, J.W., S.A. Pierce, and R.M. Maier, *Factors influencing expression of luxCDABE and nah genes in Pseudomonas putida RB1353(NAH7, pUTK9) in dynamic systems*. Appl Environ Microbiol, 1999. **65**(8): p. 3473-82.
541. Sticher, P., et al., *Development and characterization of a whole-cell bioluminescent sensor for bioavailable middle-chain alkanes in contaminated groundwater samples*. Appl Environ Microbiol, 1997. **63**(10): p. 4053-60.
542. Burlage, R.S., *Organic contaminant detection and biodegradation characteristics*. Methods Mol Biol, 1998. **102**: p. 259-68.
543. Rozen, Y., et al., *Specific detection of p-chlorobenzoic acid by Escherichia coli bearing a plasmid-borne fcbA':lux fusion*. Chemosphere, 1999. **38**(3): p. 633-41.
544. Selifonova, O.V. and R.W. Eaton, *Use of an ipb-lux Fusion To Study Regulation of the Isopropylbenzene Catabolism Operon of Pseudomonas putida RE204 and To Detect Hydrophobic Pollutants in the Environment*. Appl Environ Microbiol, 1996. **62**(3): p. 778-783.
545. Whiteley, A.S., et al., *Ecological and physiological analyses of Pseudomonad species within a phenol remediation system*. J Microbiol Methods, 2001. **44**(1): p. 79-88.
546. Wiles, S., et al., *Development of bespoke bioluminescent reporters with the potential for in situ deployment within a phenolic-remediating wastewater treatment system*. J Microbiol Methods, 2003. **55**(3): p. 667-77.
547. Wiles, S., et al., *Calibration and deployment of custom-designed bioreporters for protecting biological remediation consortia from toxic shock*. Environ Microbiol, 2005. **7**(2): p. 260-9.
548. Zaki, S., et al., *Influence of phenolics on the sensitivity of free and immobilized bioluminescent Acinetobacter bacterium*. Microbiol Res, 2006.
549. Bundy, J.G., et al., *Application of bioluminescence-based microbial biosensors to the ecotoxicity assessment of organotins*. Lett. Appl. Microbiol., 1997. **25**: p. 353-58.

550. Fabricant, J.D., J.H. Chalmers, Jr., and M.W. Bradbury, *Bioluminescent strains of E. coli for the assay of biocides*. Bull Environ Contam Toxicol, 1995. **54**(1): p. 90-5.
551. Brandt, K.K., A. Pedersen, and J. Sorensen, *Solid-phase contact assay that uses a lux-marked Nitrosomonas europaea reporter strain to estimate toxicity of bioavailable linear alkylbenzene sulfonate in soil*. Appl Environ Microbiol, 2002. **68**(7): p. 3502-8.
552. Sousa, S., et al., *Use of a lux-modified bacterial biosensor to identify constraints to bioremediation of btex-contaminated sites*. Environ. Toxicol. Chem., 1998. **17**: p. 1039-45.
553. Korpela, M.T., et al., *A recombinant Escherichia coli sensor strain for the detection of tetracyclines*. Anal Chem, 1998. **70**(21): p. 4457-62.
554. Gil, G.C., et al., *A biosensor for the detection of gas toxicity using a recombinant bioluminescent bacterium*. Biosens Bioelectron, 2000. **15**(1-2): p. 23-30.
555. Gu, M.B., et al., *A miniature bioreactor for sensing toxicity using recombinant bioluminescent Escherichia coli cells*. Biotechnol Prog, 1996. **12**(3): p. 393-7.
556. Rupani, S.P., et al., *Characterization of the stress response of a bioluminescent biological sensor in batch and continuous cultures*. Biotechnol Prog, 1996. **12**(3): p. 387-92.
557. Kobatake, E., et al., *Biosensing of benzene derivatives in the environment by luminescent Escherichia coli*. Biosens Bioelectron, 1995. **10**(6-7): p. 601-5.
558. Kelly, C.J., N. Tumsaroj, and C.A. Lajoie, *Assessing wastewater metal toxicity with bacterial bioluminescence in a bench-scale wastewater treatment system*. Water Res, 2004. **38**(2): p. 423-31.
559. Bechor, O., et al., *Recombinant microorganisms as environmental biosensors: pollutants detection by Escherichia coli bearing fabA':lux fusions*. J Biotechnol, 2002. **94**(1): p. 125-32.
560. Van Dyk, T.K., et al., *Rapid and sensitive pollutant detection by induction of heat shock gene-bioluminescence gene fusions*. Appl Environ Microbiol, 1994. **60**(5): p. 1414-20.
561. BenIsrael, O., H. BenIsrael, and S. Ulitzer, *Identification and quantification of toxic chemicals by use of Escherichia coli carrying lux genes fused to stress promoters*. Appl. Environ. Microbiol., 1998. **64**: p. 4346-52.
562. Van Dyk, T.K., et al., *Synergistic induction of the heat shock response in Escherichia coli by simultaneous treatment with chemical inducers*. J Bacteriol, 1995. **177**(20): p. 6001-4.
563. Oh, J.T., et al., *Cationic peptide antimicrobials induce selective transcription of micF and osmY in Escherichia coli*. Biochim Biophys Acta, 2000. **1463**(1): p. 43-54.
564. Belkin, S., et al., *Oxidative stress detection with Escherichia coli harboring a katG':lux fusion*. Appl Environ Microbiol, 1996. **62**(7): p. 2252-6.
565. Vollmer, A.C., et al., *Detection of DNA damage by use of Escherichia coli carrying recA':lux, uvrA':lux, or alkA':lux reporter plasmids*. Appl Environ Microbiol, 1997. **63**(7): p. 2566-71.

566. Davidov, Y., et al., *Improved bacterial SOS promoter∷lux fusions for genotoxicity detection*. Mutat Res, 2000. **466**(1): p. 97-107.
567. van der Lelie, D., et al., *The VITOTOX test, an SOS bioluminescence Salmonella typhimurium test to measure genotoxicity kinetics*. Mutat Res, 1997. **389**(2-3): p. 279-90.
568. Verschaeve, L., et al., *VITOTOX bacterial genotoxicity and toxicity test for the rapid screening of chemicals*. Environ Mol Mutagen, 1999. **33**(3): p. 240-8.
569. Elasri, M.O. and R.V. Miller, *A Pseudomonas aeruginosa biosensor responds to exposure to ultraviolet radiation*. Appl Microbiol Biotechnol, 1998. **50**(4): p. 455-8.
570. Ptitsyn, L.R., et al., *A biosensor for environmental genotoxin screening based on an SOS lux assay in recombinant Escherichia coli cells*. Appl Environ Microbiol, 1997. **63**(11): p. 4377-84.
571. Belkin, S., et al., *A panel of stress-responsive luminous bacteria for the detection of selected classes of toxicants*. Wat Res, 1997. **31**: p. 3009-16.
572. Choi, S.H. and M.B. Gu, *A portable toxicity biosensor using freeze-dried recombinant bioluminescent bacteria*. Biosens Bioelectron, 2002. **17**(5): p. 433-40.
573. Gu, M.B. and G.C. Gil, *A multi-channel continuous toxicity monitoring system using recombinant bioluminescent bacteria for classification of toxicity*. Biosens Bioelectron, 2001. **16**(9-12): p. 661-6.
574. Gillor, O., et al., *A cyanobacterial glnA::lux fusion for assessment of nitrogen bioavailability in a freshwater lake*. Appl Environ Microbiol, 2003. **69**: p. 1465-74.
575. Mbeunkui, F., et al., *Bioavailable nitrate detection in water by an immobilized luminescent cyanobacterial reporter strain*. Appl Microbiol Biotechnol, 2002. **60**(3): p. 306-12.
576. Standing, D., A.A. Meharg, and K. Killham, *A tripartite microbial reporter gene system for real-time assays of soil nutrient status*. FEMS Microbiol Lett, 2003. **220**(1): p. 35-9.
577. Gillor, O., et al., *Phosphorus bioavailability monitoring by a luminescent cyanobacterial sensor strain*. J Phycol, 2002. **38**: p. 107-15.
578. Durham, K.A., et al., *Construction and initial characterization of a luminescent Synechococcus sp. PCC 7942 Fe-dependent bioreporter*. FEMS Microbiol Lett, 2002. **209**(2): p. 215-21.
579. Boyanapalli, R., et al., *Luminescent whole-cell cyanobacterial bioreporter for measuring Fe availability in diverse marine environments*. Appl Environ Microbiol, 2007. **73**(3): p. 1019-24.
580. Turpeinen, R., M. Virta, and M.M. Haggblom, *Analysis of arsenic bioavailability in contaminated soils*. Environ Toxicol Chem, 2003. **22**(1): p. 1-6.
581. Petty, N.K., et al., *Biotechnological exploitation of bacteriophage research*. Trends Biotechnol, 2007. **25**(1): p. 7-15.
582. Hazbon, M.H., *Recent advances in molecular methods for early diagnosis of tuberculosis and drug-resistant tuberculosis*. Biomedica, 2004. **24 Supp 1**: p. 149-62.

583. Billard, P. and M.S. DuBow, *Bioluminescence-based assays for detection and characterization of bacteria and chemicals in clinical laboratories*. Clin Biochem, 1998. **31**(1): p. 1-14.
584. Goodridge, L. and M. Griffiths, *Reporter bacteriophage assays as a means to detect foodborne pathogenic bacteria*. Food Research International, 2002. **35**: p. 863-70.
585. Rees, C.E.D. and M.J. Loessner, *Phage for the detection of pathogenic bacteria*, in *Bacteriophages: Biology and Applications*, E. Kutter and A. Sulakvelidze, Editors. 2005, CRC Press: Boca Raton. p. 267-84.
586. Loessner, M.J., et al., *Construction of luciferase reporter bacteriophage A511::luxAB for rapid and sensitive detection of viable Listeria cells*. Appl Environ Microbiol, 1996. **62**(4): p. 1133-40.
587. Loessner, M.J., M. Rudolf, and S. Scherer, *Evaluation of luciferase reporter bacteriophage A511::luxAB for detection of Listeria monocytogenes in contaminated foods*. Appl Environ Microbiol, 1997. **63**(8): p. 2961-5.
588. Bardarov, S., Jr., et al., *Detection and drug-susceptibility testing of M. tuberculosis from sputum samples using luciferase reporter phage: comparison with the Mycobacteria Growth Indicator Tube (MGIT) system*. Diagn Microbiol Infect Dis, 2003. **45**(1): p. 53-61.
589. Banaiee, N., et al., *Luciferase reporter mycobacteriophages for detection, identification, and antibiotic susceptibility testing of Mycobacterium tuberculosis in Mexico*. J Clin Microbiol, 2001. **39**(11): p. 3883-8.
590. Riska, P.F., et al., *Specific identification of Mycobacterium tuberculosis with the luciferase reporter mycobacteriophage: use of p-nitro-alpha-acetylaminobeta-hydroxy propiophenone*. J Clin Microbiol, 1997. **35**(12): p. 3225-31.
591. Carriere, C., et al., *Conditionally replicating luciferase reporter phages: improved sensitivity for rapid detection and assessment of drug susceptibility of Mycobacterium tuberculosis*. J Clin Microbiol, 1997. **35**(12): p. 3232-9.
592. Riska, P.F. and W.R. Jacobs, Jr., *The use of luciferase-reporter phage for antibiotic-susceptibility testing of mycobacteria*. Methods Mol Biol, 1998. **101**: p. 431-55.
593. Riska, P.F., et al., *Rapid film-based determination of antibiotic susceptibilities of Mycobacterium tuberculosis strains by using a luciferase reporter phage and the Bronx Box*. J Clin Microbiol, 1999. **37**(4): p. 1144-9.
594. Jacobs, W.R., Jr., et al., *Rapid assessment of drug susceptibilities of Mycobacterium tuberculosis by means of luciferase reporter phages*. Science, 1993. **260**(5109): p. 819-22.
595. Sarkis, G.J., W.R. Jacobs, Jr., and G.F. Hatfull, *L5 luciferase reporter mycobacteriophages: a sensitive tool for the detection and assay of live mycobacteria*. Mol Microbiol, 1995. **15**(6): p. 1055-67.
596. Turpin, P.E., et al., *A rapid luminescent phage-based MPN method for the enumeration of Salmonella typhimurium in environmental samples*. Lett Appl Microbiol, 1993. **16**: p. 24-7.
597. Chen, J. and M.W. Griffiths, *Salmonella detection in eggs using lux⁺ bacteriophages*. J Food Protect, 1996. **59**: p. 908-14.

598. Kodikara, C.P., H.H. Crew, and G.S. Stewart, *Near on-line detection of enteric bacteria using lux recombinant bacteriophage*. FEMS Microbiol Lett, 1991. **67**(3): p. 261-5.
599. Waddell, T.E. and C. Poppe, *Construction of mini-Tn10luxABcam/Ptac-ATS and its use for developing a bacteriophage that transduces bioluminescence to Escherichia coli O157:H7*. FEMS Microbiol Lett, 2000. **182**(2): p. 285-9.
600. Kuhn, J., et al., *Detection of bacteria using foreign DNA: the development of a bacteriophage reagent for Salmonella*. Int J Food Microbiol, 2002. **74**(3): p. 229-38.
601. Ulitzur, S. and J. Kuhn, *Introduction of lux genes into bacteria, a new approach for specific determination of bacteria and their antibiotic susceptibility*, in *Bioluminescence new perspectives*, J. Scholmerich, et al., Editors. 1987, John Wiley: New York. p. 463-72.
602. Hendrie, M.S., W. Hodgkiss, and J.M. Shewan, *The identification, taxonomy and classification of luminous bacteria*. J. Gen. Microbiol., 1970. **64**: p. 151-69.
603. Bright, N.G., *A model two-component bacteriophage/bioluminescent reporter detection assay using filamentous phage M13 and an F' Escherichia coli host*. 2003, Purdue University: West Lafayette, Indiana.
604. Andersen, J.B., et al., *gfp-based N-acyl homoserine-lactone sensor systems for detection of bacterial communication*. Appl Environ Microbiol, 2001. **67**(2): p. 575-85.
605. Carbonelli, D.L., et al., *A plasmid vector for isolation of strong promoters in Escherichia coli*. FEMS Microbiol Lett, 1999. **177**(1): p. 75-82.
606. Kwan, T., et al., *The complete genomes and proteomes of 27 Staphylococcus aureus bacteriophages*. Proc Natl Acad Sci U S A, 2005. **102**(14): p. 5174-9.
607. Loessner, M.J., et al., *The two-component lysis system of Staphylococcus aureus bacteriophage Twort: a large TTG-start holin and an associated amidase endolysin*. FEMS Microbiol Lett, 1998. **162**(2): p. 265-74.
608. Vybiral, D., et al., *Complete nucleotide sequence and molecular characterization of two lytic Staphylococcus aureus phages: 44AHJD and P68*. FEMS Microbiol Lett, 2003. **219**(2): p. 275-83.
609. Sullivan, M.A., R.E. Yasbin, and F.E. Young, *New shuttle vectors for Bacillus subtilis and Escherichia coli which allow rapid detection of inserted fragments*. Gene, 1984. **29**(1-2): p. 21-6.
610. Haima, P., et al., *Development of a beta-galactosidase alpha-complementation system for molecular cloning in Bacillus subtilis*. Gene, 1990. **86**(1): p. 63-9.
611. Joseph, P., et al., *Rapid orientated cloning in a shuttle vector allowing modulated gene expression in Bacillus subtilis*. FEMS Microbiol Lett, 2001. **205**(1): p. 91-7.
612. Sambrook, J. and D. Russell, *Molecular Cloning: A Laboratory Manual, Third Edition*. 2001, Woodbury, NY: CSHL Press.
613. Schenk, S. and R.A. Laddaga, *Improved method for electroporation of Staphylococcus aureus*. FEMS Microbiol Lett, 1992. **73**(1-2): p. 133-8.
614. Stephenson, M. and P. Jarrett, *BioTechnology Techniques*. 1991. **5**(1): p. 9-12.

615. Francis, K.P., et al., *Monitoring bioluminescent Staphylococcus aureus infections in living mice using a novel luxABCDE construct*. Infect Immun, 2000. **68**(6): p. 3594-600.
616. Sau, K., et al., *Synonymous codon usage bias in 16 Staphylococcus aureus phages: implication in phage therapy*. Virus Res, 2005. **113**(2): p. 123-31.
617. Primrose, S.B., R.M. Twyman, and R.W. Old, *Cloning in bacteria other than Escherichia coli*, in *Principles of Gene Manipulation, The Sixth Edition*. 2001, Blackwell Science.
618. Rao, L., R.K. Karls, and M.J. Betley, *In vitro transcription of pathogenesis-related genes by purified RNA polymerase from Staphylococcus aureus*. J Bacteriol, 1995. **177**(10): p. 2609-14.
619. Grkovic, S., et al., *Stable low-copy-number Staphylococcus aureus shuttle vectors*. Microbiology, 2003. **149**(Pt 3): p. 785-94.
620. Hudson, M.C. and G.C. Stewart, *Differential utilization of Staphylococcus aureus promoter sequences by Escherichia coli and Bacillus subtilis*. Gene, 1986. **48**(1): p. 93-100.
621. Wang, J.D., et al., *Multicopy plasmids affect replisome positioning in Bacillus subtilis*. J Bacteriol, 2004. **186**(21): p. 7084-90.
622. Yansura, D.G. and D.J. Henner, *Use of the Escherichia coli lac repressor and operator to control gene expression in Bacillus subtilis*. Proc Natl Acad Sci U S A, 1984. **81**(2): p. 439-43.
623. Bernard, A. and M. Payton, *Selection of Escherichia coli expression systems*, in *Current Protocols in Protein Science*, J.E. Coligan, et al., Editors. 1995, John Wiley and Sons, Inc.
624. Pengov, A. and S. Ceru, *Antimicrobial drug susceptibility of Staphylococcus aureus strains isolated from bovine and ovine mammary glands*. J Dairy Sci, 2003. **86**(10): p. 3157-63.
625. Baquero, F., *Low-level antibacterial resistance: a gateway to clinical resistance*. Drug Resist Updat, 2001. **4**(2): p. 93-105.
626. Goldstein, F., *The potential clinical impact of low-level antibiotic resistance in Staphylococcus aureus*. J Antimicrob Chemother, 2007. **59**(1): p. 1-4.
627. Angeletti, R.H., *Design of useful peptide antigens*. Journal of Biomolecular Techniques, 1999. **10**: p. 2-10.
628. www.abcam.com/technical, *ABCAM troubleshooting tips-WB*.
629. Sharp, P.M. and W.H. Li, *The codon Adaptation Index--a measure of directional synonymous codon usage bias, and its potential applications*. Nucleic Acids Res, 1987. **15**(3): p. 1281-95.
630. Karlin, S., A.M. Campbell, and J. Mrazek, *Comparative DNA analysis across diverse genomes*. Annu Rev Genet, 1998. **32**: p. 185-225.
631. Ludwig, W., et al., *A phylogenetic analysis of staphylococci, Peptococcus saccharolyticus and Micrococcus mucilaginosus*. J Gen Microbiol, 1981. **125**(2): p. 357-66.
632. Balz, R.K. and K.H. Schleifer, *DNA-rRNA hybridization studies among Staphylococci and some other gram-positive bacteria*. FEMS Microbiol Lett, 1981. **10**: p. 357-62.

633. Wilkinson, B.J., *Biology*, in *The Staphylococci in Human Disease*, K.B. Crossley and G.L. Archer, Editors. 1997, Churchill Livingstone Inc.: New York. p. 1-38.
634. Kuroda, M., et al., *Whole genome sequencing of meticillin-resistant Staphylococcus aureus*. *Lancet*, 2001. **357**(9264): p. 1225-40.
635. McLaughlin, J.R., C.L. Murray, and J.C. Rabinowitz, *Plasmid-directed expression of Staphylococcus aureus beta-lactamase by Bacillus subtilis in vitro*. *J Biol Chem*, 1981. **256**(21): p. 11272-83.
636. Glick, B. and J. Pasternak, *Manipulation of gene expression in prokaryotes*, in *Molecular Biotechnology: Principles and Applications of Recombinant DNA*. 3rd ed. 2003, ASM Press: Washington, D. C. p. 121-62.
637. Sorensen, H.P. and K.K. Mortensen, *Advanced genetic strategies for recombinant protein expression in Escherichia coli*. *J Biotechnol*, 2005. **115**(2): p. 113-28.
638. Makrides, S.C., *Strategies for achieving high-level expression of genes in Escherichia coli*. *Microbiol Rev*, 1996. **60**(3): p. 512-38.
639. LaVallie, E.R., *Production of recombinant proteins in Escherichia coli*, in *Current Protocols in Protein Science*, J.E. Coligan, et al., Editors. 1995, John Wiley and Sons, Inc.
640. Dong, Y.H., et al., *Identification of quorum-quenching N-acyl homoserine lactonases from Bacillus species*. *Appl Environ Microbiol*, 2002. **68**(4): p. 1754-9.
641. Zhang, H.B., L.H. Wang, and L.H. Zhang, *Genetic control of quorum-sensing signal turnover in Agrobacterium tumefaciens*. *Proc Natl Acad Sci U S A*, 2002. **99**(7): p. 4638-43.
642. Park, S.Y., et al., *AhlD, an N-acylhomoserine lactonase in Arthrobacter sp., and predicted homologues in other bacteria*. *Microbiology*, 2003. **149**(Pt 6): p. 1541-50.
643. de Nys, R., et al., *New halogenated furanones from the marine alga Delisea pulchra*. *Tetrahedron*, 1993. **49**: p. 11213-20.
644. Kline, T., et al., *Novel synthetic analogs of the Pseudomonas autoinducer*. *Bioorg Med Chem Lett*, 1999. **9**(24): p. 3447-52.
645. Passador, L., et al., *Functional analysis of the Pseudomonas aeruginosa autoinducer PAI*. *J Bacteriol*, 1996. **178**(20): p. 5995-6000.
646. Pesci, E.C., et al., *Regulation of las and rhl quorum sensing in Pseudomonas aeruginosa*. *J Bacteriol*, 1997. **179**(10): p. 3127-32.
647. Givskov, M., et al., *Eukaryotic interference with homoserine lactone-mediated prokaryotic signalling*. *J Bacteriol*, 1996. **178**(22): p. 6618-22.
648. Manefield, M., et al., *Evidence that halogenated furanones from Delisea pulchra inhibit acylated homoserine lactone (AHL)-mediated gene expression by displacing the AHL signal from its receptor protein*. *Microbiology*, 1999. **145** (Pt 2): p. 283-91.
649. Manefield, M., et al., *Inhibition of luminescence and virulence in the black tiger prawn (Penaeus monodon) pathogen Vibrio harveyi by intercellular signal antagonists*. *Appl Environ Microbiol*, 2000. **66**(5): p. 2079-84.

650. Leadbetter, J.R. and E.P. Greenberg, *Metabolism of acyl-homoserine lactone quorum-sensing signals by Variovorax paradoxus*. J Bacteriol, 2000. **182**(24): p. 6921-6.
651. Hoang, T.T. and H.P. Schweizer, *Characterization of Pseudomonas aeruginosa enoyl-acyl carrier protein reductase (FabI): a target for the antimicrobial triclosan and its role in acylated homoserine lactone synthesis*. J Bacteriol, 1999. **181**(17): p. 5489-97.
652. Velterop, J.S., et al., *Synthesis of pyrroloquinoline quinone in vivo and in vitro and detection of an intermediate in the biosynthetic pathway*. J Bacteriol, 1995. **177**(17): p. 5088-98.
653. Ohta, K., et al., *Metabolic engineering of Klebsiella oxytoca M5A1 for ethanol production from xylose and glucose*. Appl Environ Microbiol, 1991. **57**(10): p. 2810-5.
654. Fuqua, C. and S.C. Winans, *Conserved cis-acting promoter elements are required for density-dependent transcription of Agrobacterium tumefaciens conjugal transfer genes*. J Bacteriol, 1996. **178**(2): p. 435-40.
655. Vander Byl, C. and A.M. Kropinski, *Sequence of the genome of Salmonella bacteriophage P22*. J Bacteriol, 2000. **182**(22): p. 6472-81.
656. Susskind, M.M. and D. Botstein, *Molecular genetics of bacteriophage P22*. Microbiol Rev, 1978. **42**(2): p. 385-413.
657. Bossi, L. and N. Figueroa-Bossi, *Prophage arsenal of Salmonella enterica serovar typhimurium*, in *Phages: Their Role in Bacterial Pathogenesis and Biotechnology*, M.K. Waldor, D.I. Friedman, and S.L. Adhya, Editors. 2005, ASM Press: Washington, D. C. p. 165-186.
658. O'Callaghan, D. and A. Charbit, *High efficiency transformation of Salmonella typhimurium and Salmonella typhi by electroporation*. Mol Gen Genet, 1990. **223**(1): p. 156-8.
659. Fournet-Fayard, S., B. Joly, and C. Forestier, *Transformation of wild type Klebsiella pneumoniae with plasmid DNA by electroporation*. J Microbiol Methods, 1995. **24**: p. 49-54.
660. Sorensen, K.I., et al., *Nucleotide pool-sensitive selection of the transcriptional start site in vivo at the Salmonella typhimurium pyrC and pyrD promoters*. J Bacteriol, 1993. **175**(13): p. 4137-44.
661. Ravnum, S. and D.I. Andersson, *An adenosyl-cobalamin (coenzyme-B12)-repressed translational enhancer in the cob mRNA of Salmonella typhimurium*. Mol Microbiol, 2001. **39**(6): p. 1585-94.
662. Casin, I., et al., *Salmonella enterica serovar Typhimurium bla(PER-1)-carrying plasmid pSTII encodes an extended-spectrum aminoglycoside 6'-N-acetyltransferase of type Ib*. Antimicrob Agents Chemother, 2003. **47**(2): p. 697-703.
663. Chopra, A.K., et al., *Molecular characterization of an enterotoxin from Salmonella typhimurium*. Microb Pathog, 1994. **16**(2): p. 85-98.
664. Hughes, K.T., et al., *The Salmonella typhimurium nadC gene: sequence determination by use of Mud-P22 and purification of quinolinate phosphoribosyltransferase*. J Bacteriol, 1993. **175**(2): p. 479-86.

665. Oda, M., et al., *Rapid detection of Escherichia coli O157:H7 by using green fluorescent protein-labeled PP01 bacteriophage*. Appl Environ Microbiol, 2004. **70**(1): p. 527-34.
666. Steinbacher, S., et al., *Crystal structure of phage P22 tailspike protein complexed with Salmonella sp. O-antigen receptors*. Proc Natl Acad Sci U S A, 1996. **93**(20): p. 10584-8.
667. Neal, B.L., P.K. Brown, and P.R. Reeves, *Use of Salmonella phage P22 for transduction in Escherichia coli*. J Bacteriol, 1993. **175**(21): p. 7115-8.
668. Maloy, S.R., *Phage P22*, in *Experimental Techniques in Bacterial Genetics*. 1989, Jones and Bartlett Publishers. p. 11-6.
669. Ripp, S. and R.V. Miller, *The role of pseudolysogeny in bacteriophage-host interactions in a natural freshwater environment*. Microbiology, 1997. **143**: p. 2065-70.
670. Ripp, S. and R.V. Miller, *Dynamics of the pseudolysogenic response in slowly growing cells of Pseudomonas aeruginosa*. Microbiology, 1998. **144** (Pt 8): p. 2225-32.
671. Hara-Kudo, Y., M. Miyahara, and S. Kumagai, *Loss of O157 O antigenicity of verotoxin-producing Escherichia coli O157:H7 surviving under starvation conditions*. Appl Environ Microbiol, 2000. **66**(12): p. 5540-3.
672. Fridrich, E. and C. Whitfield, *Lipopolysaccharide inner core oligosaccharide structure and outer membrane stability in human pathogens belonging to the Enterobacteriaceae*. J Endotoxin Res, 2005. **11**(3): p. 133-44.

APPENDIX

Table A. Alternative names used for plasmids in this study.

Plasmid	Alternative Name
pMOD-2-kan ^r -prom-luxI-T1T2 #7	pMO-L #7
pMK4-prom-luxI #13.3	pMK-L #13.3
pHPS9-luxI #7	pHP-L #7
pHPS9-kanR #4	pHP-K #4
pDG148-Stu-luxI #28	pDG-L #28
pHPS9-sht-Pspac-luxI-lacI #9	pHP-PL #9
pHPS9-sht-Pspac-kanR-lacI #31	pHP-PK #31
pHPS9-sht-Pspac-optluxI-lacI #5	pHP-POL #5
pCR2.1-P _L -luxI-T1T2 #3	pCR-L #3
pCR2.1-HA1-P _L -luxI-T1T2-HA2 #5	pCR-HAL #5

VITA

Aysu Ozen was born on February 12, 1972 in Kdz. Eregli, Turkey. She received her Bachelors of Science and Master of Science degrees from the Middle East Technical University in Ankara, Turkey. She worked as an assistant specialist in The Scientific and Technological Research Council of Turkey in Ankara, Turkey for three years. Then she pursued her Doctor of Philosophy degree in Microbiology at the Center for Environmental Biotechnology at the University of Tennessee in Knoxville.